Evaluation of Groundwater Resources for Communities in Rio Arriba County, New Mexico

B. Talon Newton, Daniel J. Koning, Shari A. Kelley, Ethan Mamer, Daniel J. Lavery, Cris Morton, Amanda L.M. Doherty, Laila Sturgis, and Stacy Timmons

OPEN-FILE REPORT

Open-File Report 630—Evaluation of Groundwater Resources for Communities in Rio Arriba County, New Mexico

B. Talon Newton, Daniel J. Koning, Shari A. Kelley, Ethan Mamer, Daniel J. Lavery, Cris Morton, Amanda L.M. Doherty, Laila Sturgis, and Stacy Timmons

ACKNOWLEDGMENTS

CONTENTS

Figures

Tables

EXECUTIVE SUMMARY

The New Mexico Bureau of Geology and Mineral Resources began a hydrogeologic study in regions of Rio Arriba County in 2023, funded by a state legislative appropriation. The primary goal of this study was to characterize the local and regional aquifers that currently supply local communities for domestic and municipal use. The study focused on the communities of Chama, Dixon, Abiquiu, Medanales, and El Rito. While surface water is primarily used for irrigation and farming, groundwater is the primary water source for domestic and municipal use for households, institutions, and businesses, supplied by a community system or private domestic wells. Most wells in these communities produce water from shallow alluvial aquifers that are composed of unconsolidated gravel, sand, and clay. These shallow aquifers generally offer convenient (shallow depth to water) and good-quality water but may be susceptible to contamination from the surface and changes related to variations in surface water.

These communities have experienced water shortages during drought conditions when decreased amounts of rain and snow in the recharge areas (high elevations in nearby mountains) result in decreased recharge to the shallow alluvial aquifers. Drought conditions greatly affect surface water supply, causing an increase in water demand and, therefore, an increase in groundwater pumping. The combination of decreased recharge and increased groundwater pumping can result in water levels in wells dropping below the pump, rendering the wells nonfunctional for a period of time. Therefore, as the climate warms, resulting in overall less recharge and increased evaporation, it is vital to characterize these shallow alluvial aquifers, as well as evaluate deeper aquifer systems and how the different aquifers interact with each other and the surface water system.

As part of this initial phase of study, depth to water was measured in 90 wells, and water samples were collected from 63 of these wells. All samples were analyzed for major cations and anions, trace metals, stable isotopes of water (oxygen and hydrogen), and bacteria. A subset of 25 samples was analyzed for carbon-14 and tritium (^{3}H), which were used to assess the age of the groundwater. Other data used in this study, including well depth, depth to water, and water chemistry, were obtained from well records at the New Mexico Office of the State Engineer and other state agencies.

Shallow alluvial aquifers in these communities underlie the valley bottoms and are composed of sediments deposited by the local stream or river. The accumulated sediments that make up the shallow alluvial aquifers sit on top of older rocks or sediments of lower permeability, such as clay, shale, or a crystalline rock like granite. This low-permeability boundary is essentially the "floor" or bottom of the shallow alluvial aquifer that acts as a barrier to vertical water flow, effectively defining shallow and deep aquifer systems with limited hydrologic connection. The deep aquifer systems are more difficult to characterize because significantly fewer wells are completed in them.

The shallow alluvial aquifers in all communities of interest are hydrologically connected to the surface water system. Shallow groundwater generally flows parallel to the local river or stream and moves from the aquifer to the stream or vice versa, depending on local hydrologic conditions. Depth-to-water measurements and total well depths from well records were used to estimate saturated thicknesses for local shallow alluvial aquifers. The average estimated saturated thickness for shallow

alluvial aquifers in the Abiquiu Valley (Abiquiu, Medanales, and El Rito) and the Dixon area was 11 m (36 ft). The estimated average saturated thickness of the shallow alluvial aquifer in the Chama area was 6.7 m (22 ft). The shallow alluvial aquifer in the El Rito area had the largest estimated saturated thickness, greater than 20 m (66 ft).

Groundwater produced from these shallow alluvial aquifers was mostly of good quality, with total dissolved solids concentrations of less than 500 mg/L. However, some wells completed in shallow alluvial aquifers—particularly in the communities of Chama, El Rito, Abiquiu, and Medanales—tested positive for total coliform bacteria, which is likely due to contamination from septic tanks. Water produced by some wells completed in the deep aquifer system in the Chama and Dixon areas had arsenic concentrations that were significantly higher than the U.S. Environmental Protection Agency maximum contaminant level. Water chemistry and age dating data indicate that the shallow alluvial aquifers are recharged mainly by snowmelt and rain in nearby mountains, with ages ranging from tens to a few hundreds of years old. In contrast, groundwater produced from the deeper aquifer systems exhibits a wide range of total dissolved solids concentrations, from hundreds to thousands of mg/L, along with much older ages (up to tens of thousands of years old). There is some evidence that groundwater from the deep aquifer systems can move upward into the shallow alluvial aquifer systems via faults and fractures.

While the shallow alluvial aquifers produce good-quality water for municipal and domestic uses, these aquifers are relatively thin and have limited storage. These shallow aquifers, with young waters, are highly susceptible to shallow contamination (such as septic systems) and can change quickly due to drought, surface water flow changes, or impacts of climate change. Deep regional aquifer systems are characterized by more variable water quality that comes with longer, deeper flow paths. These deep regional aquifer systems may be more stable in the long term, with less variability in water quantity.

Future work will focus on a more detailed characterization of both shallow and deep aquifer systems using existing wells and data, along with new approaches. Geophysical surveys paired with information from well logs will be used to identify the aquifer bottom (lower boundary) and the distribution of gravel, sand, and clay. Additional work will also include further characterization of the deep aquifer systems to assess their potential for supplemental water supply.

ABBREVIATIONS

cfs	cubic feet per second
DIC	dissolved inorganic carbon
EPA	U.S. Environmental Protection Agency
ft	feet
GMWL	global meteoric water line
gpm	gallons per minute
in.	inch(es)
km	kilometer(s)
LMWL	local meteoric water line
m	meter(s)
m bgs	meters below ground surface
MCL	maximum contaminant level
MDWCA	mutual domestic water consumers association
meq/L	milliequivalents per liter
mg/L	milligrams per liter
mi	mile(s)
mm	millimeter(s)
MYBP	millions of years before present
NMBGMR	New Mexico Bureau of Geology and Mineral Resources
NMOSE	New Mexico Office of the State Engineer
PMC	percent modern carbon
TDS	total dissolved solids
TU	tritium units
USGS	U.S. Geological Survey
YBP	years before present

Springs southwest of Dixon, along with gravelly Chama-El Rito Member of the Tesuque Formation. *Photo by Ethan Mamer*

CHAPTER I: HYDROGEOLOGIC STUDY IN RIO ARRIBA COUNTY

INTRODUCTION

At first glance, Rio Arriba County in northern New Mexico appears to have an abundance of water, with numerous perennial streams and three reservoirs within the Rio Chama watershed (Fig. 1.1) and Embudo Creek flowing into the Rio Grande near Dixon. This water has historically been used for subsistence farming in the valley bottoms. Today, this surface water is primarily used to irrigate an estimated 25,370 acres of land (La Calandria Associates, Inc., 2006), mainly for forage crop production and residential yard and garden space. In addition, surface water in the Rio Chama watershed is enjoyed by hunters, anglers, hikers, and boaters. The ability to divert this surface water for additional uses is limited by the Rio Grande Compact, which carefully controls new water rights applications to ensure downstream surface water users receive their allocations.

Almost all other water uses beyond agriculture rely on groundwater supplies. Groundwater is the principal water source for municipal and domestic use in households, institutions, and businesses in the region. Many small communities in Rio Arriba County have experienced problems with their groundwater supply in terms of quantity and quality (La Calandria Associates, Inc., 2006) and have valid concerns about their future water supply. While some research on the hydrogeology of this area has been conducted, much more work is needed to better understand local and regional groundwater systems.

Most small communities in Rio Arriba County use groundwater for domestic and municipal uses, not only due to legal and political limits on the surface water supply but also because of the monetary costs associated with treating surface water supplies. Groundwater supplies that are not in direct communication with surface water are generally more cost-effective sources because they typically do not contain fecal coliform and have very low turbidity. However, due to the regional geology of the Rio Arriba County area, many communities have had difficulty finding a good-quality, reliable community groundwater source (La Calandria Associates, Inc., 2006). Many communities, such as El Rito and Abiquiu, have used a variety of water sources, including collection galleries, hand-dug wells, springs, and wells tapping deeper aquifers. Shallow hand-dug wells and collection galleries tend to dry up during short-term and long-term droughts. Unfortunately, finding a deep groundwater source that produces good-quality water at adequate pumping rates to supply a community has proven very difficult. Currently, the community of Chama uses surface water from the Rio Chama because a previously used spring effectively dried up, and deep groundwater in the area tends to have quality issues such as high arsenic concentrations.

As the climate continues to change, these water supply issues will likely worsen. All surface water and groundwater in New Mexico originates as rain or snow, most of which is returned to the atmosphere by plant transpiration and evaporation (together called evapotranspiration). Some water runs off into local or regional streams, and some water recharges local or regional aquifers that eventually discharge into streams and rivers; however, the amount of groundwater recharge represents a small percentage compared to the total precipitation (Phillips and Thomson, 2022). As the average temperature continues to increase over the next 50 years, researchers predict evapotranspiration rates will increase, likely resulting in decreases in groundwater recharge and streamflow (Phillips and Thomson, 2022). Decreased streamflow and groundwater recharge will have a negative impact on water supplies for many communities in Rio Arriba County that are already experiencing water shortages.
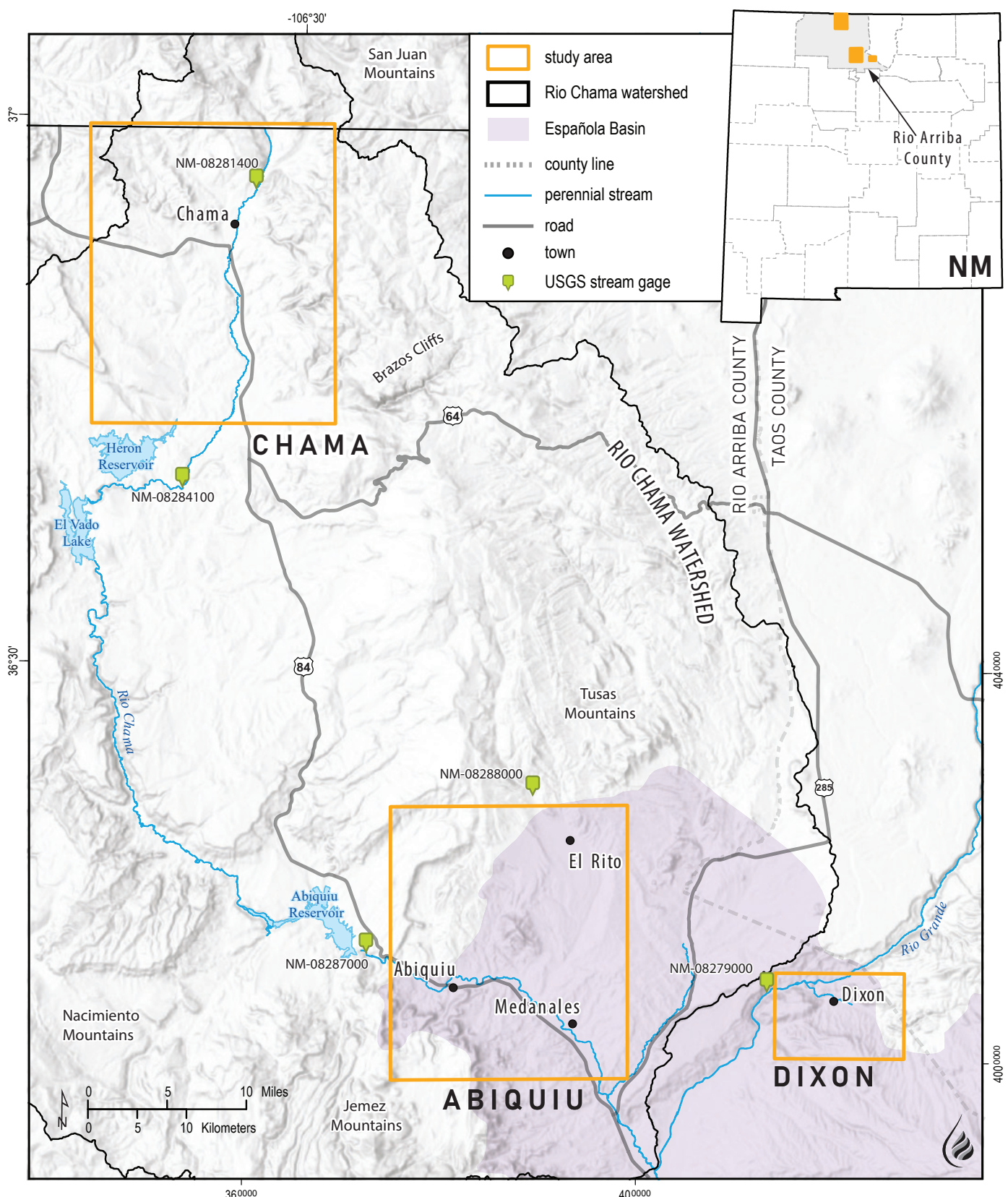
Figure 1.1. The three community areas included in this study, along with important topographic and geographic features of the Rio Chama watershed and the northern Española Basin. Locations of USGS stream gages are also shown.

Therefore, it is very important to gain a better understanding of the regional and local hydrogeologic systems that these communities rely on.

This report summarizes the first year of a project that was funded for the state fiscal year 2023–2024. Additional funding for two more fiscal years will continue this regional study, and this work will be updated and revised. This study was conducted by the New Mexico Bureau of Geology and Mineral Resources (NMBGMR), a research and service division of New Mexico Tech. The objectives of this study were to:

1. compile existing literature and hydrogeologic data for local communities of interest and surrounding areas in Rio Arriba County;

2. characterize local shallow alluvial aquifers that currently supply communities for domestic and municipal use, including geologic, hydrogeologic, and geochemical (water quality) characterization;

3. identify and assess deeper aquifer systems that also contribute to the groundwater supply; and

4. identify data gaps and clearly recommend future research needed to fill these gaps so water managers and communities can make well-informed decisions about their future water security.

The results of the first phase of this hydrogeologic study are reported in Chapters 2–4; each chapter focuses on the communities in the three study areas. Online data tables are available as appendices at https://geoinfo.nmt.edu/publications/openfile/details.cfml?Volume=630. Each chapter of this report concludes with recommendations for future research in these regions.

STUDY AREA

NMBGMR's research team focused on the communities of Chama, Abiquiu, El Rito, Medanales, and Dixon (Fig. 1.1). Except for Dixon, these communities are located in the Rio Chama watershed, which makes up more than half of Rio Arriba County (around 3,157 mi²) and is bounded by the San Juan Mountains to the north (in Colorado), the Tusas Mountains to the east, and the Jemez Mountains to the south. To the west, a relatively low-elevation surface water divide separates the Rio Chama

watershed from the San Juan Basin. The Rio Chama drains these surrounding mountains and discharges into the Rio Grande just north of Española. Chama, Abiquiu, and Medanales are located along the Rio Chama, and El Rito is located near El Rito Creek, which drains into the Rio Chama between Abiquiu and Medanales. Dixon is located on the east side of the Rio Grande along Embudo Creek, which drains a large area of the Sangre de Cristo Mountains to the southeast.

Shallow Alluvial Aquifers

Residents of these communities rely on groundwater they pump from shallow alluvial aquifers, which are typically made up of unconsolidated gravel, sand, silt, and clay. A conceptual model of a shallow alluvial aquifer is shown in Figure 1.2. The alluvial aquifers in these communities underlie valley bottoms and are composed of sediments deposited by the local stream or river (Rio Chama for Chama, Abiquiu, and Medanales; El Rito Creek for El Rito; and Embudo Creek for the Dixon area). The accumulation of sediments that make up the shallow alluvial aquifers in the study areas ranges in thickness from 5 to 50 m (16.4–150 ft) and sits on top of rocks or sediments of lower permeability, such as clay, shale, or a crystalline rock such as granite. This material is essentially the "floor" or bottom of the shallow alluvial aquifer that acts as a partial to total barrier to vertical water flow, effectively defining shallow and deep aquifer systems with limited hydrologic connection. In this report, we use the term "shallow aquifer system" to refer to groundwater that resides in and flows through the unconsolidated sediments of the shallow alluvial aquifer. The term "deep aquifer system" refers to groundwater that resides in older rocks underlying these alluvial aquifers.

Shallow alluvial aquifers in the study areas are hydrologically connected to the local streams or rivers, meaning water moves from one to the other. Whether water moves from a stream into the aquifer (losing stream) or from the aquifer into a stream (gaining stream) depends on the relative elevations of the water level in the river and the water level of the shallow aquifer or the water table. In arid and semiarid areas such as New Mexico, the distribution of gaining and losing river reaches can change significantly with space and time. Groundwater recharge primarily occurs in mountainous areas, where higher precipitation rates and lower temperatures occur. Precipitation and snowmelt at

higher elevations make their way to rivers in valleys by a variety of flow paths. Overland runoff during a snowmelt or precipitation event can reach a valley bottom in a matter of hours to days. Beneath the surface, some water moves through pores between unconsolidated grains in drainages that accumulate sediment, reaching the valley bottom on the order of weeks to years. Water may also flow along deeper and longer flow paths through fractures in crystalline rocks or through comparably consolidated and cemented, older sedimentary rocks. For these deep flow paths, groundwater flow may take hundreds to thousands of years to reach the valley bottoms from high-terrain recharge areas (Fig. 1.2).

In areas near the headwaters of a river, including those of the Rio Chama, the amount of water moving along subsurface flow paths of varying scales is sufficient to maintain base flow during dry seasons and some droughts. Base flow is the flow rate of a river or stream during seasonal dry periods or longer-term droughts when flow in the river or stream is solely due to groundwater discharge. However, as the stream flows away from the main recharge area, less or even no groundwater contributes to streamflow, resulting in losing stream conditions (meaning the river water level is higher than the water table) in which river water seeps through the streambed and recharges the shallow aquifer (Fig. 1.3). Depending on local flow conditions, the transition zone between a gaining and losing river reach likely changes by moving downstream or upstream during wetter and drier conditions, respectively. A shallow alluvial aquifer temporarily stores water that was recharged by the river under losing conditions and discharges water to the river or stream during gaining conditions.
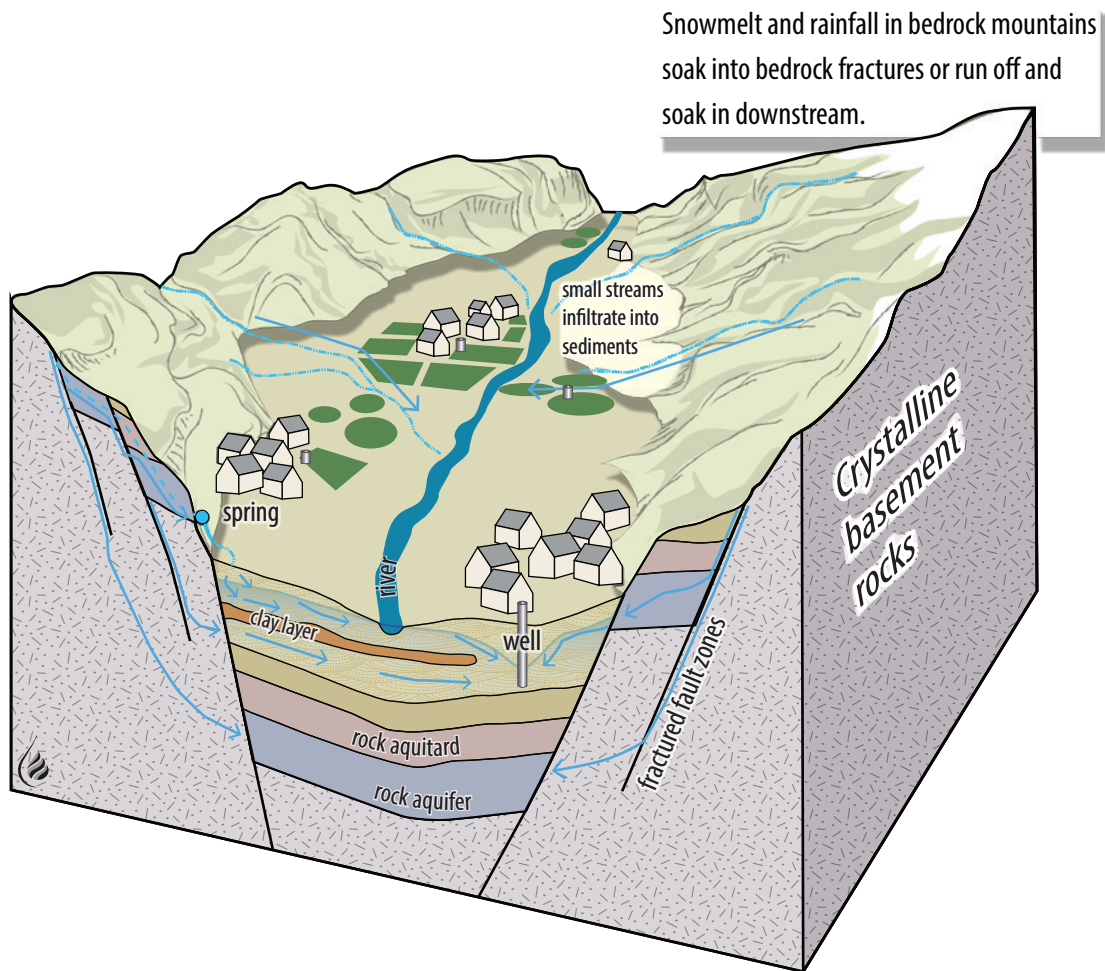
Figure 1.2. Conceptual model of a structural basin filled with sediments that compose a layered aquifer system. The shallow alluvial aquifer—the shallowest aquifer shown—is hydrologically connected to the river at the valley bottom. In this scenario, a sedimentary rock aquitard inhibits groundwater flow between the alluvial aquifer and the deep sedimentary rock aquifer.

The amount of water stored and the length of time it is stored depend on the size of the aquifer (its width and thickness), the volume of pore spaces in the aquifer (its porosity), and its permeability—a measure of the ability of water to move through pore spaces in aquifer material. Permeability in unconsolidated sediments is generally related to grain size. Water moves quickly in gravel and coarse sand, which are characterized by high permeability. Low-permeability sediments include smaller grains such as silt or clay.

These alluvial aquifers provide convenient, shallow access to good-quality groundwater with low concentrations of dissolved minerals. However, shallow aquifer systems are susceptible to contamination from the surface. Many shallow alluvial aquifers are quite thin, limiting the amount of water they can store. Significant amounts of clay are present in some shallow alluvial aquifers, which decreases the permeability or ability of water to move through pore spaces. Therefore, it is important to characterize shallow alluvial aquifers to the extent possible to evaluate them as potential water supplies for communities under current and future climate conditions.

Deep Aquifer Systems

While the majority of wells registered with the New Mexico Office of the State Engineer (NMOSE) in the study area produce water from shallow alluvial aquifers, some wells in all three community study areas produce water from older rocks that underlie the alluvial aquifer. While data are scarce, it appears that many wells produce good-quality water from the deep aquifer systems. However, as discussed in detail below, some water produced from deeper aquifers is
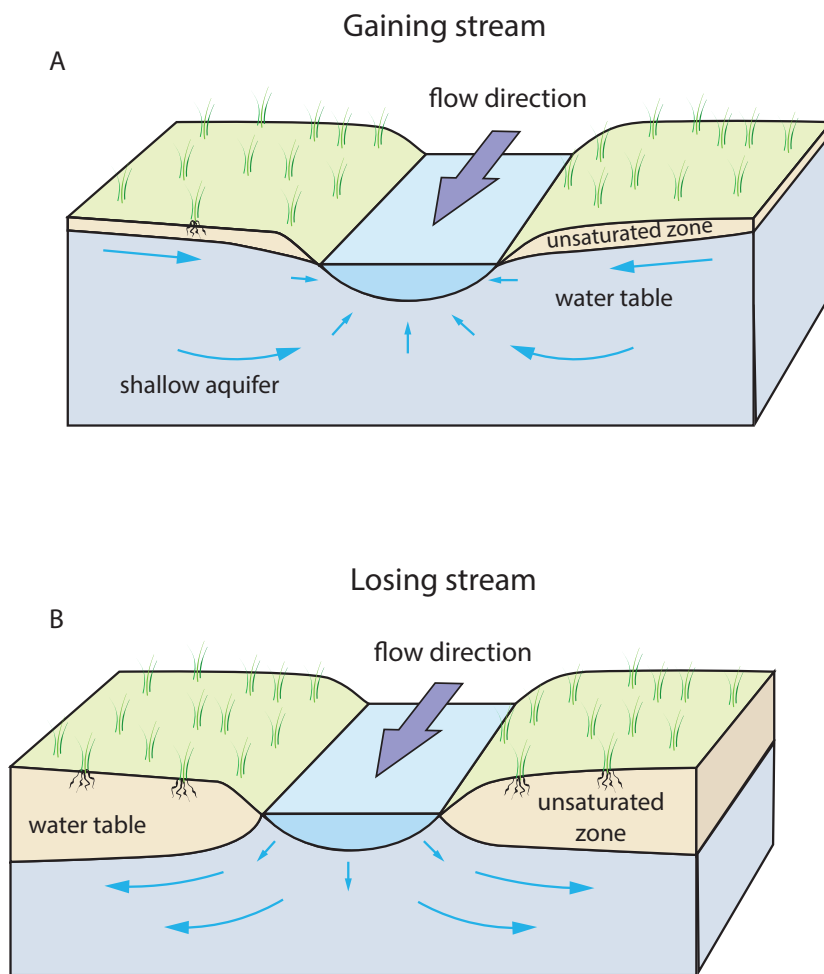
Figure 1.3. Diagrams illustrating interactions between the shallow aquifer and a stream. (A) For a gaining stream, groundwater discharges to the stream. (B) For a losing stream, water from the stream recharges the shallow alluvial aquifer. Modified from Winter et al. (1998).

of very poor quality, with high total dissolved solids (TDS) concentrations and high levels of inorganic contaminants such as arsenic and uranium. Initial examination of the deep aquifer system in all three community study areas suggests that these complex systems may reflect mixing of water from unique sources or different depths. Such mixing may be facilitated by upwelling of water in fault or fracture zones in cemented sedimentary rocks or crystalline rocks. Alternatively, faults may juxtapose different rock layers in less consolidated strata. If the fault zone is incompletely sealed by fault-zone clay gouge or fault-zone cementation, groundwater may flow between permeable stratigraphic layers across the fault. Water in these deeper formations is typically much older than water in the shallow aquifers and has had more time to dissolve minerals from the host rock into the aquifer and to interact with these minerals. Much more research is needed to understand these deep hydrologic systems before we can evaluate these aquifers as potential community water supplies.

Regional Geologic Differences

The following discussion about regional geology is very general and points out important geologic differences among regions. A more detailed geologic description of the different aquifers in this study is presented in subsequent chapters. The regional geologic framework, including lithology and structural geometry, greatly influences many hydrogeologic parameters, such as groundwater flow direction, velocity, and residence time, which strongly affect groundwater chemistry. The communities of El Rito, Abiquiu, Medanales (together referred to as the Abiquiu Valley), and Dixon are located in the Española Basin (Fig. 1.1), one of the major Rio Grande rift basins. For these communities, the deep aquifer system is primarily composed of Santa Fe Group rocks, which are generally sandstones, siltstones, and clay deposited between 27 and 10 million years ago by paleodrainages flowing to the south-southwest and south-southeast (Ekas et al., 1984; Ingersoll et al., 1990; Smith, 2004; Koning et al., 2011a, 2011b). While the rocks just below the shallow alluvial aquifer are largely Santa Fe Group rocks for both the Abiquiu Valley and the Dixon area, the underlying geology is very different between these two areas. Rocks underlying the Santa Fe Group in the Abiquiu Valley include a thick (up to 500 m [1,640 ft]) sequence of older sedimentary

rocks (sandstones, siltstones, and limestones), ranging in age from about 300 to 27 million years old. These older sedimentary rocks overlie Proterozoic granites and schist, which are 1.7 to 1.4 billion years old and usually do not make good aquifers. In contrast, in the Dixon area, these Proterozoic rocks are located directly beneath Santa Fe Group rocks and are less than 200 m (656 ft) below the surface. The shallow occurrence of Proterozoic rocks in this area is due to ancient tectonic uplift that occurred east of Abiquiu 70 to 50 million years ago, which eroded away 300- to 17-million-year-old strata between the Santa Fe Group and Proterozoic rocks.

Although Chama is also located in the Rio Chama watershed, which drains water into the Rio Grande, the geology in the area is not influenced by Rio Grande rift faulting and deposition (i.e., Santa Fe Group rocks are not present). Rather, surficial rocks at higher elevations and rocks underlying the shallow alluvial aquifer in valley bottoms include shales, sandstones, and siltstones that range in age from 250 to 90 million years old. These geologic differences have implications for finding potentially new groundwater sources in these areas.

METHODS AND DATA DESCRIPTIONS

To achieve the study objectives stated above, we initially compiled existing groundwater, well, and surface water data, including well locations, groundwater levels, and water quality. Well records from NMOSE were filtered to include only wells with an estimated depth-to-water measurement at the time the wells were drilled. In addition, we measured depth to water in 91 wells and collected water samples from 65 wells in the study regions (Fig. 1.4). These water samples were analyzed for different parameters, including general chemistry, trace metals, stable isotopes, and bacteria. A subset of samples was analyzed for carbon-14 and tritium to estimate the age of the water.

Groundwater Levels

Groundwater levels are the primary datasets for hydrologic research. Measurements of groundwater levels are made in wells, usually as the depth to water or the distance between the ground surface and the top of the water surface in the well.
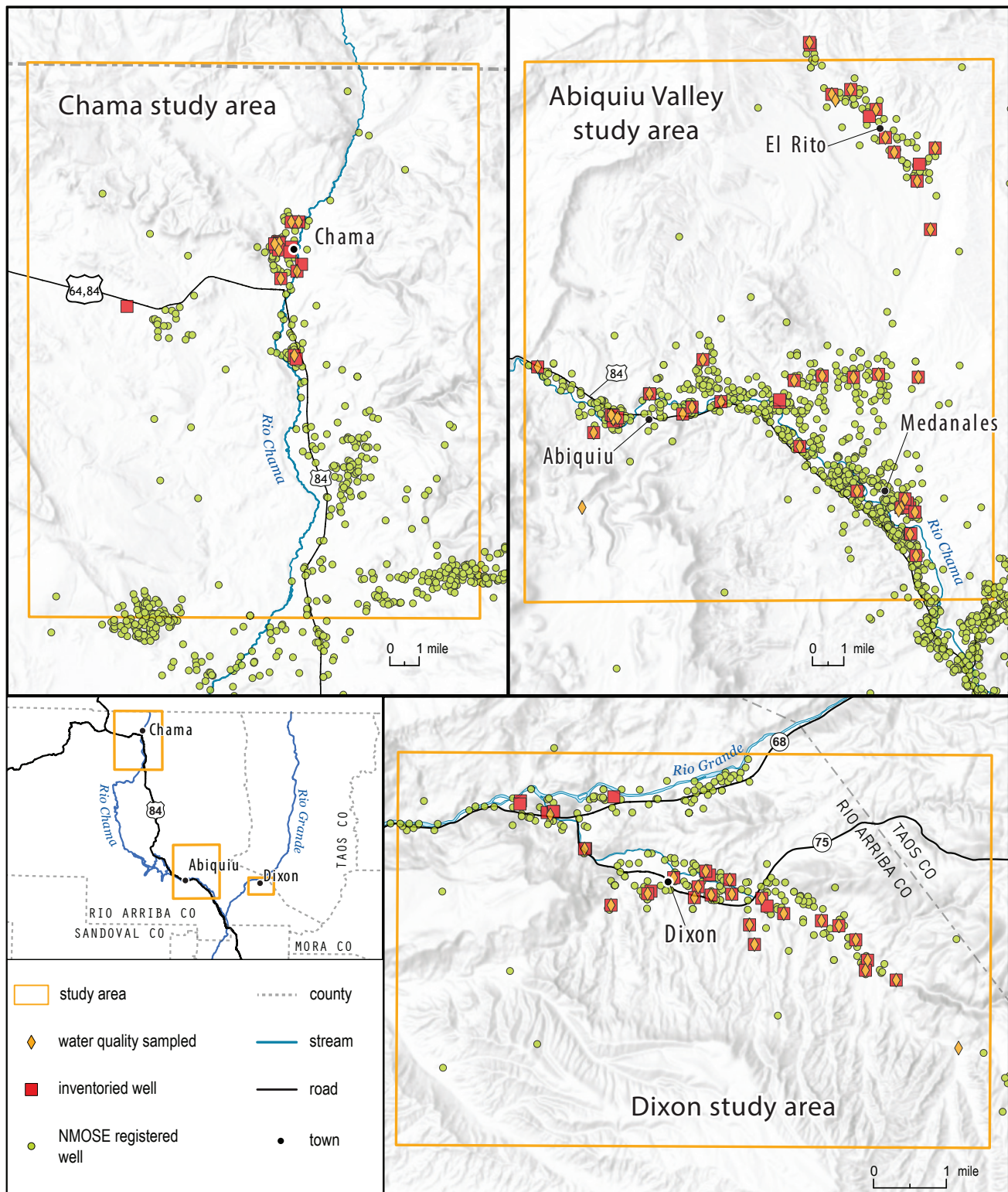
Figure 1.4. Important data in this investigation are depth-to-water observations and borehole cutting descriptions from wells registered with the New Mexico Office of the State Engineer (green dots). A subset of these wells was inventoried during this project for current depth-to-water measurements (red squares) and to collect chemistry samples (yellow diamonds).

Subtracting this distance from the surface elevation (extracted from SPADTM 4.5-m digital elevation model) yields the groundwater level elevation with respect to mean sea level. These data are very useful for evaluating hydraulic gradients and groundwater flow directions. In this study, depth-to-water measurements were very useful for determining whether a well was producing water from the shallow alluvial aquifer or the deep aquifer system. Many areas had enough depth-to-water data for the shallow alluvial aquifer to construct water-table maps, which are basically topographical maps of the surface of the shallow alluvial aquifer (the water table).

Data for the registered wells shown in Figure 1.4 were acquired from the NMOSE (2024) website (refer to Appendix C of this report). Data such as depth-to-water measurements and total well depth were extracted from drillers' notes and well records and were used to identify and characterize the shallow alluvial aquifer in the study area. Interpretations of these data are complicated by the fact that the depth-to-water measurements were taken at different times over the last 75 years. Additionally, the quality of the drillers' measurements is unknown. However, general spatial trends in depth to water can be observed and provide helpful information for delineating different aquifers. Also, in many areas, well density was high enough to evaluate the local water table, even with high uncertainties associated with the data. Water-table maps constructed from these data for these areas are presented in the following sections of this report. Assuming the total depth of a well is the bottom or effective floor of the aquifer, subtracting depth to water from total well depth yields the saturated thickness of the aquifer; this is the thickness of alluvial sediments that are saturated with water, meaning the pore spaces between grains are completely full of water. We present maps showing the spatial distribution of saturated thickness for the shallow alluvial aquifers in the three study areas.

As part of the inventory process, most depth-to-water measurements collected as part of this study were measured with a steel tape. We applied chalk on the first 6 m (20 ft) of the tape, which was washed off by the groundwater when the tape reached the surface of the water in the well. The distance between the water line in the chalk and the surface is the depth to water. Other data were also collected during inventory, including the GPS locations of the wells and the heights of well casings visible above ground.

Estimated Yield

Groundwater is extracted by a pump through a well. As a well is being pumped, the water level in the well goes down; this decrease in water level in the well during pumping is called drawdown. The rate of drawdown depends on aquifer permeability and pumping rate. For highly permeable sediments such as gravel, high pumping rates in the hundreds of gallons per minute (gpm) result in low drawdown rates because water easily moves through the large pore spaces in the gravel. However, in materials of low permeability such as siltstone or clayey sand, pumping rates as low as 1 to 2 gpm can result in very large drawdowns very quickly. The estimated yield, which is included in some well records, is a rough estimate by the drillers of the pumping rate at which drawdown will not cause the water level in the well to drop below the pump during extended periods of pumping. Estimated yields for wells in the different aquifer systems in the study areas are discussed below.

Water Chemistry

It is very important to test groundwater for dissolved constituents, both inorganic and organic, because some constituents (natural and anthropogenic) at certain concentrations may be harmful to human health. In addition, from a hydrogeologic perspective, the concentrations and relative distributions of dissolved minerals provide important information about what type of rocks the water has come in contact with along its flow path and possibly how long the water has been in the subsurface. For each study area, we present water chemistry data, with a focus on evaluating hydrogeochemical controls on water chemistry for the shallow and deep aquifer systems. Timmons et al. (2013) described the sampling methods we used in detail.

Water Quality and Drinking Water Standards

In each chapter of this report, we refer to two different drinking water standards established by the U.S. Environmental Protection Agency (EPA; 2024). The primary maximum contaminant levels (MCLs), as defined by the EPA, were established to protect against consumption of drinking water contaminants that present a risk to human health. Drinking water MCLs are legally enforceable standards that apply

to public water systems to protect public health. These standards are not enforceable for private wells. Secondary MCLs are an unenforceable guideline regarding cosmetic or aesthetic effects. While these contaminants do not pose a threat to health, if present at levels above the secondary MCL, these constituents may cause water to appear cloudy or colored or to taste or smell bad. Because these standards are not enforceable for domestic water sources, the following information is provided to inform readers about general groundwater quality in the communities of Rio Arriba County.

We tested all groundwater samples for the presence or absence of total coliform and *E. coli* bacteria. Total coliform is a group of bacteria present all around us, most of which are not dangerous to human health. However, these bacteria are not naturally present in groundwater and are an indication that more harmful organisms might be present. Fecal coliform and *E. coli* are subgroups within the total coliform group that primarily come from the feces of warm-blooded animals. The presence of *E. coli* indicates water has been exposed to feces and an immediate risk to human health exists.

Major Cations and Anions

Major ions include calcium (Ca^{2+}), magnesium (Mg^{2+}), sodium (Na^+), potassium (K^+), bicarbonate (HCO_3^-), chloride (Cl^-), and sulfate (SO_4^{2-}), and these constitute a large amount of the elements dissolved in groundwater. Positively charged ions are called cations and negatively charged ions are called anions. Precipitation at a recharge area infiltrates through the soil, where carbon dioxide partial pressures are high due to plant root respiration in the soil. This carbon dioxide slightly acidifies the water, which begins dissolving minerals in the soil and unsaturated zone as it percolates to the water table. Because calcium carbonate ($CaCO_3$) is a very common mineral and is quite soluble in water, young groundwaters usually have higher Ca^{2+} and HCO_3^- relative to other major ions that make up other minerals. As groundwater moves along a flow path, it continues to interact with the rocks that make up the aquifer. These interactions include continued dissolution of minerals, adsorption of ions to minerals, cation exchange, and mixing with other groundwaters of different chemical compositions. Over time, less-soluble minerals are dissolved and other geochemical reactions occur, resulting in the water chemistry evolving over time,

usually with higher TDS concentrations and different ion distributions. Older water, therefore, often looks very different chemically than it did when it started its journey in the recharge area hundreds or thousands of years prior.

A Piper diagram (Fig. 1.5) is used to characterize different water types based on relative concentrations of cations (Ca^{2+}, Mg^{2+}, Na^+, and K^+; left triangular graph) and anions (HCO_3^-, SO_4^{2-}, and Cl^-; right triangular graph). Piper diagrams allow us to define a water type based on the dominant cations and anions, as well as to identify trends that are indicative of different geochemical processes, such as dissolution of a specific rock type and mixing of different water sources. The example water chemistry data plotted on the Piper diagram in Figure 1.5 is characterized by the dominant cations of Na^+ and K^+ and the dominant anion of SO_4^{2-}. For all water samples discussed below, K^+ concentrations are much lower than Na^+ concentrations. Therefore, we do not consider K^+ and refer to the water type as sodium-sulfate (Na^+-SO_4^{2-}), with the dominant cation and anion being Na^+ and SO_4^{2-}, respectively. By projecting the position of the point from each triangular graph onto the diamond, water samples can be compared based on relative cation and anion concentrations.

Stable Isotopes

The stable isotopes of oxygen and hydrogen that make up the water molecule are useful tools for tracing the hydrologic cycle. The stable isotopes of hydrogen are H and ^2H (also called deuterium, denoted as D), and the stable isotopes of oxygen are ^{18}O and ^{16}O. The isotopic composition of a water sample refers to the ratio of the heavier isotopes to the lighter isotopes (R) for hydrogen (D/H) and oxygen (^{18}O/^{16}O). Because these stable isotopes are part of the water molecule, small variations in these ratios act as labels that allow tracking of waters with different stable isotopic signatures. All isotopic compositions in this report are presented as relative concentrations, or the per mil deviation of R of a sample from R of a standard, as shown in this equation:

$$\delta = \frac{R_{sample} - R_{standard}}{R_{standard}} * 1,000‰$$

It is useful to plot stable isotope data on a δD versus δ¹⁸O graph, as shown in Figure 1.6. In general, most precipitation plots on or near the global meteoric water line (GMWL) with a slope of 8 and a deuterium excess (y-intercept) of 10, as demonstrated by Craig (1961). However, the linear trend that characterizes local precipitation in a specific area may deviate from the global meteoric water line. This deviated trend usually has a similar slope but a different deuterium excess (y-intercept) and is referred to as a local meteoric water line (LMWL). Figure 1.6 includes local meteoric water lines that have been constructed for the Rocky Mountains and the Rio Hondo watershed in the Sangre de Cristo Mountains to the north of Taos (Tolley et al., 2015).

In the southwestern United States and New Mexico specifically, the stable isotopic composition of precipitation varies seasonally, with heavier isotopic values (fewer negative values that are closer to zero) during the summer monsoon season and lighter isotopic values during winter. This seasonal change in the average isotopic composition of precipitation is largely due to the large temperature
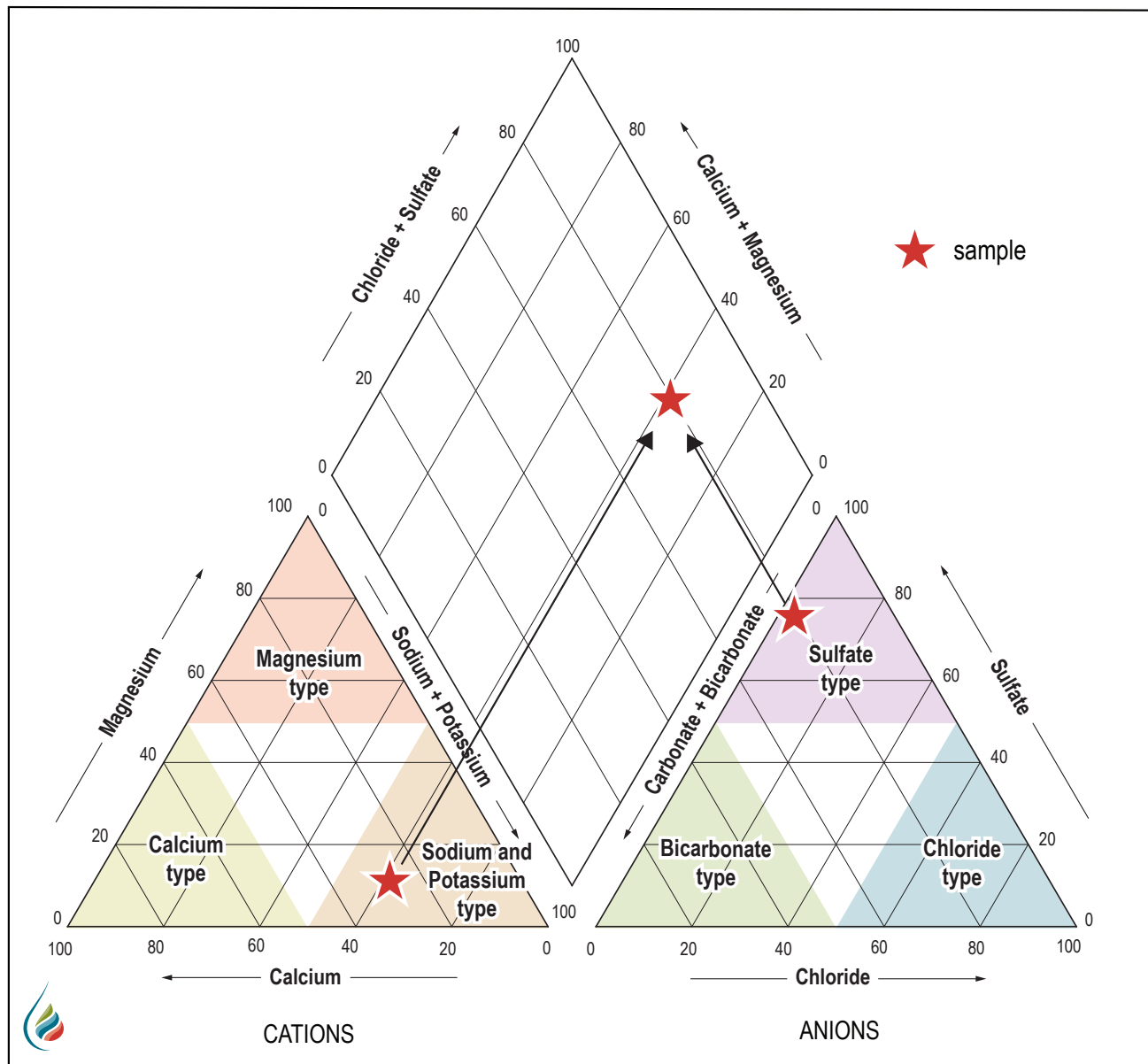
Figure 1.5. Example of how major ion data are plotted on a Piper diagram. The example point represents a water sample with the dominant cation and anion of Na^+ and SO_4^{2-}, respectively.

difference and the different sources of moisture (summer monsoons versus winter frontal storms). Figure 1.6 shows the range of typical values for summer precipitation (the orange oval) and winter and spring precipitation (the blue oval) defined for the Sangre de Cristo Mountains to the east and northeast by Tolley et al. (2015). Other researchers have observed similar ranges of isotopic compositions for summer and winter precipitation in other parts of the state (Johnson et al., 2002; Newton et al., 2012).

Stable isotopes of water can also be useful for identifying water that has undergone evaporation (Fig. 1.6). Isotopically lighter water molecules evaporate at a slightly higher rate than isotopically heavier water molecules, resulting in isotopic

fractionation; this causes the residual water to become isotopically heavier and evolve along an evaporation line that deviates from the local meteoric water line with a slope between 4 and 6 (Dansgaard, 1964).

Groundwater Age Estimates

A subset of 25 water samples was tested for tritium (^{3}H) and carbon-14 (^{14}C), which are used to determine how old groundwater is or how long ago the sampled water recharged a local or regional aquifer in the recharge area. Measuring tritium concentrations in water allows us to identify young waters that are less than 50 years old. Carbon-14 is used to determine ages for much older water, on the order of hundreds of years to tens of thousands of
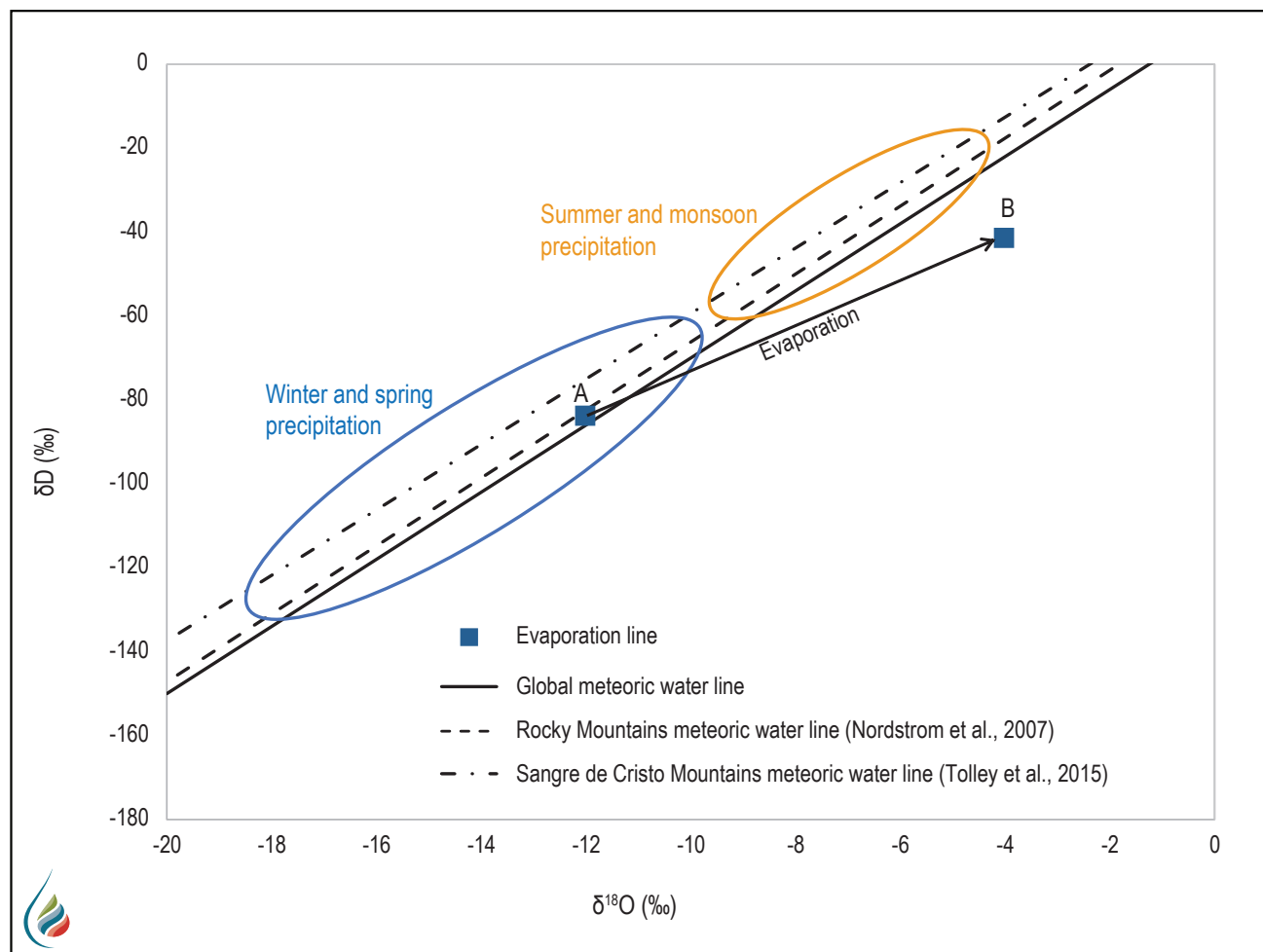
Figure 1.6. Example δD versus δ^{18}O graph with the global meteoric water line, different local meteoric water lines, and areas of expected isotopic composition for winter and summer precipitation. The arrow (an evaporation line) shows the linear path along which the isotopic composition of the residual water evolves during evaporation. A volume of water with the initial isotopic composition of point A on the line A–B evaporates under a set of conditions (relative humidity, temperature, wind speed, etc.). The volume of water decreases as evaporation continues, and the isotopic composition of the residual water evolves along an evaporation line such as the line A–B.

years. Below, we present background information about the different methodologies to help the reader better understand our interpretations of these data.

Tritium

Tritium (^{3}H), a radioactive isotope of hydrogen with a half-life of 12.4 years, is produced naturally in the atmosphere by cosmic radiation and enters the hydrologic cycle via precipitation as part of a water molecule. Tritium concentration is measured in tritium units (TU), where one TU indicates a tritium-to-hydrogen atomic ratio of 10^{-18}. The tritium content of precipitation varies spatially and temporally, with average values in the southwestern United States and Mexico ranging from 2 to 10 TU (Eastoe et al., 2011). Between 1991 and 2005, the tritium content of precipitation in Albuquerque, New Mexico, ranged from 4.5 to 19.1 TU, with an average of 8.8 TU (International Atomic Energy Agency, 2017). Newton et al. (2012) observed tritium concentrations in precipitation in the Sacramento Mountains in southern New Mexico to range from 3 to 10 TU. For groundwater samples collected over the last 20 years or so, the general interpretation of tritium in groundwater is (1) tritium concentrations between 5 and 10 TU represent modern water less than 10 years old; (2) tritium concentrations between 1 and 5 TU indicate a mixture of modern recharge and older, "tritium-dead" water over the past 50 years or so; and (3) groundwater with tritium concentrations of 1 TU or less indicates that most recharge is more than 50 years old.

Carbon-14

Atmospheric carbon dioxide gas, which has an approximate carbon-14 activity of 100 percent modern carbon (PMC; Clark and Fritz, 1997), is incorporated into the groundwater system (as bicarbonate, $H^{14}CO_3^-$) during infiltration of recharge through the vadose zone (the portion of the subsurface between the ground level and the water table). After infiltration crosses the water table, dissolved inorganic carbon (DIC) is isolated from modern carbon-14 input from the atmosphere and soil zone reservoirs. The carbon-14 decays with time as the water travels along a flow path in the aquifer system. As a result, the amount of carbon-14 measured in the groundwater along a flow path gives an age, or the approximate amount of time that has passed since the water recharged

the aquifer system. In general, lower PMC indicates older groundwater. However, to properly quantify groundwater age, it is usually necessary to correct the measured carbon-14 activity to account for hydrogeologic processes such as carbonate dissolution, isotopic exchange, and mixing of older and younger waters. These processes usually result in apparent (uncorrected) ages that are older than the actual age.

Carbon-13 for Dissolved Inorganic Carbon ($\delta^{13}C_{DIC}$)

The stable carbon isotopic composition for DIC in groundwater ($\delta^{13}C_{DIC}$) refers to the fraction R ($^{13}C/^{12}C$) for the dissolved carbon that is usually in the form of HCO_3^-. The $\delta^{13}C_{DIC}$ is primarily a function of the carbon isotopic composition of the soil carbon dioxide in the recharge area and the carbon isotopic composition of the carbonate rock that has been dissolved (Clark and Fritz, 1997). The $\delta^{13}C$ of soil carbon dioxide is very similar to that of the local vegetation, which is a function of the metabolic pathway by which carbon dioxide is converted to carbohydrates during photosynthesis. We used $\delta^{13}C_{DIC}$ to correct the carbon-14 dates for the dissolution of carbonate rocks, with an assumed $\delta^{13}C_{DIC} = 0$ per mil for some samples but not others, as discussed below.

OVERALL FINDINGS

Despite the differences in the hydrogeologic systems in the study areas, the results and, to a degree, the conclusions for the different areas were similar. The majority of registered wells in all areas are completed in shallow alluvial aquifers. All of these aquifers are limited in size, with lateral widths coinciding with modern valley bottom widths, ranging from tens of meters to 5 km (a few hundred feet to about 3 mi). Estimated saturated thicknesses for shallow alluvial aquifers are relatively thin, ranging from 5 to 30 m (16–100 ft). However, many registered wells produce water from the deep aquifer system. Some of these are located at slightly higher elevations and were drilled directly into older rocks; others are in valley bottoms, penetrating both the shallow alluvial aquifer and the deep aquifer system. Estimated yields for wells completed in shallow alluvial aquifers ranged from 5 to 30 gpm. Estimated yields for wells completed in the deep aquifer system ranged from 2 to 40 gpm. We sampled one well in the Chama area that was

completed in the deep aquifer system and is a flowing artesian well (in which natural pressure causes groundwater to move to the surface through the well).

Groundwater samples from the shallow alluvial aquifers in this study exhibited measurable tritium concentrations, indicating the presence of young, modern water less than 50 years old mixing with older, tritium-dead water. Groundwater samples from the deep aquifer systems all show essentially no tritium, with apparent carbon-14 ages of tens of thousands of years before present (YBP). Figure 1.7 shows the stable isotopic composition of all water samples plotted on a δD versus δ¹⁸O graph. All groundwater plots within the observed range of values for winter and spring precipitation. While the isotopic composition of groundwater is likely a mixture of winter and summer precipitation in the surrounding mountain ranges, the observed isotopic

compositions for groundwater indicate the winter recharge component is significantly higher than the summer recharge component.

Shallow alluvial aquifer waters are generally of good quality with very low TDS concentrations (<500 mg/L). However, several of these waters tested positive for total coliform, and a few tested positive for the presence of *E. coli*, demonstrating the susceptibility of the shallow alluvial aquifers to contamination from the surface. Many deep aquifer system waters and a few shallow aquifer system waters exhibited high arsenic concentrations that exceeded the primary MCL.

Major ion chemistry for groundwater samples from the three study areas shows similar trends. The Piper diagram in Figure 1.8 shows that most shallow aquifer system waters for all study areas exhibit a
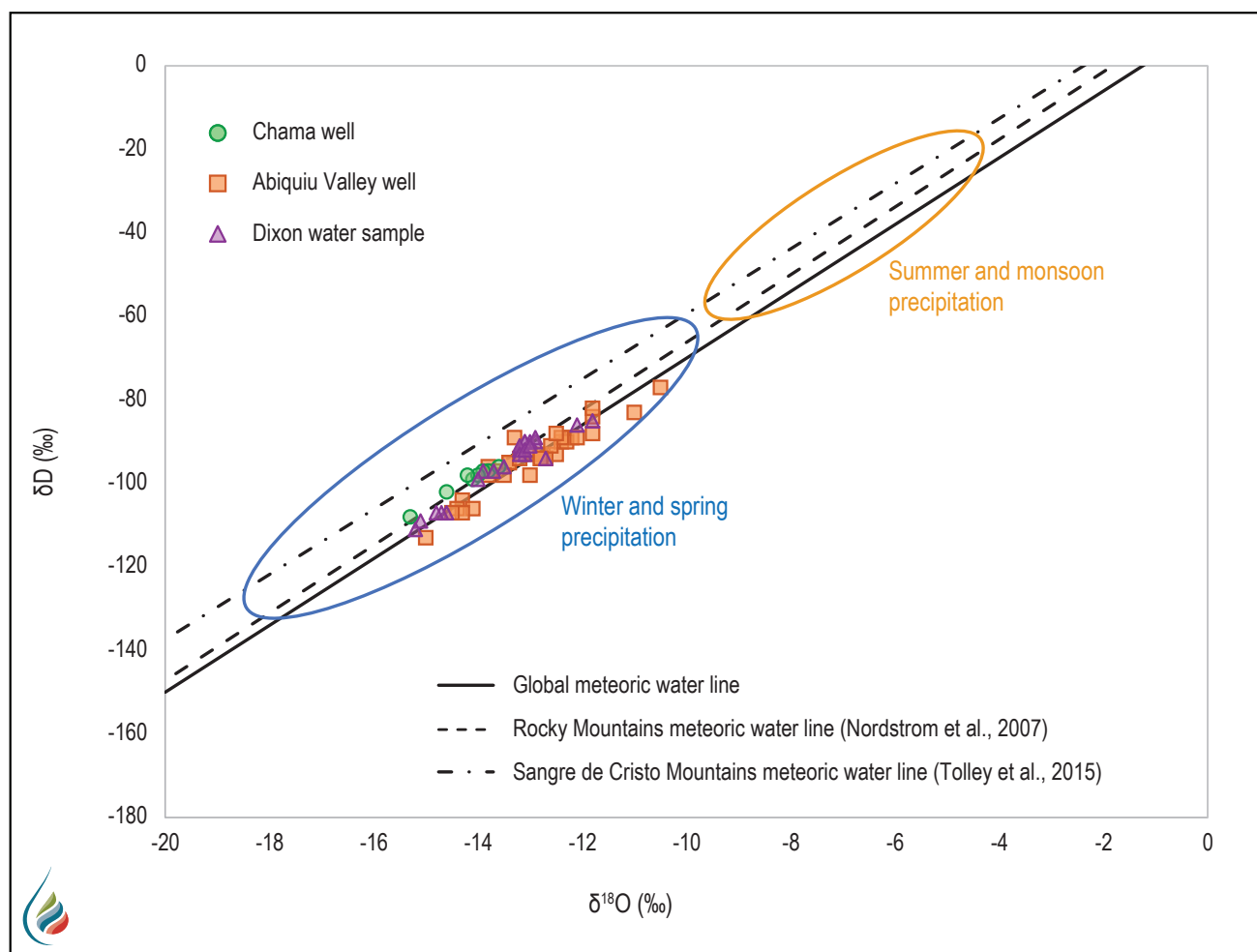
Figure 1.7. Stable isotope data for all groundwater samples collected for this study. The isotopic compositions for all samples plot within expected values for winter and spring precipitation as defined by Tolley et al. (2015) for the Sangre de Cristo Mountains.

calcium-bicarbonate (Ca^{2+}-HCO_3^-) water type (the blue dashed circle in the figure). This water type is consistent with the young ages observed for shallow aquifer system waters because calcium carbonate is a very common mineral and is quite soluble. For most of the deep aquifer system waters, sodium (Na^+) was the dominant cation (orange oval in the figure). The linear trend for the cations from calcium water type to sodium water type is commonly associated with a process called cation exchange. Cation exchange is a water/mineral interaction where Na^+ ions that are adsorbed to clay minerals exchange with Ca^{2+}

and Mg^{2+} ions that are dissolved in the groundwater. Because Ca^{2+} and Mg^{2+} have twice the charge of Na^+, for every one molecule of Ca^{2+} or Mg^{2+} that adsorbs to a mineral surface, two molecules of Na^+ are released into solution in the groundwater. This process is quite common, and evidence from this study indicates that all water samples have undergone cation exchange to some degree. However, there are several deep aquifer system waters in the Abiquiu Valley and the Dixon area that exhibit TDS concentrations less than 1,000 mg/L but have relative sodium concentrations greater than 95%
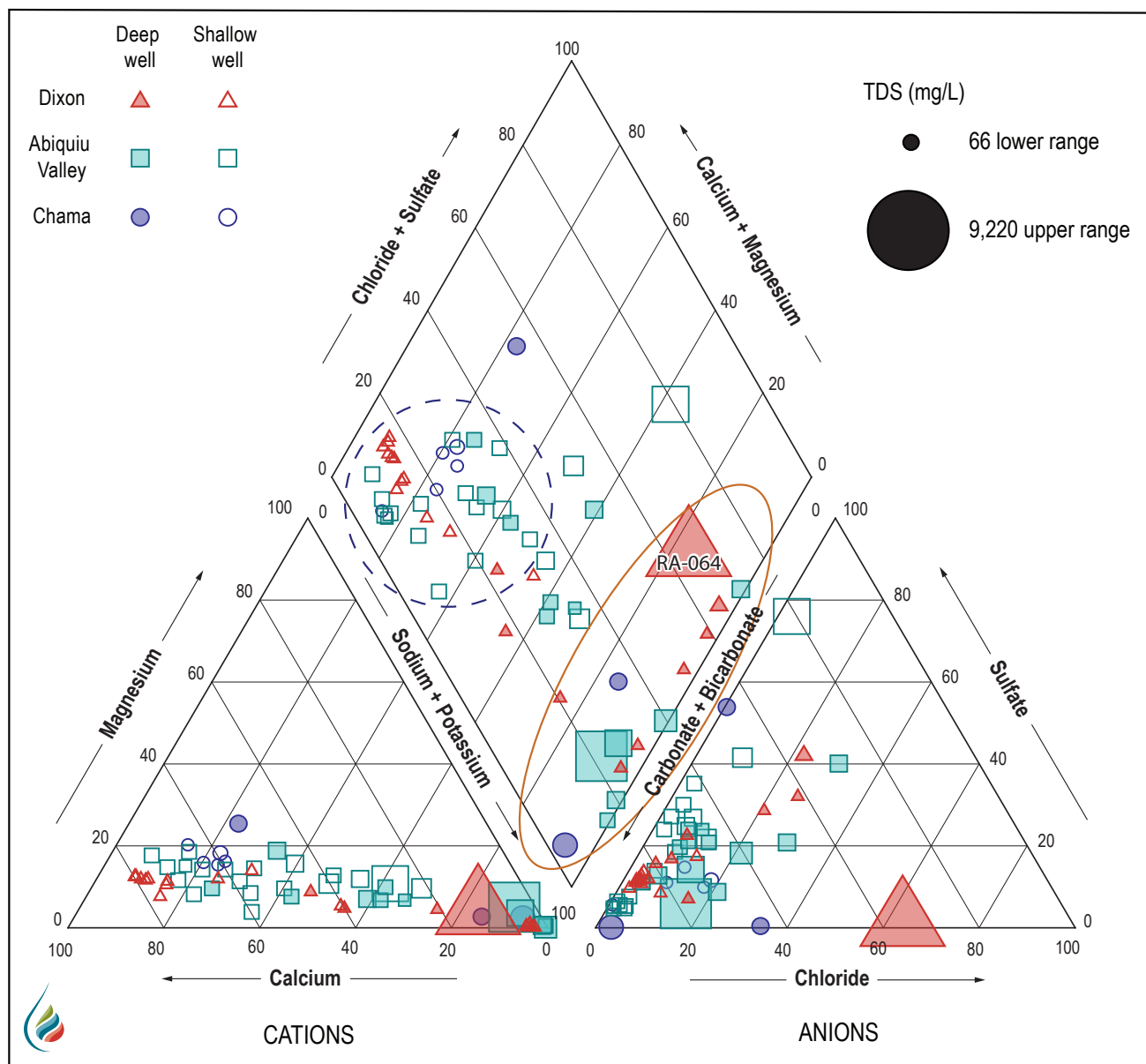
Figure 1.8. Major ion data for all groundwater samples collected for this study. Most shallow aquifer system waters exhibit calcium-bicarbonate (Ca^{2+}-HCO_3^-) water type (circled by a blue dashed line). Most deep aquifer system waters exhibit sodium (Na^+) water type, with relative sodium (Na^+) concentrations representing over 75% of total cations (orange oval). The size of the data points is proportional to the TDS concentration. Sample number RA-064 is highlighted.

of total cations. These waters show a variety of anion compositions; thus, these waters plot on the right bottom edge of the diamond portion of the Piper diagram (orange oval). These waters are produced from Santa Fe Group rocks, and they also exhibit high pH values (greater than 8.5). It is thought that abundant sodium and high pH are due to the dissolution of sodium feldspars from volcaniclastic sediments. In addition to water/mineral interactions such as cation exchange and mineral dissolution, our study results also show evidence of the mixing of waters from different sources. A few deep aquifer system waters with relatively high TDS concentrations appear to be mixing into the shallow system, likely by moving upward via faults and fractures, which are common in all the study areas.

FUTURE WORK

Early in this study, it became clear that limited geologic and hydrogeologic research has been done in this region compared with many other areas in the state. This lack of research is mainly due to groundwater use being a very small percentage of total water use (La Calandria Associates, Inc., 2006). However, with small communities depending on uncertain groundwater supplies, it is necessary to conduct continuing geologic and hydrogeologic research in Rio Arriba County. It is largely recognized by researchers and water managers that the shallow alluvial aquifers in these regions are greatly limited as long-term community water supplies. Their areal extent and thicknesses are relatively small. However, water quality in the shallow aquifer systems tends to be very good, with low TDS concentrations. Further research on these shallow alluvial aquifers may identify specific areas within the shallow alluvium that would be more suitable community water sources.

We highly recommend continued research to thoroughly assess both the shallow and deep aquifer systems in these study areas for sufficiency as water sources. Future work over the next two years should focus on the following activities:

- Groundwater level monitoring
  - o Identify specific aquifers to be monitored
  - o Identify current wells or install new long-term monitoring wells
  - o Install instrumentation

- Regional and local geology
  - o Critically review existing geological data
  - o Identify specific data gaps
  - o Develop recommendations on how to fill those data gaps
- Deep groundwater resources
  - o Collect additional samples
  - o Conduct geochemical analyses

Monitoring groundwater levels is very important. Continuous water level measurements in wells provide important information about aquifers. Fluctuations in groundwater levels and how these fluctuations correlate to changes in river flow rates, precipitation events, and droughts can help us understand recharge and discharge processes, as well as how climate change may be affecting the local and regional groundwater systems. Continuous water level data allow water planners to forecast possible crises resulting from a quickly decreasing water table during a short-term or long-term drought. We recommend installing data loggers in several wells that tap both the shallow and deep aquifer systems within these communities.

Much geological research remains to be done in these areas, especially in the northern part of the Rio Chama watershed near Chama. The geologic map of the 15-minute Chama quadrangle (Muehlberger, 1967) needs to be updated to be more consistent with our current understanding of the geology of the southwestern United States. Geological work ranging from regional geophysical surveys to local-scale mapping would further our understanding of the local and regional hydrogeology. Shallow geophysical surveys may allow for quantification of water in the shallow alluvial aquifer system, and deeper geophysical surveys can help identify deep water sources of different salinities. By collecting water samples for water chemistry analyses from wells that tap the deep aquifer throughout the Rio Chama watershed, we may be able to locate alternative groundwater sources for some of these communities. The next three chapters present specific future work suggestions for each study area.

Rio Chama at Chama, New Mexico, in June 2024 at approximately 250 cfs. *Photo by Talon Newton*

CHAPTER 2: ASSESSMENT OF GROUNDWATER RESOURCES FOR CHAMA, NEW MEXICO

STUDY AREA

The extent of the study area that focused on the Chama region is shown in Figure 2.1. The village of Chama is situated in the southern Rocky Mountains near the New Mexico/Colorado border and was home to 917 people in 2020 (U.S. Census Bureau, 2024).

The Rio Chama's surface water supplies irrigation water for local farmers and ranchers through an acequia system (community irrigation ditches) that has been in use for hundreds of years. Currently, Chama residents rely solely on the Chama Water System, which is operated by the Village of Chama, to divert surface water from the Rio Chama for up to approximately 1,600 residents. The Chama Water System includes four storage tanks and a treatment plant.

The Chama Water System has had issues with turbidity in public water supplies, leading to boil water advisories in 2020 and 2023 (New Mexico Environment Department, 2024). Past efforts to supplement the community water supply with groundwater have not been successful, largely due to groundwater quality issues such as high arsenic concentrations. Finding a reliable groundwater source is important to build a sustainable water supply for this community, complement surface water supplies, and help eliminate the potential for water outages.

Local Geology

Chama, New Mexico, lies in the north-central portion of Rio Arriba County and represents the northernmost site in this regional assessment. Chama lies well outside the Española Basin, with geology distinct from that of the other study areas. Figure 2.2 shows the geologic map of the 15-minute Chama quadrangle (Muehlberger, 1967), which focuses on the area surrounding the community

of Chama. The village of Chama mainly sits on Quaternary terrace deposits, labeled Qtg, Qtk, and Qtb; these are the units in which most domestic wells are currently completed. Exposed rocks above the terrace deposits include young landslide deposits (Ql) and Cretaceous rocks, including the Mesaverde Group (Kmv) to the west, as well as various members of the Mancos Shale, including (from youngest to oldest) the Niobrara (Kn), Carlile (Kcl), Greenhorn Limestone (Kgr), and Graneros Shale (Kg). East of Chama, the oldest Cretaceous rock in the area, Dakota Sandstone (Kd), is exposed at the surface.

A north-south geologic cross section (Fig. 2.3) through the village of Chama was developed using data from NMOSE water-well drillers' logs, information from six oil wells, and unit thickness measurements from Muehlberger (1967). Three buried faults underlie Chama, which is located on a horst block that brings fractured sandstones of the Dakota Formation closer to the surface. Most wells in the vicinity of Chama that are not completed in the shallow alluvium (and not shown in the cross section) penetrate Mancos Shale, and a few penetrate the top of the Dakota. In general, these wells produce good-quality water, but high arsenic concentrations are sometimes observed. The following discussion will briefly cover pre-Cretaceous geologic units, followed by a more detailed description of Cretaceous rocks and overlying Cenozoic sediments. While a small amount of water from the pre-Cretaceous units may be moving upward into shallower formations along faults and fractures, we focus more on the shallow geology because almost all wells in the study area are completed in Cenozoic sediments and underlying Cretaceous rocks. The following descriptions of geologic units are largely based on those of Muehlberger (1967).
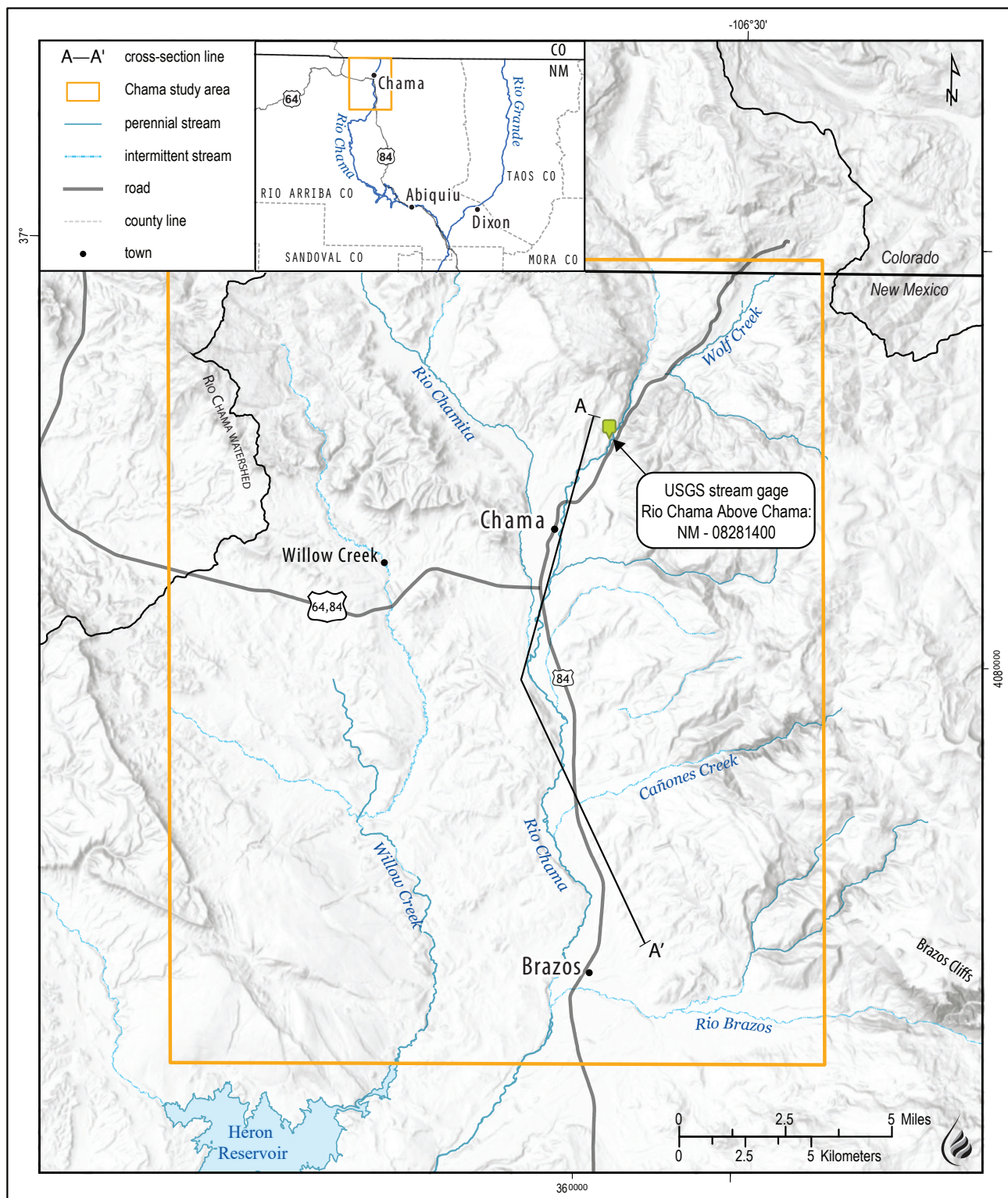
Figure 2.1. Study area boundary for Chama region. The location of the cross section shown in Figure 2.3, indicated by the line A–A′, is shown here.
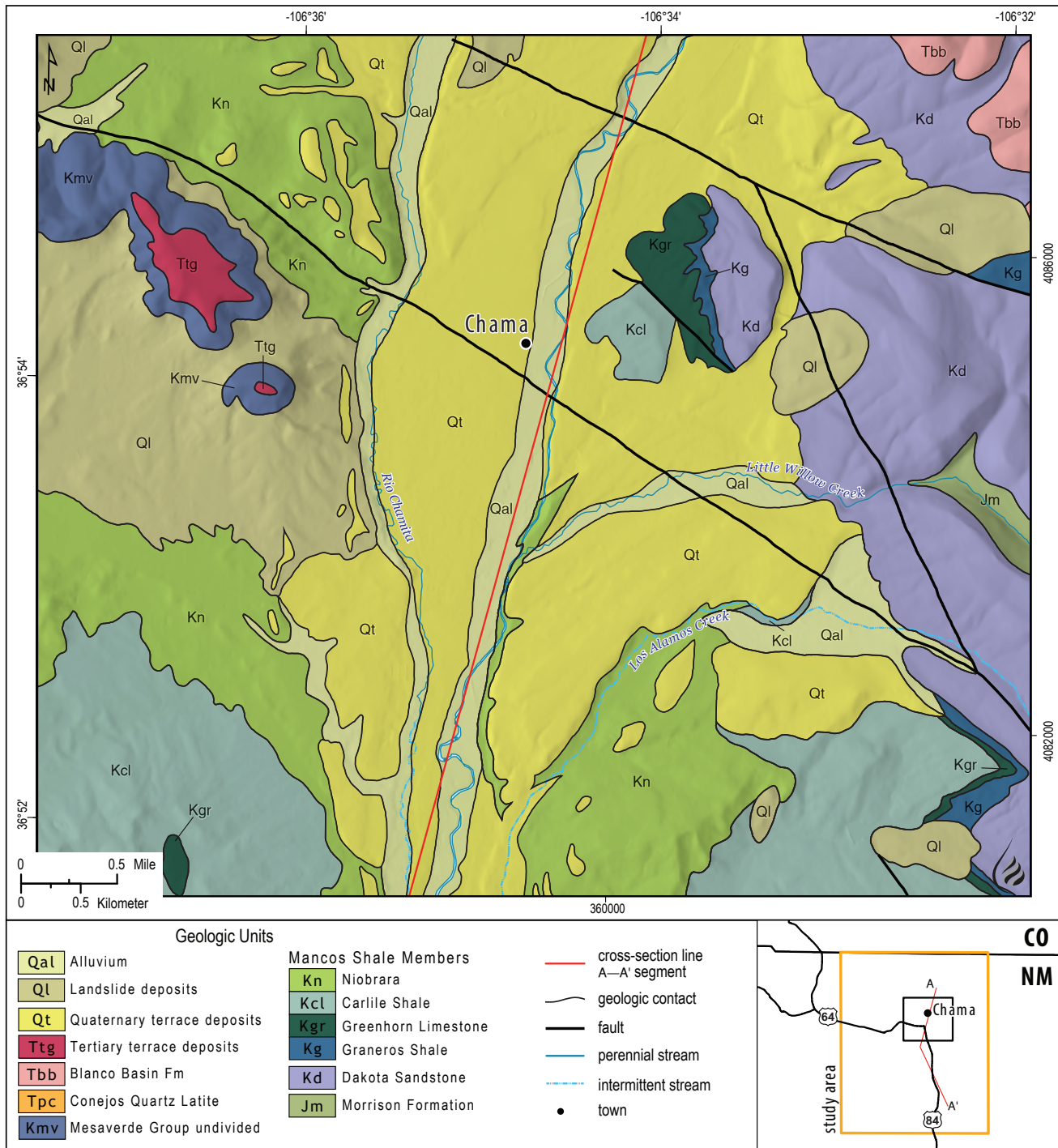
Figure 2.2. Geologic map of the 15-minute Chama quadrangle (Muehlberger, 1967), focused on the community of Chama. A partial cross-section line A–A´ is shown here; see Figure 2.1 for full cross-section line. For geologic maps, the area covered is denoted by the small black square shown on the inset map.
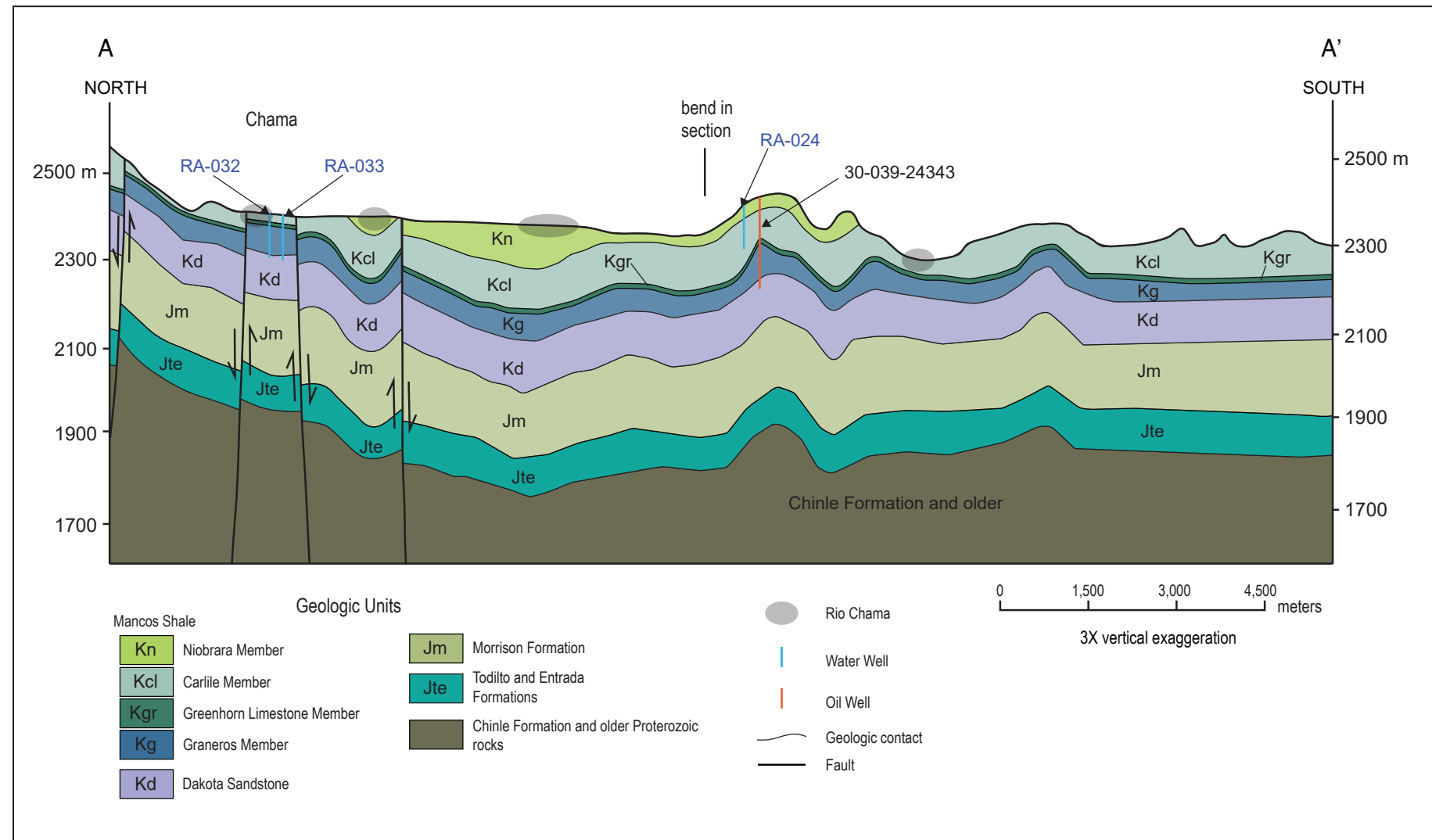
Figure 2.3. North-south geologic cross section (3x vertical exaggeration). The three deep wells sampled are shown.

Pre-Cretaceous Units

In the area immediately around Chama, these older, pre-Cretaceous rocks are at least 150 m (500 ft) below the surface. The basement rock is Precambrian Kiawa Mountain Formation, which is a massive quartzite that crops out in the Tusas Mountains southeast of Chama. Unconformably overlying the Kiawa Mountain Formation is the Triassic Chinle Formation, which is predominantly siltstones and thin sandstones of fluvial origin; this unit is generally an aquitard. Above the Chinle lies a stack of Jurassic sedimentary rocks consisting of (from oldest to youngest) the Entrada, Todilto, and Morrison Formations. The Entrada and Todilto Formations are grouped and are the oldest unit shown in the cross section (Fig. 2.3). The Entrada is a massive, cliff-forming sandstone that has significant outcrops in the area, while the overlying gypsum-bearing Todilto sediments are thin and discontinuous in the Chama area. The upper Jurassic in this area is represented by the Morrison Formation. The Morrison Formation is a very thick unit, predominantly consisting of interbedded sandstones and mudstones.

Cretaceous Units

The Dakota Formation makes up the base of the Cretaceous units in the Chama area. The Dakota Formation is a moderately thick (about 60–120 m [200–400 ft]) stack of massive sandstones with alternating mudstone members that have significant surface exposures to the east of Chama. The component sandstone units are fine grained, well sorted, and moderately rounded, but they exhibit silica cementation. The rounding and sorting of the Dakota Sandstone units could make them suitable aquifer units; however, the silica cementation could impact the permeability of these intervals. Research by Muehlberger (1967) suggested the Dakota unconformably overlies the Precambrian basement in the Tusas Mountains. The uppermost sandstone unit of the Dakota grades up into the Graneros Shale, which is the lowermost unit of the overlying Mancos Shale.

The Mancos Shale is composed of several member units that are designated differently by different researchers. Here, we use the member designation of Graneros, Greenhorn Limestone, Carlile, and Niobrara. The Graneros and Carlile are predominantly thick-bedded, fine-grained sequences of muddy to silty sediments, and the Niobrara is shaly with a calcareous interval. Septarian calcareous concretions are common in the shale units of the Mancos and are often more than 0.3 m (1 ft) thick and around 1 to 1.5 m (3–5 ft) in diameter. The Greenhorn Limestone is distinct from adjacent shales and consists of about 9 to 20 m (30–70 ft) of interbedded shales and heavily fractured limestones that lie between the underlying Graneros and overlying Carlile units (Muehlberger, 1967; Ridgley and Hatch, 2013). The Carlile Shale hosts a member unit known as the Juana Lopez Member, which consists of interbedded shale, calcarenite, and sandstone (Muehlberger, 1967; Molenaar, 1977). Taken all together, the Mancos Shale is predominantly fine-grained deposits, with multiple sandstone or limestone intervals. Very little has been reported about the degree of cementation in the sandstone members, but the thin fractured limestone interval of the Greenhorn appears to have permeability.

Above the Mancos lies the Mesaverde Group, which is typically divisible into the Point Lookout Sandstone, Menefee Formation, and Cliff House Sandstone. These units are exposed at the surface to the west of Chama (Fig. 2.2) and thus are not aquifers beneath the village of Chama. This unit is likely to be in the subsurface to the west and northwest of Chama. In the Chama area, these units are difficult to distinguish and were referred to by Muehlberger (1967) as the Mesaverde Group, undivided. Outcrops of the Mesaverde Group exhibit massive, cliff-forming beds composed of poorly sorted, very fine to fine sandstones. Small-scale apparent channel deposits occur in the upper part of the group and are less cemented than adjacent rocks. A thin shale unit (likely discontinuous in the area) can be used to distinguish the lower and upper sandstone units of the group. The upper sandstones are very fine to fine grained and are quite well cemented. The Mesaverde Group as a whole is predominantly sandy, without extensive silt or finer units, and is generally coarser grained than the adjacent stratigraphic units (Muehlberger, 1967). Other researchers variously report calcite, iron oxide, and clay cementation in the Mesaverde (Craigg, 2001), which could inhibit permeability.

The Lewis Shale, which is exposed just west of the map area in Figure 2.2, defines the top of the Cretaceous sediments in the Chama area. Like the upper Mancos, the Lewis Shale is a thick sequence of dark-gray shale with septarian calcareous concretions (Muehlberger, 1967). The basal contact of the Lewis

Shale with the Mesaverde Group is a gradational contact, and the top contact with the Tertiary sequence is an erosional unconformity.

Cenozoic Units

The Eocene Blanco Basin Formation is a conglomeratic sandstone interbedded with sandstone and siltstone composed of detritus shed from the Tusas Mountains during Laramide uplift and erosion (Brister, 1992). This rock unit is exposed in cliffs well above the elevation of the village of Chama and thus is not an important component of the hydrogeologic story. However, volcanic rocks of the San Juan volcanic field that were deposited on the Blanco Basin Formation—the andesitic Conejos Formation and the ash-flow tuffs in the Treasure Mountain Group exposed in Colorado in the upper watershed of the Rio Chama—have contributed detritus incorporated into the sediments that form the shallow aquifer. The volcanic component in the terrace and landslide deposits has influenced the water quality in Chama, as described in a later section.

Tertiary terrace deposits in the Chama area are remnants of erosion by the paleo Chama River and consist mainly of coarse sands to boulders originating from stratigraphically nearby units down to the Mesaverde Group. The terrace gravels, which likely represent two erosional surfaces, tend to cap modern ridges. Younger (Quaternary) terrace gravels lie topographically much closer to modern drainage levels than do the Tertiary deposits, with the youngest of these gravels underlying the village of Chama to a thickness of less than 10.5 m (35 ft). Quaternary glacial deposits exist northeast of the village of Chama but are not extensive, whereas Quaternary landslide deposits are at the surface near Chama and are far more extensive at the surface than the glacial sediments. The young age and coarse clast sizes in the Tertiary and Quaternary gravels suggest high permeability in these deposits.

Local Hydrogeology

The climate in the Chama area can be characterized by large seasonal fluctuations in temperature from winter to summer (Western Regional Climate Center, 2024). Minimum daily temperatures can approach -14.2°C (6.4°F) in December and January. Summer temperatures are warm, reaching about 30°C (about 90°F) in July and August. Average annual temperatures decrease with elevation, and it is therefore much cooler in the adjacent mountains to the north and east. Annual precipitation in Chama averages 548 mm (21.3 in.), with approximately 40% of annual precipitation supplied by summer monsoons between July and October. Average annual precipitation increases with elevation, and it is much wetter in the adjacent mountains to the north and east.

Chama is located in a relatively wide-open area within the Rio Chama valley. The Rio Chamita is to the west of the village of Chama and feeds into the Rio Chama south of town. The Rio Chama drains both groundwater and surface water from the San Juan Mountains to the north. Discharge rates in the Rio Chama vary seasonally, with the highest flow rates resulting from runoff in the late spring and early summer months (Fig. 2.4). In late summer, the monsoons increase discharge rates in the Rio Chama.

Most wells in the Chama area are completed in the shallow alluvial aquifer, which is composed of a relatively thin layer of young gravel terrace deposits. The shallow alluvial aquifer is hydrologically connected to the river, providing base flow to the Rio Chama. Groundwater in the shallow aquifer likely originates as precipitation and snowmelt from the mountains to the north and east. Several wells in the area are drilled to depths between 76 and 107 m (250 and 350 ft) below the surface and appear to penetrate the upper part of the Cretaceous-aged Dakota Formation.

DATA ASSESSMENT

Figure 2.5 shows registered wells that included depth-to-water estimates in the well records. While existing water chemistry data for groundwater are scarce, some data are available for the Chama Water System (Rio Chama) and the well called RA-026 in this study (Table 2.1). The data source is Drinking Water Watch (New Mexico Environment Department, 2024). These data are included in the analyses below. We also extracted water chemistry data from the U.S. Geological Survey (USGS) that included cation (Ca^{2+}, Mg^{2+}, Na^+, K^+) concentrations for the Rio Chama near La Puente between the years 2000 and 2010. These data are available in the appendices of this report, which are available for download at https://geoinfo.nmt.edu/publications/openfile/details.cfml?Volume=630
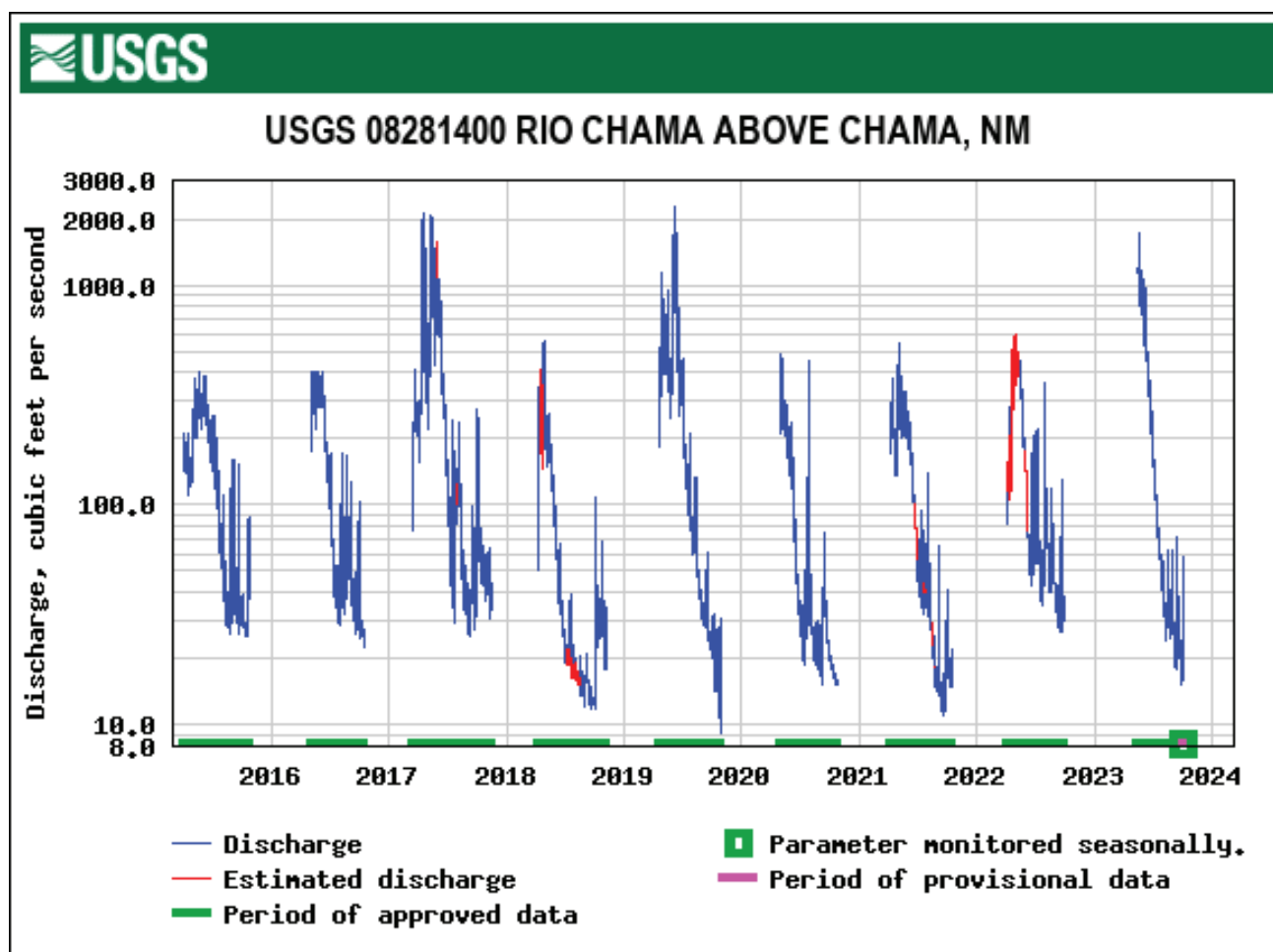
Figure 2.4. Hydrograph for the Rio Chama above the village of Chama. See Figure 1.1 for gage location.

Table 2.1. Existing water chemistry data for RA-026 and the Rio Chama Community System (NM3501021), retrieved from Drinking Water Watch (New Mexico Environment Department, 2024). The groundwater (GW) sample type refers to existing chemistry data for water produced from the RA-026 well that was also sampled for this study. The surface water (SW) sample type refers to previously analyzed water samples from the Chama Mutual Domestic Water Consumers Association, which diverts water from the Rio Chama.

Water system number	Sample type	Date	Calcium (Ca^{2+}) (mg/L)	Magnesium (Mg^{2+}) (mg/L)	Sodium (Na^+) (mg/L)	Potassium (K^+) (mg/L)	Bicarbonate (HCO_3^-) (mg/L)	Chloride (Cl^-) (mg/L)	Sulfate (SO_4^{2-}) (mg/L)	Total dissolved solids (mg/L)
NM3503821	GW	10/08/2008	110	28	80	11	240	15	350	780
NM3501021	SW	04/08/1997	29.3	3.1	13.9	2.1	96.4	13	23	
NM3501021	SW	12/30/1998	18.3	2.97	5	5	62.6	<10	11.7	158
NM3501021	SW	06/22/1999	8.07	1.26	5	5	21.2	<10	<10	126
NM3501021	SW	08/14/2001	15.1	2	3.8	2.5	51.9	0.5	14	
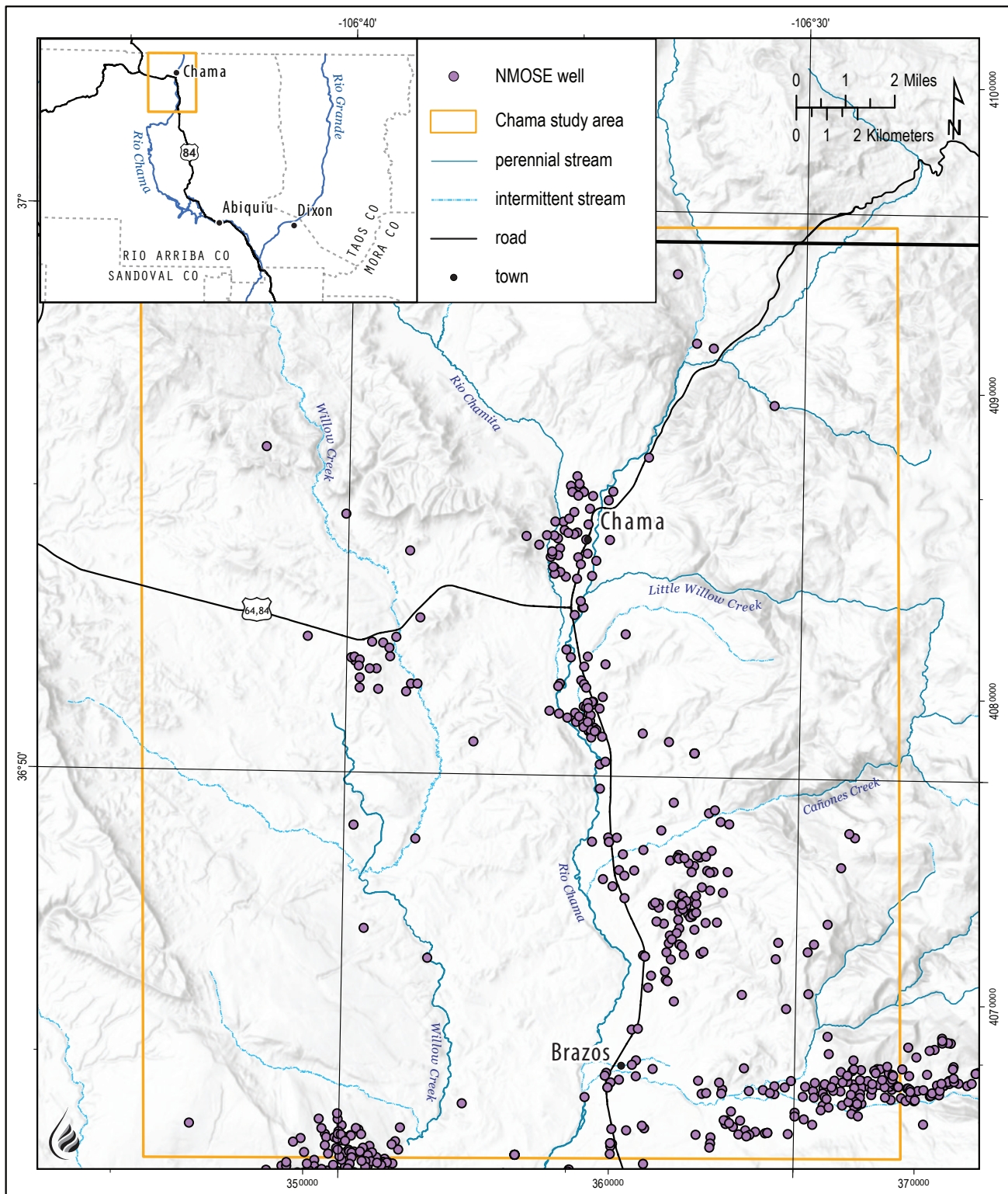
Figure 2.5. Registered wells in the study area with depth-to-water measurements included in the well record.

As part of this study, we inventoried 16 existing wells in the Chama area. This entailed documenting well location and condition, assigning a unique well ID number for the project (RA-###), and collecting a measurement of the static depth to water in the well. Of the 16 wells inventoried, we sampled eight for water quality parameters (Fig. 2.6). Criteria for water quality site selection included maximized well coverage over the study area, accessibility, the ability of the well to be sampled, and the goal to sample wells completed in both shallow and deep aquifer systems. All samples were analyzed for general chemistry (major cations and anions), trace metals, the presence of bacteria, and the stable oxygen and hydrogen isotopes of water. A subset of four samples was tested for carbon-14 and tritium, which provides information about how long the water has been in the subsurface.

RESULTS

Water Levels

Figure 2.7 shows depth-to-water measurements that range from 0.61 to 381 m (2–1,250 ft) below the surface. Most wells north of the Rio Brazos exhibit a much shallower depth to water than those just south of Chama, with many wells showing depth to water of less than 5 m (16.4 ft) below the surface. Figure 2.7 shows that the majority of wells exhibit depth-to-water values of 10 m (33 ft) or less below the surface. Most wells with depth to water of less than 6 m (19.5 ft) are completed in the shallow alluvial aquifer. Figure 2.8 shows the spatial distribution of total well depth for wells in the area. A rough bimodal distribution is observed for well depth, with the majority of wells being 38 m (125 ft) or less below the surface. The deeper distribution includes well depths ranging from 38 to 457 m (125–1,500 ft).

Figures 2.9, 2.10, and 2.11 show well locations on the 15-minute Chama quadrangle geologic map (Muehlberger, 1967) from north to south, respectively. The colors of the points represent the depth to water for each well. Wells that are most likely completed in the shallow alluvial aquifer (blue points, depth to water ≤6 m) are almost all located in Quaternary terrace deposits (Qtk and Qtg). Wells with greater depth to water are likely part of a deeper aquifer system in the southern part of the study area (Fig. 2.11) on the east side of the Rio Chama, where Cretaceous rocks, including Mancos Shale and the Dakota Formation, are exposed at the surface.

However, some of these deeper wells are also located in Quaternary sediments among the wells completed in the shallow alluvial system, suggesting that the drillers of these wells drilled past the shallow alluvial system to tap a deeper groundwater system. Depth to water for these deep wells is generally between 9 and 15 m (30 and 50 ft) below the surface, usually with a thin (0.6–3 m [2–10 ft]) water-bearing unit approximately 61 to 91 m (200–300 ft) below the surface. However, for some wells depth to water can be much shallower. There is at least one flowing artesian well within the community of Chama, discussed in more detail below.

Figure 2.12 shows a map of the water-table contours for the shallow alluvial aquifer in the study area. The contours represent the surface elevation of the water table. In general, groundwater flows perpendicularly to the contours from high elevation to low elevation. In the Chama area, our findings indicate that the shallow alluvial aquifer is being recharged from the San Juan Mountains to the north and the Tusas Mountains to the east. The Rio Chama and the Rio Chamita appear to be gaining in the study area reach, meaning that groundwater is discharging to the river. This can be inferred from the water-table contour map because the contour lines extend upstream from where they intersect the stream. Water from the surrounding shallow aquifer is therefore supporting flow in the river. Groundwater flow in the area is generally north to south and angles toward the Rio Chama, where it ultimately discharges. Throughout much of the area, the slope of the water table does not exceed a gradient of 2% (1 m of head drop over 50 m of lateral distance). The saturated thickness map (Fig. 2.13) indicates a very thin shallow alluvial aquifer. In the village of Chama, the saturated thickness is between 3 and 10 m (10 and 33 ft).

Depth-to-water measurements for wells inventoried are shown in Figure 2.14 and Table 2.2. For many wells, we were not able to find well logs that identified the total well depth, depth of the water-bearing unit, and unit description. For the deep aquifer system wells RA-024, RA-026, and RA-032, depth-to-water measurements were greater than 10 m (33 ft). However, the deep aquifer system well RA-033 exhibits the smallest depth-to-water measurement (0 m) because this well is a flowing artesian well, meaning the aquifer is under pressure, which pushes water to the surface.
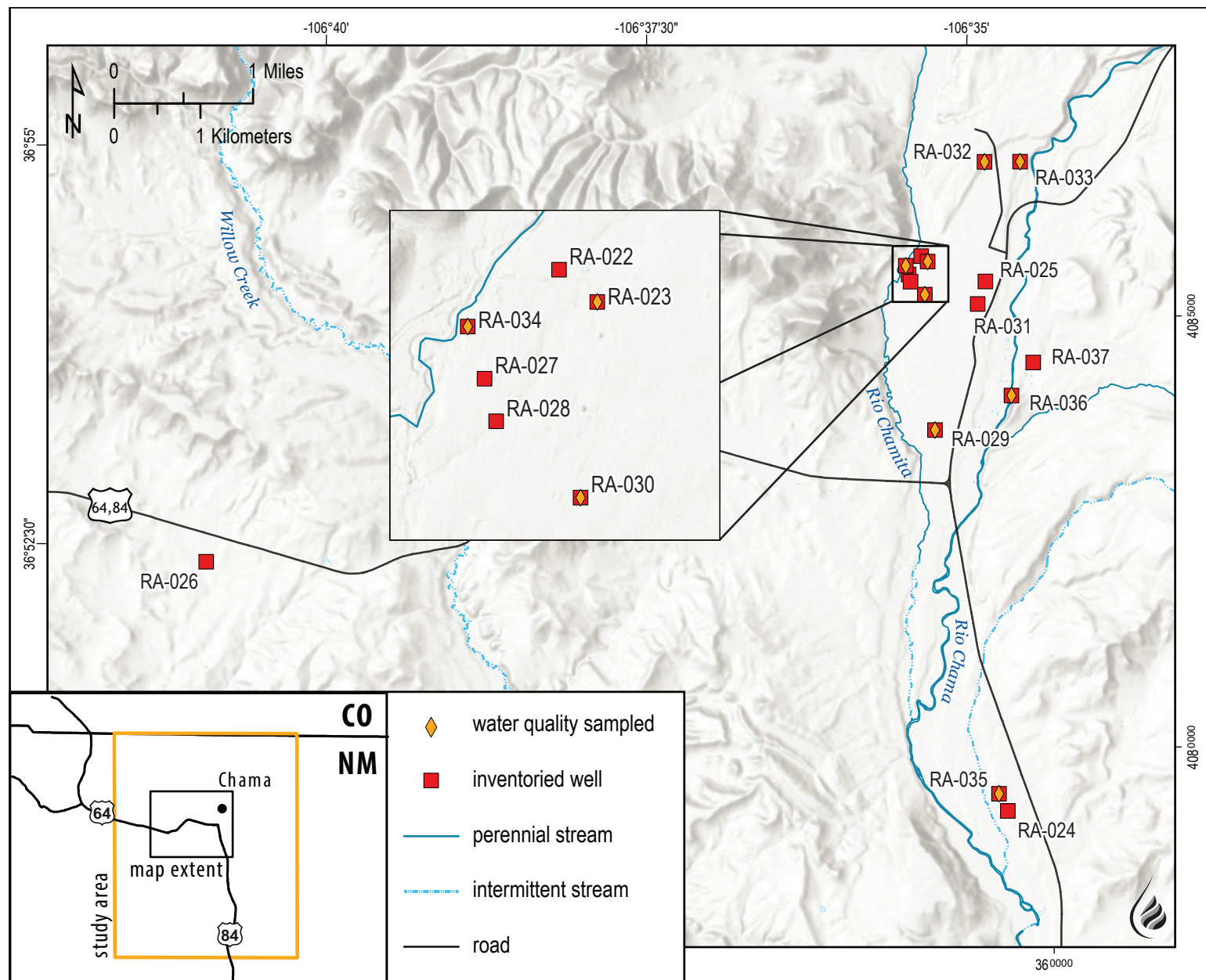
Figure 2.6. Location map of wells that were inventoried and sampled for this study. For information about these wells, see Appendices B and C.
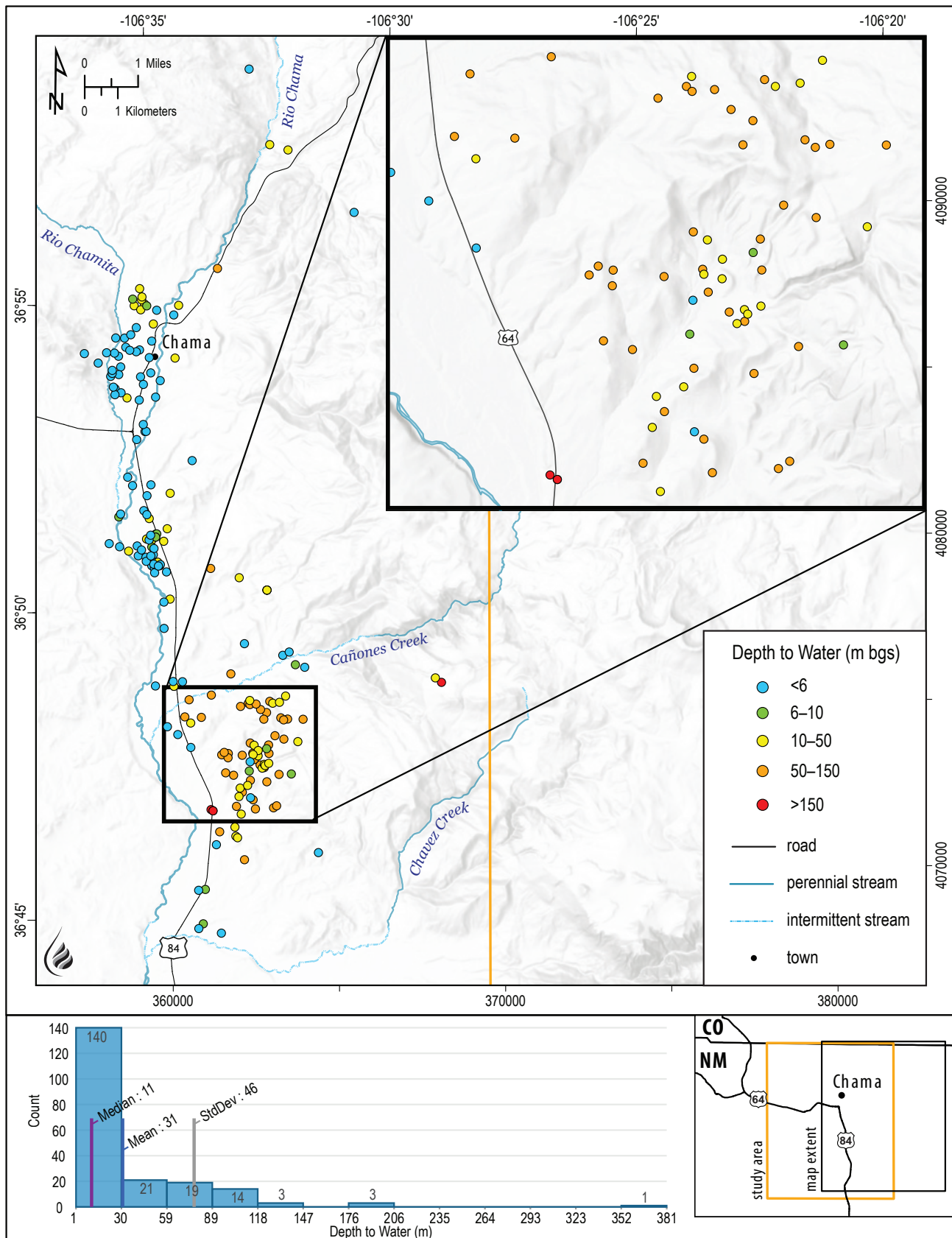
Figure 2.7. Depth-to-water measurements for existing wells in the study area in meters below ground surface (m bgs). An expanded view of wells located in the southern part of this map is shown in the upper right corner. The histogram shows that most wells exhibit a depth to water of less than 30 m (100 ft) below the surface.
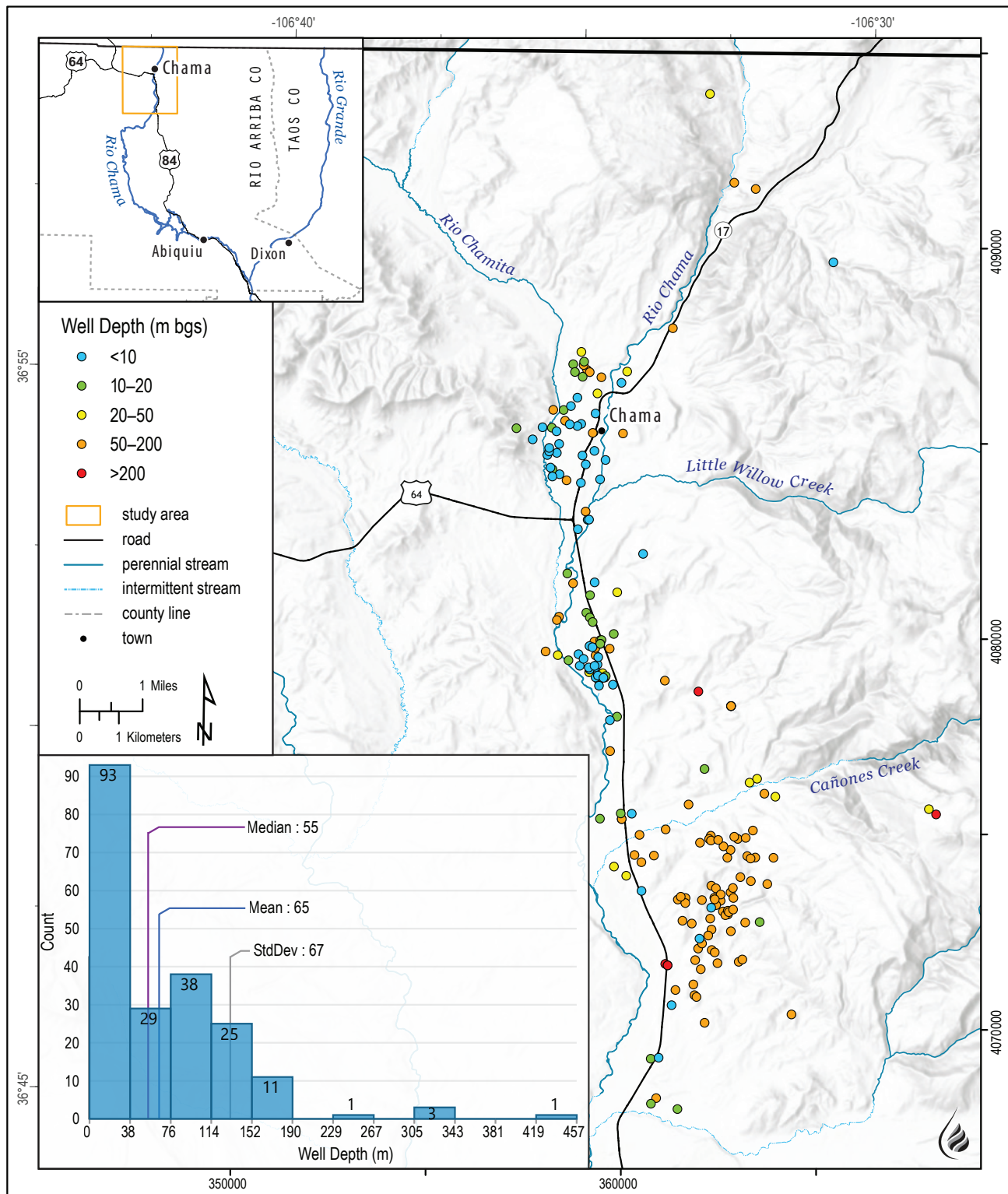
Figure 2.8. Depth of existing wells in the study area in meters below ground surface. The histogram shows that the majority of wells have total depths of less than 38 m (125 ft) below the surface.
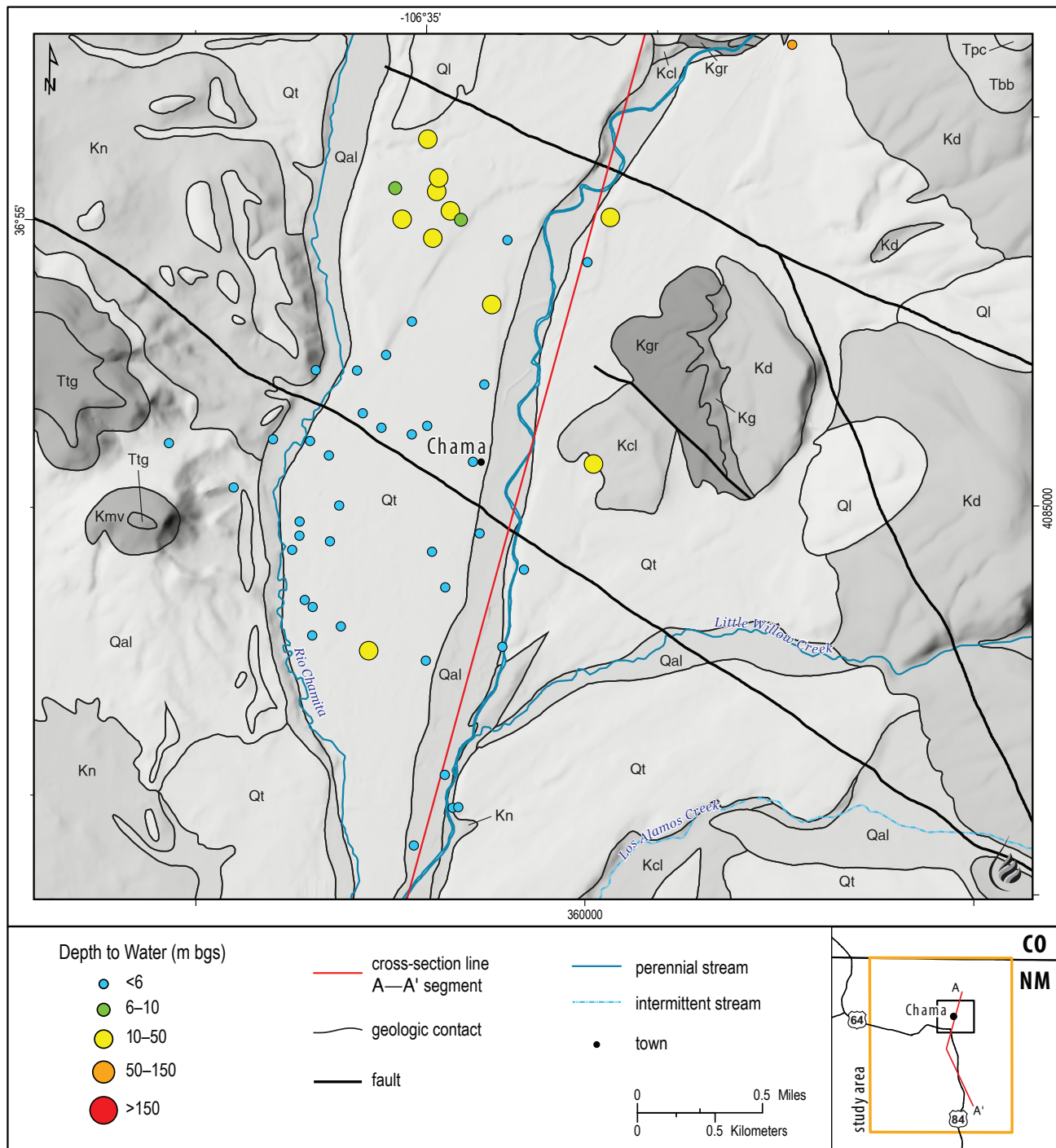
Figure 2.9. Well locations to the north on the 15-minute Chama quadrangle geologic map (Muehlberger, 1967). The size of the points is proportional to depth to water.
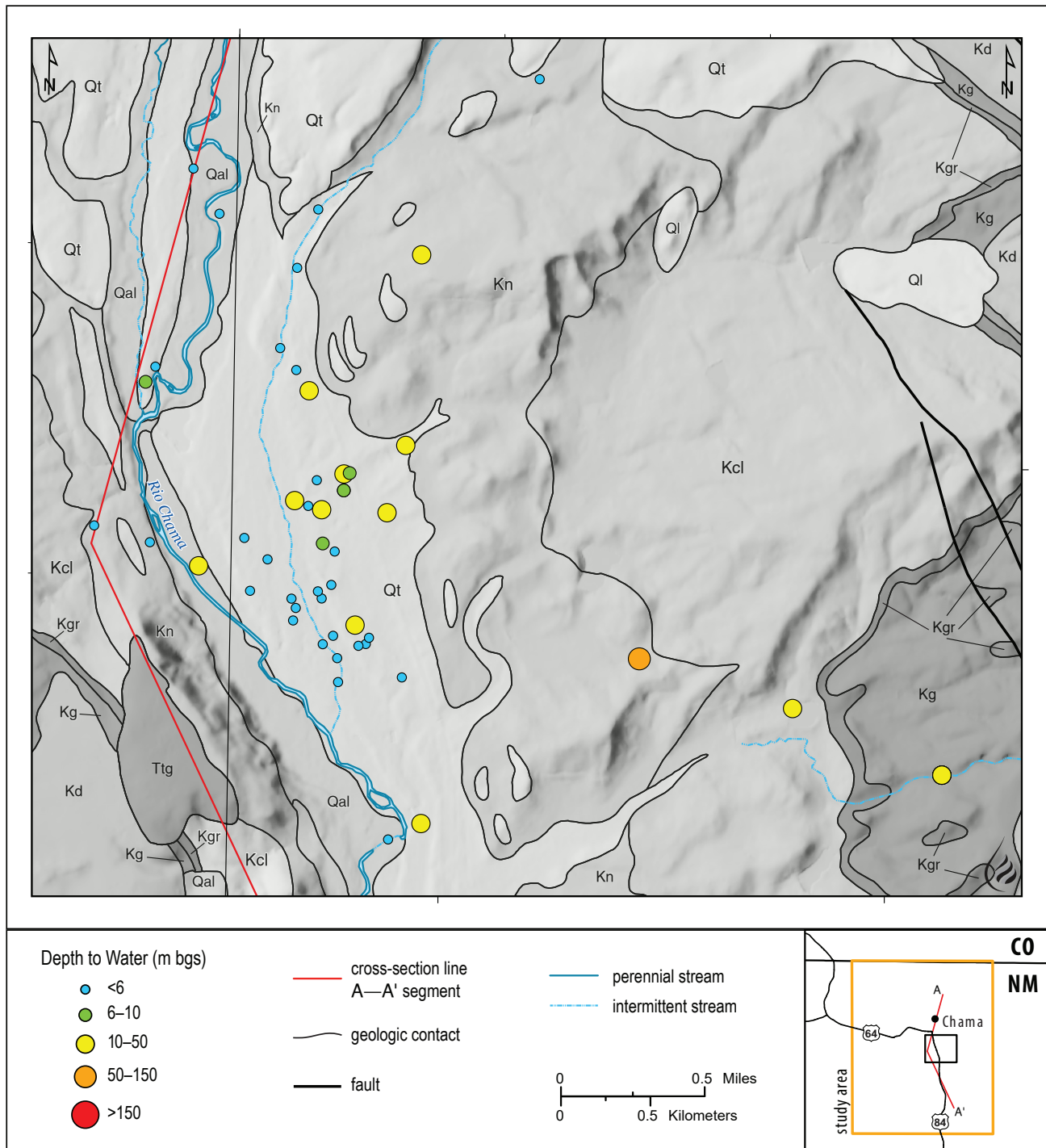
Figure 2.10. Well locations in an intermediate area on the 15-minute Chama quadrangle geologic map (Muehlberger, 1967). The size of the points is proportional to depth to water.
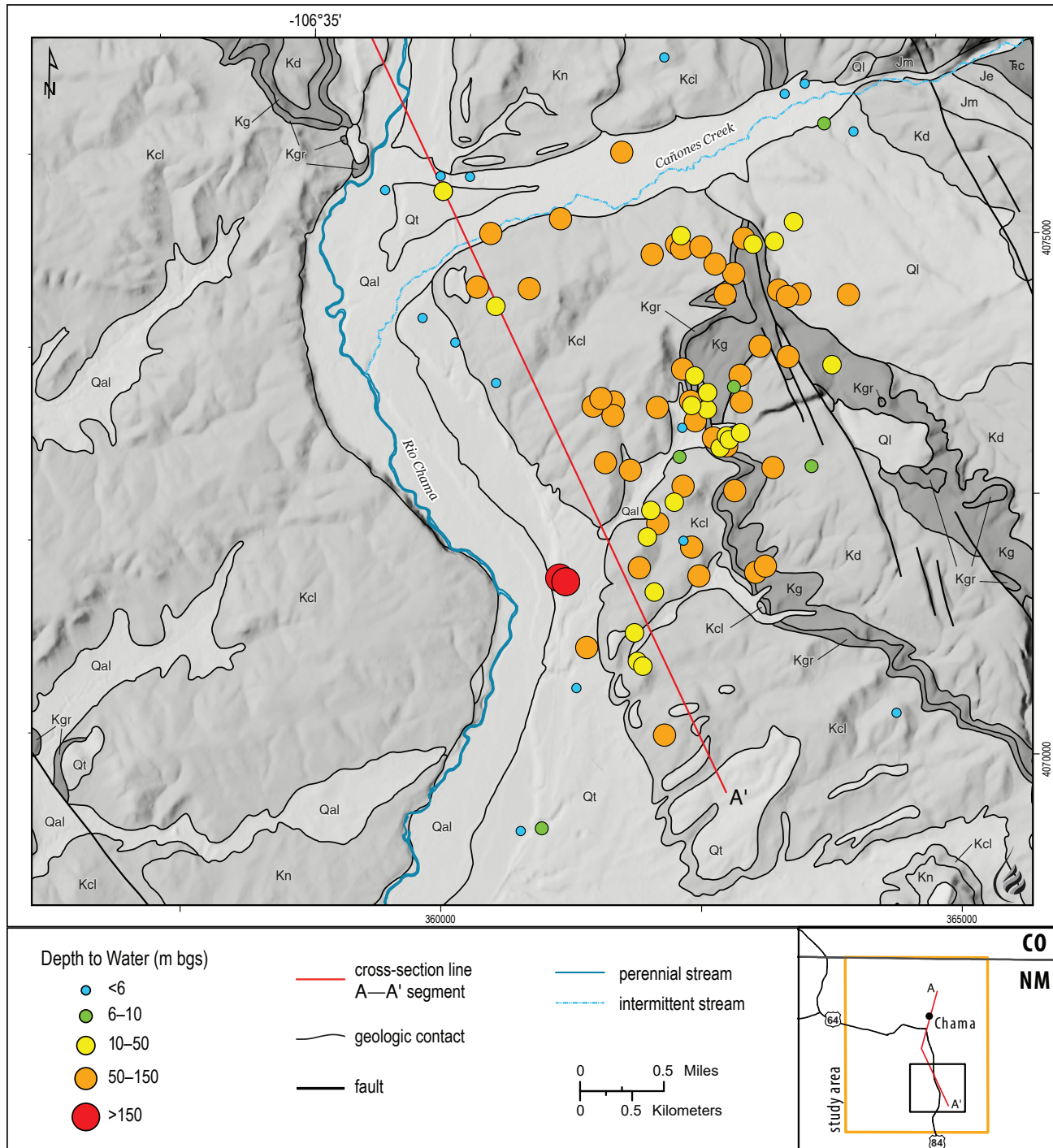
Figure 2.11. Well locations to the south on the 15-minute Chama quadrangle geologic map (Muehlberger, 1967). The size of the points is proportional to depth to water.

31
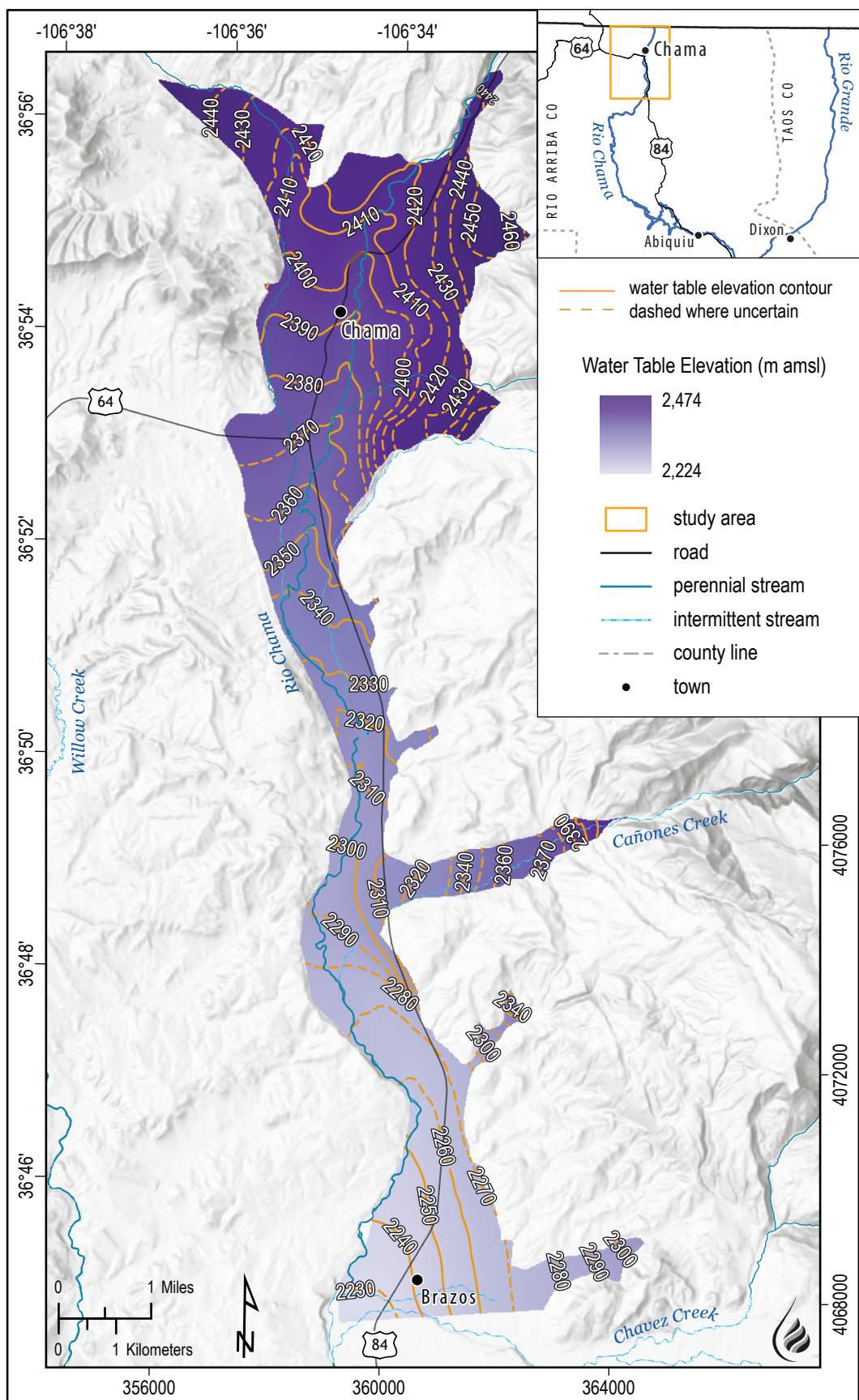
Figure 2.12. Water-table elevation map for the shallow alluvial aquifer in the Rio Chama valley near Chama.
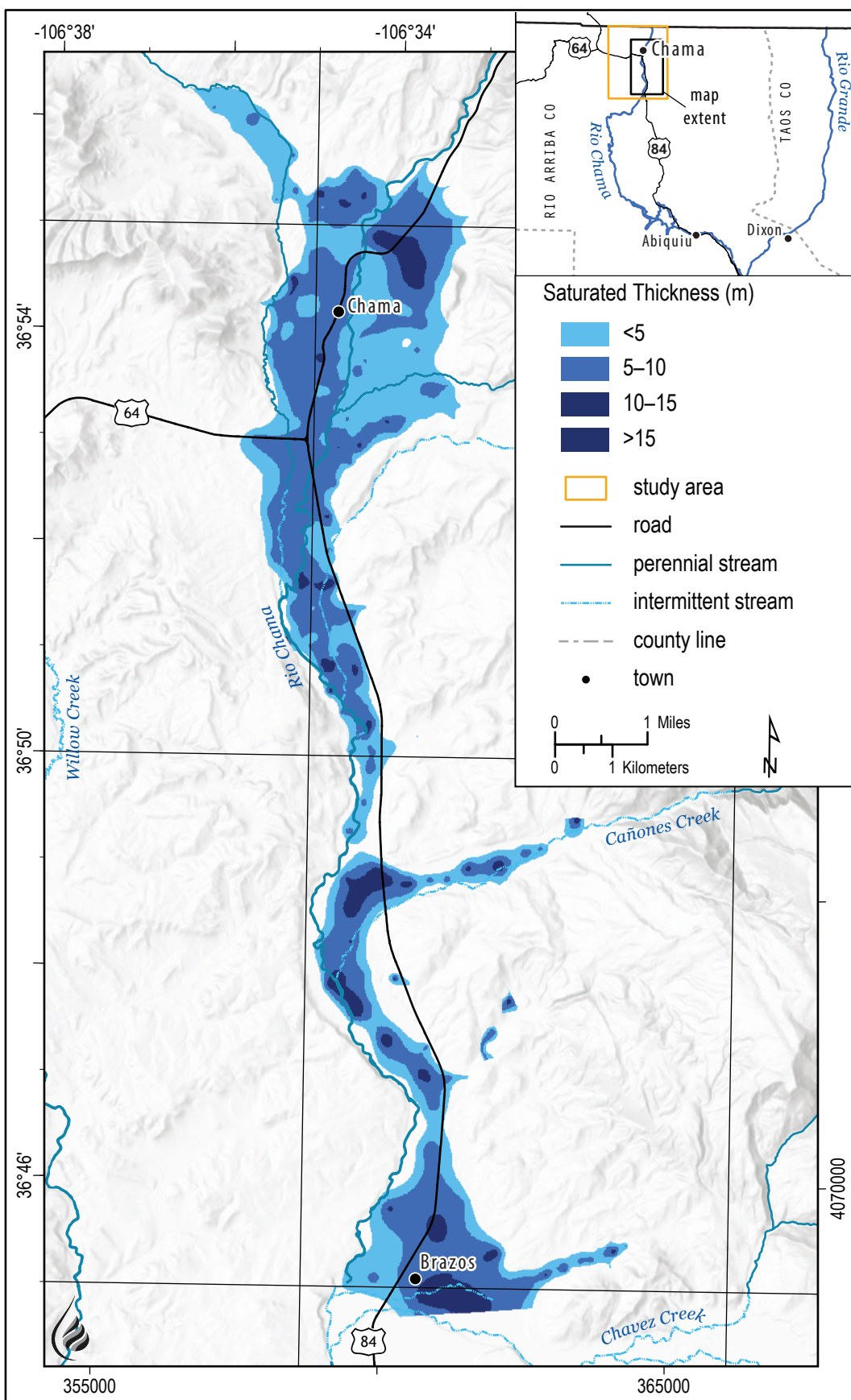
Figure 2.13. Estimated saturated thickness of the shallow alluvial aquifer in meters.
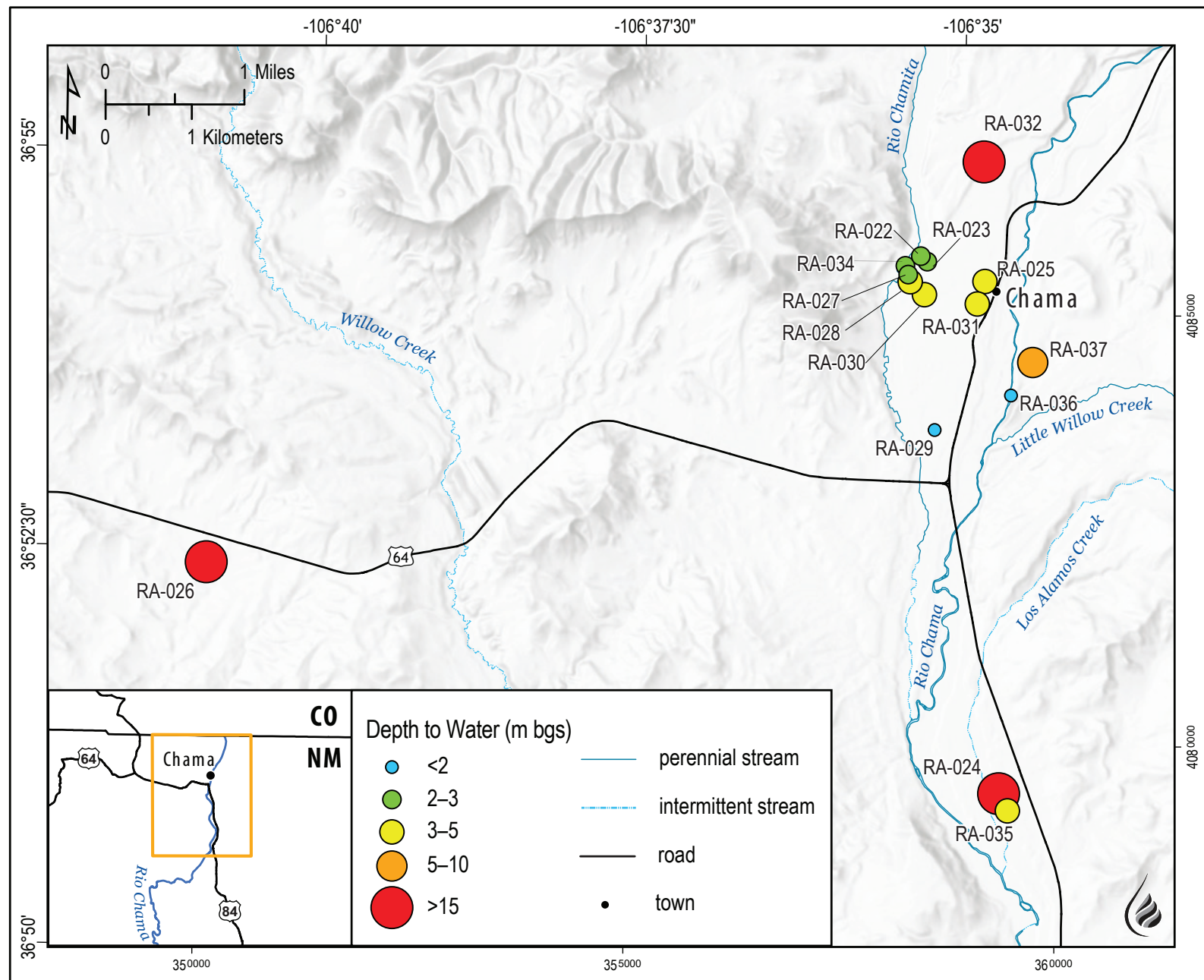
Figure 2.14. Depth-to-water measurements for wells inventoried for this study.

Table 2.2. Summary of notes taken during well drilling, such as the water-bearing unit description, yield, and depth, as found in NMOSE well records. Wells were categorized as completed in either the shallow or deep aquifer system as part of this research.

Well ID	Total depth (m)	Depth to water (m)	Depth of water-bearing unit (m)	Description	Aquifer system	Approximate yield (gpm)
RA-022		2.0			shallow	
RA-023	12.2	2.5	6–10	sand and gravel	shallow	
RA-024	91.4	12.9	88–89	fractured sandstone	deep	
RA-025		4.3			shallow	
RA-026	189	10.4	165–189	limestone/shale/white	deep	40
RA-027		2.3			shallow	
RA-028		3.4			shallow	
RA-029		1.9			shallow	
RA-030		3.6			shallow	
RA-031		3.3			shallow	
RA-032	103.6	14.0	96–103.6	brown sandstone	deep	20
RA-033	107	0	98–107	white sandstone and shale	deep	100
RA-034		2.3			shallow	
RA-035		3.0			shallow	
RA-036	2.4	1.3	1.2–1.5	gravel	shallow	15+
RA-037		6.9			shallow	

Wells determined to be completed in the shallow aquifer system all exhibited depth-to-water measurements of less than 10 m (33 ft) below the surface.

Water Chemistry Data

Water Quality

Table 2.3 shows major ion concentrations and other parameters for water samples. Wells were identified as part of the shallow or deep aquifer system mostly based on the measured depths to water and estimated well depths. In general, water quality in the Chama area is quite good, with TDS concentrations ranging from 117 to 1,260 mg/L (Fig. 2.15). For shallow aquifer system waters, TDS concentrations range from 117 to 211 mg/L—well below the secondary MCL of 500 mg/L. However, some constituents were found to be above the primary and secondary MCLs. These contaminants are discussed here.

All of the Chama shallow aquifer system waters tested positive for the presence of total coliform (Table 2.4). However, the presence of *E. coli* was detected in only two wells (RA-030 and RA-036). A likely source of these bacteria is septic tanks buried in the shallow alluvial aquifer. Significant groundwater

contamination from septic tanks should also result in high concentrations of dissolved nitrate (NO_3). While nitrate was detectable in all shallow aquifer system wells, concentrations were well below the primary MCL (Table 2.4). It is possible the nitrate concentrations have been lowered in this system by plant uptake of nitrate. RA-033 produces the only water that exceeded the primary MCL for arsenic (As), and water from RA-024 exceeded the secondary MCL for fluoride (F; Fig. 2.16). For iron (Fe) and manganese (Mn; Fig. 2.17), the flowing artesian deep aquifer system well RA-033 exhibited concentrations exceeding the secondary MCLs. Interestingly, the shallow aquifer system well RA-036 also exhibited iron and manganese concentrations exceeding the secondary MCLs.

General Chemistry

Table 2.3 shows concentrations of major ions for the eight wells sampled in the Chama area. Other parameters shown include estimated well depth, depth to water, TDS, silica (SiO_2), pH, and temperature. A quick review of the table reveals many differences in chemistry data from the different systems, including higher TDS concentrations and pH values exhibited by water produced from the deep aquifer system.

Table 2.3. Water chemistry data for groundwater samples. Data include major ion concentrations (mg/L), pH, alkalinity (mg/L of CaCO₃), and temperature (°C).

Aquifer system	Point ID	Calcium (Ca²⁺) (mg/L)	Magnesium (Mg²⁺) (mg/L)	Sodium (Na⁺) (mg/L)	Potassium (K⁺) (mg/L)	Bicarbonate (HCO₃⁻) (mg/L)	Chloride (Cl⁻) (mg/L)	Sulfate (SO₄²⁻) (mg/L)	Total dissolved solids (mg/L)	Silica (SiO₂) (mg/L)	pH	Alkalinity (mg/L)	Temperature (°C)
Shallow	RA-023	24.3	3.66	7.67	2.4	84	7.5	13.2	136	33.1	6.31	69	13.3
	RA-029	35.7	6.7	13.2	4.57	114	17.2	14.7	211	41.7	6.76	93	12.8
	RA-030	32.7	5.4	13.9	3.5	119	16.9	12.6	192	44.6	6.54	98	11.6
	RA-034	28	4.23	11.1	2.56	106	7.15	11.6	156	35.4	6.28	87	10.9
	RA-036	22.7	4.29	5.49	0.90	96	<1	4.43	117	28.1	6.67	79	12.1
Deep	RA-024	31.5	3.98	242	1.8	507	155	<5	716	20.3	7.97	416	9.1
	RA-032	19	6.49	468	19.8	1,400	29.6	<1	1,260	8.54	7.37	1,150	13.8
	RA-033	99	29.4	43.6	11.1	262	1.4	244	584	6.42	8	215	9.7

Table 2.4. Concentrations of contaminants of interest, with primary and secondary maximum contaminant levels (MCLs). P = present, A = absent, ND = non-detect.

EPA secondary drinking water MCL						**2 mg/L**	**0.3 mg/L**	**0.05mg/L**
EPA primary drinking water MCL				**10 mg/L**	**0.01 mg/L**	**4 mg/L**		
	Point ID	**Total coliform**	**E. coli**	**Nitrate as nitrogen (NO₃ as N) (mg/L)**	**Arsenic (As) (mg/L)**	**Fluoride* (F⁻) (mg/L)**	**Iron (Fe) (mg/L)**	**Manganese (Mn) (mg/L)**
Shallow aquifer system	RA-023	P	A	0.28	0.0011	<0.1	ND	ND
	RA-029	P	A	4.41	0.0016	<0.1	ND	ND
	RA-030	P	P	0.58	0.0011	0.11	ND	ND
	RA-034	P	A	0.63	0.0008	ND	ND	ND
	RA-036	P	P	ND	0.0043	0.11	1.2	0.204
Deep aquifer system	RA-024	A	A	ND	ND	2.88	0.204	ND
	RA-032	A	A	ND	ND	1.41	0.164	ND
	RA-033	A	A	0.06	0.0718	1.08	15.5	0.21

* Fluoride (F⁻) has two drinking water standards—an enforceable maximum of 4 mg/L and the recommended limit of 2 mg/L.
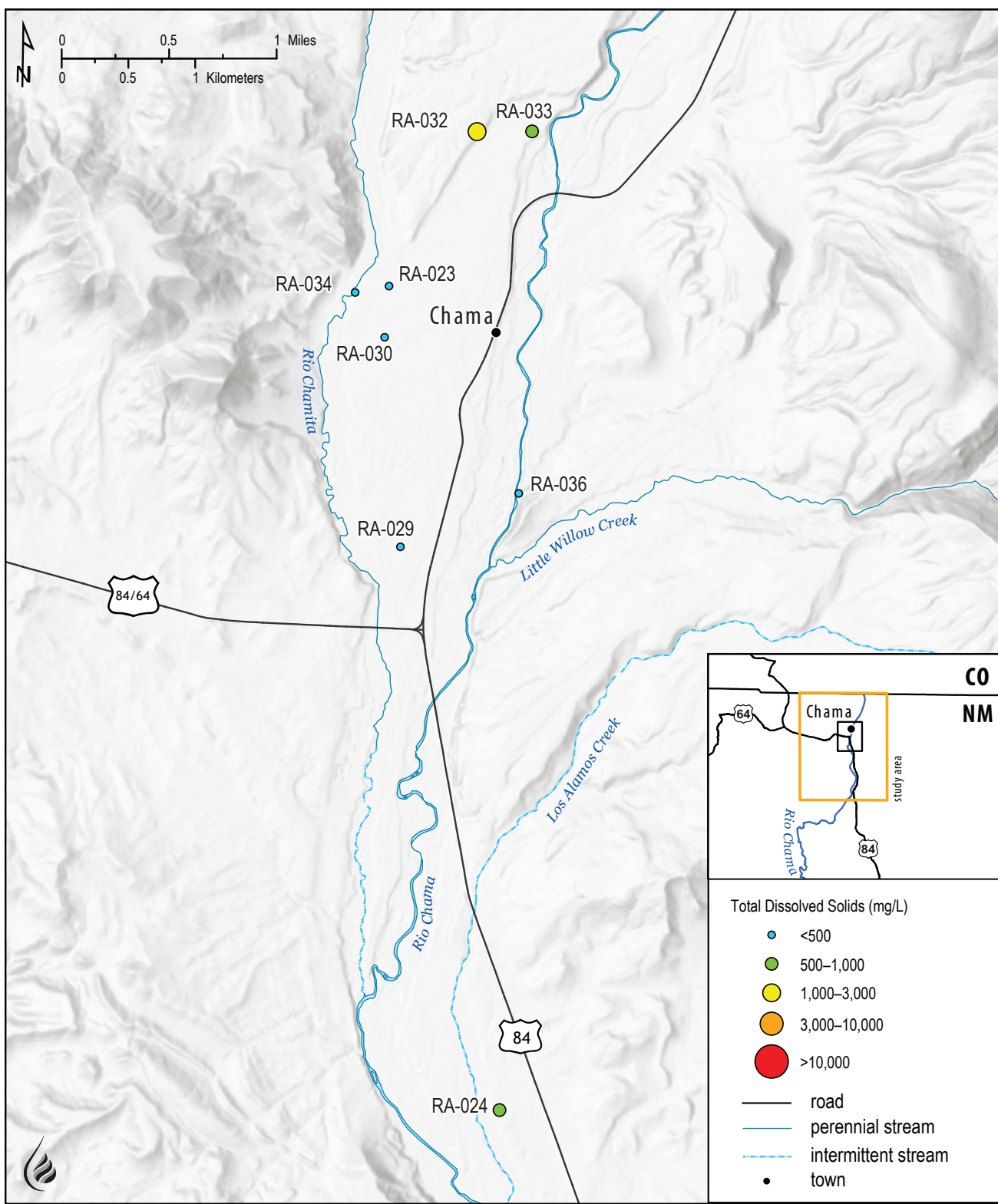
Figure 2.15. Sample locations for total dissolved solids concentrations, with the size of each point proportional to TDS concentration.
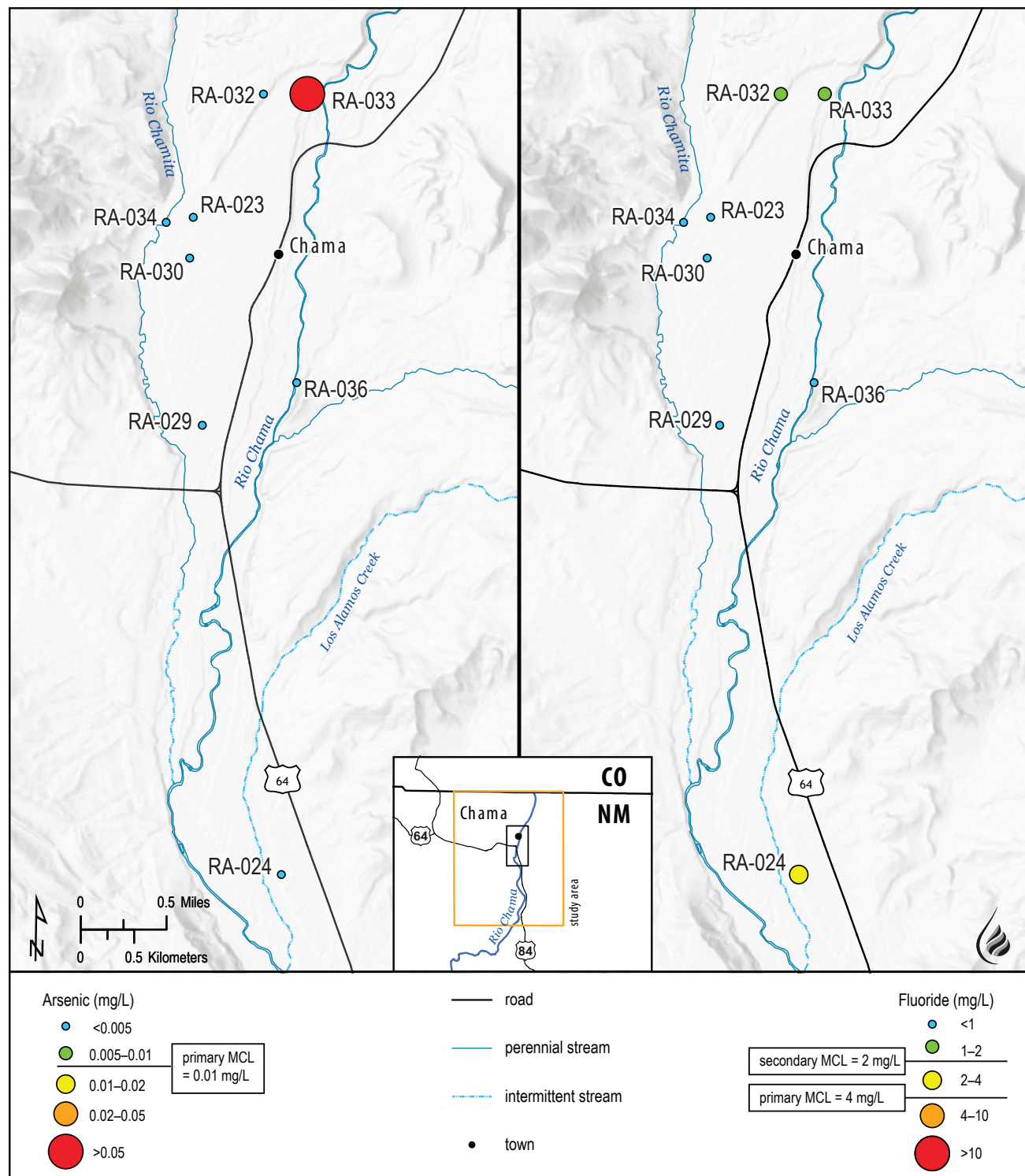
Figure 2.16. Arsenic (As; left) and fluoride (F⁻; right) concentrations for water samples. Yellow, orange, and red points represent exceedance of the primary EPA arsenic MCL. Fluoride also has a secondary MCL of 2 mg/L, shown with a yellow point.
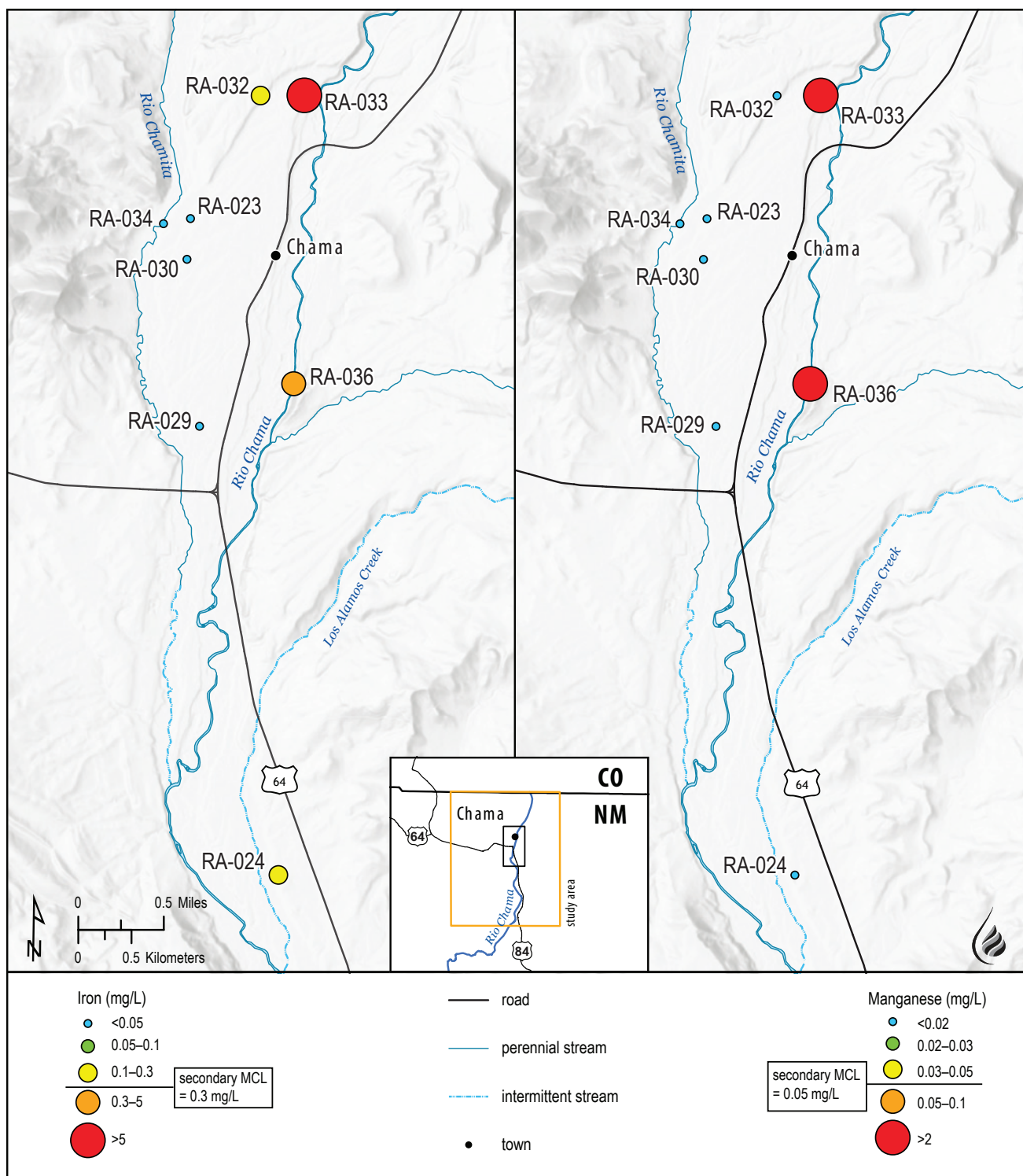
Figure 2.17. Iron (Fe; left) and manganese (Mn; right) concentrations for wells sampled in the study area. Orange and red points represent exceedance of the secondary MCL.

Initial analysis of the relative distribution of the major dissolved constituents for the different water samples is exhibited in Figure 2.18, which shows concentrations of individual constituents as a proportion of TDS concentrations. For shallow aquifer system wells, which are characterized by low TDS concentrations (<250 mg/L) on the x-axis, silica accounts for about 20% of the TDS concentration by mass, just above Ca^{2+} concentrations. For the deep aquifer system groundwaters, silica accounts for only 0.6 to 2.8% of TDS concentrations.

The element silicon (Si) combines with oxygen to form minerals called silicates, which make up more than 90% of the earth's crust. We can measure aqueous silicon concentrations, but usually we do not know the form or chemical species that it existed as in solution. Therefore, silica concentrations are reported as mg/L SiO_2. Most silica concentrations in groundwater range from 5 to 85 mg/L (Langmuir,

1997), with a median value of 17 mg/L. Silica has been used by researchers to estimate residence time (Marçais et al., 2018) and as a geothermometer for geothermal and low-temperature waters (Fournier and Potter, 1982). Silica concentrations for water from the deep aquifer system ranged from 6.42 to 20.3 mg/L and for shallow aquifer system waters from 28.1 to 44.6 mg/L. These high silica concentrations were unexpected because the water from the shallow aquifer system appears, from many other lines of evidence, to be relatively young groundwater with limited water/mineral interactions. While only five water samples were collected over a fairly small area, these high silica concentrations may provide important information about what type of rock this water has interacted with between the primary recharge area and the well where it was sampled. Silicate weathering is the primary control on the water chemistry for the shallow aquifer system waters.
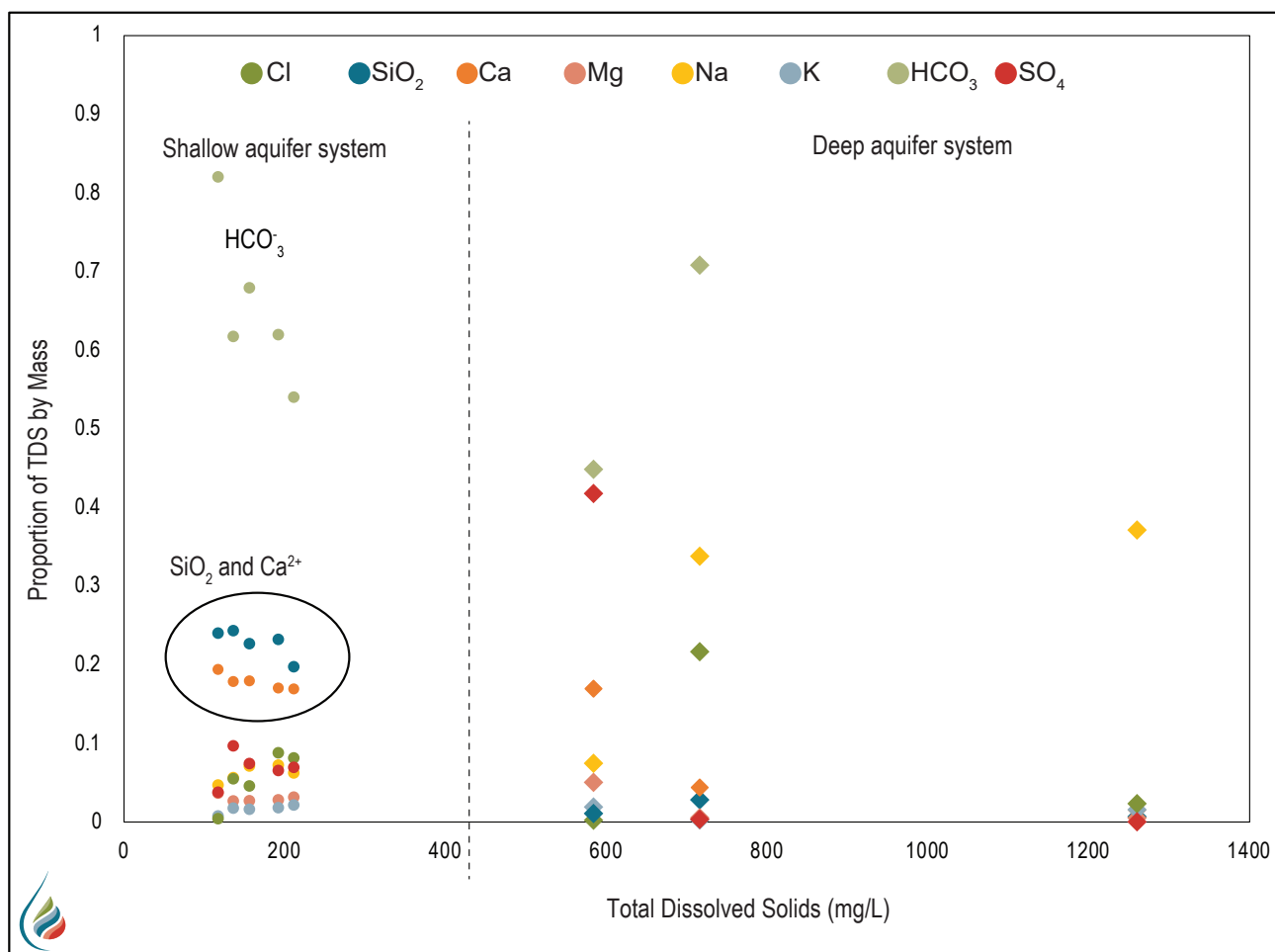
Figure 2.18. Graph showing the concentrations of major ions and silica (SiO_2) as a proportion of TDS by mass.

Figure 2.19 shows the groundwater chemistry for the water samples plotted on a Piper diagram. For all the shallow aquifer system samples, Ca^{2+} is the dominant cation and HCO_3^- is the dominant anion, resulting from the dissolution of calcite. A sample from the Chama community water system (river water) in 2001 plots within this group. For cations, four of the five shallow aquifer waters group tightly together, while RA-036 has slightly higher relative Mg^{2+} and Ca^{2+} concentrations. For the anions, the sample RA-036 has a relative HCO_3^- concentration of over 90% of total anions, while the other shallow aquifer system waters plot with slightly lower

HCO_3^- concentrations and slightly higher SO_4^{2-} and Cl^- concentrations. The water sample collected from RA-033 in the deep aquifer system shows the dominant cations and anions are Ca^{2+} and SO_4^{2-}, respectively, which is indicative of the dissolution of gypsum $(CaSO_4)$. Interestingly, existing water chemistry data for well RA-026, located several miles west of Chama, plot close to water chemistry data for well RA-033. While the dominant cation and anion for samples RA-024 and RA-032 were Na^+ and HCO_3^-, respectively, RA-024 exhibits significantly more Cl^- than RA-032.
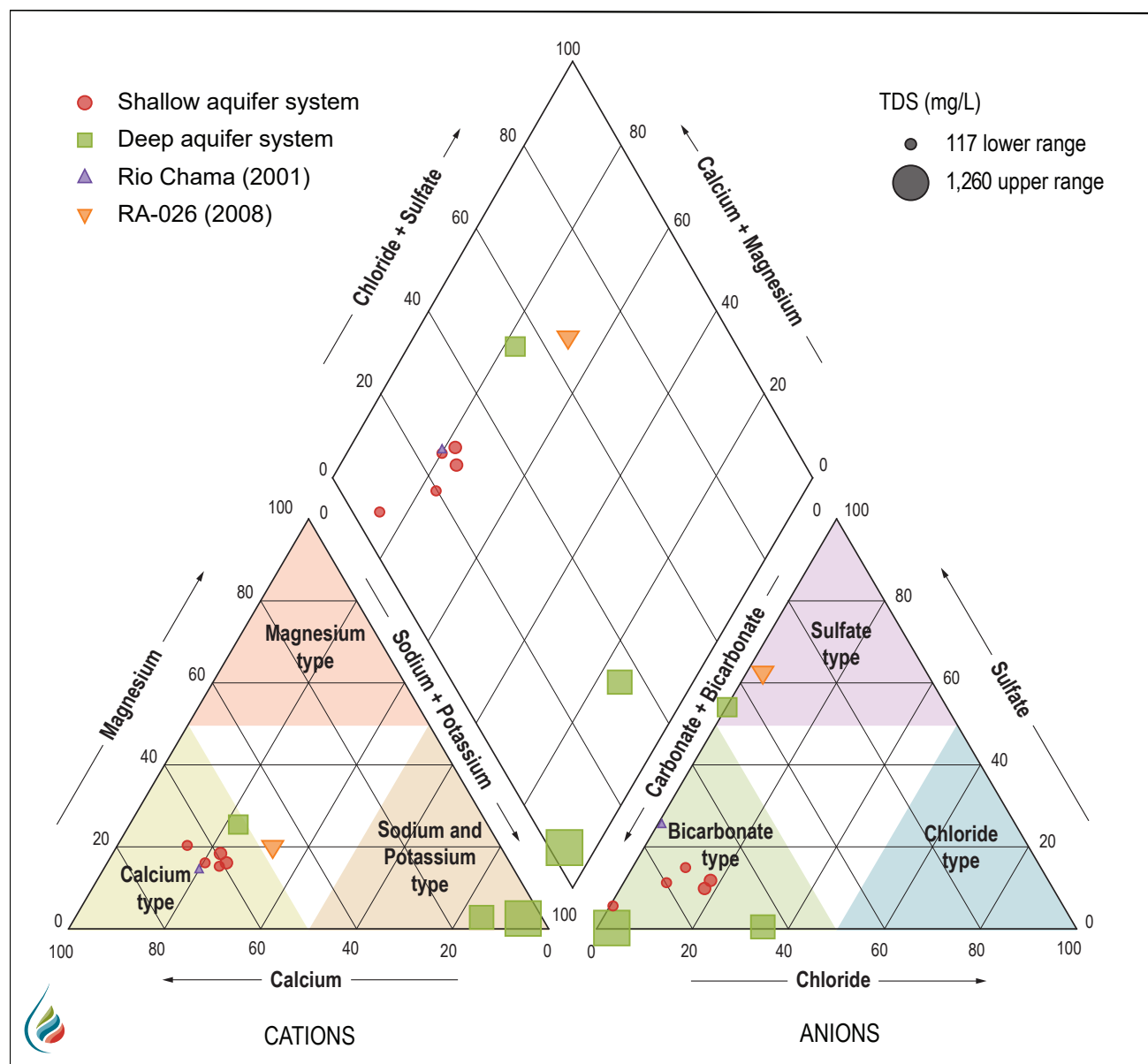
Figure 2.19. Piper diagram showing water chemistry data for water samples and existing data. The size of the data point is proportional to the measured TDS.

The high Na^+ concentrations and Na^+ water type (Fig. 2.19) observed for RA-024 and RA-032 suggest that a process called cation exchange may be occurring. Cation exchange is a water/mineral interaction where Na^+ ions that are adsorbed to clay minerals exchange with Ca^{2+} and Mg^{2+} ions that are dissolved in the groundwater. Because Ca^{2+} and Mg^{2+} have twice the charge of Na^+, for every one molecule of Ca^{2+} or Mg^{2+} that adsorbs to a mineral surface, two molecules of Na^+ are released into solution in the groundwater. Stoichiometric analyses (not shown) confirm that almost all water samples showed some degree of cation exchange. It appears that cation exchange has significantly altered the chemical composition of water from RA-024 and RA-032, altering the cation chemistry of the water compared to that resulting from the dissolution of minerals.

From the above discussion, we can conclude that the water chemistry for shallow aquifer system waters is controlled by silicate weathering (interactions with rocks high in silica) and the dissolution of $CaCO_3$. For the deep aquifer system, geochemical controls include the dissolution of $CaCO_3$ and $CaSO_4$ (in the case of RA-033) as well as significant cation exchange. When looking at the anions in the Piper diagram (Fig. 2.19), the three deep aquifer system water samples each show quite different water chemistry, unlike the shallow aquifer system samples, suggesting that these deep aquifer system waters may have interacted with different types of rock and therefore represent water sources from distinct aquifers.

While the shallow aquifer system waters are chemically similar, variations that are present suggest their chemical composition is affected by mixing with a small amount of water(s) from other sources. Figure 2.20 shows concentrations for selected dissolved constituents, including SiO_2, Cl^-, and Ca^{2+}, as a function of TDS concentrations. We observe direct correlations to some degree for all of these constituents. An increase in SiO_2 is
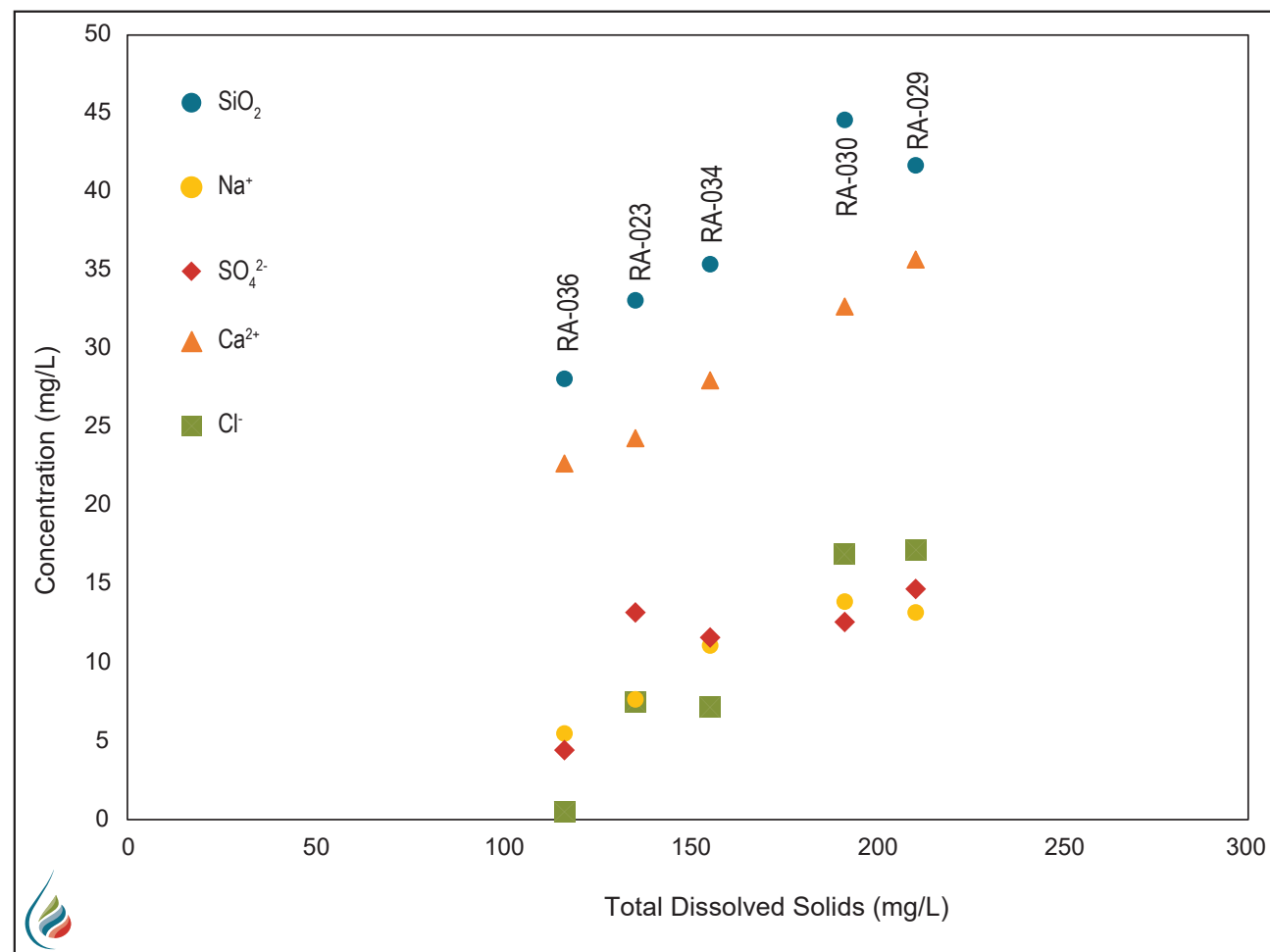
Figure 2.20. Concentrations for selected constituents plotted as a function of TDS concentrations for shallow aquifer system waters.

related to water/mineral interactions and likely correlates to residence time (age of the groundwater). However, the increase of Cl⁻ concentrations is not likely due to the same water/mineral interactions because Cl⁻ is not commonly associated with volcanic rocks with high SiO_2 content that are present near Chama, such as ash-flow tuff. The increase in SO_4^{2-} as TDS increases is also not likely due to water/mineral interactions but rather due to mixing. The water sample RA-036 exhibits the lowest observed concentration for TDS and many other dissolved constituents, with Cl⁻ concentrations being below the detection limit. Therefore, we will assume that RA-036 is representative of the shallow groundwater end member, with little to no mixing with other waters.

Examination of the water chemistry in the three deep aquifer system samples (RA-024, RA-032, and RA-033) indicates that the addition of any single deep water source to the shallow water systems could not account for the increase in both Cl⁻ and SO_4^{2-} concentrations in the samples. Figure 2.21 shows Cl⁻ and SO_4^{2-} plotted versus TDS concentrations. Water from RA-033 is the only possible source of SO_4^{2-} for the three deep water samples, but Cl⁻ concentrations are too low to account for the increase in Cl⁻ concentrations for shallow waters. Therefore, water from RA-024 looks like the most likely source of Cl⁻. Small amounts of groundwater from the deep aquifer system mix into the shallow aquifer system, affecting TDS concentrations and relative ion distribution of shallow aquifer system waters.
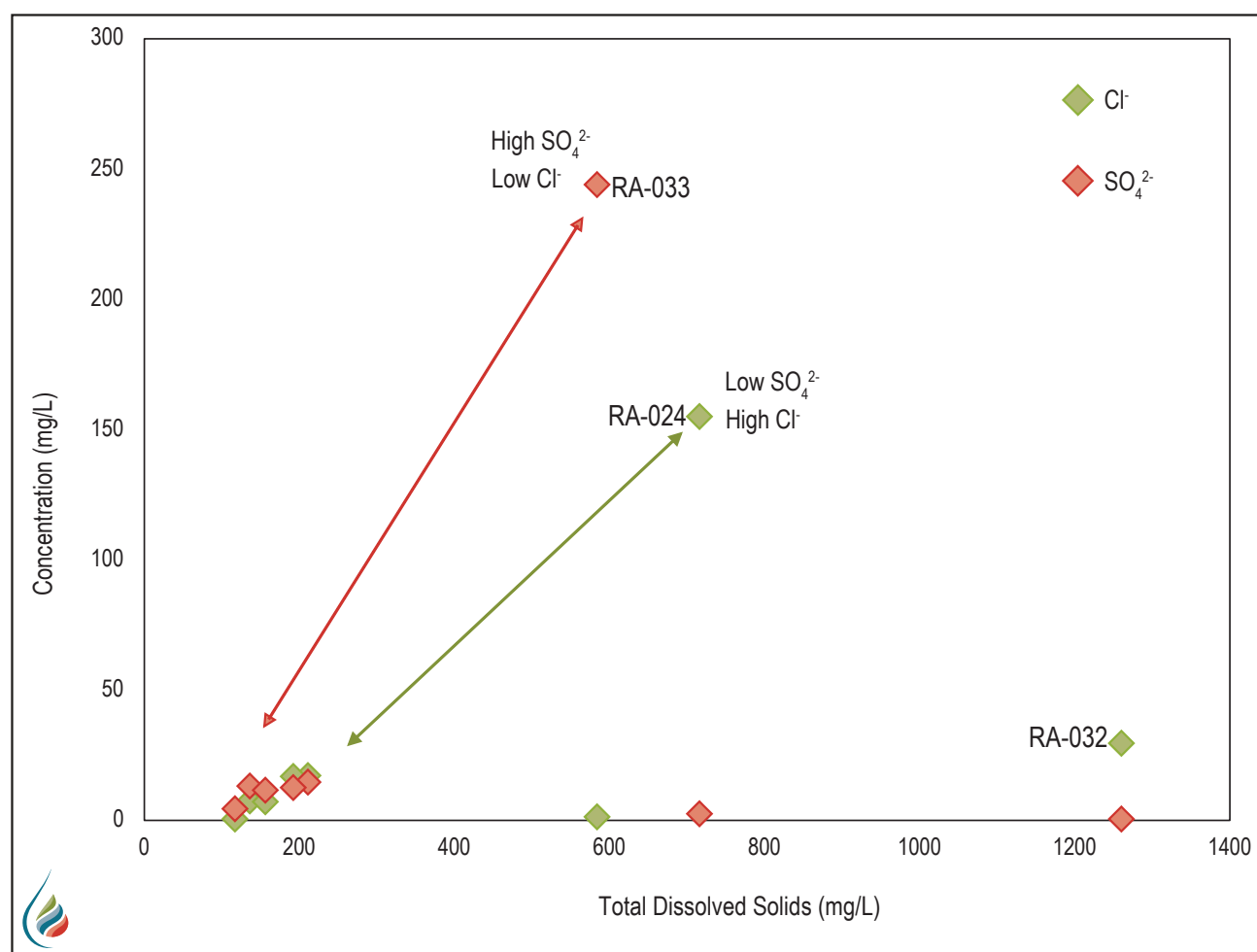
Figure 2.21. Cl⁻ and SO_4^{2-} concentrations plotted as a function of TDS concentrations. The double-arrowed lines represent probable mixing of deep waters that affect Cl⁻ and SO_4^{2-} concentrations in shallow system waters. Shallow alluvial system waters all have TDS concentrations less than 500 mg/L.

Stable isotope data show no evidence that any of the water samples had undergone evaporation. Therefore, both the deep and shallow aquifer systems appear to be largely recharged by snowmelt and winter precipitation in the mountains that has infiltrated into the subsurface without being exposed to the atmosphere (Fig. 1.6).

Groundwater Age Estimates

Table 2.5 shows age dating data, including tritium and carbon-14 ages. The shallow aquifer system waters from RA-029 and RA-036 exhibit ^{3}H concentrations of 5.11 and 4.21 TU, respectively, indicating that a large proportion of this water is less than 50 years old. Corrected carbon-14 ages for RA-029 and RA-036 agree with ^{3}H data, yielding relatively young ages of 120 and 51 YBP, respectively. Virtually no ^{3}H was found in water from the two deep aquifer system wells RA-032 and RA-033, and corrected carbon-14 ages were greater than 39,000 and 14,818 YBP, respectively.

For water from RA-036, the ^{13}C-based correction for carbon-14 age changed the estimated age from 770 YBP to 51 YBP, making it younger than water from RA-029. Considering that RA-036 exhibits the lowest TDS and SiO_2 concentrations for the shallow aquifer system waters, it makes sense that RA-036 also produces the youngest water. Using the corrected ages and SiO_2 concentrations for RA-029 and RA-036, we were able to estimate ages for the other shallow aquifer system wells based on SiO_2 concentrations. Shallow aquifer system water appears to range in age from 51 to 135 years old.

DISCUSSION AND CONCLUSIONS

Characterization of the Shallow Alluvial Aquifer

For the following sections, refer to Figure 2.22—a hydrogeologic conceptual model of the region based on the information and analyses above. In general, the shallow alluvial aquifer in the Chama area is very limited in size and permeability. While some Chama residents use groundwater from this aquifer, and the quality of this water is quite high, it does not appear to be sufficient for a community water supply. Existing wells in the area that tap deeper aquifers show that water levels in the wells are much higher than the apparent water-bearing unit, indicating that these aquifers are confined and under pressure. In the presence of open fractures and faults, this deep aquifer system water can move upward into the shallow aquifer system.

Hydrogeologic Description

The shallow aquifer system comprises Quaternary sediments, including 11 different terrace deposits that follow the Rio Chama valley floor (Figs. 2.9, 2.10, and 2.11). The width of the aquifer is limited by the lateral extent of these deposits and is widest where tributaries feed into the Rio Chama, such as the area near Chama (Fig. 2.9). In other areas, such as just north of mouth of the Rio Brazos (bottom of Fig. 2.10), the width of the aquifer is much smaller. These terraces were not described in detail by Muehlberger (1967), but he did identify a young terrace deposit (Qtg) as a gravel deposit measuring less than 10 m thick. The term "gravel" that is in buried sediments suggests large grain sizes and high permeability, making this thin terrace a favorable aquifer unit within this layered system.

Table 2.5. Tritium (^{3}H) concentrations, estimated ages, and $\delta^{13}C_{DIC}$ data for groundwater. TU = tritium unit, DIC = dissolved inorganic carbon, PMC = percent modern carbon, YBP = years before present.

System	Point ID	Tritium [3]H (TU)	Carbon-13 (DIC) $\delta^{13}C_{DIC}$ (‰)	Carbon-14 [14]C (PMC)	Carbon-14 ^{14}C age (YBP)	^{13}C-based corrected age (YBP)	SiO_2-based age (YBP)
Shallow aquifer system	RA-023						76
	RA-029	5.11	-13.6	98.48	120	120	120
	RA-030						135
	RA-034						88
	RA-036	4.21	-11.7	90.84	770	51	51
Other aquifer(s)	RA-024						
	RA-032	0.08	-1.4	<0.44	>43,500	>39,000	
	RA-033	-0.09	-8.4	10.93	17,780	15,000	
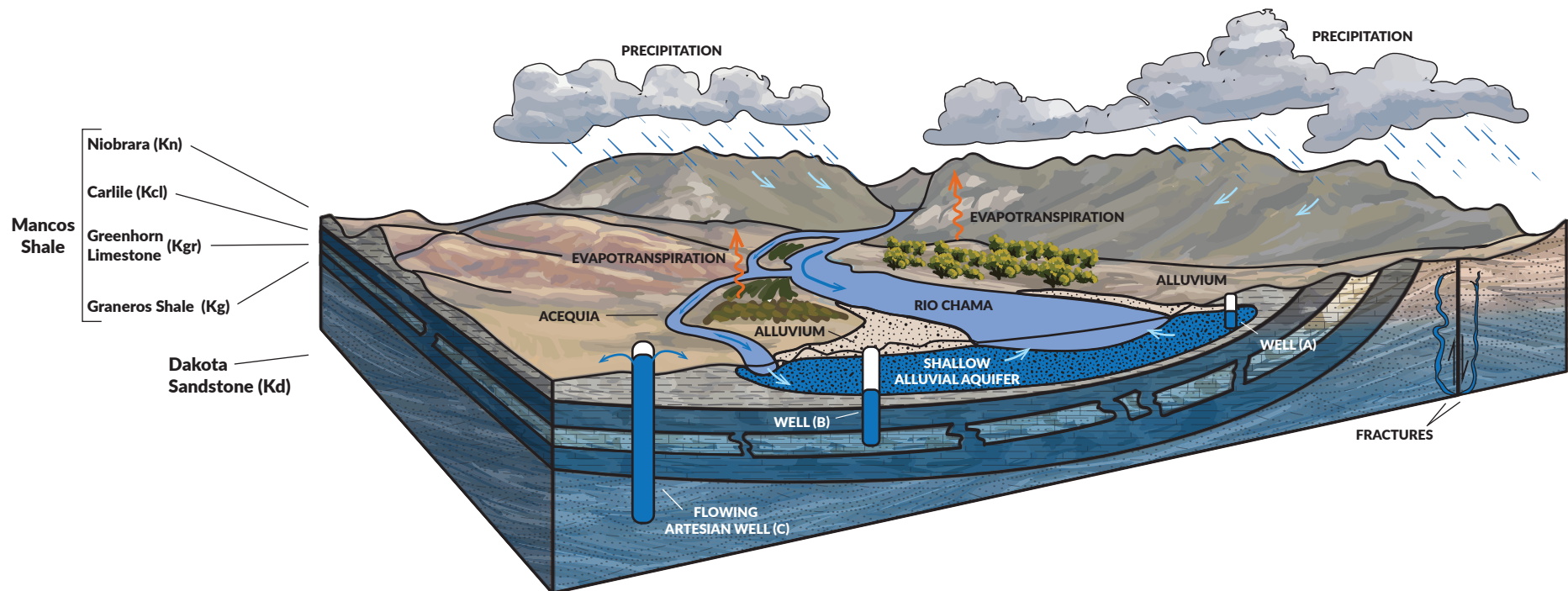
Figure 2.22. Hydrogeologic conceptual model for the Chama area. The width of the valley limits the extent of the shallow alluvial aquifer, which is primarily recharged by rain and snow in the mountains to the north and east. In this area, the Rio Chama is primarily a gaining stream, where groundwater from the shallow alluvial aquifer discharges into the river. The deep aquifer system includes the Mancos Shale (Graneros [Kg], Greenhorn Limestone [Kgr], Carlile [Kcl], and Niobrara [Kn]) and the Dakota Sandstone. The distribution of water-bearing zones in the Mancos Shale that are composed of more permeable rock, such as sandstone, is highly variable both vertically and laterally. The Greenhorn Limestone generally produces water of good quality. For most wells penetrating water-bearing zones in the deep aquifer system, water levels in the wells rise significantly above the water-bearing zone, indicating that this aquifer system is under confined conditions (under pressure).

A review of well-drilling logs reveals that although much of the material being drilled through in the shallow alluvial aquifer was described as sand and gravel, the term "clay" is also used occasionally. From the estimated yields of these wells, which can be as low as 2 to 5 gpm, it appears enough clay material is present to significantly decrease the average permeability of the aquifer. Drillers tended to stop drilling when they reached gray or black shale, presumed to be the top of the Mancos Shale—a very low-permeability formation. Future work is required to characterize the thickness, extent, and hydrologic properties of these deposits.

Based on carbon-14 and tritium dating results, the groundwater residing in the shallow alluvial aquifer is primarily sourced from precipitation or snowmelt that infiltrated to the water table in the high mountains approximately 105 to 50 years ago.

Water-table contours in Figure 2.12 indicate that recharge is coming from the San Juan Mountains to the north and the Tusas Mountains to the east. High SiO_2 concentrations confirm that the water has interacted with volcanic rocks incorporated in the Quaternary sediments.

Once recharged groundwater meets the valley floor, it flows generally parallel to and toward the Rio Chama in shallow deposits. Figure 2.13 shows the estimated saturated thickness of the shallow alluvial aquifer. While some uncertainty is associated with this estimate due to lack of data in some areas, it is apparent that the saturated thickness is very thin, with a median value of 6 m (20 ft). Groundwater in this aquifer ultimately discharges into the Rio Chama.

The strong hydrologic connection between the river and the shallow aquifer is demonstrated in Figure 2.23, which shows a USGS time series
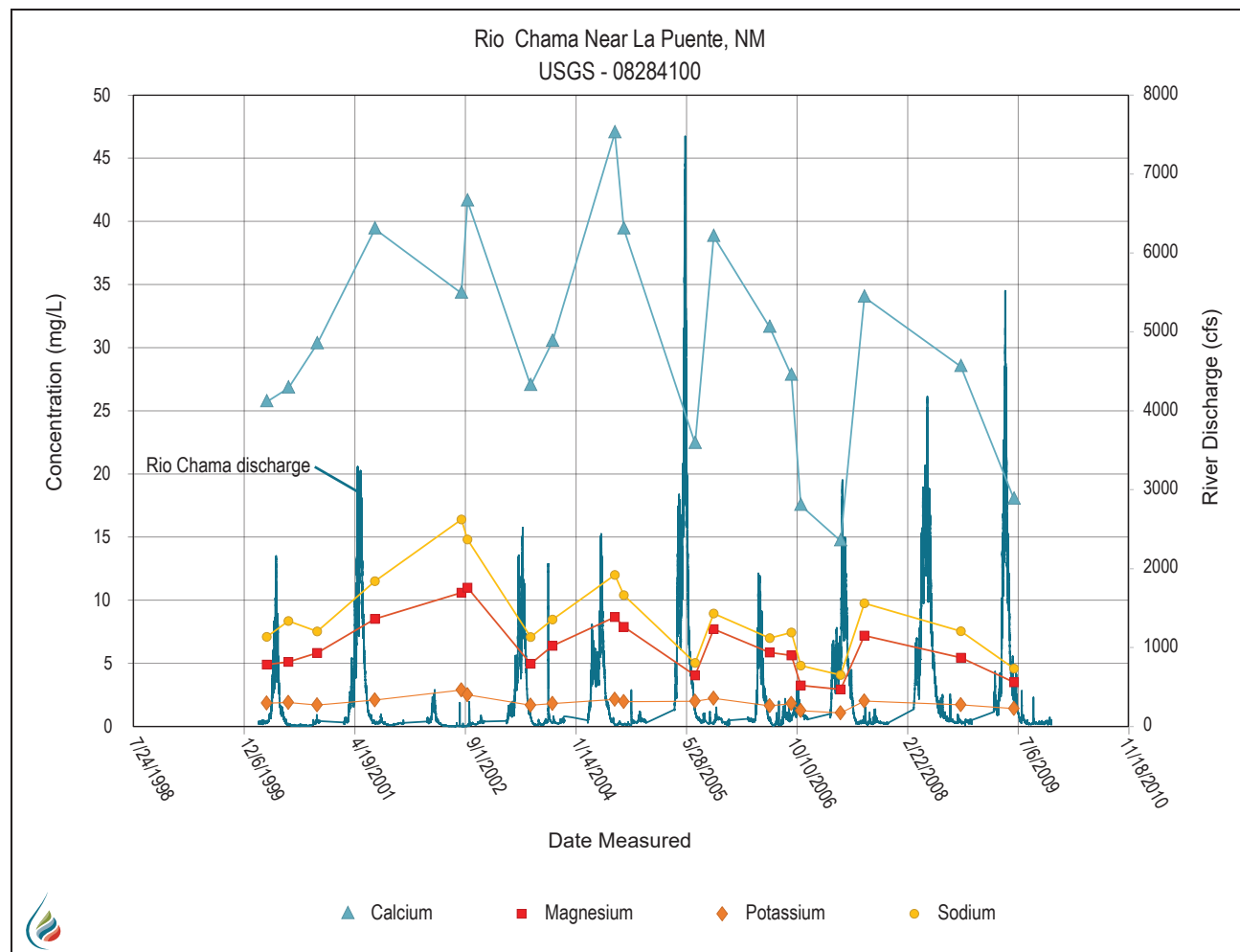
Figure 2.23. USGS time series of cation (Ca^{2+}, Mg^{2+}, Na^+, K^+) concentrations in the Rio Chama near La Puente between the years 2000 and 2010.

of cation (Ca^{2+}, Mg^{2+}, Na^+, K^+) concentrations in the Rio Chama near La Puente between the years 2000 and 2010. The ranges of all these cations bracket all major cation concentrations observed in shallow aquifer system groundwaters (Fig. 2.24). Also, the relative cation distribution for all the different Rio Chama samples (Fig. 2.24) is very similar to those observed for the shallow groundwater samples, with Ca^{2+} as the dominant cation. These data verify the Rio Chama gains water from the shallow alluvial aquifer in the area around Chama.

Geochemical Description

In general, groundwater in the shallow alluvial aquifer is of good quality, with low TDS concentrations (<250 mg/L). Well RA-036 exhibited iron and manganese concentrations that exceed the EPA secondary MCLs of 0.3 and 0.05 mg/L, respectively. The source of these metals is not known, but iron and manganese are common constituents in many alluvial aquifers. Interestingly, all five shallow

aquifer system wells tested positive for the presence of total coliform, and two of the wells produced water that also tested positive for the presence of *E. coli.* The most likely source of this contamination is effluent from septic tanks in the shallow subsurface.

Groundwater from the shallow aquifer system exhibits high SiO_2 concentrations, ranging from 28.1 to 44.6 mg/L, which is a distinguishing feature for water in the shallow alluvial aquifer but does not present a health risk. These SiO_2 concentrations are due to being in contact with and interacting with clasts of high-silica volcanic rocks such as volcanic tuff. In addition to dissolved silica, shallow aquifer system water chemistry shows evidence of the dissolution of $CaCO_3$ and minor cation exchange. While Cl^- and SO_4^{2-} concentrations in the shallow aquifer system are quite low (<20 mg/L; Table 2.3), the source of these ions is groundwaters from the deep system, which are likely moving upward along faults and fractures beneath Chama.
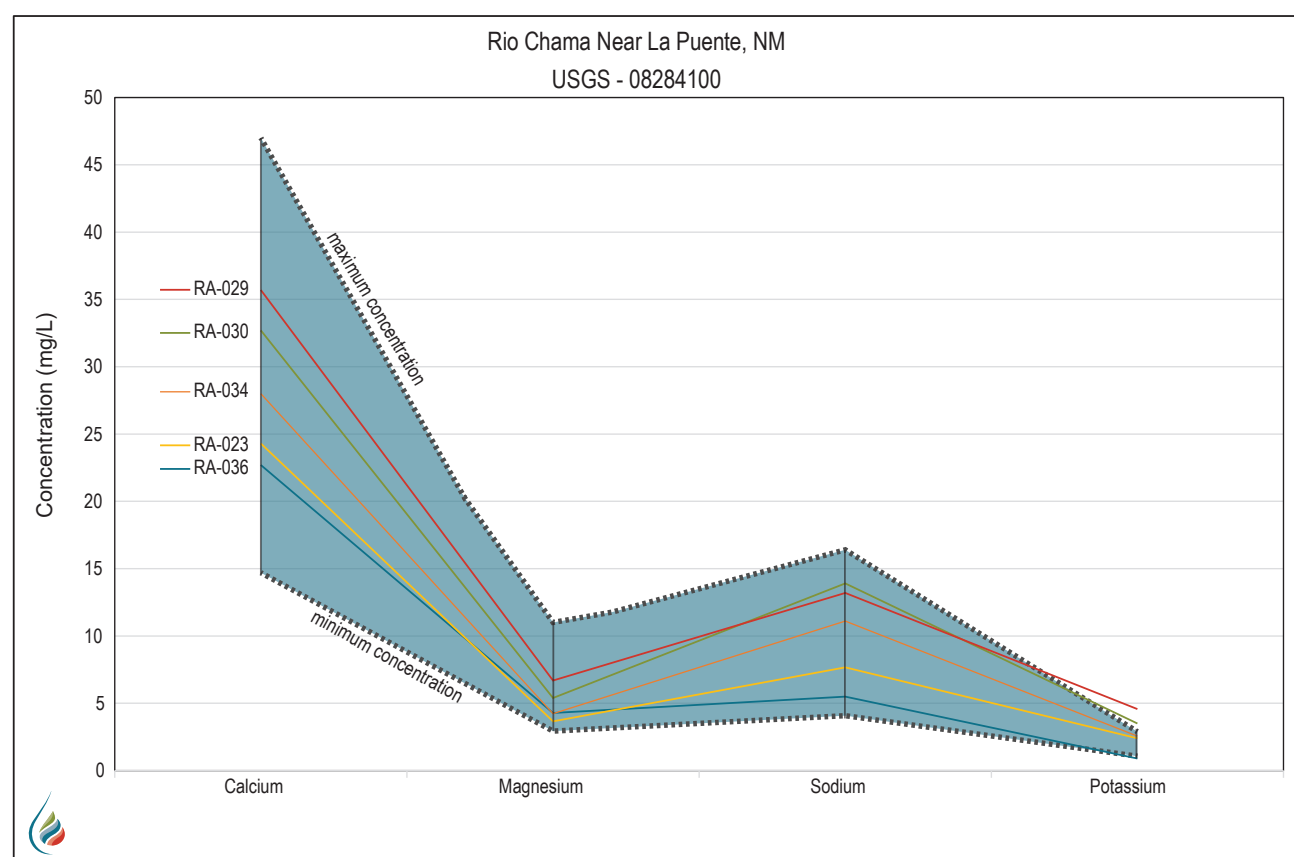
Figure 2.24. Each colored line represents the cation composition of one of the groundwater water samples (labeled). Maximum and minimum concentrations are defined by the USGS cation dataset shown in Figure 2.23. Those samples were collected between 1999 and 2009 from the Rio Chama.

Characterization of the Deep Aquifer Systems

Of the eight groundwater samples collected in the Chama area, three produce water from a deeper system. According to well logs, many deep aquifer system wells are drilled to between 60 and 120 m (200 and 400 ft) below the surface, with the water-bearing unit defined as a relatively thin unit of rock located close to the bottom of the well. Many such wells in the Chama area appear to be completed in the Cretaceous Mancos Shale or the top of the Dakota Sandstone (Fig. 2.3). However, most of these wells show depth to water of less than 30 m (100 ft) below the surface, indicating that groundwater from the water-bearing unit moved upward under pressure along the well bore after being tapped by the well. These data indicate the deeper aquifers are confined.

Interestingly, the three deep water samples all exhibit different chemical signatures. Water from the flowing artesian well RA-033 exhibits the lowest TDS concentration (584 mg/L) of the deep wells. This water sample is the only one with significant SO_4^{2-} content, with a Ca-SO$_4$ water type. Preliminary findings suggest very small amounts of water with a geochemical signature similar to that of RA-033 are leaking into the shallow aquifer system. RA-026 is located about 8.6 km west of Chama and is reported to be about 180 m (600 ft) deep, penetrating a water-bearing zone composed of limestone and white shale from 165 to 180 m (540–600 ft) below the surface. The presence of limestone indicates the geologic formation is very likely the Greenhorn Limestone, which is part of the Mancos Shale. Water from RA-026 is defined as a Ca-SO$_4$ water type and plots very close to RA-033 (Fig. 2.19). Therefore, RA-033 is likely producing water from the Greenhorn Limestone. The fact that RA-033 is a flowing artesian well demonstrates that the water in this deeper aquifer is confined and under pressure. Therefore, it is possible for this water to move toward the land surface along faults and fractures and thus mix with shallow groundwater. As mentioned above, it appears that a small amount of this deeper groundwater is mixing with the shallow aquifer system, resulting in an increase in SO$_4$ and TDS (Fig. 2.21). We do not know what formations the other two deep aquifer system wells (RA-024 and RA-032) are producing water from, but their different water chemistry suggests they have interacted with different rocks.

Figure 2.25 provides more evidence for the upwelling of deep groundwater into the shallow aquifer system. Interestingly, the fluctuation of cation concentrations in the river (Fig. 2.23) appears to be inversely related to river discharge rates, with higher concentrations during low discharge rates and lower concentrations during times of high discharge rates. Seasonal increases in river discharge are due to spring runoff, when snow in the mountains melts and feeds local and regional streams. During these times of high discharge, much of the water in the river is very young, coming directly from the snowmelt and effectively mixing with groundwater discharge in the channel and diluting dissolved ion concentrations. Figure 2.25 shows Ca^{2+}/Mg^{2+} ratios for river water and our shallow groundwater samples (horizontal lines). For much of that time period, Ca^{2+}/Mg^{2+} ratios in river water fluctuated closely around the value of 5, which correlates well with Ca^{2+}/Mg^{2+} ratios for the shallow aquifer system aquifer wells RA-029 and RA-036. However, the Ca^{2+}/Mg^{2+} ratio of river water began decreasing in early 2001, reaching a low value of 3.2, which is between the observed Ca^{2+}/Mg^{2+} ratios for water from the deep aquifer system wells RA-033 and RA-032 (3.37 and 2.93, respectively). This time period correlates with a very dry period in 2001 and 2002, when spring runoff events were very small. This suggests that during dry periods with very low runoff events, water from the deeper aquifers can discharge into the river, significantly affecting the quality of river water. This observation has implications for the effects of climate change on water quality in the Rio Chama.

FUTURE WORK

It was very difficult to find geologic and hydrogeologic data and literature for this region compared with many other regions in New Mexico studied by the NMBGMR. The few consultant reports cited in the Regional Water Plan (La Calandria Associates, Inc., 2006) are quite old and difficult to find. The 2016 Regional Water Plan (New Mexico Interstate Stream Commission, 2016) confirms the scarcity of hydrogeologic data because there are no current USGS groundwater monitoring sites. That plan also stated, "Though quantitative data were limited, the 2006 plan indicated that based on qualitative assessment of the available data, there are no aquifer systems within the Rio Chama watershed

that can support large volumes of groundwater withdrawals." Before reaching that conclusion here, we highly recommend continued research to thoroughly assess the deep aquifer system for sufficiency as a water source.

A review of available geologic and hydrogeologic data for this study revealed that we do not have enough information to make educated decisions regarding groundwater availability in the Chama area. While it would be beneficial to thoroughly update the geologic map by Muehlberger, for next steps, we instead recommend focusing on specific areas where information is missing, such as developing better lithologic descriptions for the shallow alluvial aquifer. We also recommend focusing on areas of potential deep aquifer system water extraction. Tasks should include on-the-ground geologic assessment, small-scale mapping investigations, and constructing multiple detailed cross sections in areas of interest.

For the initial phase of the study described in this report, we focused our water sampling on the immediate area around the community of Chama. We sampled only three deep aquifer system wells, and they all exhibited different water chemistry from one another. We clearly do not have enough data to effectively characterize the deep aquifer system. Future work should include the sampling of the deep aquifer system over a larger area, focusing on areas circled in Figure 2.26. It appears many of these wells are completed in the Dakota Sandstone, which may be a suitable aquifer. By analyzing water from several deep aquifer system wells, we may be able to identify multiple wells that produce water from the same aquifer. Understanding the spatial relationship between wells that are apparently completed in the same aquifer may help to identify areas potentially suitable for well installation.
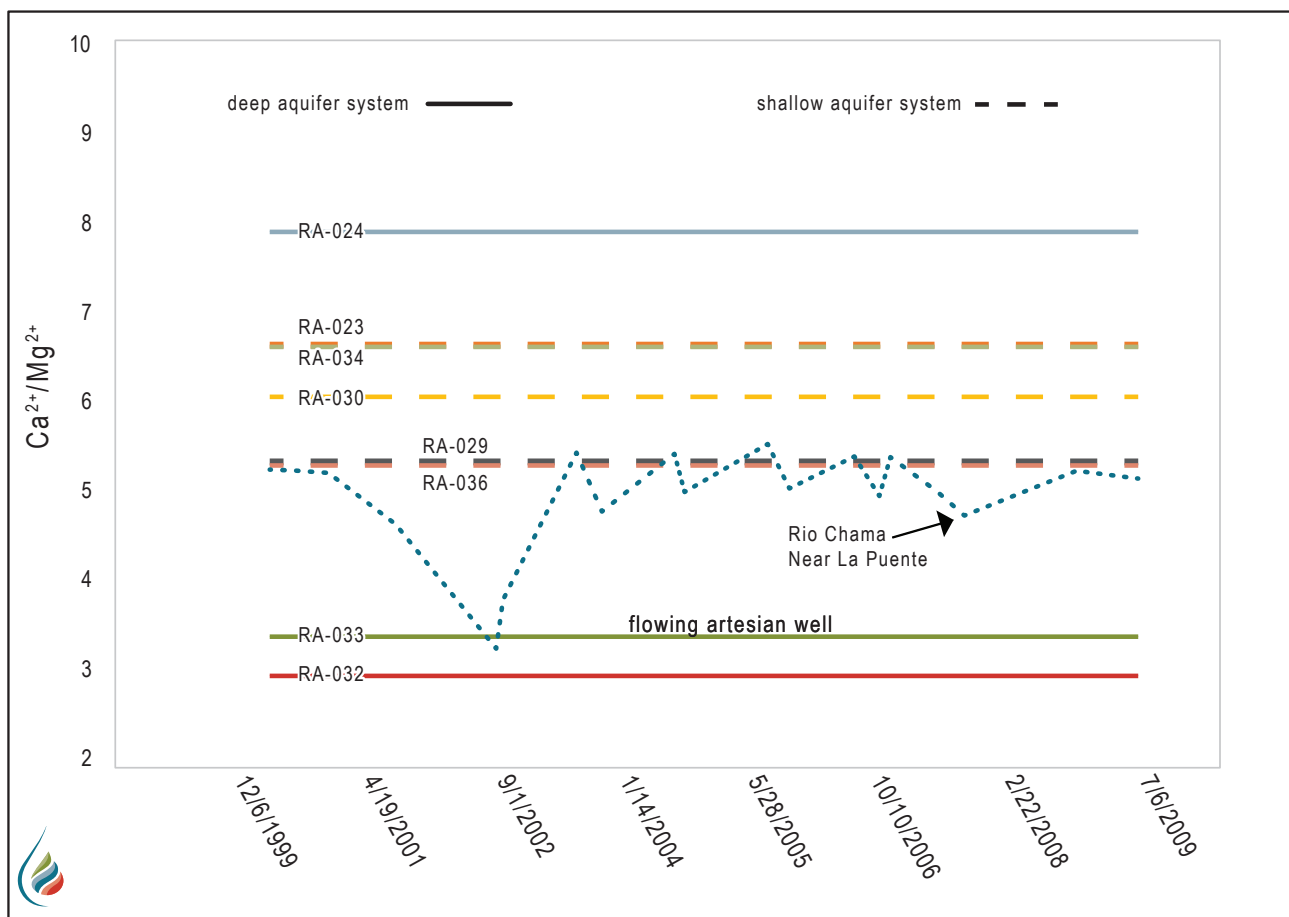
Figure 2.25. The Ca^{2+}/Mg^{2+} ratio for the Rio Chama at La Puente, calculated from USGS data shown in Figure 2.23. The horizontal lines represent the Ca^{2+}/Mg^{2+} ratios for groundwater samples collected in this study.
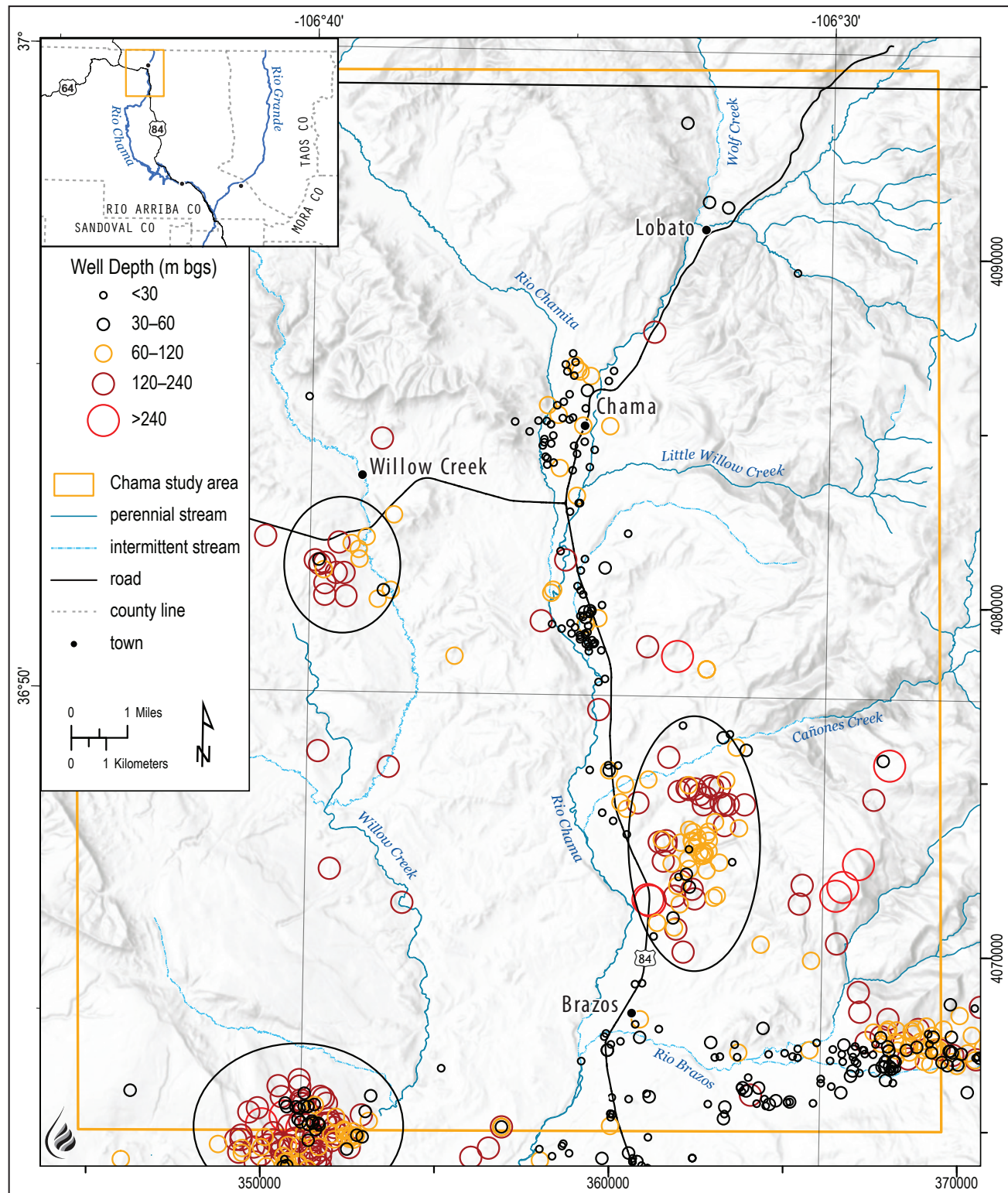
Figure 2.26. Wells with total depths greater than 60 m (200 ft) below the surface (orange and red points). Wells in areas circled in black should be considered for future sampling.

CHAPTER 3: ASSESSMENT OF GROUNDWATER RESOURCES FOR THE COMMUNITIES OF EL RITO, ABIQUIU, AND MEDANALES, NEW MEXICO

THE ABIQUIU VALLEY: EL RITO, ABIQUIU, AND MEDANALES

The villages of El Rito, Abiquiu, and Medanales are situated in adjoining watersheds in the southern part of the Rio Chama watershed (Fig. 3.1). Groundwater is limited in these communities, and surface water supplies irrigation water for local farmers and ranchers through acequias, which have been used for hundreds of years.

El Rito is surrounded by the Carson National Forest, about 12 mi north of Abiquiu, and had a population of 749 in 2020 (U.S. Census Bureau, 2024). Groundwater in the El Rito area is used for domestic and public supply through individual, private domestic, and irrigation wells and two community water systems. El Rito Canyon Mutual Domestic Water Consumers Association (MDWCA) serves approximately 300 users, supplied by one well. El Rito Regional Water and Waste Water Association serves approximately 1,200 users with groundwater from one active well. Historically, finding a secure groundwater source has been challenging in El Rito (La Calandria Associates, Inc., 2006), which has limited sustained growth and development. In general, Santa Fe Group rocks, which are important aquifers in most other areas of the northern Española Basin, are thinner and finer grained in the area surrounding El Rito and therefore have limited potential as an effective community water supply. Studies in the area (Geohydrology Associates, Inc., 1979) have shown that groundwater resources vary greatly from one location to another, with wells (including test holes) ranging in depth from 102 to 731 ft below the surface and yields ranging from 0 to 80 gpm.

Abiquiu, most famous as the home of artist Georgia O'Keeffe, is located 40 mi north of Santa Fe on the Rio Chama and had a population of 181 in 2020 (U.S. Census Bureau, 2024). The primary use of surface water in Abiquiu is irrigation, with water distributed through a network of acequias. Abiquiu's primary groundwater uses are domestic and commercial wells that mainly tap shallow alluvial deposits and deeper Santa Fe Group rocks. The Abiquiu MDWCA serves about 400 people with water discharging from a spring approximately 10 mi southwest of Abiquiu along Abiquiu Creek. With the current flow rate, this spring is barely adequate to meet the demands of Abiquiu. The nearby community of Barranca, which is located just west of Abiquiu, relies on groundwater pumped from one well to the Barranco MDWCA.

Medanales is located about 8 mi downstream of Abiquiu on the Rio Chama and had a population of 224 in 2020 (U.S. Census Bureau, 2024). The primary uses of groundwater and surface water are similar to those in Abiquiu: domestic wells supply households and surface water is used for irrigation through a network of acequias. There are no public water systems in Medanales. In general, due to limited thickness and areal extent, alluvial aquifers are not a reliable groundwater source. Deeper aquifers in the Santa Fe Group show some promise for domestic water supplies in this area (La Calandria Associates, Inc., 2006). Securing a stable long-term groundwater source in this area is crucial to Medanales's ability to respond resiliently to changes in future water supply and demand.
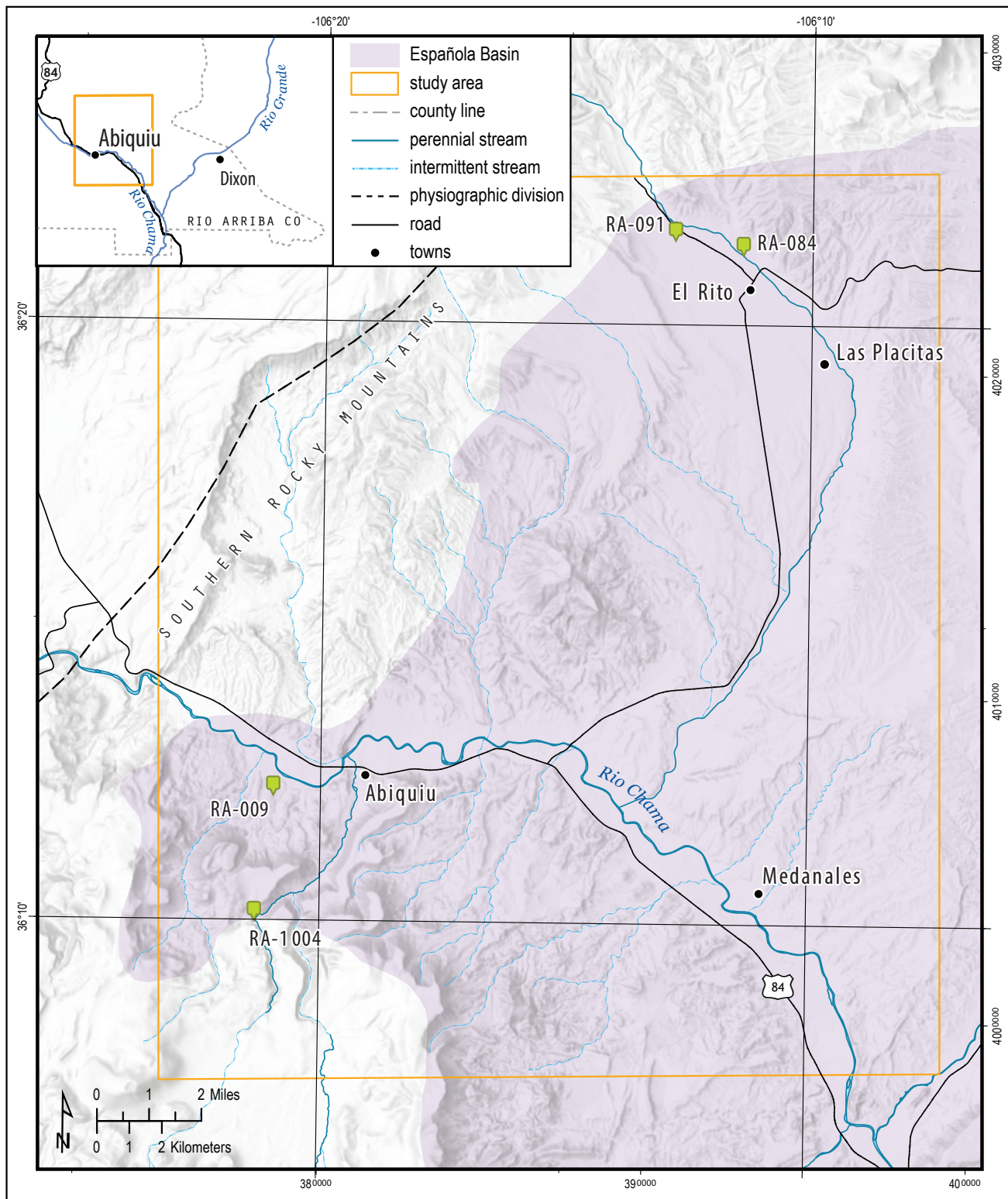
Figure 3.1. Location of the Abiquiu Valley study area, which includes the communities of El Rito, Abiquiu, and Medanales. Community mutual domestic wells serving El Rito include RA-091 and RA-084. The municipal well (RA-009) and the spring (RA-1004) that provide Abiquiu with water are to the south.

Local Geology

The Española Basin is one of the main geologic basins that define the Rio Grande rift and is located south of the San Luis Basin and north of the Albuquerque Basin (Fig. 3.1). This study focuses on the northwest portion of the Española Basin, largely coinciding with the Abiquiu embayment and the lower Rio Chama watershed, where El Rito, Abiquiu, and Medanales are located. The stratigraphy of the Abiquiu embayment portion of the northern Española Basin is dominated by Santa Fe Group basin-fill deposits and minor interfingering tongues of volcanic units (May, 1979, 1984a, 1984b; Koning et al., 2004a, 2008, 2011a). The Santa Fe Group basin-fill deposits include the Abiquiu and Tesuque Formations (Fig. 3.2) and cover a time period ranging from the late Oligocene to the middle Miocene (about 27 to 8 million years ago; Koning et al., 2011a, 2011b). The Ritito Conglomerate (pebble to cobble gravel conglomerate) and the El Rito Formation (red lithified conglomeratic sandstone, sandstone, and mudstone) unconformably overlie Proterozoic–Mesozoic rocks. Much focus in this section is given to the sedimentary member units of the Tesuque Formation because these units of the Santa Fe Group are important aquifers. However, we also discuss overlying Quaternary sediments due to their implications for groundwater storage and flow.

Quaternary surficial units in the Abiquiu embayment of the Española Basin are predominantly divided between colluvial and alluvial features (Koning et al., 2004a, 2008; Maldonado, 2008). The colluvial units consist of undivided colluvium with landslide, eolian, and sheetwash deposits. The alluvial features consist of valley-floor alluvium, alluvial fan deposits, and gravel terraces associated with local modern tributaries and minor drainages. Valley-floor alluvial sequences range in age from latest Pleistocene to the present and are generally composed of silty sands, sands, and gravels underlying modern valley floors of the Rio Chama and its tributaries. These alluvial deposits generally occur in planar to lenticular beds. Compositionally, they primarily reflect erosion of upstream basin-fill sediment of the Santa Fe Group and older bedrock units. Alluvial fan deposits are generally found at the mouths of modern canyons, but some older fans are found at higher topographic positions in the valleys. Gravel terraces range in age from late Miocene to Quaternary.

The upper and middle part of the Santa Fe Group generally correlates to the Tesuque Formation (Fig. 3.2). The Miocene Ojo Caliente Sandstone (thickness up to 200–400 m [650–1,300 ft]) is the uppermost member unit of the Tesuque Formation near the communities we studied. The Ojo Caliente here is composed of light-tan to tan, typically upper-fine to upper-medium sands that are interpreted to reflect deposition in a wind-blown (eolian) dune field depositional environment (May, 1979; Koning et al., 2004a, 2011b). The lower Ojo Caliente interfingers with the underlying Miocene Chama-El Rito Member, which is distinguished from the overlying Ojo Caliente sandstone by its slight orange color and presence of interbedded mudstones and variably cemented gravels (conglomerates; May, 1979; Ekas et al., 1984; Koning et al., 2004a). Outside of the cemented gravel beds, the sands are mainly lower fine to upper fine (Koning et al., 2004a). The Chama-El Rito Member may be up to
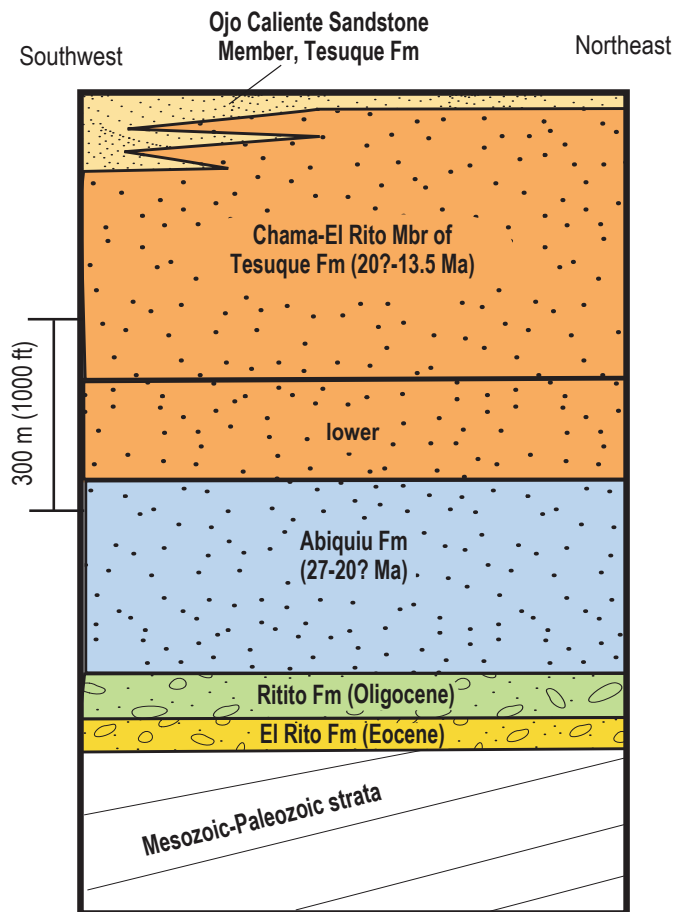
Figure 3.2. Stratigraphic column for the Abiquiu embayment of the northern Española Basin (modified from Koning et al. [2008]).

600 m (2,000 ft) thick and becomes increasingly consolidated downward, probably corresponding to a decrease in permeability. The lower part of the Chama-El Rito Member, exposed southeast of El Rito, is lighter colored, better consolidated and cemented, and commonly exhibits more distinctive bedding than sandy intervals upsection (Koning et al., 2008). The Chama-El Rito Member becomes increasingly gravelly to the north-northeast.

Underlying the Chama-El Rito Member are 300 m (985 ft) of strata composed of either the Cordito Member of the lower Los Pinos Formation or the Abiquiu Formation (Koning et al., 2011a). The Cordito Member grades laterally southwest into the Abiquiu Formation, but near El Rito, a tongue of the upper Cordito 30 to 60 m (100–200 ft) thick extends over the Abiquiu Formation (Koning et al., 2008). The Cordito Member is composed of volcaniclastic sandstones (fine to very coarse grained) and gravels (Manley, 1981; Koning et al., 2008). The Abiquiu Formation is a whitish sandstone, pebbly sandstone, and clayey-silty sandstone with minor sandy gravel beds (Smith, 1935, 1938; Vazzana and Ingersoll, 1981; Smith, 1995; Moore, 2000; Koning et al., 2008, 2011a; Maldonado, 2008). This unit is around 150 m (500 ft) thick near Abiquiu (Maldonado, 2008). Erosion of the Abiquiu Formation has created the picturesque, whitish badlands seen near the town of Abiquiu (Koning et al., 2008).

The underlying Ritito Conglomerate and El Rito Formation are significantly thinner collectively (200–300 m [650–1,000 ft]) in the Abiquiu area (Maldonado, 2008) than the two overlying Santa Fe Group formations. They are generally coarse-grained sedimentary rocks containing notable proportions of gravel and medium- to very coarse-grained sandstones (Smith, 1938; Barker, 1958; Kelley, 1978; Moore, 2000; Maldonado and Kelley, 2009; Kelley et al., 2013). The El Rito Formation unconformably overlies a sequence of Proterozoic–Mesozoic rocks that generally do not crop out in the northern Española Basin (Kelley, 1978).

From a hydrogeologic perspective, Quaternary alluvial deposits make the best aquifers because these deposits have higher permeability than the units of the Santa Fe Group (Koning et al., 2007). Aquifer tests in the Quaternary alluvium near El Rito showed high hydraulic conductivity and relatively thick alluvium depths (Geohydrology Associates, Inc.,

1979). However, the areal extents and thicknesses of these deposits vary significantly throughout the Rio Chama watershed. The Ojo Caliente Member of the Tesuque Formation exhibits lower permeability than alluvial sediments (Koning et al., 2007) but is inferred to be more permeable than the middle to lower Chama-El Rito Member (Tesuque Formation). In general, the permeability of the Tesuque Formation decreases with depth. However, there appear to be multiple permeable zones within the Chama-El Rito Member that produce good-quality water under confined conditions in the Medanales and Abiquiu regions.

Figure 3.3 shows the study region on a simplified geologic map, along with cross-section lines, including a west–east cross section (Fig. 3.4) perpendicular to El Rito Creek, from the El Rito 7.5-minute quadrangle (Koning et al., 2008); a west–east cross section (Fig. 3.5) approximately parallel to the Rio Chama, based on geologic map data from the Abiquiu 7.5-minute quadrangle (Maldonado, 2008) and NMOSE well data; and a northwest–southeast cross section (Fig. 3.6) approximately parallel to the Rio Chama based on surface geology from Koning et al. (2004a) and NMOSE well data.

El Rito is located along El Rito Creek, about 15 mi upstream from the confluence with the Rio Chama. The small community of Las Placitas is located just downstream of El Rito. These communities are located where the valley widens, with Quaternary terrace deposits (Qt) to the west of El Rito Creek and associated Quaternary alluvium deposits (Qa) under the modern river. The terrace deposits are associated with El Rito Creek and are generally 6 to 25 m (20–80 ft) above the present-day channel elevations (Koning et al., 2008). Quaternary alluvium is located at the valley bottoms adjacent to El Rito Creek and the Rio Chama.

Over much of the study area, Santa Fe Group rocks are exposed at the surface, with the Ojo Caliente Member of the Tesuque Formation (Tto) cropping out in the southern and southeastern portion of the study area, south of Abiquiu and surrounding Medanales. Moving downsection, the Chama-El Rito Member of the Tesuque Formation is exposed in the lower slopes of mesas to the east and northeast of Abiquiu. The Chama-El Rito Member is relatively extensive south of El Rito.
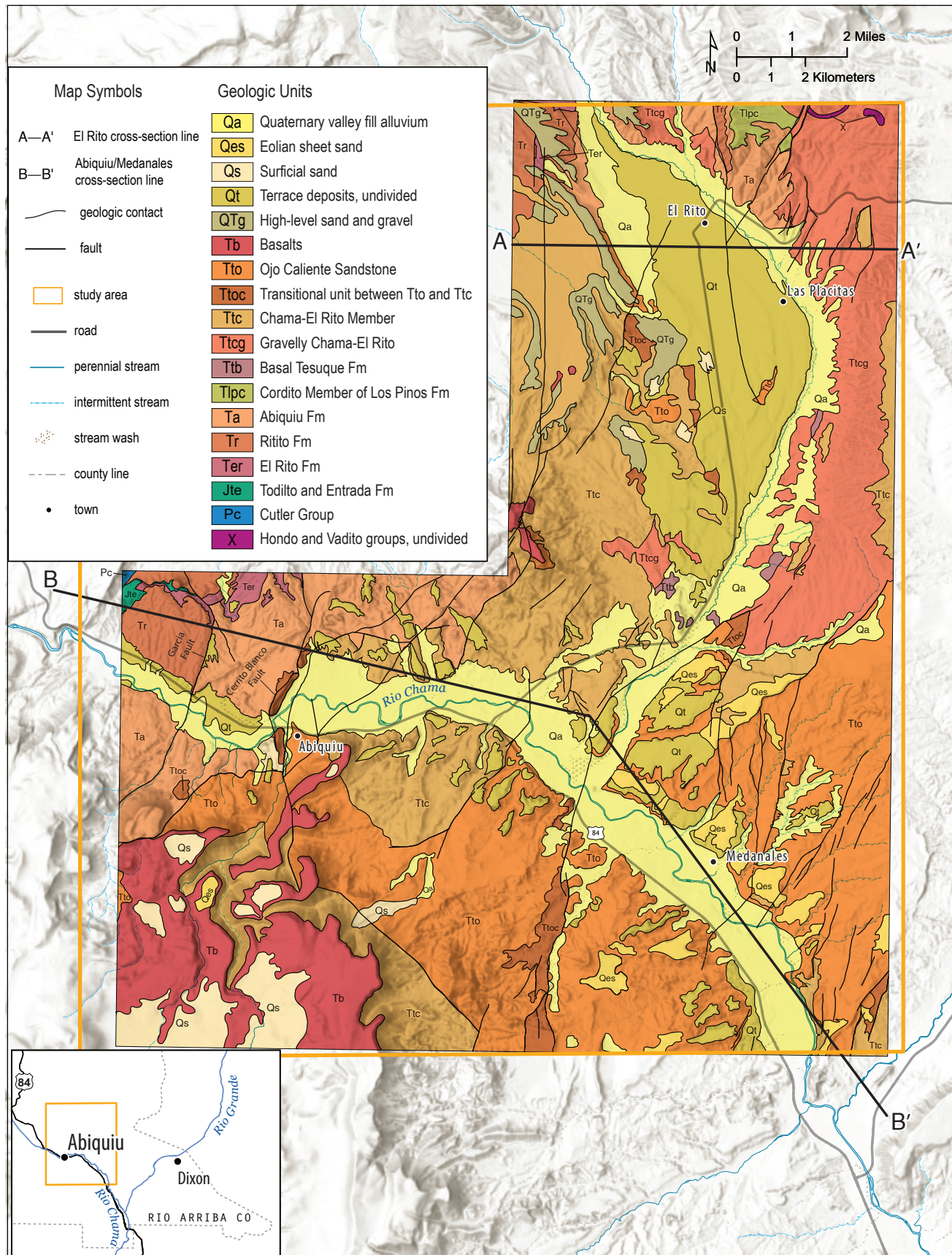
Figure 3.3. Overall study area along with a simplified geologic map modified from Koning et al. (2008) and Maldonado (2008). Cross-section lines for Abiquiu, Medanales, and El Rito are also shown.
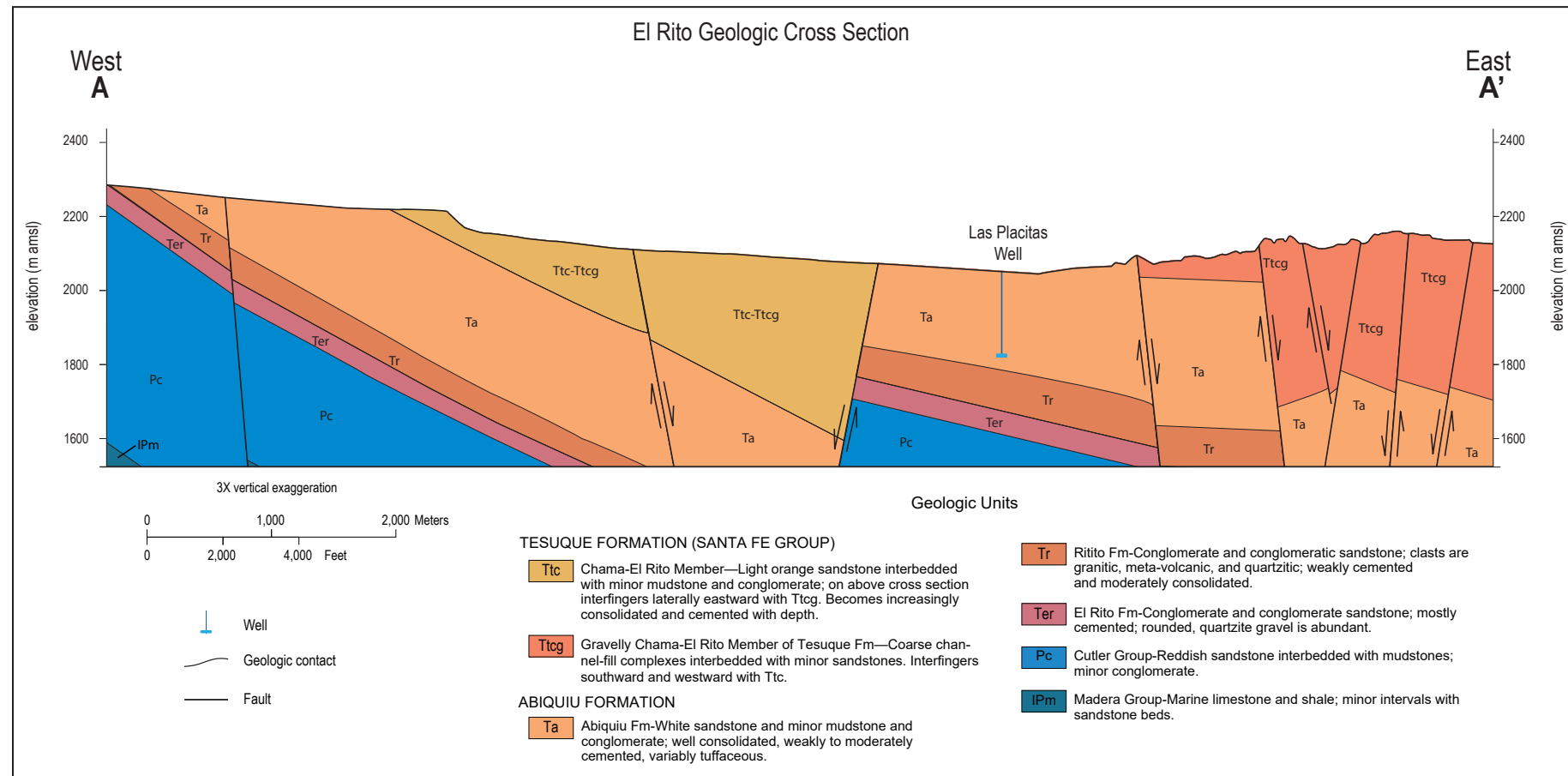
Figure 3.4. Geologic cross section for the El Rito area (vertical exaggeration = 3×; Koning et al., 2008).
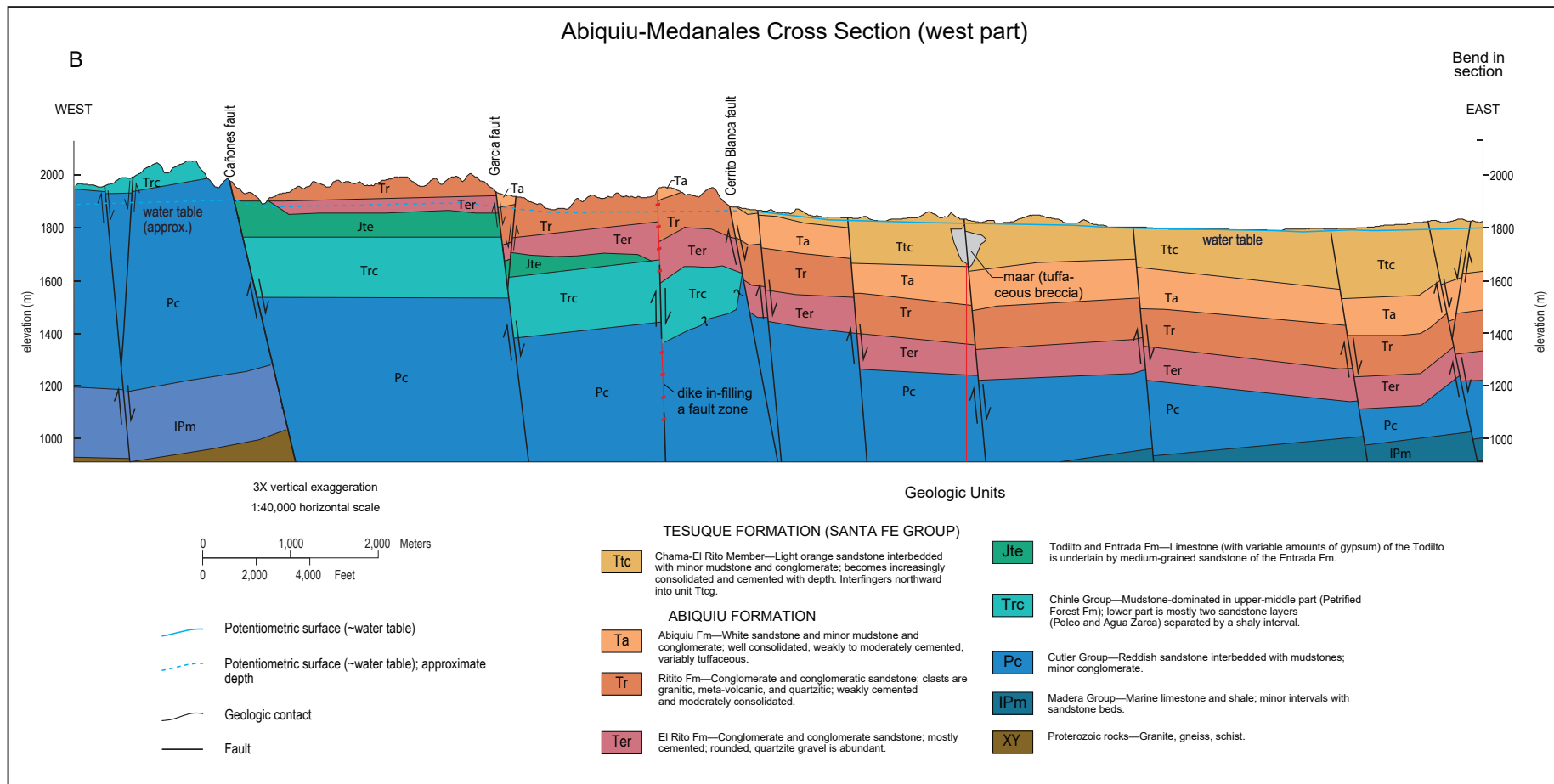
Figure 3.5. Geologic cross section for the Abiquiu area, based on the Abiquiu 7.5-minute quadrangle geologic map (Maldonado, 2008), NMOSE well records, and seismic data in Baldridge et al. (1994). Vertical exaggeration is 3x.
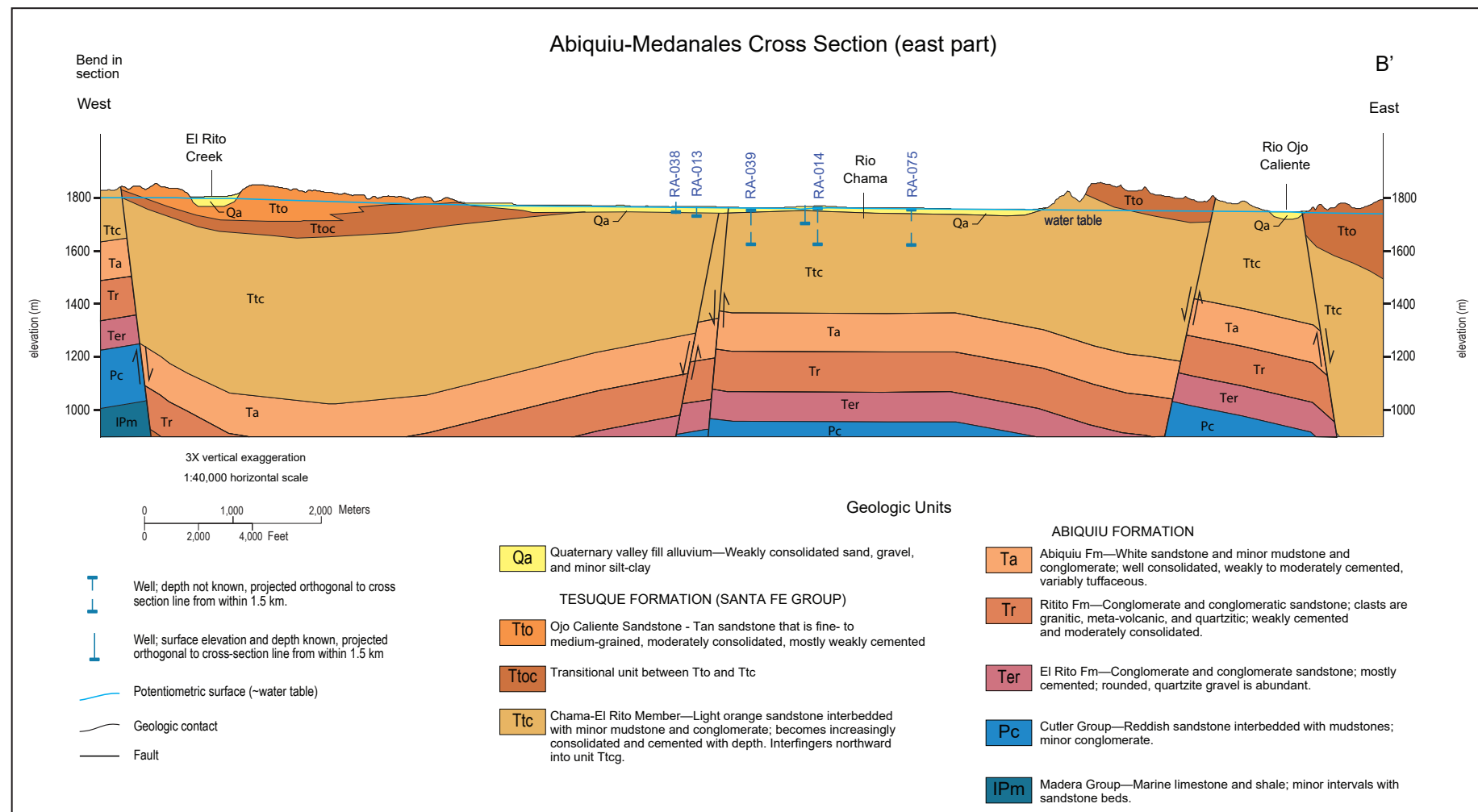
Figure 3.6. Geologic cross section for the Medanales area, based on the Medanales 7.5-minute quadrangle geologic map (Koning et al., 2004a) and NMOSE well records. Vertical exaggeration is 3x.

The Abiquiu Formation is exposed just north and southwest of Abiquiu. Important faults include the Cañones fault about 6 km (3.7 mi) to the west of Abiquiu, the Garcia fault 3 km (1.8 mi) west of Abiquiu, the Cerrito Blanca fault near Abiquiu, and the fault system that somewhat parallels southern El Rito Creek (i.e., the El Rito fault).

Local Hydrogeology

Average precipitation in Rio Arriba County displays general seasonal and spatial trends; it is usually greater at higher elevations, during summer, and to the north. Average annual precipitation at El Rito and Abiquiu Reservoir is 308 and 247 mm (12 and 9.7 in.), respectively, with about 50% of precipitation falling during the summer monsoons between July and September. Flow in the Rio Chama in the Abiquiu and Medanales areas is primarily controlled by water releases from Abiquiu Reservoir (Fig. 3.7). The original purpose of Abiquiu Dam was to control flooding and sediment loads to the Rio Grande.

The majority of wells in the Abiquiu area are located in the Rio Chama valley, while wells in the Medanales area are largely located in the hills to the north and south of the river valley. Depth-to-water values of less than 15.2 m (50 ft) are common in and near the river valley and increase with distance from the Rio Chama to over 122 m (400 ft) at 1.6 km (1 mi) north of the river, to the west and east of El Rito Creek. The primary use of groundwater around Abiquiu is domestic, with some wells for irrigation, livestock, and commercial use. Wells in Medanales are almost all used as domestic wells, with some used for livestock watering.

Streamflow in El Rito Creek has not been monitored since the 1950s, but available data (Fig. 3.8) suggest streamflow is perennial at the old USGS site, which was very close to well RA-080. Flow-rate data in El Rito Creek show a native flow regime with spring runoff peak flows ranging from about 20 to 800 cfs. Observations from aerial photography suggest that El Rito Creek is perennial down to about 5.5 km (3.4 mi) north of the confluence of El Rito Creek and the Rio Chama. The primary use of groundwater in this area is domestic, with some wells used for irrigation and a few for livestock watering and community use. Wells in the El Rito area are mostly completed in a shallow alluvial aquifer composed of boulders, gravel, sand, and clay, locally overlying gray clay or sandstone. The majority of wells are completed at depths less than 46 m (150 ft), but a few domestic wells have been completed near 91 m (300 ft) deep. This shallow aquifer is likely replenished by precipitation and melting snow from the surrounding hills and is connected to El Rito Creek.

During the 1950s and 1960s, several shallow (around 7 m [23 ft]) collection galleries supplied the communities of El Rito and Las Placitas (Geohydrology Associates, Inc., 1979), and hundreds of private wells tapping shallow gravel deposits supplied water to local residents. Wells drilled into the shallow aquifer ranged from 12 to 24 m (40–80 ft) deep. Groundwater levels fluctuate seasonally, with the highest water levels occurring in spring when excess water in the acequias is diverted from El Rito Creek. Groundwater levels in the shallow alluvial aquifer are lowest during late fall and winter when flow in the acequias is low; hand-dug wells up to 8 m (26 ft) deep would sometimes go dry during winter months. Geohydrology Associates, Inc. (1979) conducted an aquifer test on a well located northwest of El Rito on a former sawmill site. The sawmill well, with a total depth of about 31 m (102 ft), apparently penetrated a buried channel deposit composed of an unusually thick sequence of gravel and had an approximate sustained production of about 80 gpm. Water from this well was of good quality, with TDS below 500 mg/L. The existence of this well in the shallow alluvial aquifer indicates that, in some areas of the thin alluvial aquifer, there may be zones that can produce enough good-quality water to supply local communities.

An exploratory well in Las Placitas (shown in Fig. 3.4 as Las Placitas Well) was drilled to the depth of 223 m (731 ft), penetrating the Los Pinos and Abiquiu Formations (Geohydrology Associates, Inc., 1979). The well log for this well shows permeable materials, such as medium- and coarse-grained sand and some gravel. However, an abundance of clay impacts the permeability of this aquifer; it has an estimated sustained pumping rate of 14 gpm. This water exhibited a low TDS concentration of 220 mg/L, a sodium-bicarbonate water type, and a pH of 8.87.
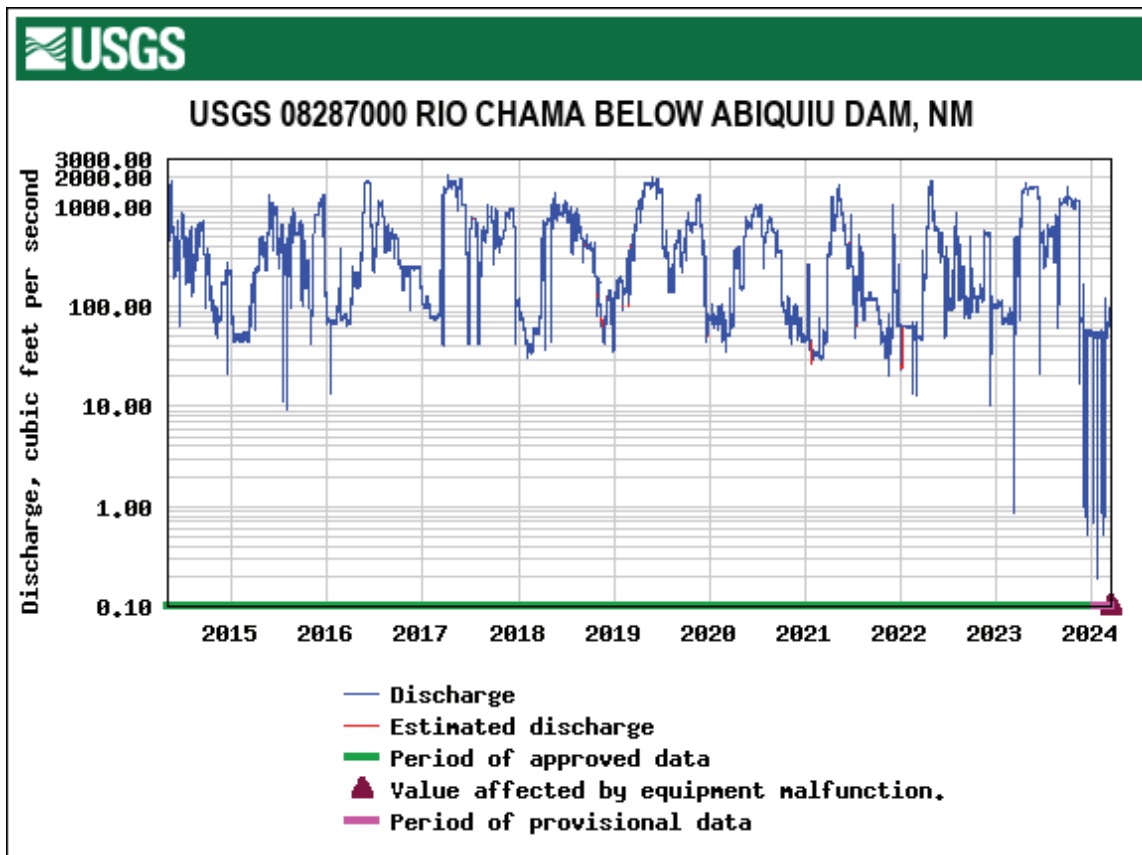
Figure 3.7. Discharge data for the Rio Chama below Abiquiu Dam (USGS gage 08287000). See Figure 1.1 for gage location.
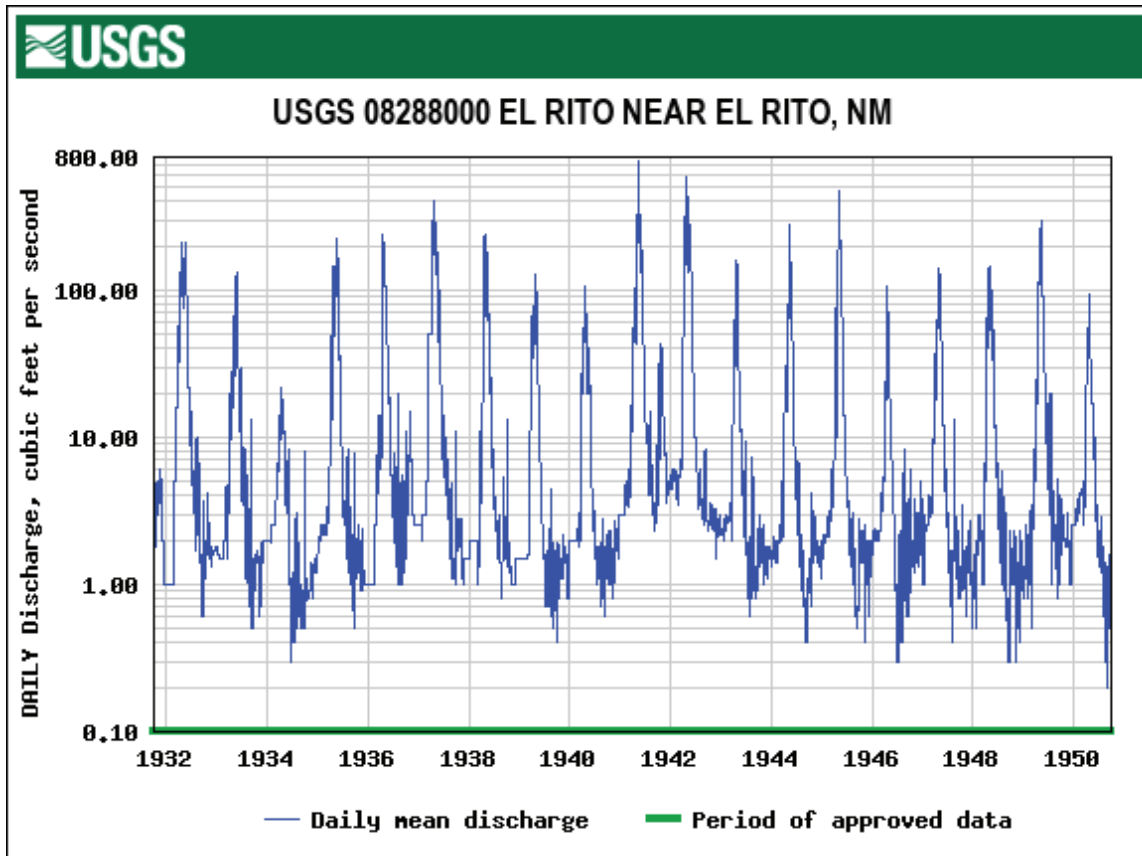
Figure 3.8. USGS hydrograph for El Rito Creek between 1930 and 1950 (USGS gage 08288000). See Figure 1.1 for gage location.

DATA ASSESSMENT

Existing Data

Figure 3.9 shows wells for which depth-to-water measurements were included in the well-drilling records (NMOSE, 2024). These data were used to differentiate wells producing water from the shallow alluvial aquifer from those producing water from the deep aquifer system.

New Data Collection

For this regional study area, we inventoried 42 wells, 34 of which were sampled (Fig. 3.10) for general chemistry (major cations and anions), trace metals, the presence of bacteria, and the stable oxygen and hydrogen isotopes of water. A subset of 24 samples was tested for carbon-14 and tritium, which provides information about how long the water has been in the subsurface. Timmons et al. (2013) described the sampling procedures we used in more detail.

RESULTS

Water Levels

Figure 3.11 shows depths to water reported in well-drilling logs (NMOSE, 2024), ranging from 0.9 to 207 m (3–680 ft) below the surface. Total well depths range from 2.4 to 317 m (8–1,000 ft) below the surface. Similar spatial variability is observed for both depth to water and total well depth, with wells with the smallest depth-to-water values and shallowest total depths occurring in close proximity to the Rio Chama and El Rito Creek. Obviously, these wells likely tap the shallow alluvial aquifer. A notable feature of the spatial distribution of wells is the large group of wells north of Medanales with depth-to-water measurements greater than 10 m (33 ft) below the surface (Fig. 3.11). These wells tap groundwater at greater depths within the Santa Fe Group rocks.

Figure 3.12 shows the same depth-to-water measurements as a function of total well depth. The rectangle at the bottom left defines the 80th percentile for both depth to water and total well depth. About 75% of all the wells are within this group and are likely completed in the shallow alluvial aquifer. Assuming these wells fully penetrate the shallow alluvial aquifer (meaning the bottom of the well coincides with the bottom of the aquifer), we can estimate the saturated thickness of the aquifer in the vicinity of the well by subtracting depth to water from the total well depth. Assuming that depth to water and total well depth for those wells are representative of most of the shallow alluvial aquifers, the maximum saturated thickness is about 30 m (100 ft).

As well depth increases, so does the maximum observed depth to water, indicating the groundwater being tapped by deeper wells is located significantly below the shallow alluvial aquifer. However, for most wells with total depth between 50 and 250 m (160 and 820 ft) below the surface, depth-to-water measurements range from just a few meters above the bottom of the well to tens of meters above the total well depth (close to the surface). Well records for many of these wells identify the depth of the water-bearing unit to be near the total well depth. Water from this unit is usually under pressure that causes the water level to rise in the well above the water-bearing unit, sometimes bringing it very close to the surface.

Figure 3.13 focuses on the El Rito area, which is located at a higher elevation than Abiquiu or Medanales. The depth to water for most wells in this area is less than 10 m (33 ft) below the surface, and most wells are located near the valley bottom, which correlates to young Quaternary alluvium and terrace deposits (Fig. 3.13). A few wells with deeper depth-to-water measurements are scattered throughout the area.

Along the Rio Chama between Abiquiu and Medanales, spatial trends for depth to water in existing wells are much more apparent, with most wells with depth to water of less than 5 m (16 ft) located closest to the river, on or just above the valley bottom (Fig. 3.14). In general, as the distance of the wells from the river increases (and elevations increase), depth to water increases, until about 20 m (66 ft) below the surface. Most wells with depth-to-water values greater than 20 m (66 ft) are located at slightly higher elevations to the north of Abiquiu and Medanales and in the area where El Rito Creek feeds into the Rio Chama. Most of these wells are likely completed in the Tesuque Formation (Chama-El Rito or Ojo Caliente Members).

The contoured water table in the Abiquiu and Medanales area (Fig. 3.15) shows that the shallow alluvial aquifer is being recharged from the surrounding mountains. This can be discerned from contoured water-table lines running parallel to the valley slopes on the north side of the valley.
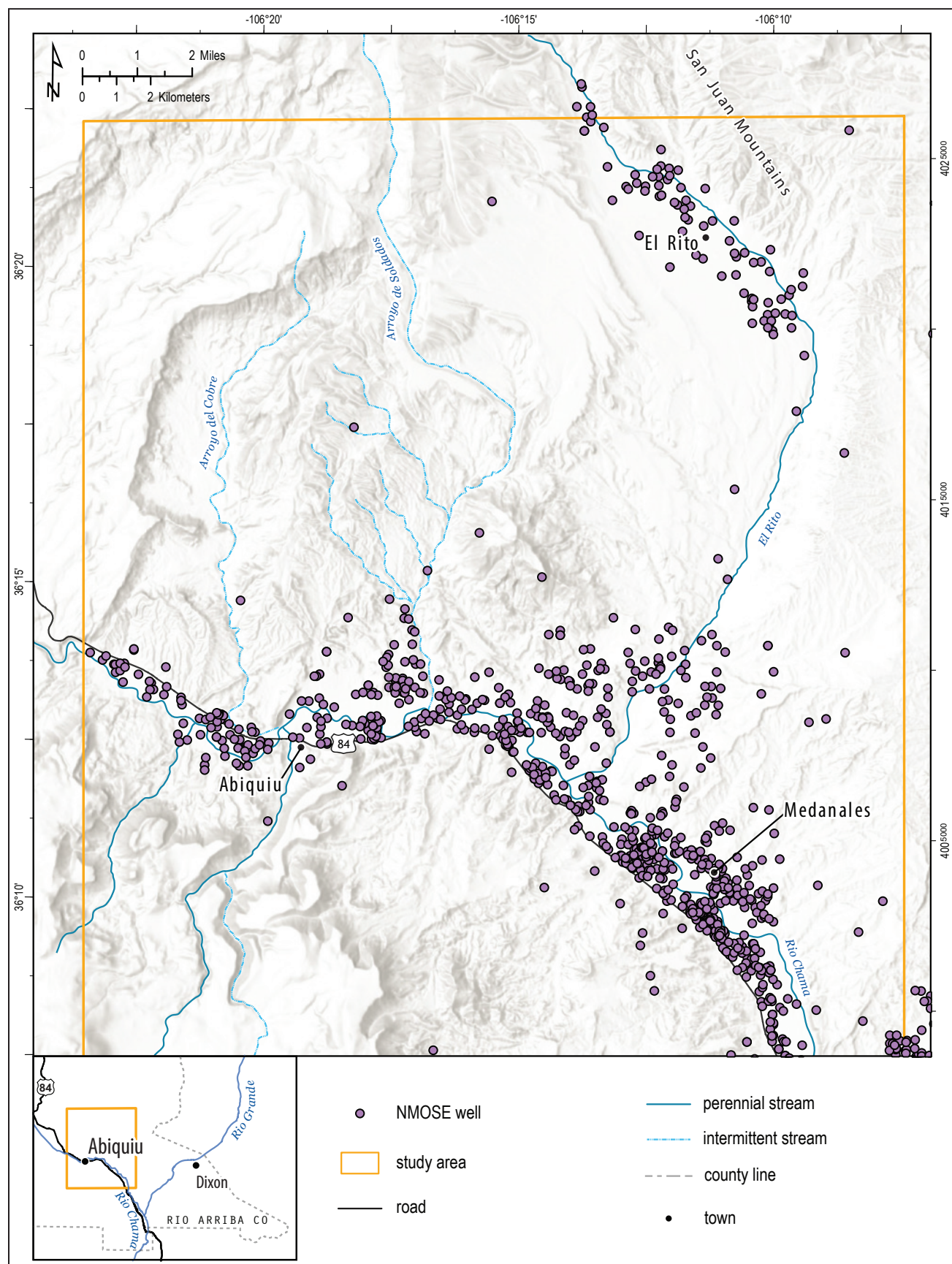
Figure 3.9. Registered wells for which depth-to-water measurements were included in the well logs.
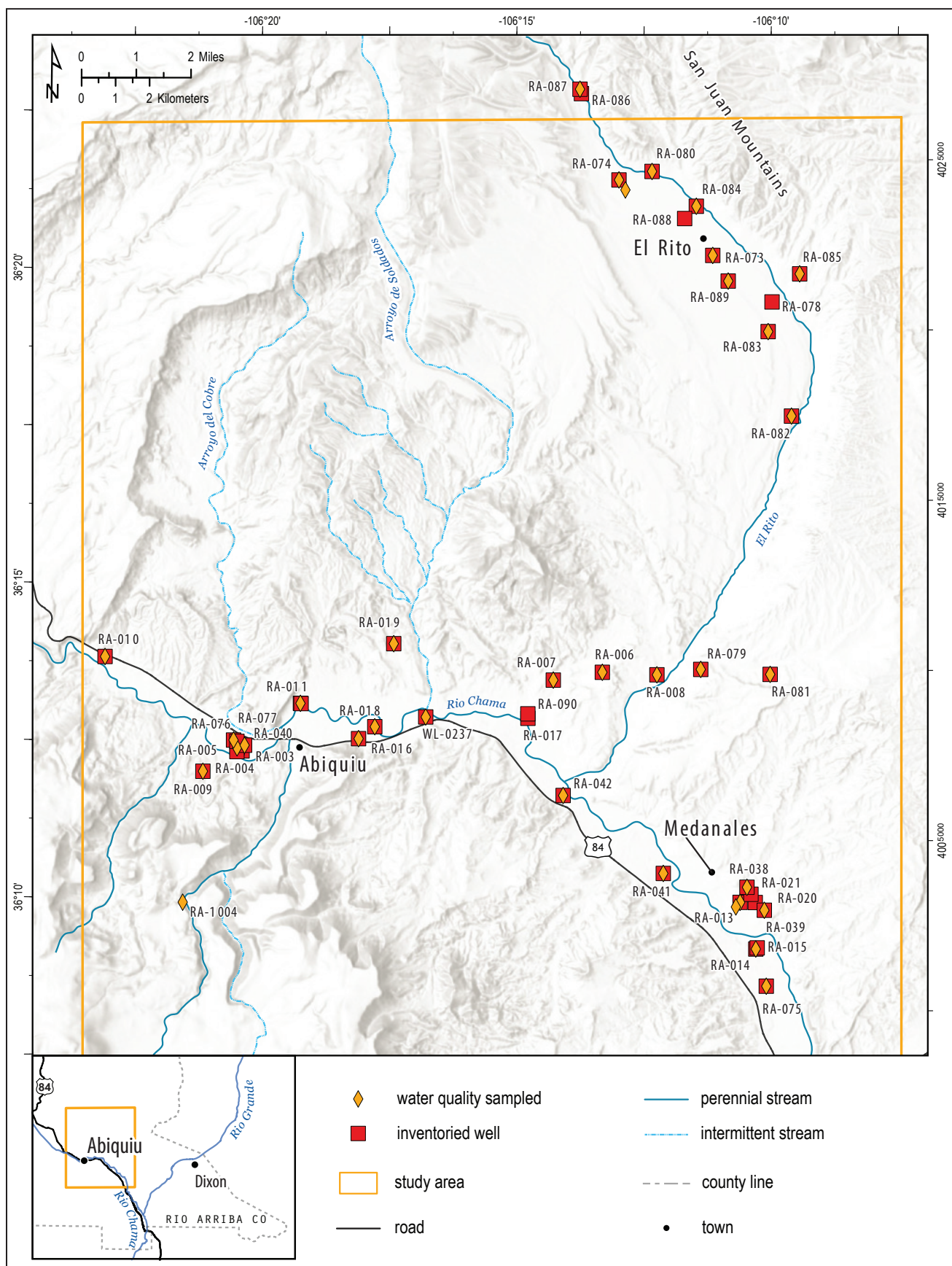
Figure 3.10. Location of sampled and inventoried wells.
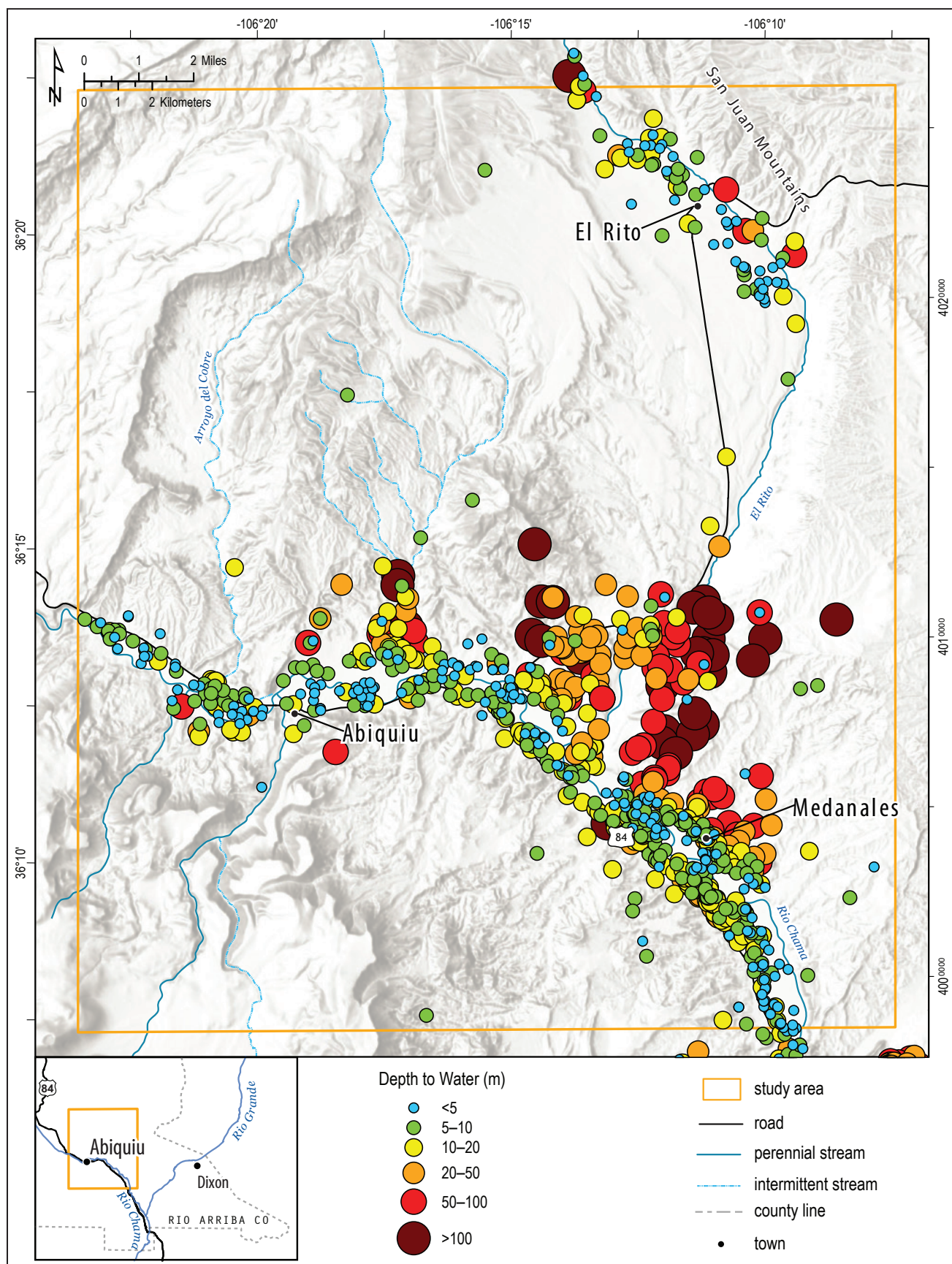
Figure 3.11. Depth-to-water measurements represented by the size and shape of the well location markers.

The water table in this valley near the Rio Chama contributes water to the river flow in some reaches, while in others the river loses water to the aquifer. These gaining and losing reaches, the location of which also changes with time, are controlled by local flow conditions in the Rio Chama. Generally, the flow through the shallow alluvium is parallel to the valley's axis and slightly toward the river. The slope of the water table is fairly shallow at around a 1% gradient (1 m of head drop over 100 m of lateral distance). The saturated thickness of the alluvial aquifer is between 10 and 20 m (33 and 66 ft; Fig. 3.16).

The water table near El Rito and Las Placitas (Fig. 3.15) is different compared to that in the other study areas because El Rito Creek is only a perennial stream in the uppermost reaches of the valley. In the northernmost section of the valley where El Rito Creek flows out of the Tusas Mountains, the valley

is quite narrow, and the water table appears to show gaining conditions (groundwater discharging to El Rito Creek). As the valley widens, the water-table contours flatten out and run perpendicular to the river channel. Farther southeast in the valley, the contours start to bend downstream, indicating the river is losing water to the shallow aquifer. The gradient of the water table in this area is around 2%. The saturated thickness in the El Rito valley is greatest near the center of the basin. Mapping shows there may be as much as 30 m (100 ft) of saturated alluvial aquifer (Fig. 3.16).

Figure 3.17 shows depth-to-water measurements for wells inventoried in the study area, with most wells exhibiting depth-to-water values of less than 20 m (66 ft); this includes all wells inventoried in and around El Rito and in the immediate vicinity of Abiquiu. Wells RA-020 and RA-038 in the eastern
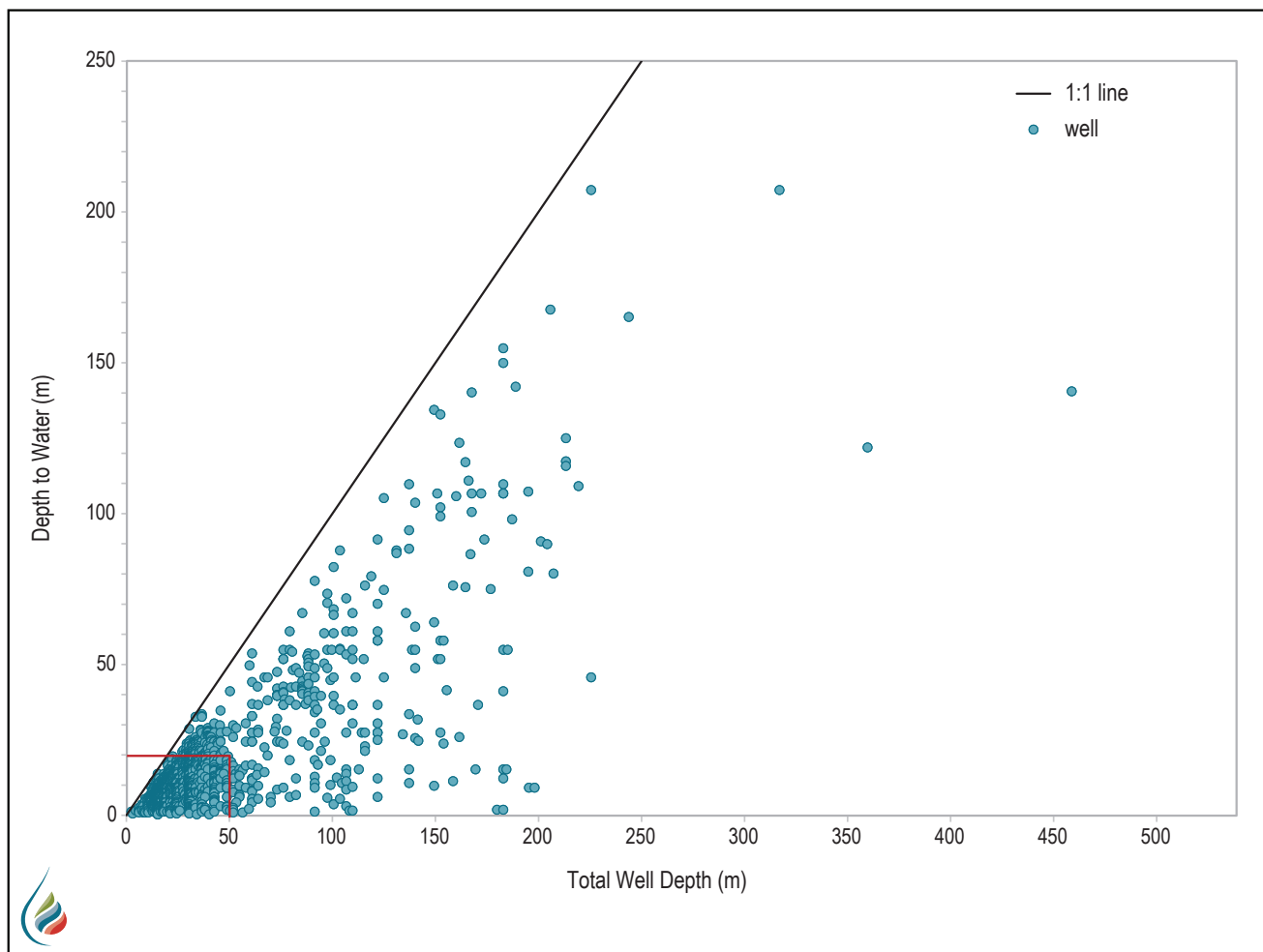
Figure 3.12. Depth-to-water measurements plotted versus total well depth. The rectangle represents the 80th percentile for both depth to water and total well depth.

part of Medanales show slightly deeper depth-to-water measurements of greater than 50 m (164 ft). The greatest depths to water (in RA-007, RA-079, and RA-081) were measured north of the mouth of El Rito Creek among the large group of deep wells shown in Figure 3.11.

Table 3.1 shows depth-to-water measurements for all wells inventoried for this study. If available, total well depth, depth of water-bearing unit, and water-bearing unit description are included. From the depth-to-water measurements and total well depths, we were able to determine whether the well tapped the shallow alluvial aquifer or an aquifer from the

deeper system. This division between shallow aquifer system waters and deep aquifer system waters is used below in the discussion of water chemistry. Note that wells RA-013 and RA-082 are screened in both the shallow alluvial aquifer and the deeper system.

Water level observations in an 18-m-deep (60-ft) well (WL-0237) about 121 m (400 ft) from the Rio Chama suggest the water level of the Rio Chama ultimately controls the groundwater levels in the alluvial aquifer. The shallow alluvial aquifer stores water during high flows and releases water over the course of several months in the winter and spring (Fig. 3.18).
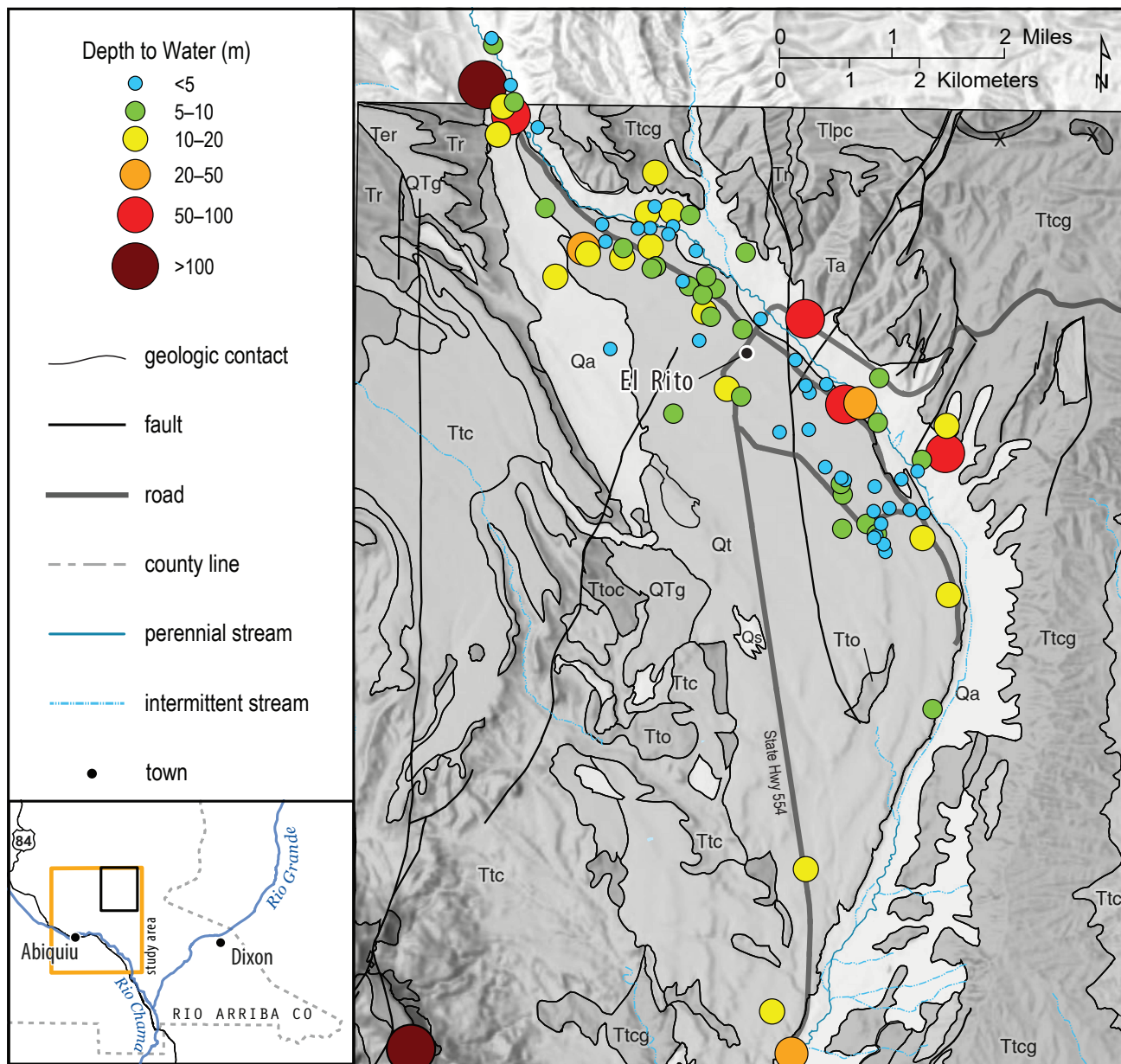
Figure 3.13. Depth-to-water measurements for wells in the El Rito and Las Placitas area, along with local geology (modified from Koning et al. [2008]). Refer to Figure 3.3 for a description of geologic units.
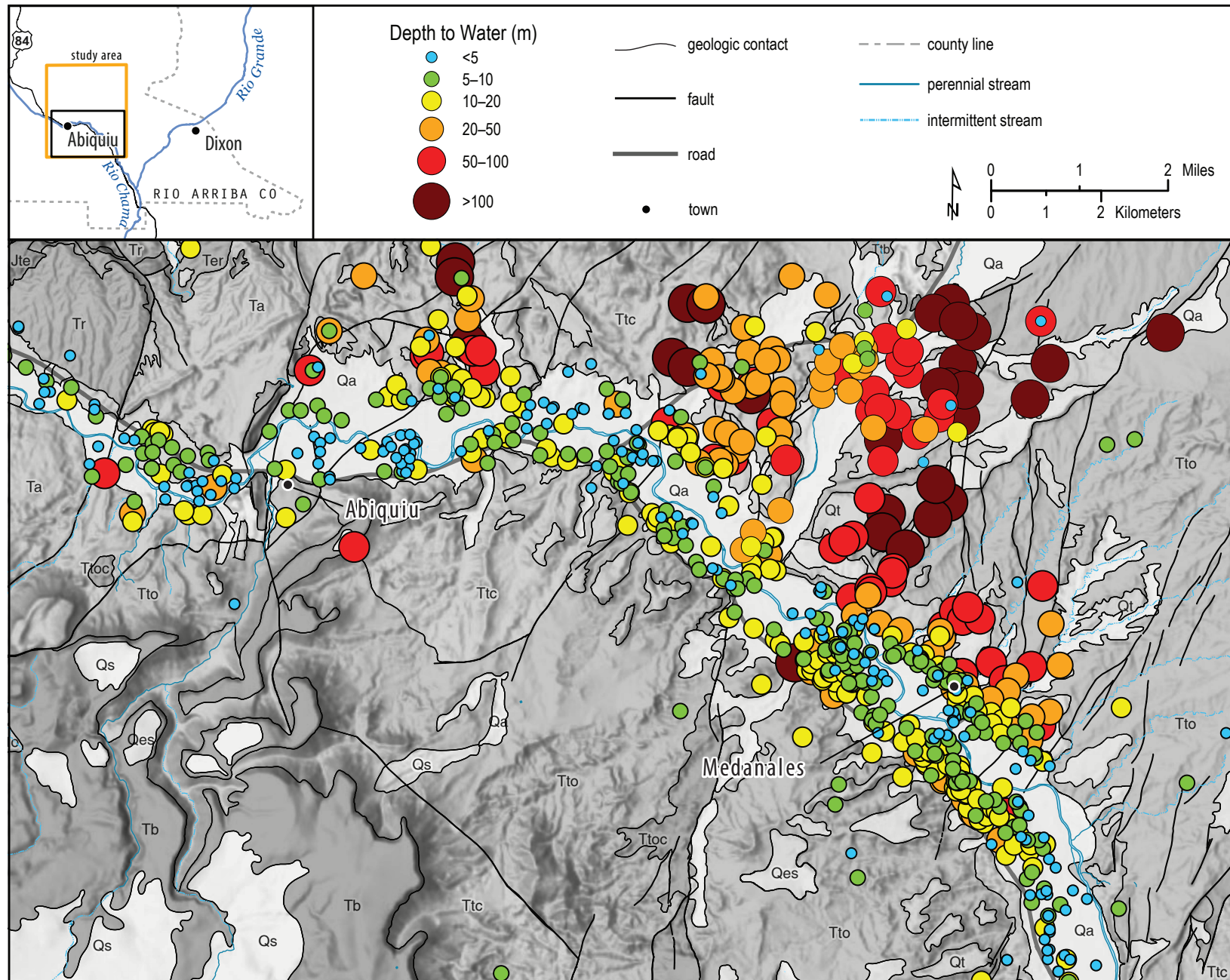
Figure 3.14. Depth-to-water measurements for wells in the Abiquiu and Medanales area, with local geology modified from Maldonado (2008) and Koning et al. (2004a). Refer to Figure 3.3 for a description of geologic units.
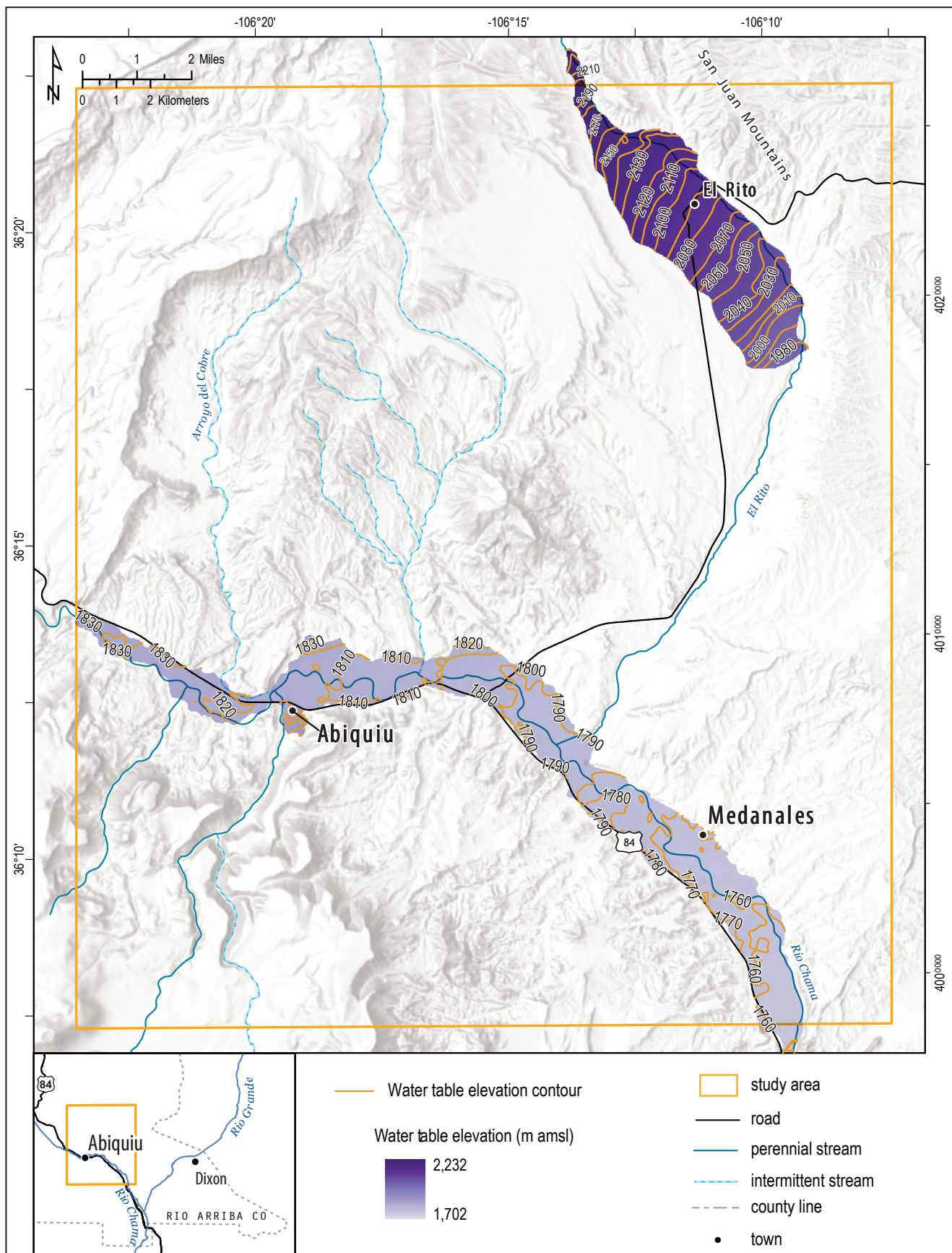
Figure 3.15. Map showing groundwater elevation contours for the shallow alluvial aquifer in the study area.
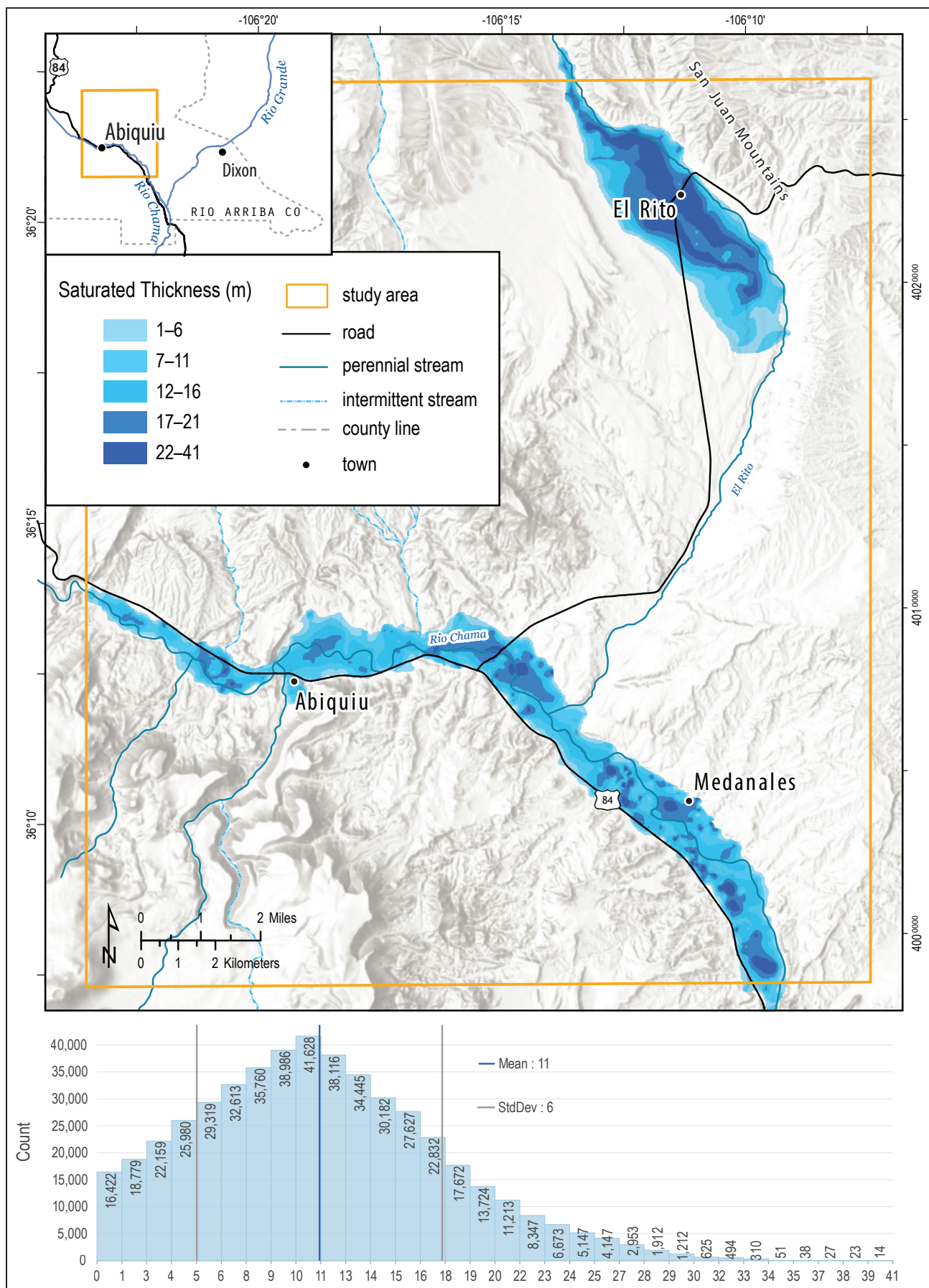
Figure 3.16. Map showing estimated saturated thickness for the shallow aquifer. The saturated thickness was not evaluated in the area between El Rito and the Rio Chama because very few wells are located in this area.
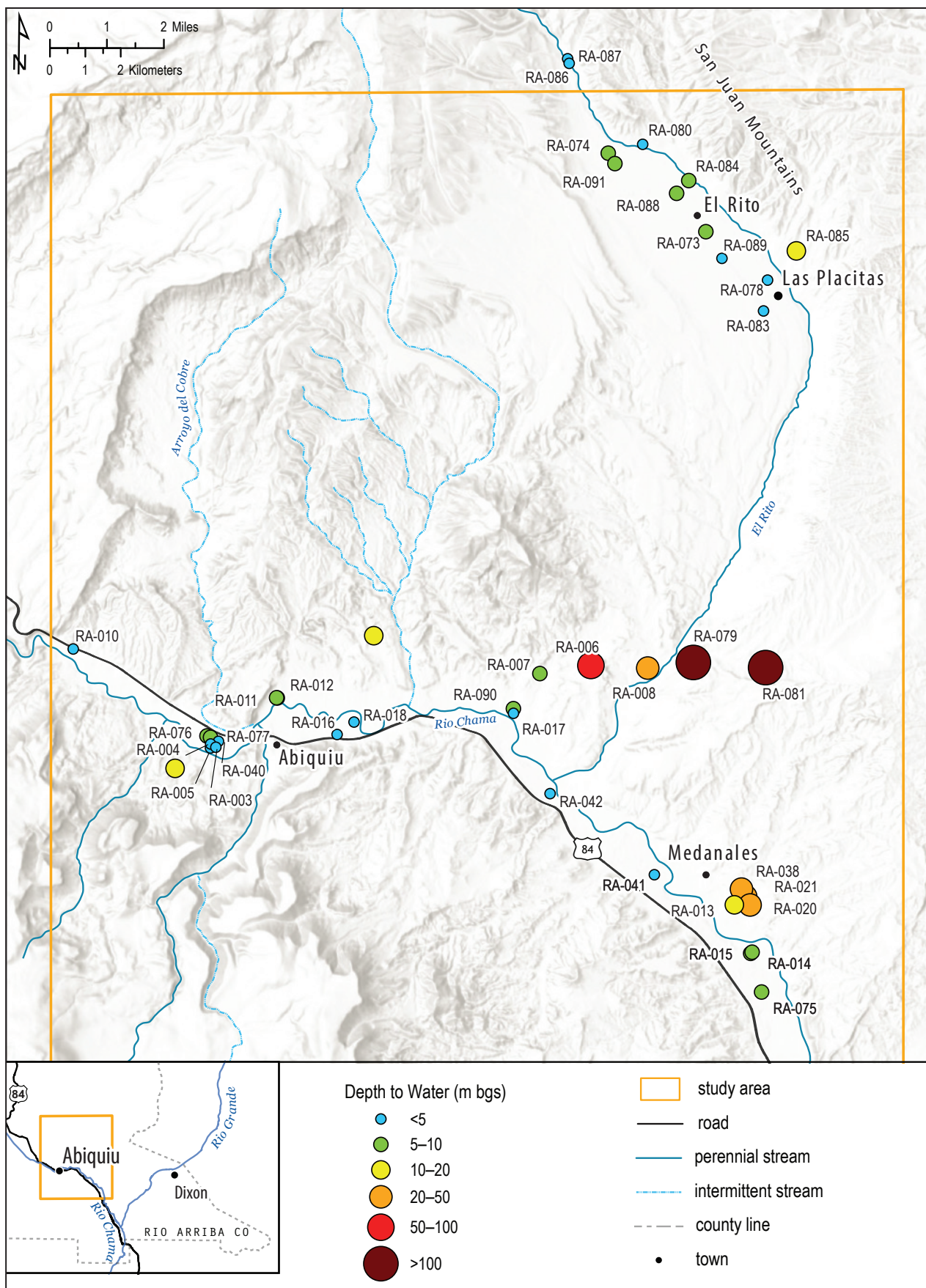
Figure 3.17. Depth-to-water measurements for wells inventoried in the El Rito/Abiquiu/Medanales area.

Table 3.1. Total well depth, depth to water, depth of water-bearing units, lithologic description, and approximate yield for wells inventoried for this study.

Well ID	Area	Total well depth (m)	Depth to water (m)	Depth of water-bearing unit (m)	Water-bearing unit description	Aquifer system	Approximate yield (gpm)
RA-004	Abiquiu	15.24	1.66	3.0–5.5	multicolored sand and gravel	shallow	20+
RA-006	Medanales	51.8	69.3	41.8–42.1	sandstone and red clay	deep	
RA-007	Medanales	108.2	8.83	64.0–108.2	brown clay/sandstone	deep	10
RA-008	Medanales	91.4	37.2	77.7–91.4	fractured sandstone	shallow	
RA-009	Abiquiu	56.4	16.33	16.8–36.6	ash conglomerate	deep	22
RA-010	Abiquiu	15.2	1.34	3.0–5.8	light-brown sand and gravel	shallow	20+
RA-011	Abiquiu	18.3	6.68	7.8–12.5	multicolored coarse gravel	deep	18
RA-013	Medanales	42.7	17.6	36.6–42.7	brown and white sandstone	shallow and deep	10+
RA-014	Medanales	18.6	7.4	6.1–13.4	multicolored fine gravel	shallow	20+
RA-016	Abiquiu	16.8	4.67	5.5–11.9	multicolored coarse gravel, cobbles	shallow	20
RA-018	Abiquiu	15.2	1.95	7.0–13.7	sand with black gravel	shallow	20
RA-019	Abiquiu	121.9	17.5	76.2–77.7	conglomerate	deep	4.5
RA-038	Medanales	45.8	30.7	23.8–45.7	sandstone and light gravel	deep	5
RA-039	Medanales		NA			deep	
RA-040	Abiquiu	50.3	1.9	2.7–8.2	multicolored coarse sand and gravel	shallow	18–20
RA-041	Medanales		1.1			shallow	
RA-042	Medanales	16.8	6.3	1.2–11.6	multicolored fine and coarse gravel, boulders	shallow	18–20
RA-073	El Rito		6.07			shallow	
RA-074	El Rito		8.87			shallow	
RA-075	Medanales		6			shallow	30+
RA-076	Abiquiu	18.3	6.29	8.5–11.9	coarse gravel	shallow	18
RA-079	Medanales		104			deep	25
RA-080	El Rito	42.7	2.57	12.2–30.5	sand and gravel	deep	10
RA-081	Medanales	182.9	121.2	150–182	sandstone/gravel	deep	5
RA-082	El Rito	76.2	9.14	57.9–70.0	gravel	shallow and deep	
RA-083	El Rito		3.31			shallow	
RA-084	El Rito	24.1	8.5	4.6–7.6	cobbles and boulders with some coarse sand	shallow	
RA-085	El Rito	93.0	14.7	71.6–90.5	sand and gravel	deep	8
RA-087	El Rito	15.2	3.8	8.5–15.2	sand and gravel	shallow	6
RA-089	El Rito		10.5			shallow	
RA-091	El Rito		6.9			shallow	
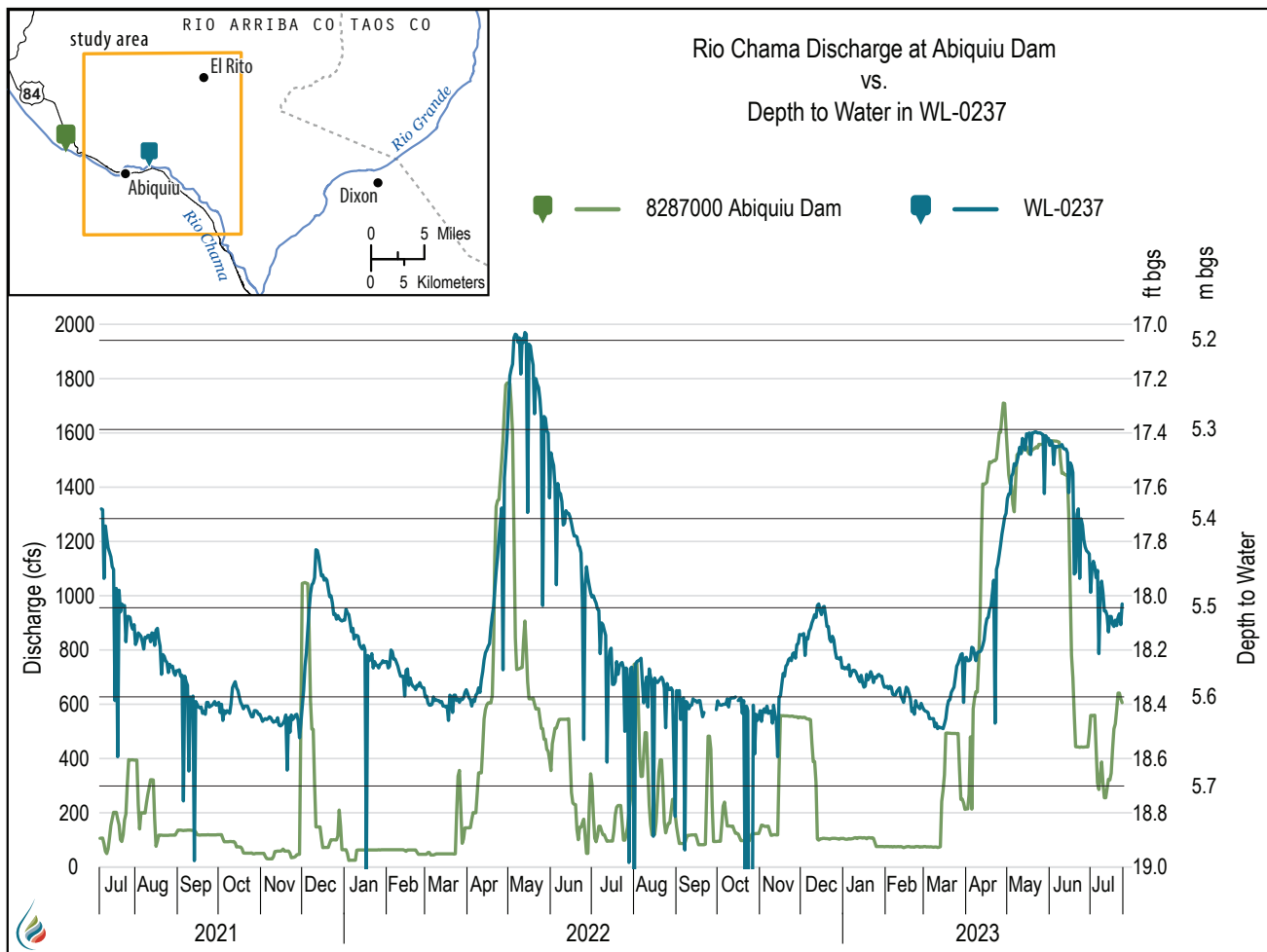
Figure 3.18. Continuous water level data for well WL-0237, along with Rio Chama discharge data for the Rio Chama below Abiquiu dam.

Water Chemistry Data

Water Quality

Table 3.2 shows major ion concentrations and other parameters for water samples, including TDS, pH, alkalinity, and temperature. In general, water quality in the study area is quite good, with about 70% of the samples exhibiting TDS concentrations less than 500 mg/L. TDS concentrations for shallow aquifer system waters averaged 466 mg/L. Only three samples exhibited TDS concentrations greater than 1,000 mg/L, which is the upper boundary of what is referred to as fresh water (USGS, 2019). Water produced by well RA-010 in the shallow aquifer system stands out with a TDS concentration of 2,760 mg/L, which is the second-highest TDS value after that of the deep aquifer system water sample from RA-007, which had a TDS concentration of 4,200 mg/L (Fig. 3.19). The average TDS

concentration for deep aquifer system waters is 891 mg/L. However, about 50% of deep aquifer system wells produced water with TDS concentrations less than 500 mg/L.

Table 3.3 shows concentrations of constituents for which at least one water sample was found to exceed a primary or secondary MCL. We tested all groundwater samples for the presence or absence of total coliform and *E. coli*. One water sample showed the presence of both total coliform and *E. coli*, and five water samples showed just the presence of total coliform. All wells producing these waters were completed in the shallow alluvial aquifer.

Figure 3.20 shows arsenic concentrations for water samples. Several wells completed in both the shallow and deep aquifer systems produced water that exceeded the primary MCL for arsenic (0.01 mg/L).

Table 3.2. Major ion and silica concentrations (in mg/L), pH, alkalinity (as mg/L CaCO$_3$), and temperature (°C). Ab = Abiquiu, ER = El Rito, Med = Medanales, S = shallow, D = deep, Sp = spring.

Point ID	Community	Aquifer system	Calcium (Ca^{2+}) (mg/L)	Magnesium (Mg^{2+}) (mg/L)	Sodium (Na$^+$) (mg/L)	Potassium (K$^+$) (mg/L)	Bicarbonate (HCO$_3^-$) (mg/L)	Chloride (Cl$^-$) (mg/L)	Sulfate (SO$_4$) (mg/L)	Total dissolved solids (mg/L)	Silica (SiO$_2$) (mg/L)	pH	Alkalinity (mg/L)	Temperature (°C)
RA-009	Ab	D	71.5	17.2	56.9	5.85	327	57.2	31.6	478	65.3	7.26	268	16
RA-019	Ab	D	2.19	0.279	382	1.33	607	131	150	1,000	14.7	8.78	522	16.5
RA-004	Ab	S	88.2	18.6	86.4	5.4	442	24.3	125	605	32.5	6.69	362	13.2
RA-010	Ab	S	229	53.3	557	47.3	541	42.5	1,530	2,760	14	7.01	444	14.1
RA-011	Ab	S	46.6	7.49	30.6	1.6	159	4.46	72	268	24.2	7.62	130	13.3
RA-016	Ab	S	45.8	5.24	40	4.04	225	9.28	30.8	283	32.7	7.57	184	14.6
RA-018	Ab	S	113	18.2	154	6.4	430	50.8	288	880	32	7.54	352	14.5
RA-040	Ab	S	52	13.8	186	6.73	491	54	127	728	32.6	6.76	402	16.4
RA-076	Ab	S	53.1	11.3	97.9	3.74	315	19.5	101	477	30.8	7.38	258	16.2
RA-1004	Ab	Sp	12.5	4.76	10.9	1.1	84	1.81	2.04	127	49.9	8.08	68	17.8
WL-0237	Ab	S	42.8	8.54	61.1	3.23	222	6.81	79.1	347	32.5	7.94	182	14.8
RA-085	ER	D	1.9	<0.1	206	<1	405	22.6	55.3	539	23.4	9.17	364	16.5
RA-082	ER	S&D	0.897	0.128	129	0.444	256	8.88	29.4	350	27.1	9.23	240	14.2
RA-073	ER	S	73.6	12.5	20.6	0.805	311	3.1	12.3	311	28.3	7.16	255	13.3
RA-074	ER	S	53.9	5.29	14.1	1.52	198	2.15	10.9	219	26.1	7.12	162	13.9
RA-080	ER	S	42.8	1.61	28.7	2.32	190	4.53	7.66	221	35.1	7.53	156	11.6
RA-083	ER	S	69.1	9.76	33.7	0.638	305	7.22	20.2	332	36.3	7.11	250	14.4
RA-084	ER	S	53.1	6.54	10.9	1.17	195	3.09	8.9	216	26.5	7.09	160	11.7
RA-087	ER	S	11.2	1.51	2.84	0.705	47	<1	1.94	66	19.8	6.68	38	12
RA-089	ER	S	91.7	13.3	12	0.825	336	8.03	14.7	342	31.3	7.13	275	13
RA-091	ER	S	57.7	3.98	20.1	1.92	202	6.04	20.5	247	28.7	7.17	166	13.2
RA-006	Med	D	2.66	<0.1	247	<1	187	124	220	716	11.9	8.9	169	23.1
RA-007	Med	D	71.2	43.3	1,510	8.04	3,710	449	217	4,200	30.7	6.51	3,060	18.8
RA-008	Med	D	24.1	11.3	579	2.94	1,270	133	199	1,650	44.9	7.08	1,050	15.7
RA-038	Med	D	15.2	2.25	41.5	3.17	106	9.89	30.7	190	23.6	8.17	87	16.1
RA-079	Med	D	34.9	3.22	33.7	1.79	145	9.23	40.1	225	22.3	7.87	119	17.9
RA-081	Med	D	19.4	3.96	45.2	2.63	131	10	31.3	220	30.4	8.23	108	18.2
RA-013	Med	S&D	22	2.79	47.9	3.21	145	9.12	31.3	235	27.1	8.13	119	15.7
RA-014	Med	S	64.5	8.61	22.8	2.25	212	4.24	64.5	307	30.6	7.42	174	15.1
RA-039	Med	S	39.9	3.56	15.2	4.87	116	13.7	28.9	206	26.9	7.55	96	16.3
RA-041	Med	S	76.7	8.87	44.4	2.21	284	16.6	56	392	31.3	7.38	233	14.6
RA-042	Med	S	78.3	6.77	51.1	3.35	302	5.76	77.1	409	31.9	7.21	248	13.6
RA-075	Med	S	66.4	8.17	128	4.69	302	105	99.8	625	43.4	7.43	248	15.8
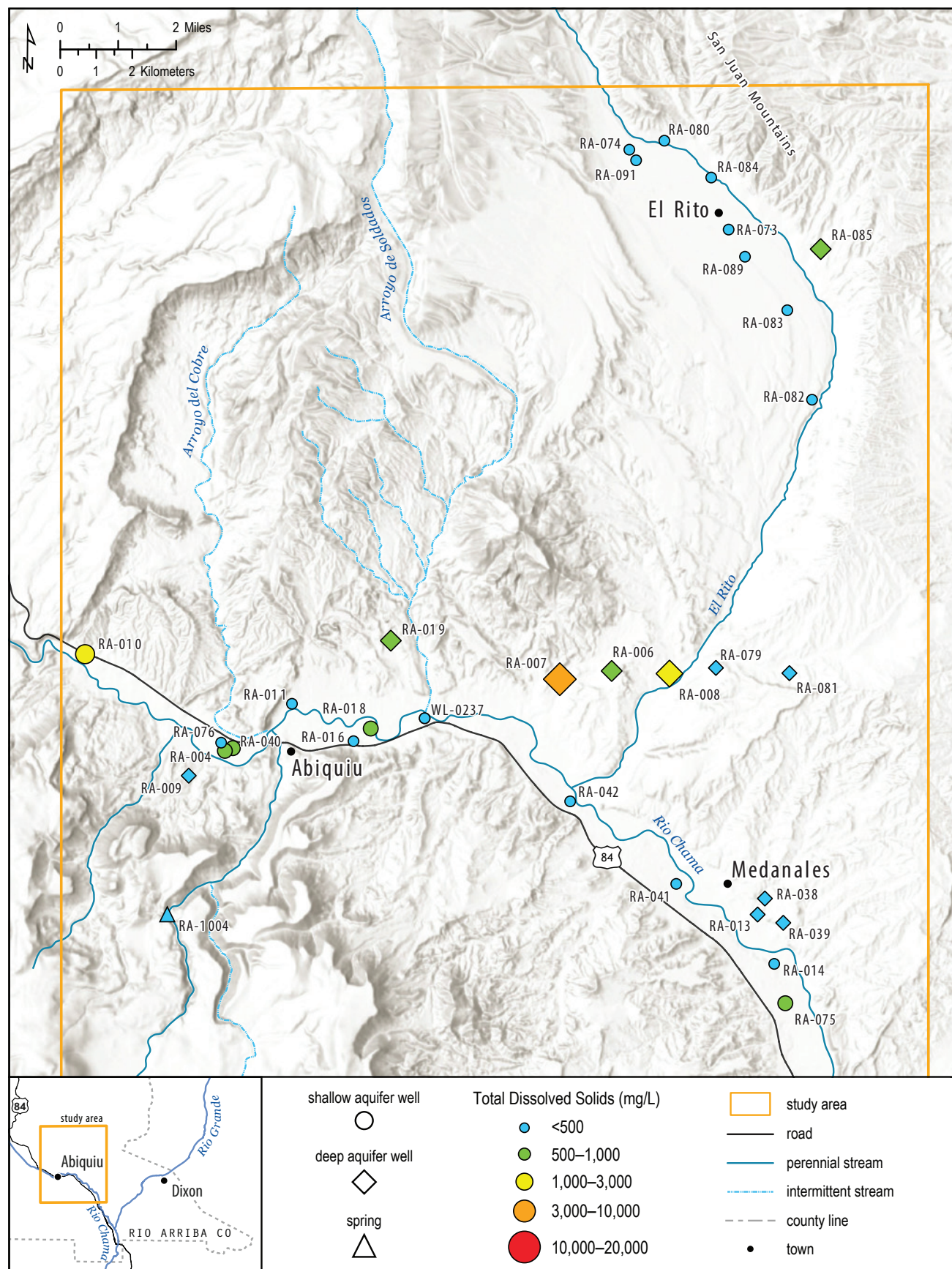
Figure 3.19. Sample locations for total dissolved solids concentrations. TDS concentrations are proportional to the size of the data point for shallow and deep aquifer system waters.

Table 3.3. Concentrations of contaminants for which the EPA has established primary and secondary MCLs. Concentrations that exceed the primary MCL are highlighted in red, and concentrations that exceed the secondary MCL are highlighted in yellow. Bacterial tests show the presence (P) or absence (A) of total coliform and *E. coli*.

Point ID	Area	System	Total coliform	E. coli	Arsenic (As) (mg/L)	Fluoride (F⁻) (mg/L)	Uranium (U) (mg/L)	Chloride (Cl⁻) (mg/L)	Iron (Fe) (mg/L)	Manganese (Mn) (mg/L)	pH	Sulfate (SO₄) (mg/L)
EPA secondary drinking water MCL						2		250	0.3	0.05	<6.5 >8.5	250
EPA primary drinking water MCL					0.01	4	0.03					
RA-004	Abiquiu	shallow	P	A	0.0072	0.4	0.0062	24.3	1.1	0.731	6.69	125
RA-009	Abiquiu	deep	A	A	0.0063	0.33	0.0057	57.2	<0.01	<0.001	7.26	31.6
RA-010	Abiquiu	shallow	P	A	<0.0025	3.63	0.004	42.5	1.44	0.116	7.01	1,530
RA-011	Abiquiu	shallow	A	A	0.0047	0.26	0.0006	4.46	<0.01	0.191	7.62	72
RA-016	Abiquiu	shallow	A	A	0.0131	0.2	0.0036	9.28	<0.01	0.005	7.57	30.8
RA-018	Abiquiu	shallow	P	A	0.0071	<0.5	0.0032	50.8	0.972	0.694	7.54	288
RA-019	Abiquiu	deep	A	A	0.004	3.42	0.0411	131	<0.05	<0.005	8.78	150
RA-040	Abiquiu	shallow	A	A	0.0119	0.8	0.0098	54	8.07	0.149	6.76	127
RA-076	Abiquiu	shallow	A	A	0.0063	0.63	0.0059	19.5	<0.01	0.006	7.38	101
RA-1004	Abiquiu	spring	A	A	0.0026	0.18	0.0006	1.81	<0.01	<0.001	8.08	2.04
WL-0237	Abiquiu	shallow	A	A	0.0095	0.78	<0.0005	6.81	0.211	0.365	7.94	79.1
RA-073	El Rito	shallow	A	A	0.0026	0.75	0.0063	3.1	<0.01	<0.001	7.16	12.3
RA-074	El Rito	shallow	A	A	0.0014	0.19	0.005	2.15	<0.01	<0.001	7.12	10.9
RA-080	El Rito	shallow	A	A	0.001	0.26	0.0061	4.53	<0.01	<0.001	7.53	7.66
RA-082	El Rito	shallow/deep	A	A	0.0495	4.85	0.0193	8.88	<0.01	<0.001	9.23	29.4
RA-083	El Rito	shallow	P	A	0.0021	0.65	0.0042	7.22	0.019	0.001	7.11	20.2
RA-084	El Rito	shallow	A	A	0.0012	0.22	0.0015	3.09	<0.01	<0.001	7.09	8.9
RA-085	El Rito	deep	A	A	0.0086	0.85	0.0357	22.6	0.206	<0.005	9.17	55.3
RA-087	El Rito	shallow	P	P	0.0015	0.1	<0.0005	<1	2.73	0.204	6.68	1.94
RA-089	El Rito	shallow	A	A	0.0029	0.19	0.0039	8.03	<0.01	0.017	7.13	14.7
RA-091	El Rito	shallow	A	A	0.0012	0.22	0.0068	6.04	<0.01	<0.001	7.17	20.5
RA-006	Medanales	deep	A	A	0.0134	5.26	0.115	124	<0.05	<0.005	8.9	220
RA-007	Medanales	deep	A	A	0.0053	<1	0.133	449	<0.1	0.343	6.51	217
RA-008	Medanales	deep	A	A	0.0105	1.05	0.0507	133	<0.05	<0.005	7.08	199
RA-013	Medanales	shallow/deep	A	A	0.0073	0.58	0.0035	9.12	<0.01	<0.001	8.13	31.3
RA-014	Medanales	shallow	A	A	0.0134	0.48	0.003	4.24	<0.01	0.004	7.42	64.5
RA-038	Medanales	deep	A	A	0.0194	0.84	0.0008	9.89	<0.01	<0.001	8.17	30.7
RA-039	Medanales	shallow	A	A	0.0046	0.25	0.0044	13.7	0.017	0.002	7.55	28.9
RA-041	Medanales	shallow	P	A	0.0029	0.27	0.0078	16.6	0.033	0.014	7.38	56
RA-042	Medanales	shallow	A	A	0.0019	0.63	0.0081	5.76	<0.01	<0.001	7.21	77.1
RA-075	Medanales	shallow	A	A	0.0129	1.56	0.0129	105	<0.05	<0.005	7.43	99.8
RA-079	Medanales	deep	A	A	0.0016	0.26	0.0049	9.23	<0.01	<0.001	7.87	40.1
RA-081	Medanales	deep	A	A	0.0037	0.69	0.0139	10	<0.01	<0.001	8.23	31.3

The southern sampled well in the El Rito area (RA-082), which is completed in both the shallow and deep aquifer systems, exhibited the highest arsenic concentration at about 0.05 mg/L. All other water samples that had arsenic concentrations exceeding the primary MCL had arsenic concentrations less than 0.02 mg/L. Interestingly, RA-007 and RA-010, the wells that produced water with the highest TDS concentrations, had arsenic concentrations of 0.0053 mg/L and less than 0.0025 mg/L, respectively.

Figure 3.21 shows uranium concentrations for water samples. All five wells that produced water exceeding the primary MCL of 0.03 mg/L are completed in the deep aquifer system. The two deep aquifer system wells with the highest uranium concentrations are RA-007 (highest TDS concentration of 4,200 mg/L) and RA-006 (TDS concentration of 716 mg/L) at 0.133 mg/L and 0.155 mg/L, respectively.

Figure 3.22 shows fluoride concentrations for all water samples. Two wells, RA-082 (shallow and deep aquifer systems) and RA-006 (deep aquifer system), produced water that exceeds the primary MCL of 4 mg/L. Wells RA-010 (shallow aquifer system) and RA-019 (deep aquifer system) produced water exceeding the secondary MCL of 2 mg/L.

The remaining cations we measured include iron and manganese (Figs. 3.23 and 3.24, respectively). Iron concentrations that exceeded the secondary MCL of 0.3 mg/L were observed for water produced by wells completed in the shallow aquifer (Fig. 3.23), and most of these wells (RA-010, RA-004, RA-040, and RA-018) are located in the Abiquiu area. In El Rito, the only well that produced water that exceeded the secondary MCL for iron was RA-087, which is the northernmost well sampled in the El Rito area. Both iron and manganese are relatively heavy minerals that can be concentrated in sediments deposited by running water in streams and rivers. Therefore, manganese concentrations (Fig. 3.24) that exceeded the secondary MCL of 0.05 mg/L were produced by most of the same wells (RA-010, RA-004, RA-040, RA-011, RA-018, and RA-087) that showed exceedance of the secondary iron MCL. An exception is well RA-007, which exhibited the highest manganese concentration at 0.343 mg/L but comparably low iron concentrations. The four wells that showed a pH value greater than 8.5 (RA-019,

RA-006, RA-085, and RA-082) are wells that stand out chemically and are discussed in more detail below.

General Chemistry (Major Ions)

Figure 3.25 shows the groundwater chemistry for the water samples plotted on a Piper diagram. Cation data (left triangle) exhibit a roughly linear trend from Ca^{2+}-dominant waters to Na^+-dominant waters. While the cation composition for shallow aquifer system waters spans most of the observed range, deep aquifer system waters do not exhibit Ca^{2+} as the dominant cation (Fig. 3.25), suggesting that deep aquifer system waters are likely older and have undergone water/mineral interactions to a larger degree than water in the shallow aquifer system.

Most shallow wells in El Rito and Medanales produce water of a Ca^{2+}-HCO_3^- water type that is also low in TDS (66–342 mg/L for El Rito and 206–409 mg/L for Medanales), indicating young groundwater that is likely recharged in nearby mountains (Fig. 3.25, Table 3.3). The spring that supplies Abiquiu (RA-1004) stands out from other data points and exhibits mixed cations and the highest relative Mg^{2+} concentrations. Water from RA-010, the shallow aquifer system well with the highest TDS (2,760 mg/L), shows Na^+ as the dominant cation. The deep aquifer system wells in Medanales (RA-007 and RA-008) exhibit high TDS concentrations and high relative Na^+ (90% and 92%, respectively). However, four deep aquifer system wells (RA-082, RA-085, RA-019, and RA-006) are from all three areas of interest and exhibit extremely high relative Na^+ concentrations (>98% of cations) and low TDS concentrations. These are the same waters with pH values that exceed the secondary MCL of 8.5 (Table 3.3).

For anions (Fig. 3.25, right triangle), all but four water samples exhibit HCO_3^- as the dominant anion. The shallow aquifer system well RA-010 again stands out because it is the only water sample with SO_4^{2-} as the dominant anion. To a lesser degree, the shallow aquifer system well RA-018 and the deep aquifer system well RA-006 show elevated relative SO_4^{2-} concentrations. RA-006, one of the wells that produced high Na^+, high pH, and relatively low TDS concentrations, also shows the highest relative Cl^- concentration. The shallow aquifer system well RA-075 exhibits the second-highest relative Cl^- concentration.
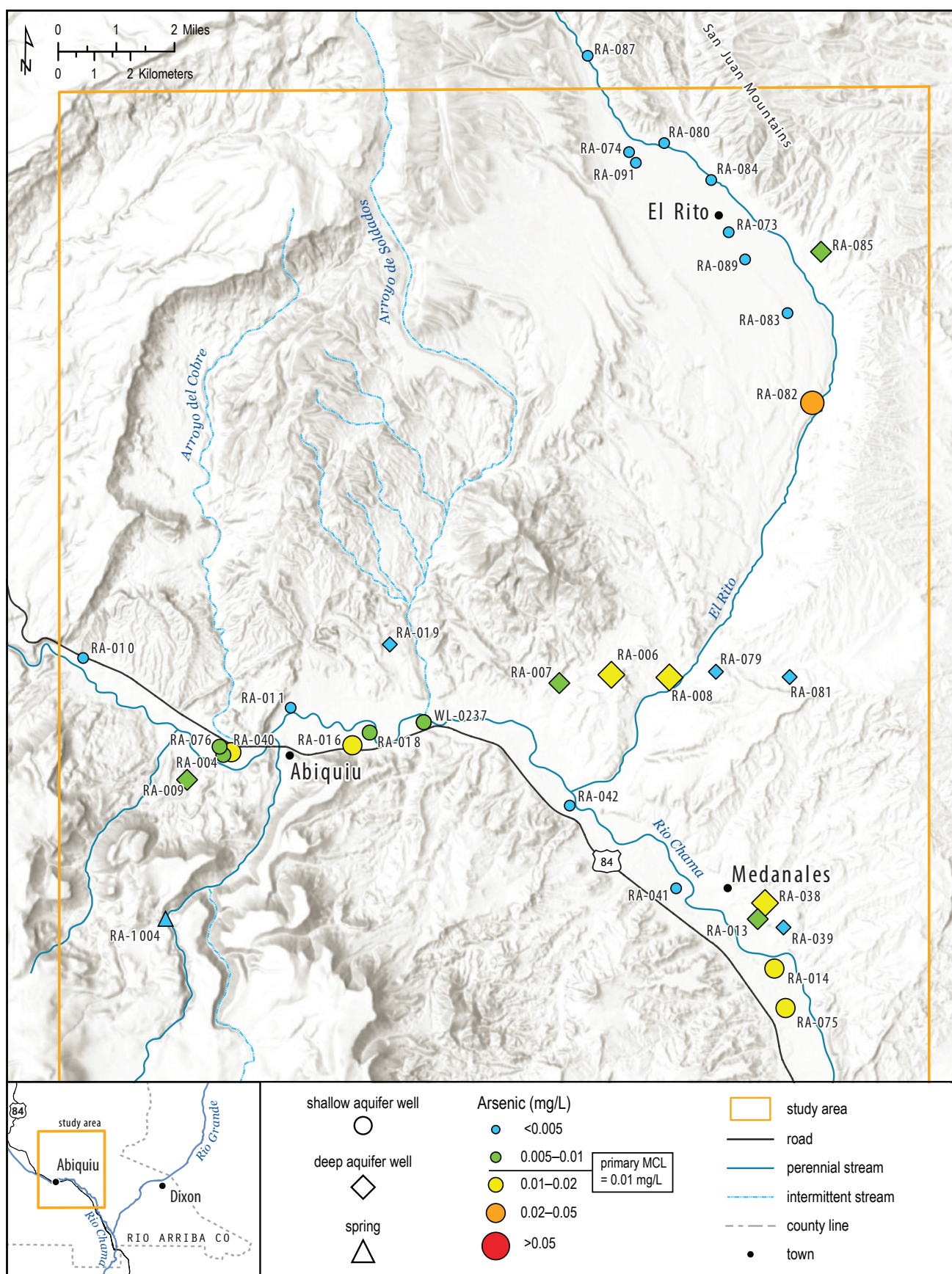
Figure 3.20. Arsenic concentrations for water from shallow and deep system wells. Primary MCL = 0.01 mg/L. Yellow, orange, and red points indicate exceedance of the MCL.
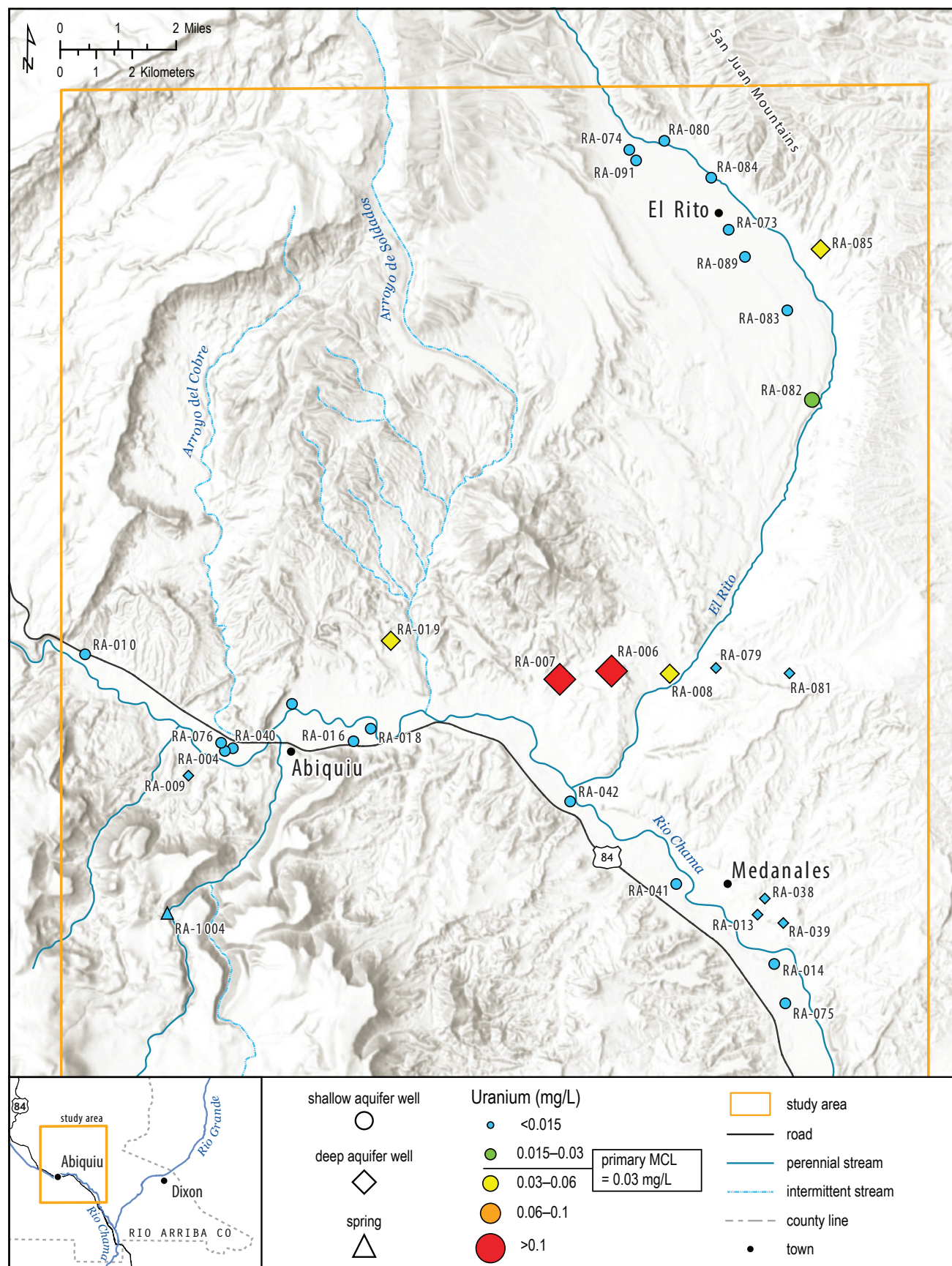
Figure 3.21. Uranium concentrations for water from shallow and deep system wells. Primary MCL = 0.03 mg/L. Yellow, orange, and red points indicate exceedance of the MCL.
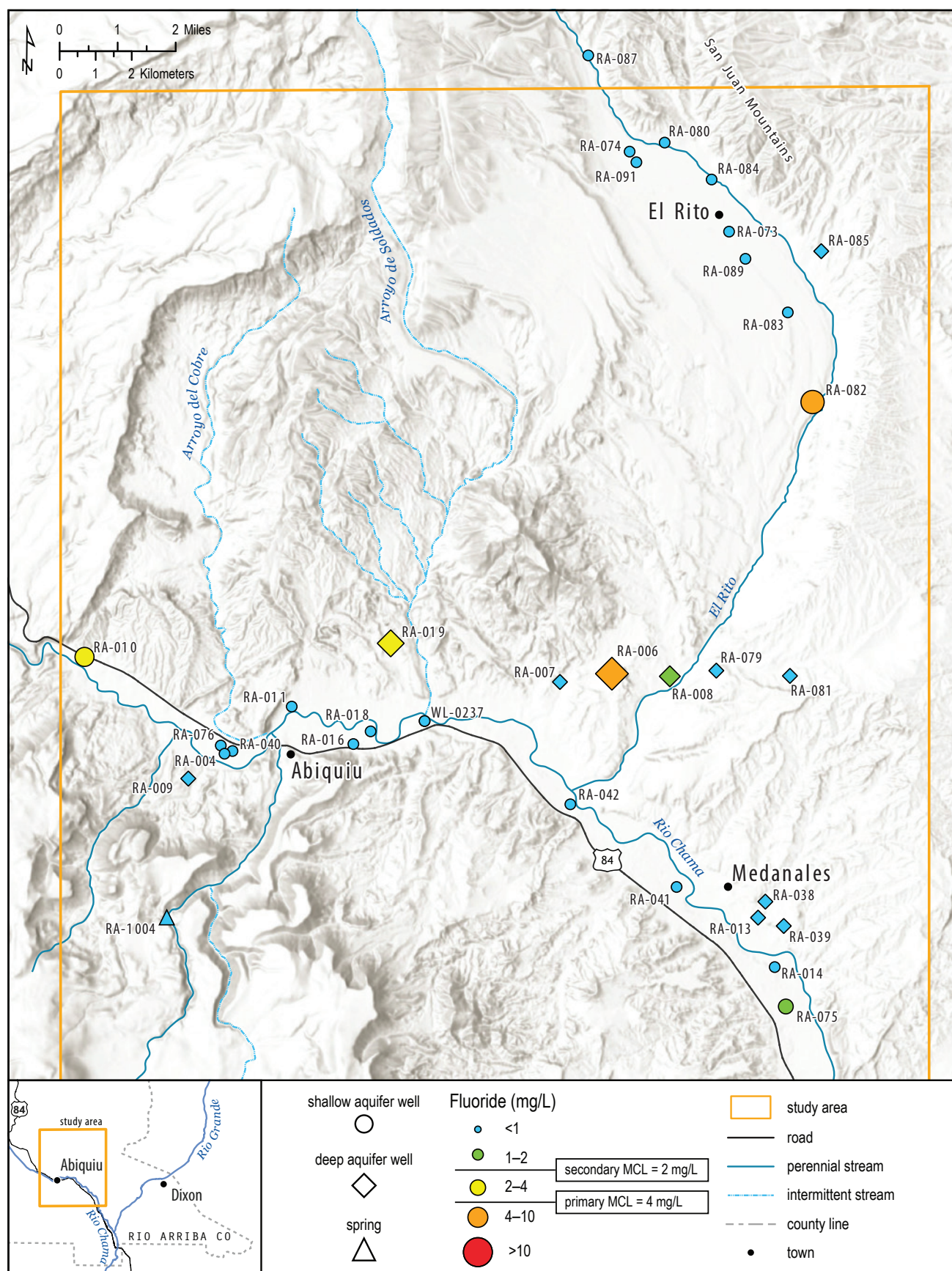
Figure 3.22. Fluoride concentrations for water from shallow and deep system wells. Primary MCL = 4 mg/L, secondary MCL = 2 mg/L. Yellow points indicate exceedance of the secondary MCL; orange and red points indicate exceedance of the primary MCL.
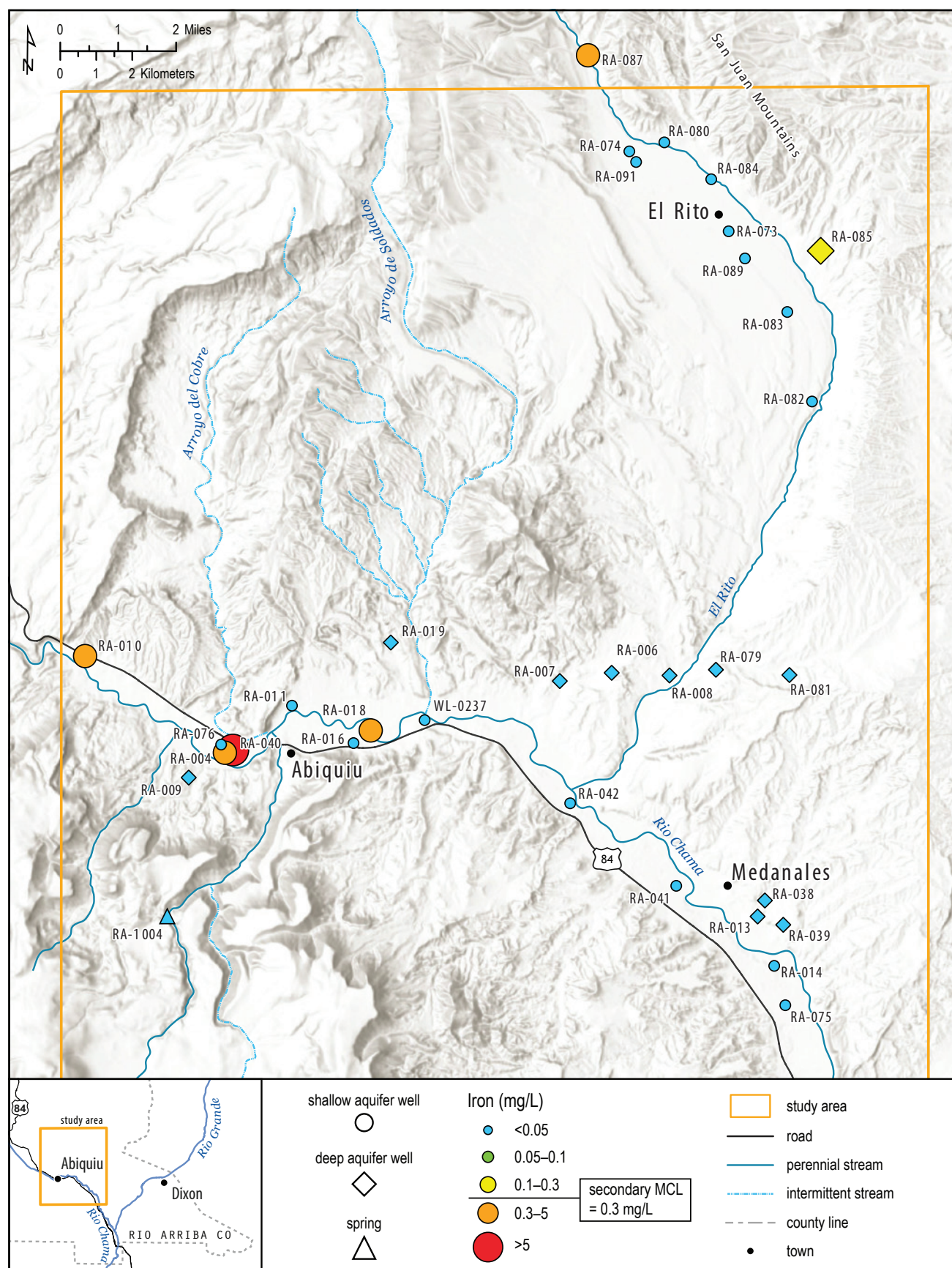
Figure 3.23. Iron concentrations for water from shallow and deep system wells. Secondary MCL = 0.3 mg/L. Orange and red points indicate exceedance of the secondary MCL.
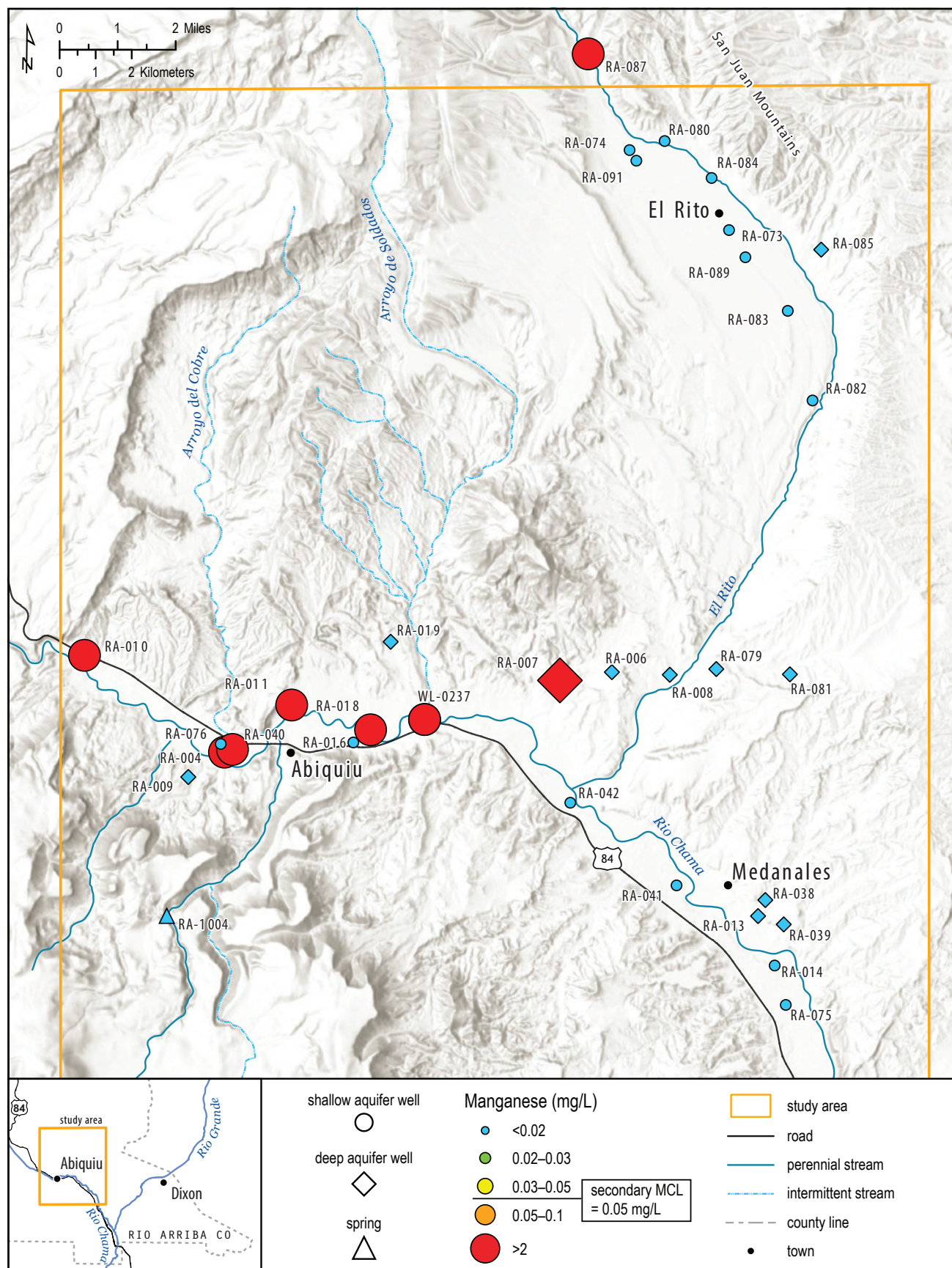
Figure 3.24. Manganese concentrations for water from shallow and deep system wells. Secondary MCL = 0.05 mg/L. Orange and red points indicate exceedance of the secondary MCL.

Figure 3.26 shows locations of sampled wells, indicating the dominant cation exhibited by the water sample. Most shallow wells produce water of Ca^{2+} type, and this is especially true for the El Rito area. In the Abiquiu and Medanales areas, some shallow aquifer system waters are identified as both mixed-cation and Na^+ water types. As mentioned above, there are no Ca^{2+} water types for deep aquifer system waters. Figure 3.27 shows TDS as a function of relative Na^+ concentrations (as a proportion of cations, meq/L). As seen in the Piper diagram in

Figure 3.25, the cation compositions for all water samples are relatively low in magnesium (<25% of cations) and define a roughly linear trend between Ca^{2+} water types and Na^+ water types. Again, shallow aquifer system waters with low TDS and Ca^{2+} as the dominant cation are likely very young waters that were recharged in the nearby mountains to the north. Two processes are likely to cause groundwater to evolve from a Ca^{2+} water type toward a Na^+ water type: (1) mixing with other water sources with high relative Na^+ concentrations and (2) cation exchange.
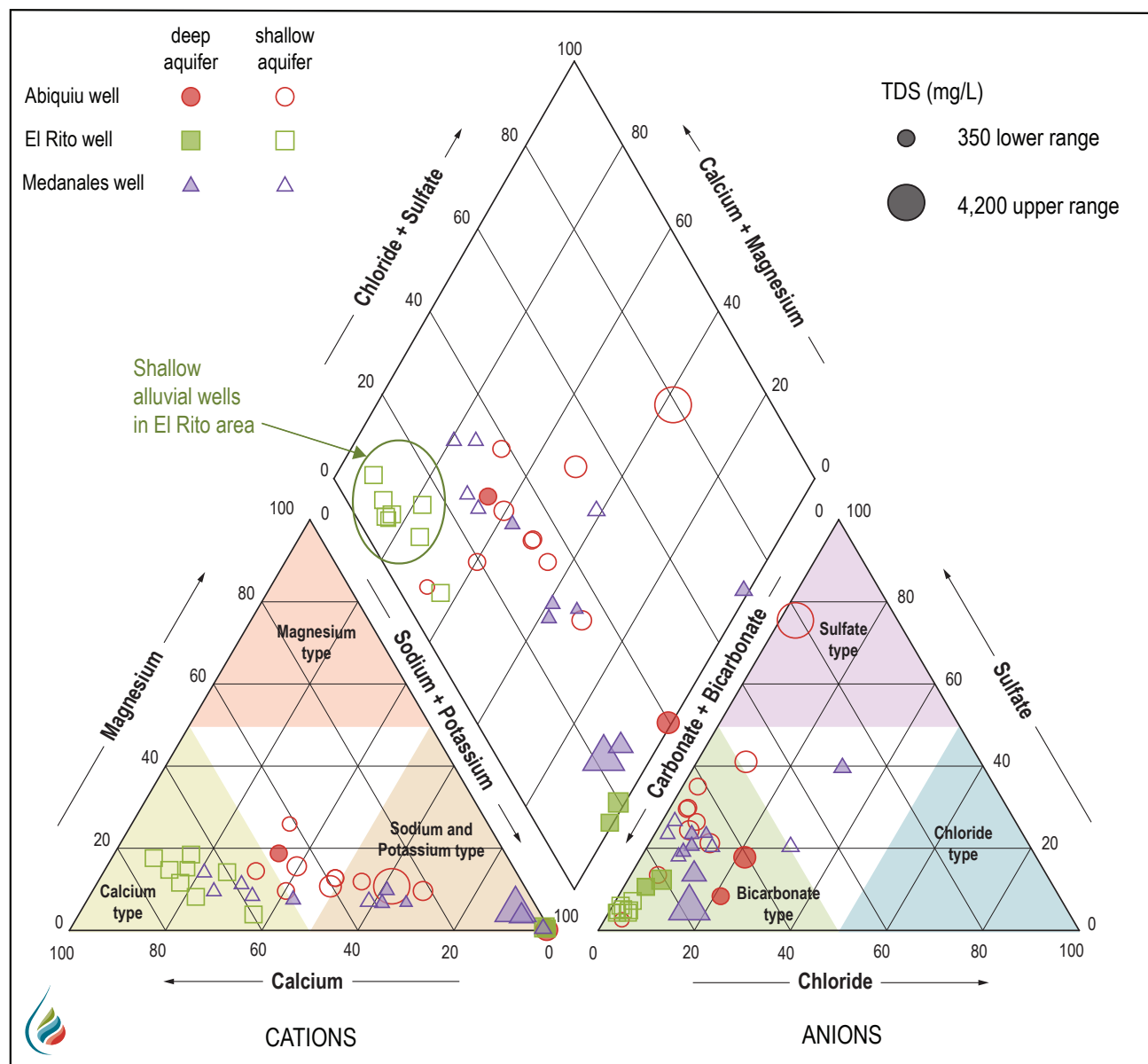
Figure 3.25. Piper diagram showing data for all water samples in the Abiquiu Valley. The different regions are defined by the shape of the data point, and water from the shallow and deep aquifer systems is differentiated by open and filled symbols, respectively. The size of the data point is proportional to the measured TDS.
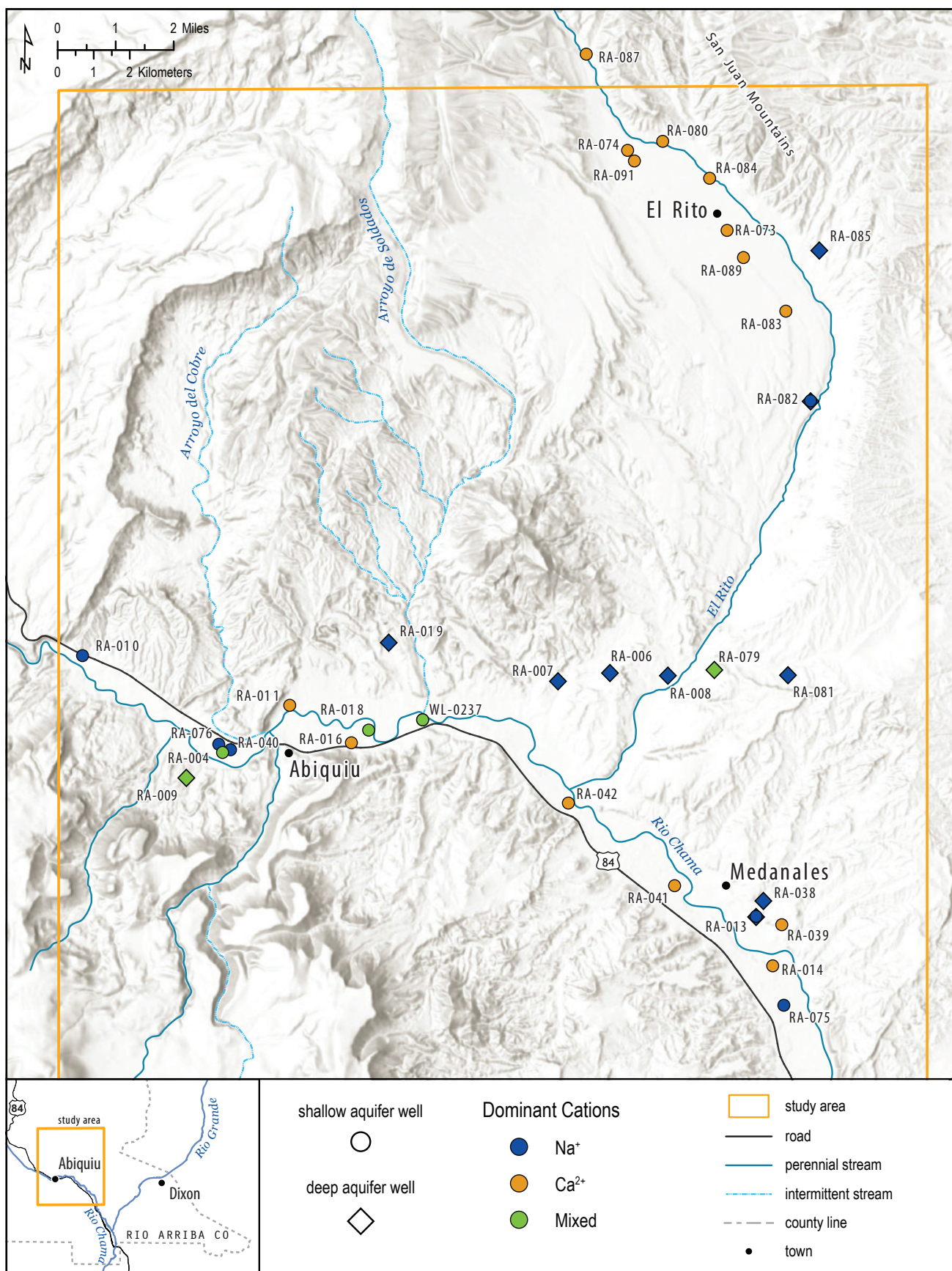
Figure 3.26. Well locations indicating the dominant cation for deep and shallow aquifer systems.

The graph in Figure 3.27 shows examples of both mixing and cation exchange. The increase in relative Na⁺ concentration accompanied by significant increase in TDS indicates mixing with a groundwater source that has high TDS and a Na⁺ water type. This is most apparent for shallow aquifer system wells in the Abiquiu area (red arrow) with a relative Na⁺ concentration between 0.3 and 0.7; these are apparently mixing with groundwaters chemically similar to waters produced by deep aquifer system wells, such as RA-007 and RA-008. Most shallow aquifer system waters in the El Rito and Medanales areas are Ca^{2+} water types (low relative Na⁺ concentrations) and show very small increases in TDS between the relative Na⁺ concentrations of 0.1 and 0.4. In this case, increases in relative Na⁺ concentrations are mostly due to cation exchange reactions, which are not expected to increase TDS (purple arrow). Interestingly, it appears that the five

deep aquifer system wells in the Medanales area with TDS concentrations less than 250 mg/L have relative Na⁺ concentrations ranging from 0.2 to 0.7. These waters (in wells RA-013, RA-038, RA-039, RA-079, and RA-081) may come from the same formation (Chama-El Rito Member of the Tesuque Formation) and are discussed in more detail below.

The graph in Figure 3.27 also clearly shows waters with high pH and low TDS aligned close to the relative Na⁺ concentration of 1 (about 98–99% of cations), with TDS concentrations ranging from 350 to 1,000 mg/L. These wells are all screened in the deep aquifer. Initial analyses suggest this water chemistry is due to the dissolution of feldspars, which range from about 5 to 40% in the Abiquiu Formation and are dominantly plagioclase (Vazzana and Ingersoll, 1981).
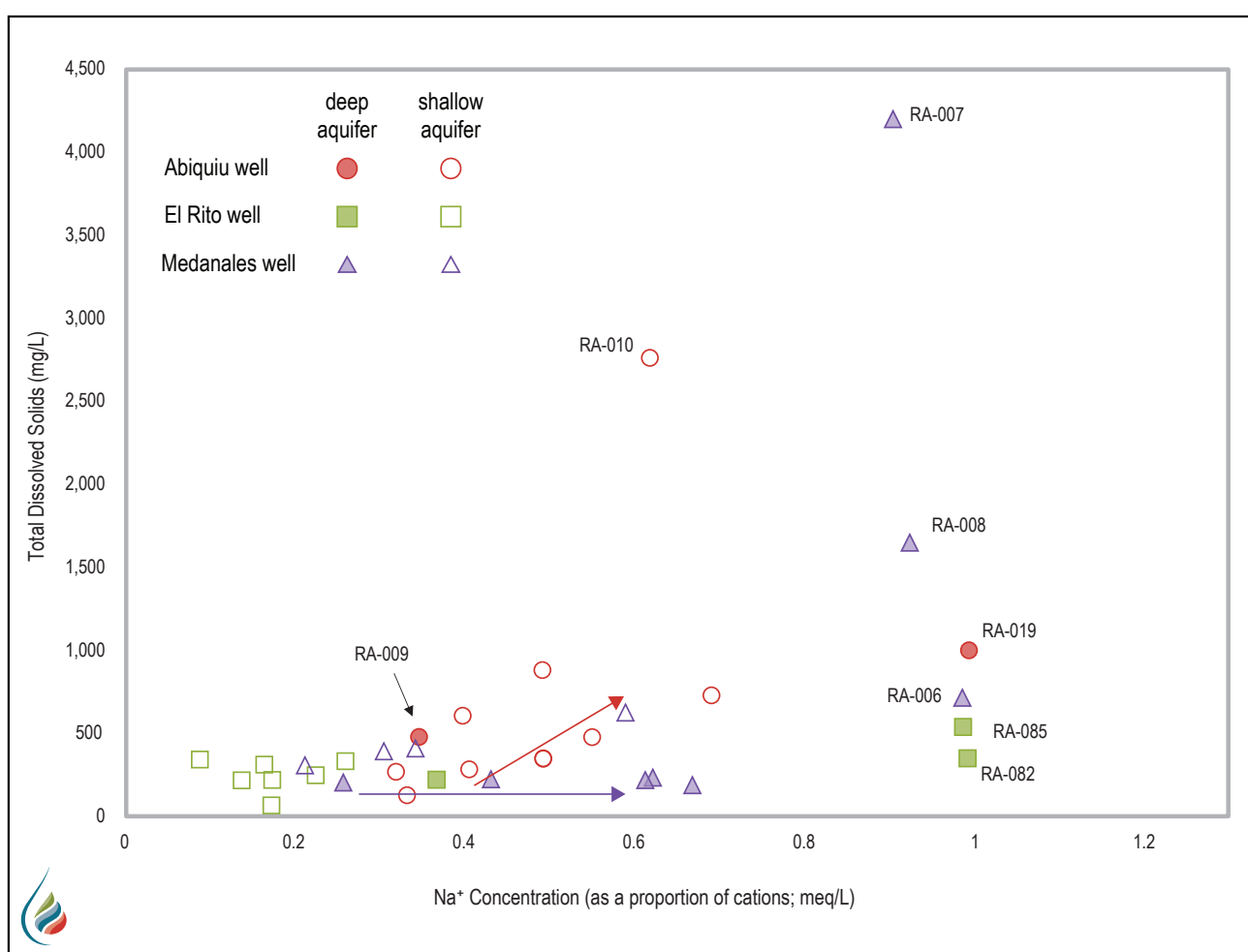
Figure 3.27. TDS plotted as a function of relative Na⁺ concentrations as a proportion of cations. The arrows show different chemical evolution pathways, with the red arrow representing the mixing of waters with different TDS concentrations. The purple arrow represents cation exchange, which does not significantly affect the TDS concentrations.

Figure 3.28 shows additional evidence of groundwaters with high TDS and chemical signatures similar to those of RA-010 and RA-007, likely upwelling along fractures and faults and mixing with shallow aquifer system waters; these significantly impact shallow groundwater quality in the Abiquiu area. The graph shows the molar ratio (ratio of molar concentrations, mol/L) of HCO_3^-/SO_4^{2-} versus SO_4^{2-} concentrations (in meq/L). The top graph presents all the data, showing water from RA-010 with the highest SO_4^{2-} concentration of 31.9 meq/L (1,530 mg/L). The estimated mixing line (dashed) suggests that a small amount of water chemically similar to that sampled from RA-010 is mixing with most water in the shallow aquifer system. The bottom graph in Figure 3.28 zooms in to show other possible mixing processes. The dashed line and arrows show that groundwater with a chemical signature similar to that of water from RA-007 appears to be mixing into the shallow aquifer system, impacting water quality for shallow groundwaters, especially in the Abiquiu area. The deep aquifer system waters with low TDS labeled in Figure 3.28 are the same waters (solid purple triangles) shown in Figure 3.27 that show a range of relative sodium concentrations but low TDS concentrations.

Groundwater Ages

Figures 3.29 and 3.30 show that tritium concentrations above 1 TU are observed for waters produced by shallow wells in the El Rito and Abiquiu areas, which all exhibit depth-to-water measurements less than 10 m (33 ft) below the surface. In general, carbon-14 data agree with tritium data. With the exception of well RA-010, all waters with tritium concentrations greater than 1 TU exhibit apparent carbon-14 ages less than 1,000 YBP. Well RA-010, which produces water with an apparent carbon-14 age of 11,930 YBP, is located just east of the Cañones fault (Figs. 3.5 and 3.10); this fault juxtaposes the Permian Cutler Formation and the Oligocene Ritito Conglomerate (about 27 million years old). In this area, the Todilto Formation is very close to the surface and likely the main source of shallow groundwater. However, a tritium concentration of 1.37 TU indicates young water from the Rio Chama recharges the shallow aquifer, mixing with older water in this area. Well RA-075, the southernmost well sampled, is located in an area where the Tesuque Formation is very close to the surface (Fig. 3.6) and where the Tesuque is probably the source of shallow groundwater in that area. However, with a tritium concentration of 0.37 TU, a small amount of young river water apparently does recharge the shallow alluvial aquifer in this area as well. As discussed in more detail below, several deep aquifer system waters with similar apparent ages (10,000–15,000 YBP) seem to also be coming from the Chama-El Rito Member of the Tesuque Formation. The water sample exhibiting the oldest apparent age of 22,740 YBP is from RA-006, which also appears to be completed in the Chama-El Rito Member.

Stable Isotopes of Water

As shown in Figure 1.6, the stable isotopic composition of all groundwater samples plots within the range of values expected for winter precipitation. Figure 3.31 shows that the groundwater system is quite complicated, with different water sources evaporating and mixing. These data allow us to identify the three water samples (RA-1004, RA-016, and RA-009) that appear to have been recharged in the Jemez Mountains to the south. RA-1004 is the spring located up Abiquiu Creek that supplies Abiquiu with community water; RA-016 is located close to the mouth of Abiquiu Creek, where Abiquiu Creek feeds into the Rio Chama; and RA-009 is located in a small drainage coming from the south. The apparent linear trend exhibited by these waters is likely an evaporation line, where water from RA-1004 has undergone the least amount of evaporation and water from RA-016 has undergone the most evaporation. These data indicate groundwater on the southern flank of the Rio Chama valley near Abiquiu was likely recharged by stream water in the northern flank of the Jemez Mountains, such as Abiquiu Creek, where water is exposed to the atmosphere and undergoes evaporation before it infiltrates through the stream bed to recharge the shallow alluvial aquifer.

Note how the shallow groundwater wells near El Rito extend rightward from the Rocky Mountains meteoric water line. This indicates that shallow aquifer system groundwater in much of the El Rito area is recharged by water that has undergone evaporation, including water from El Rito Creek, irrigation return flow, and water in the acequias.
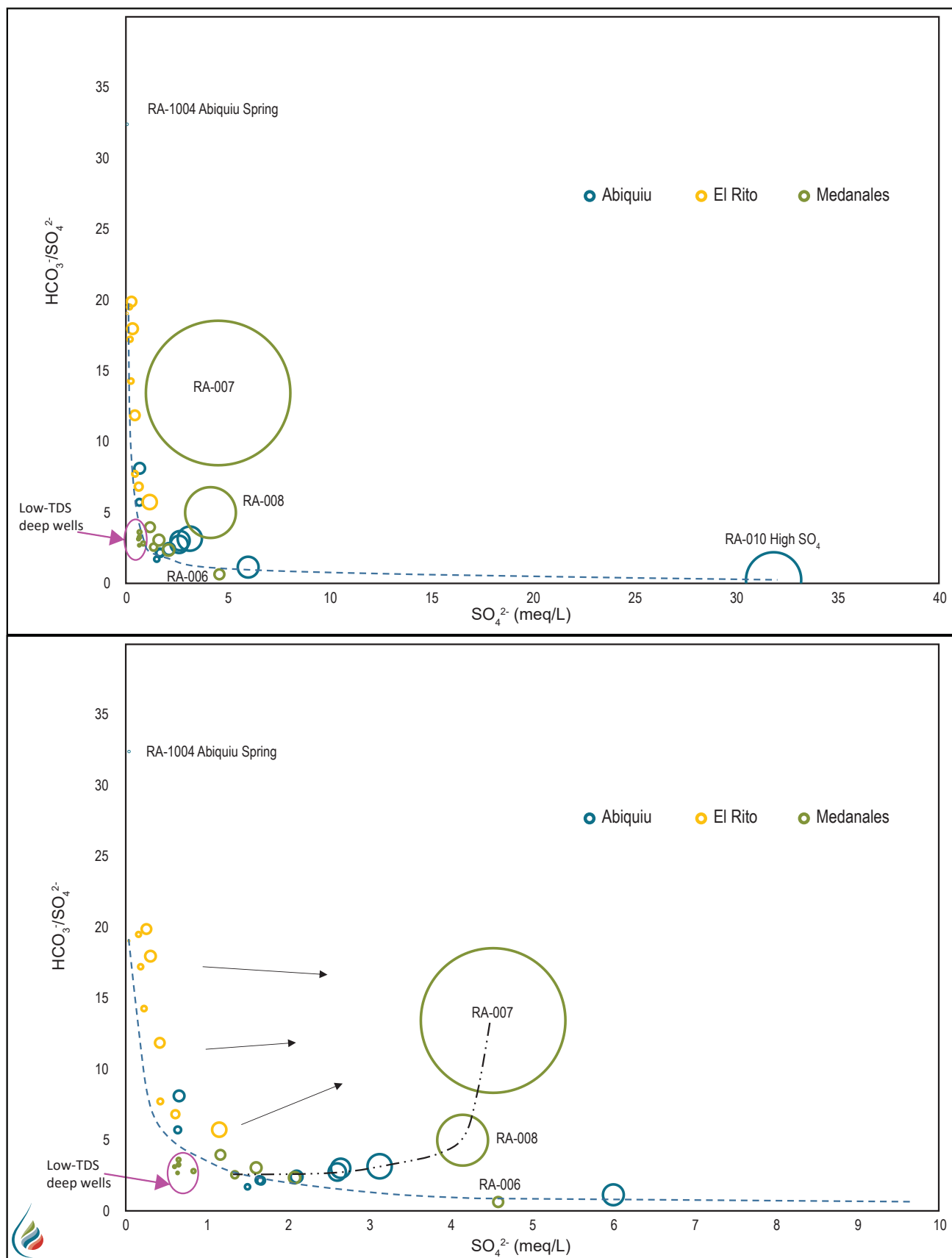
Figure 3.28. Molar ratio of HCO_3^-/SO_4^{2-} plotted as a function of SO_4^{2-} concentrations. Almost all water samples appear to be affected by mixing with groundwater that is chemically similar to water produced by RA-010 (top graph) and RA-007 (bottom graph). Dashed lines are hypothetical mixing lines. The size of the data points is proportional to TDS concentrations.

Shallow aquifer system waters for the Abiquiu and Medanales areas plot along the bottom evaporation line. They show larger degrees of evaporation, with the southernmost well (RA-075) showing the largest degree. This indicates water originating from the Rio Chama has undergone evaporation before recharging the shallow alluvial aquifer. In this area, the Rio Chama may sometimes be a losing stream, where stream water that has undergone evaporation seeps into the streambed and recharges the aquifer.

The isotopically lightest groundwaters, with the exception of RA-010, are all deep aquifer system waters based on their depth and depth-to-water measurements; these include wells RA-007, RA-085, RA-019, and RA-038. These waters appear to be separated from most of the shallow aquifer system

and are likely related to Pleistocene recharge identified in the San Luis Basin by Drakos et al. (2004). These waters represent older recharge under a different climatic regime. Many researchers have observed that some old groundwaters, likely recharged tens of thousands of years ago, exhibit much lighter isotopic compositions than those observed today due to cooler climatic conditions in past ice ages. Interestingly, most deep aquifer system waters in the Medanales area appear to represent recharge that originally plotted along the global meteoric water line but shows evidence of the mixing of a small amount of Pleistocene water that changed the isotopic composition toward lighter values (red arrows in Fig. 3.31), with the result being compositions lying in between that of pure Pleistocene recharge (red circle in Fig. 3.21) and the global meteoric line.
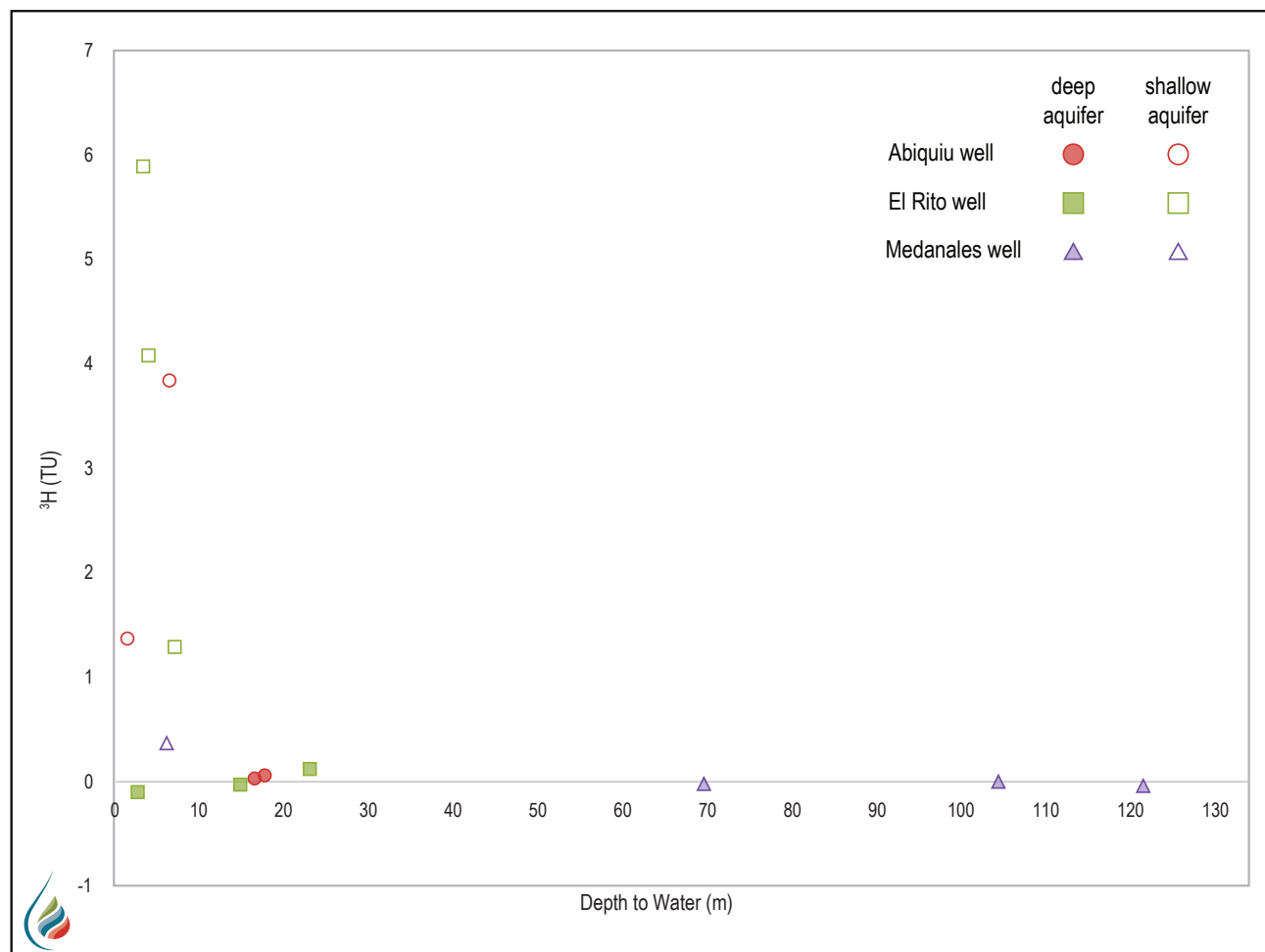
Figure 3.29. Tritium concentrations as a function of depth-to-water measurements.
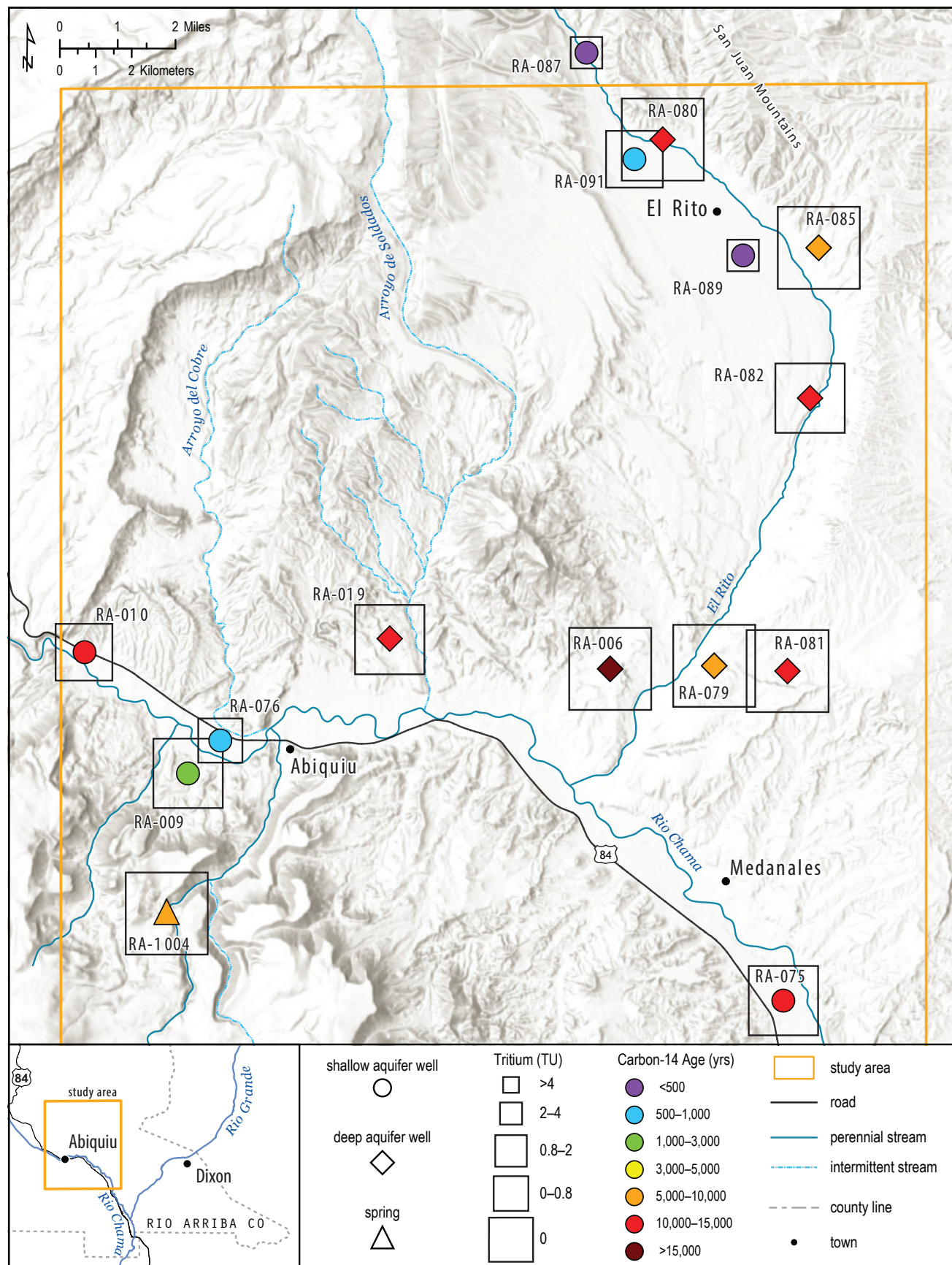
Figure 3.30. Location of wells tested for carbon-14 and tritium, with the color of the filled points representative of the apparent age of the water and the size of the open points inversely proportional to the tritium concentration in TU.
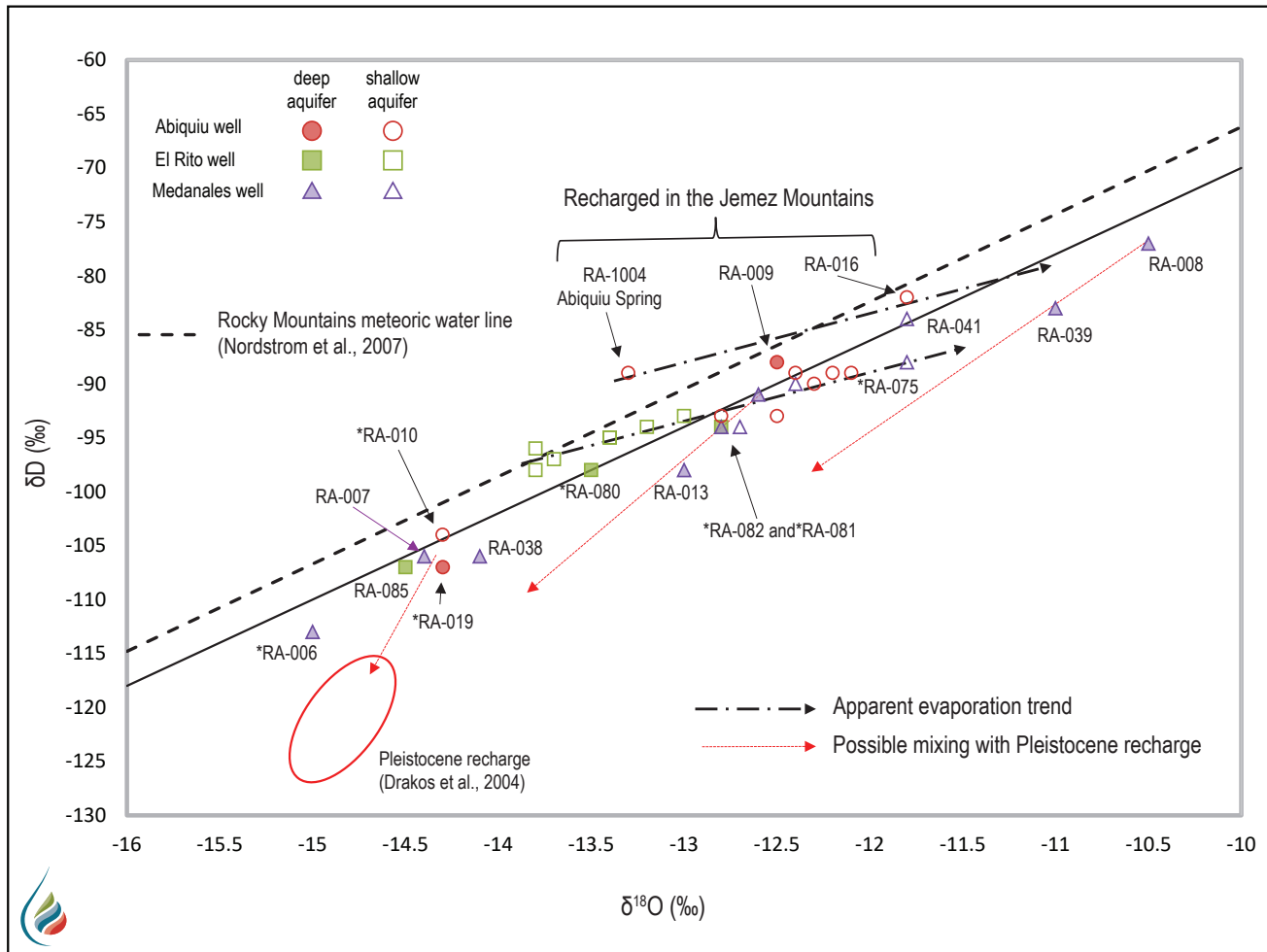
Figure 3.31. Stable isotopic composition of water samples. The dashed arrows indicate different processes, such as the mixing of different water sources and evaporation.

DISCUSSION AND CONCLUSIONS

For the following sections, refer to Figure 3.32, which is a block diagram demonstrating the hydrogeologic conceptual model based on the information and analyses discussed above. In general, the shallow alluvial aquifer in the Abiquiu area is very limited in size but has relatively high permeability. Existing wells in the area that tap deeper aquifers show that water levels in the wells are much higher than the elevation of the apparent water-bearing unit, indicating these aquifers are confined and under pressure. However, while the deep aquifer system appears to be confined to some degree, the water levels in the wells are still lower than the surface of the shallow alluvial aquifer (water table). In the presence of open fractures and faults, this deep aquifer system water can move upward into the shallow aquifer system.

Characterization of Shallow Alluvial Aquifers

The shallow alluvial aquifers that supply groundwater for residents and communities in the Abiquiu Valley study area are located in the valley bottom adjacent to the Rio Chama and El Rito Creek. The aquifer is composed of Quaternary sediments, including Quaternary alluvium and young terrace deposits in the El Rito area and Quaternary alluvium along the Rio Chama (Figs. 3.13 and 3.14). The width of the aquifer is limited by the lateral extent of these deposits. The widest portion of the shallow aquifer is in the vicinity of El Rito, which is where the greatest saturated thickness is measured (Fig. 3.16). To the south toward the mouth of El Rito Creek, the shallow alluvial aquifer is not well defined because there are very few existing wells in this area (Fig. 3.13). The water-table contours along the Rio Chama show a
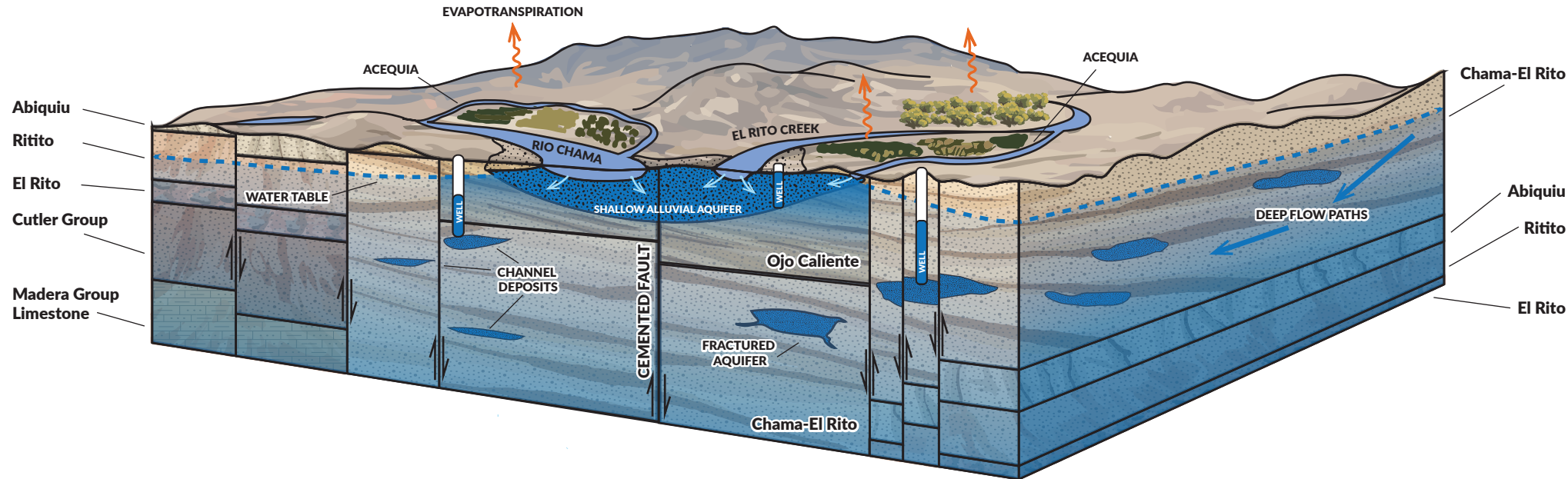
Figure 3.32. Conceptual model of the hydrogeologic system in the Abiquiu Valley area. The shallow alluvial aquifer is primarily recharged by El Rito Creek, the Rio Chama, and acequias. While the Ojo Caliente Member of the Tesuque Formation is less permeable than the overlying alluvium, the general lack of clay beds strongly suggests it is hydrologically connected to the shallow aquifer system. Most deep aquifer system wells tap the Chama-El Rito Member of the Tesuque Formation, where higher degrees of compaction, cementation, and clayey strata create a permeability regime intermediate between that of bedrock (e.g., Madera Group Limestone and Cutler Group) and the shallow alluvial aquifer. Within the Chama-El Rito Member, water-bearing units are likely mostly in channel deposits, which are composed of coarser materials. The fault zone in the center appears to be cemented, resulting in compartmentalization. Deep aquifer system wells to the west (left) of the cemented fault tend to produce water with high total TDS concentrations (700–4,200 mg/L) and high arsenic and uranium concentrations. Deep aquifer system wells to the east (right) of the cemented fault produce good-quality water from 122 to 183 m (400–600 ft) below the surface. This area is highly faulted and possibly fractured if the Chama-El Rito Member is cemented at depth.

relatively flat hydraulic gradient, with some apparent gaining reaches and some losing reaches. Water level data used to construct water level elevation contours span from the 1970s to the present, and we know groundwater levels in this area can fluctuate well over 0.3 m (1 ft) due to fluctuations in the Rio Chama (Fig. 3.18). Near El Rito, where the hydraulic gradient is steeper, water level contours can be identified despite the uncertainty of the water level data. However, in areas with very flat gradients (<1%), like those along the Rio Chama, these uncertainties make it difficult to define water level contours. Furthermore, because the flow in the Rio Chama in the Abiquiu Valley is controlled by releases from Abiquiu Reservoir, this reach of the Rio Chama likely loses water to the aquifer during high flows and gains water back from the aquifer during low flows. In general, groundwater flows parallel to the Rio Chama and El Rito Creek, and saturated thickness ranges from 20 to 30 m (66–98 ft).

Geochemistry

In general, water quality in the study area is quite good, with about 70% of the samples exhibiting TDS concentrations less than 500 mg/L. TDS concentrations for shallow aquifer system waters averaged 466 mg/L. Only three samples exhibited TDS concentrations greater than 1,000 mg/L. Water produced by the shallow aquifer system well RA-010 stands out, with a TDS concentration of 2,760 mg/L; this is the second-highest TDS value after the deep aquifer system water sample from RA-007. Unlike all other water samples, RA-010 exhibits SO_4^{2-} as the dominant anion (Fig. 3.25) and shows evidence of the dissolution of the mineral gypsum, which does not occur in alluvial or Santa Fe Group sediments in the area. Well RA-010 is located on the western edge of the study area just east of the Cañones fault (Fig. 3.10). In that area, the Jurassic Todilto/Entrada Formation, which does contain gypsum, is very close to the surface. With a total depth of 15.24 m (50 ft) and a depth to water of 1.34 m (4.4 ft), the well appears to be completed in the shallow alluvium. If this is the case, then this water, rich in SO_4^{2-} and with high TDS, is likely moving upward along fractures and faults into the shallow alluvial aquifer. There is evidence that a small amount of this water is mixing into the shallow aquifer system, affecting water quality for almost all shallow aquifer system wells (Fig. 3.28).

There are slight differences between the shallow aquifer system of the El Rito area and that of the Abiquiu-Medanales area. The shallow waters farthest to the north in the El Rito area have TDS concentrations less than 300 mg/L. Shallow wells along El Rito Creek farther to the south have slightly higher TDS concentrations, mostly due to evaporation in the stream as it recharges the shallow aquifer. Other shallow aquifer system waters along the Rio Chama have TDS concentrations between 250 and 500 mg/L (Fig. 3.19). The cation water type for these waters ranges from Ca^{2+} to Na^+ water types. These waters evolve toward Na^+ water type due to cation exchange and mixing with deep aquifer system waters with higher TDS concentrations and high Na^+ concentrations relative to total cations (Fig. 3.27). These shallow aquifer system waters also appear to be recharged by seepage from the Rio Chama when river levels are higher than the local water table or from acequias transporting water for irrigation. Both river and acequia waters would be expected to show the evaporation signature observed in shallow groundwater farther downstream.

Several shallow aquifer system wells along the Rio Chama in the Abiquiu and Medanales areas produce water that exceeds the primary MCL for arsenic (0.01 mg/L; Fig. 3.20). All shallow aquifer system waters in the El Rito area are below the MCL. The deep aquifer system well RA-082 exhibits the highest arsenic concentration of 0.05 mg/L. While some naturally occurring arsenic may be present in waters from the deep aquifer system, it appears that arsenic is also present in groundwater in the shallow alluvial aquifer.

Water quality for almost all shallow aquifer system waters appears to be impacted to at least a small degree by mixing with groundwater with high TDS from deeper aquifers upwelling into the shallow aquifer system. This upwelling may be controlled by faults (acting as a barrier to flow), fractures in shallow bedrock, or the three-dimensional arrangement of low-permeability and high-permeability sediments in the Tesuque Formation. Shallow groundwater in the Abiquiu area is significantly affected by mixing with a small amount of water chemically similar to water sampled from RA-010 and RA-007 (Fig. 3.28).

Recharge to the Shallow Alluvial Aquifers

Stable isotope data for shallow aquifer system waters show three different recharge sources (Fig. 3.33). With the exception of well RA-010, all other shallow aquifer system waters plot on or near one of two apparent evaporation lines. When precipitation with an isotopic composition that plots on a local meteoric water line makes its way to a local stream, it will undergo evaporation to some degree. As the water evaporates, the stable isotopic composition of the water in the stream becomes isotopically heavier and evolves along an evaporation line. If the stream is recharging the shallow alluvial aquifer, the isotopic composition of groundwater will plot along an evaporation line that connects it to its initial composition before it evaporated.

We interpret an evaporation trend for the three samples on the southern flank of the Rio Chama near Abiquiu (Fig. 3.33). The location of the spring that supplies Abiquiu with water (RA-1004) indicates that its water likely originates as precipitation in the Jemez Mountains. The fact that the isotopic composition of this water plots above the Rocky Mountains meteoric water line indicates that it is likely plotting on a different local meteoric water line, representative of different environmental conditions (such as relative humidity) that presumably are present in the northern Jemez Mountains. Near the headwaters of Abiquiu Creek flows, the water is likely isotopically similar to water discharging from the spring RA-1004. As it flows on the surface, the water undergoes evaporation before infiltrating through the streambed to recharge the shallow alluvial aquifer. Well RA-016, which produces water with an isotopic composition plotting on the evaporation line, is located on the south side of the Rio Chama near the mouth of Abiquiu Creek, located approximately 8 km (5 mi) downstream of RA-1004.
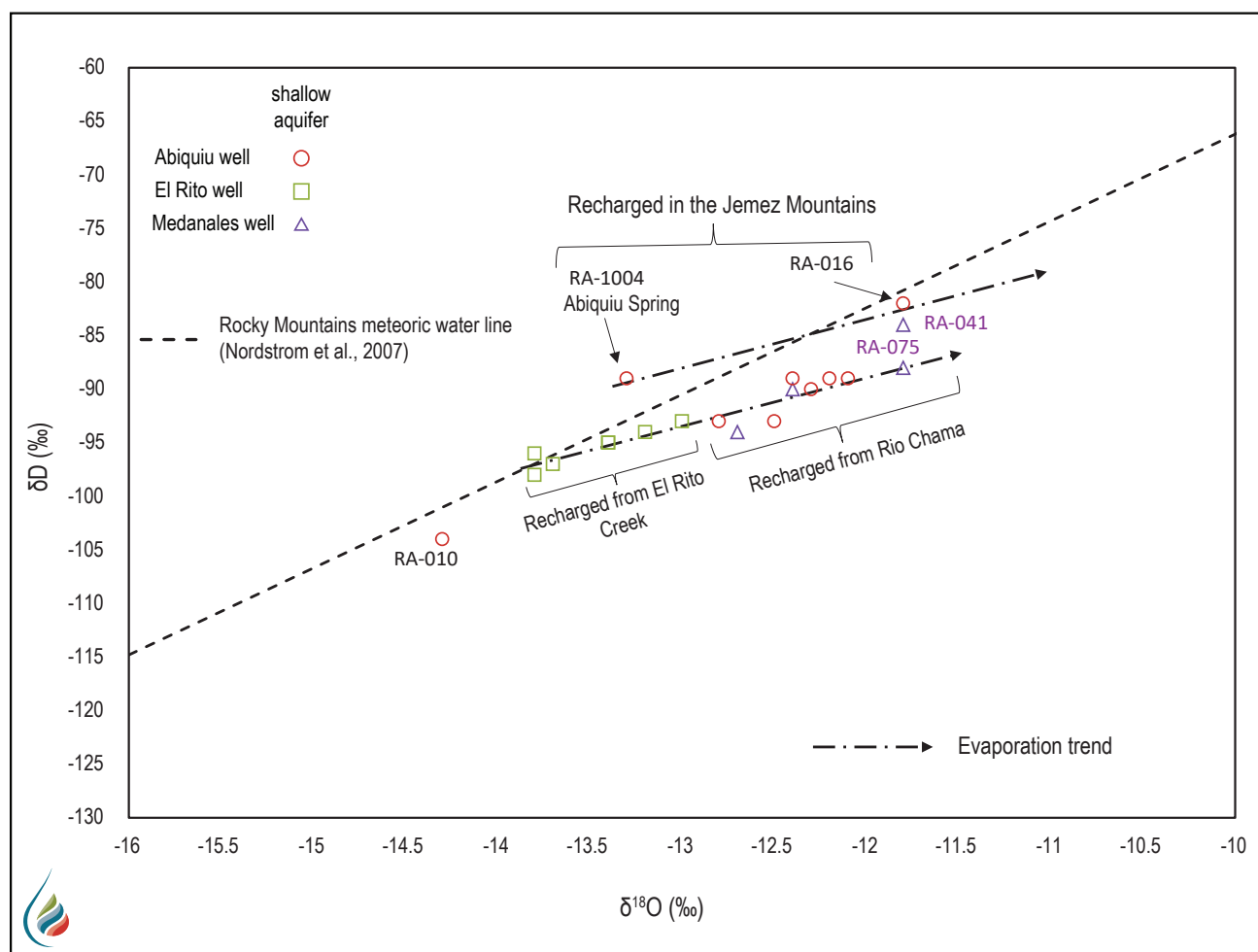

Figure 3.33. Stable isotopic compositions for shallow aquifer system waters. Most points plot along two apparent evaporation lines.

Shallow groundwater in the El Rito area and the Rio Chama has an isotopically similar source in the San Juan and Tusas Mountains, corresponding to the Rocky Mountains meteoric water line, but the fact that they plot separately in Figure 3.33 reflects the larger degree of cumulative evaporation in the Rio Chama, much of which occurs while the water is being stored in Abiquiu Reservoir. Shallow aquifer system waters in El Rito with isotopic compositions plotting on the Rocky Mountains meteoric water line represent relatively unevaporated water in El Rito Creek. Groundwaters with isotopic compositions that plot along the lighter section of the evaporation line were recharged by water from El Rito Creek that had undergone evaporation. Groundwaters with isotopic compositions plotting on the heavier end of this evaporation line of Figure 3.33 represent river water from the Rio Chama with an initial isotopic composition similar to water in Abiquiu Reservoir, which already has an evaporation signature. Irrigation return flow and seepage from the acequias also recharge the shallow alluvial aquifer with what is ultimately evaporated river water. The result of these phenomena is that shallow water from the Rio Chama lies toward the right on the evaporation line of Figure 3.33.

Discharge from Shallow Alluvial Aquifers

Referring to the hydrographs in Figure 3.18, additional water released from Abiquiu Reservoir during November 2022 resulted in the groundwater level gradually increasing by around 0.1 m (0.3 ft) over a period of about a month. During this time, the Rio Chama recharged the shallow alluvial aquifer due to river levels being above groundwater levels. This gradient was reversed shortly after river discharge rates decreased to less than 200 cfs, resulting in groundwater levels being higher than the river level. It was during this period that the river was gaining water from the aquifer; the shallow alluvial aquifer discharged into the river until groundwater levels dropped to be closer to the level of the river. In other words, fluctuation of streamflow results in the Rio Chama being both a gaining stream and a losing stream depending on the relative water levels in the river and the shallow aquifer. There are also periods of time when river flow rates stabilize and equilibrate with the water table, such as August through November 2022.

Characterization of the Deep Aquifer Systems

Most deep aquifer system wells appear to be completed in the Tesuque and Abiquiu Formations, both of which are part of the Santa Fe Group. The Chama-El Rito Member of the Tesuque Formation is the primary deep aquifer in this area, with some wells being screened (at least partly) in the Ojo Caliente area. The TDS for deep aquifer system waters varies widely, ranging from 190 to 4,200 mg/L (Figs. 3.19 and 3.25). With the exception of a few deep aquifer system water samples, all deep aquifer system waters are dominantly Na^+-type waters, with Na^+ representing over 90% of cations (Fig. 3.25, left triangular graph, bottom-right corner). The following discussion focuses on chemistry data for the deep aquifer system wells RA-007, RA-006, RA-008, RA-079, RA-081, RA-013, RA-038, and RA-039 (Fig. 3.34), all of which are completed in the Chama-El Rito Member of the Tesuque Formation. Wells RA-007, RA-006, and RA-008 are separated from the other wells by El Rito Creek, which has a long fault paralleling the creek to the west (Fig. 3.3). This subset of deep aquifer system wells exhibits the full range of TDS. Water produced by wells west of El Rito Creek (RA-006, RA-007, and RA-008) differs significantly from that produced by the deep aquifer system wells east of the creek (RA-079, RA-081, RA-038, RA-039, and RA-013) in several ways. Table 3.4 shows that water level elevations for wells to the west range from 1,820 to 1,870 m (5,971–6,135 ft) above sea level, while the eastern wells exhibit lower water level elevations ranging from 1,757 to 1,780 m (5,764–5,840 ft). Other observed differences include TDS concentrations (Fig. 3.34) and water type (Fig. 3.35). Western wells produce water with TDS concentrations greater than 500 mg/L, and eastern wells produce water with TDS concentrations less than 250 mg/L. The Piper diagram in Figure 3.35 shows that the eastern wells have HCO_3^- as the dominant anion, but the cations show an evolution of water chemistry from Ca^{2+} water type to Na^+ water type, indicative of cation exchange. For the wells to the west of El Rito Creek, all show Na^+ as the dominant cation. All western wells except RA-006 exhibit HCO_3^- as the dominant anion. RA-006 is the only well other than RA-010 to have a significant amount of SO_4^{2-}. The only western well tested for carbon-14 is RA-006, which has the oldest water age of 22,740 YBP. Water from the eastern wells RA-079 and RA-081 shows apparent ages of 9,360 and 11,440 YBP, respectively.
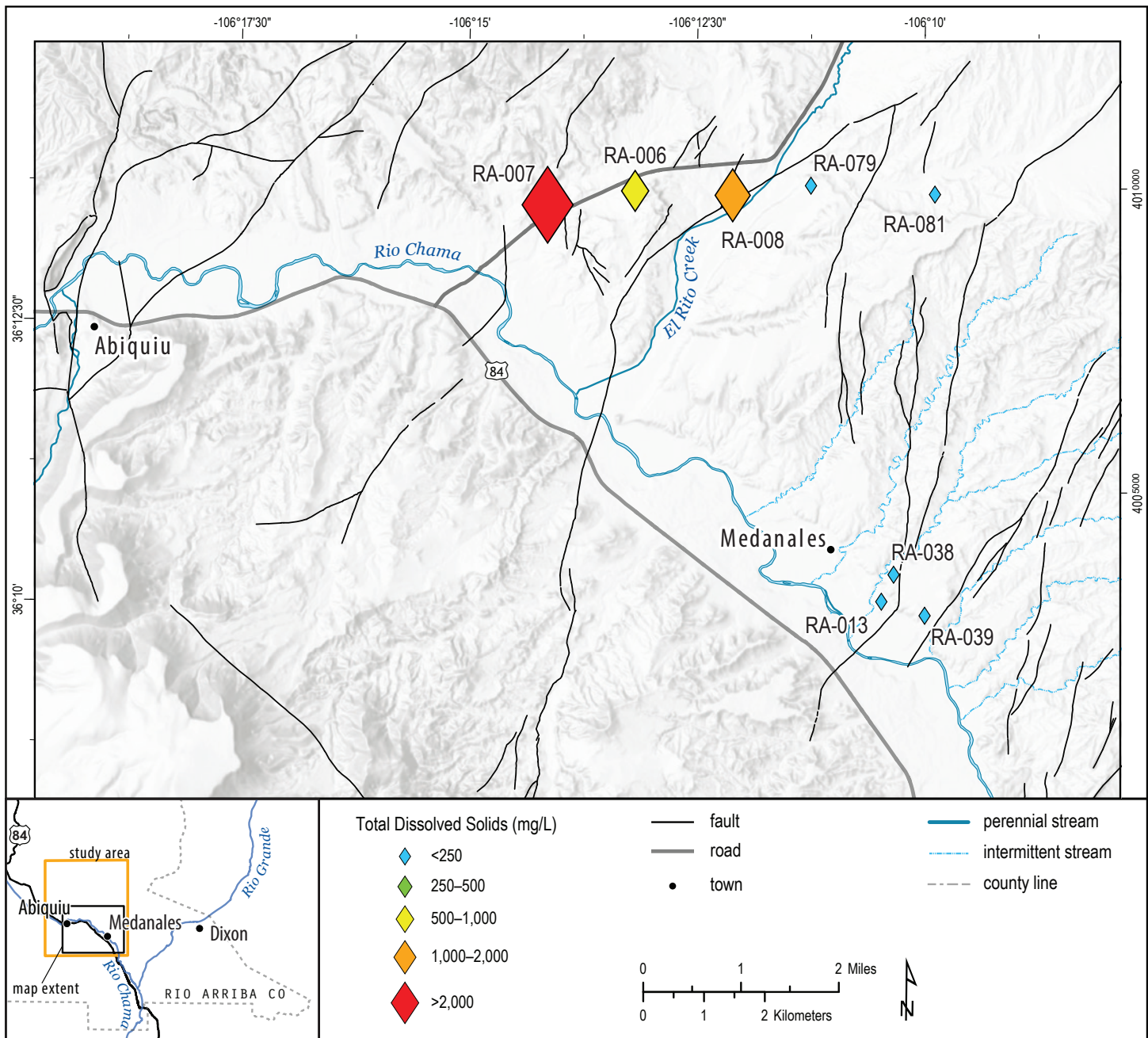
Figure 3.34. Deep aquifer system wells apparently completed in the same geologic formation show a large range in TDS concentrations.

Table 3.4. Well data for specific deep aquifer system wells, including depth to water, water level elevation, total depth, depth range of water-bearing unit, and water-bearing unit description. bgs = below ground surface, NA = not available.

Well ID	Depth to water (m)	Water level elevation (m)	Total depth (m)	Depth range (m bgs)	Description
RA-006	69.7	1,869.7	51.8	40–42	sandstone
RA-007	8.8	1,824.7	108.2	64–108	brown clay/sandstone
RA-008	37.5	1,840.5	91.4	77.7–91.4	fractured sandstone
RA-079	105.7	1,779.6	161.5	131–152.4	fine sand
RA-081	121.2	1,786.4	182.9	150–183	sandstone/gravel
RA-038	30.7	1,769.6	45.7	23.7–45.7	sandstone and light gravel
RA-039	NA	NA	NA	NA	no log
RA-013	17.6	1,757.8	42.7	36.6–42.7	brown and white sandstone
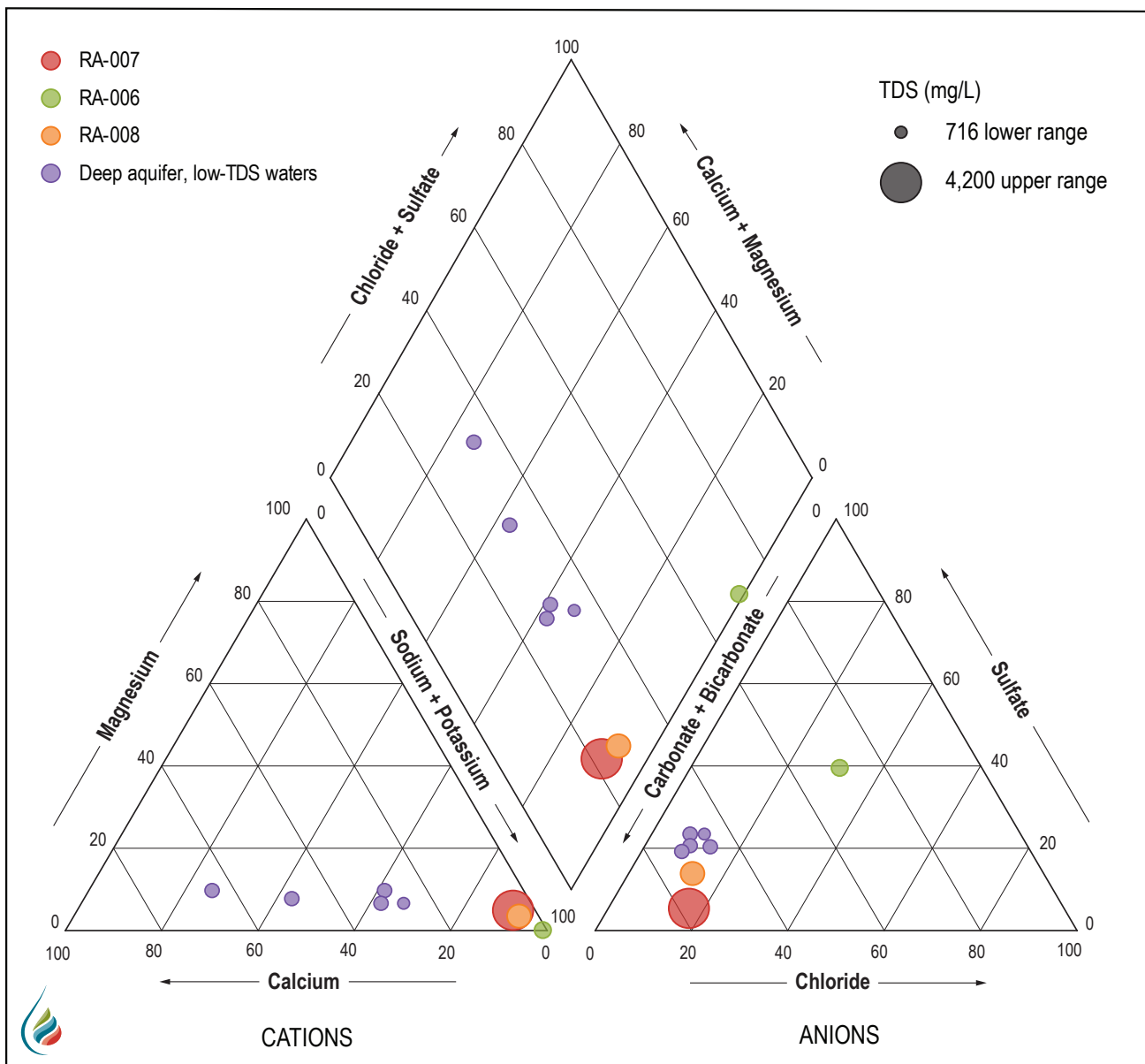
Figure 3.35. Water chemistry data for specific deep aquifer system waters plotted on a Piper diagram.

Unlike the eastern wells, the western wells RA-006, RA-007, and RA-008 produce water that exceeds the primary MCL for uranium (Fig. 3.21). Although the wells east of El Rito Creek produce old water from several hundreds of feet below the surface, it is of excellent quality, with very low TDS concentrations. For this set of wells, the two northern wells RA-079 and RA-081 are approximately 7 km (4.3 mi) from the southern wells RA-013, RA-038, and RA-039, and all of these wells produce water with similar TDS concentrations, similar anion compositions, and cation compositions that show different degrees of cation exchange. It appears that the west-down fault adjoining lower El Rito Creek on the west acts as a notable hydrogeologic barrier separating these two types of groundwaters. The more deleterious quality of groundwater on the west may reflect closer proximity to uplifted bedrock groundwater sources or closer proximity to major fault zones that bound the western side of the Rio Grande rift. The water-bearing unit from which the eastern wells are extracting water may possibly be continuous over a large area. This hypothesis merits further research.

Water produced by RA-006 is representative of a unique water type, with relative Na^+ concentrations greater than 98% of cations; this is also observed for the deep aquifer system wells RA-082, RA-085, and RA-019 (Fig. 3.25). These waters also exhibit high pH values (Table 3.2) and tend to have high uranium concentrations (Fig. 3.21). Geohydrology Associates, Inc. (1979) described the "Las Placitas Well," shown on the geologic cross section in Figure 3.4. The exploratory hole was 731 ft deep, penetrated the Abiquiu Formation, and produced water very chemically similar to water produced by RA-082 and RA-085, with a TDS concentration of 220 mg/L and a pH of 8.87. Wells RA-085, RA-082, and RA-019 all appear to be completed in the Abiquiu Formation, which is the oldest member of the Santa Fe Group. This unit probably has a different lithology (perhaps a high proportion of initial sodium feldspars) that results in this unique groundwater chemistry.
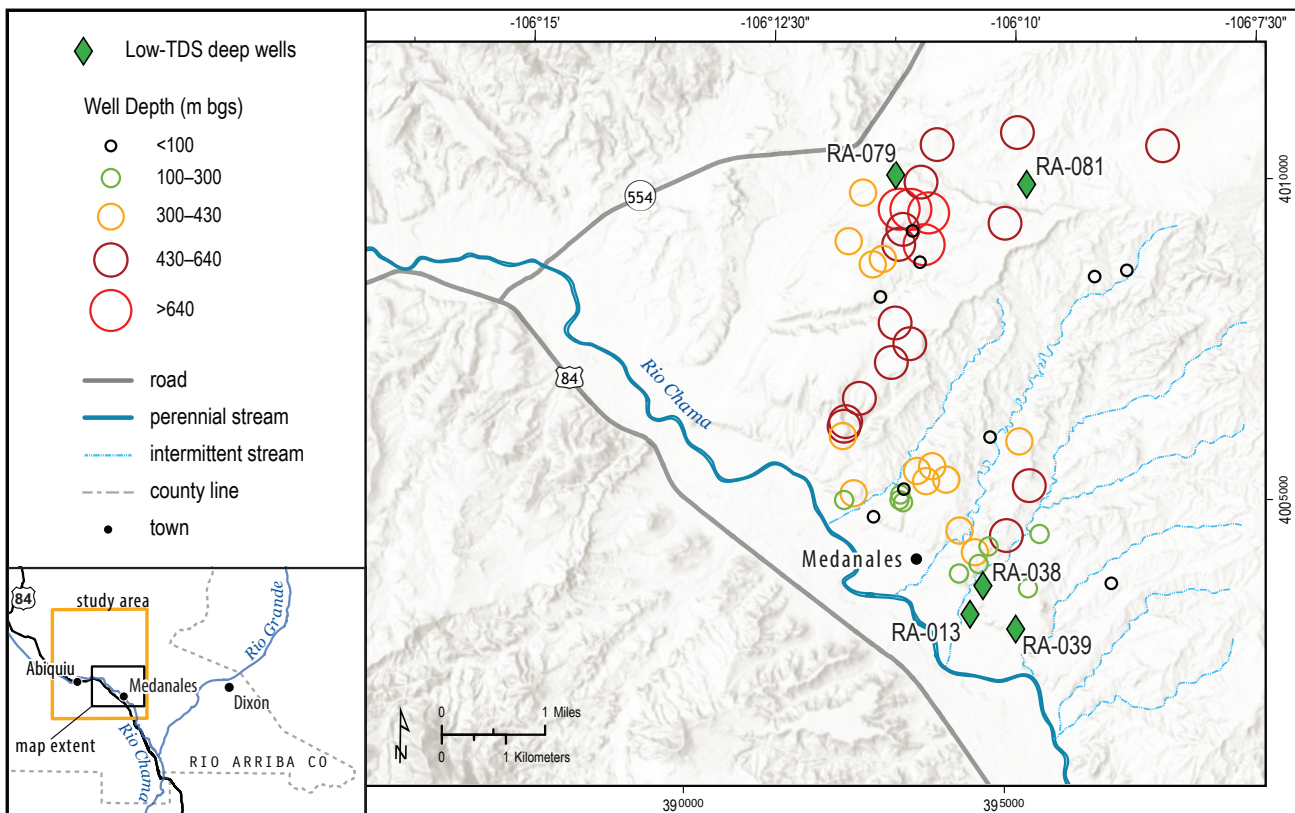
Figure 3.36. Location of deep aquifer system water with low TDS, along with other wells in the area that were studied as potential supply wells.

FUTURE WORK

In addition to the recommended future work described in Chapter 1, further study of the deep aquifer system wells completed in the Chama-El Rito Member of the Tesuque Formation on the east side of El Rito Creek is also suggested. Of the deep aquifer system waters analyzed for this study, the waters sampled from wells RA-079, RA-081, RA-038, RA-039, and RA-013 are of good quality and have low TDS concentrations (Fig. 3.36). These wells appear to produce water from the same water-bearing unit in the Chama-El Rito Member of the Tesuque Formation, with water level elevations ranging from 1,750 to 1,790 m (5,741–5,872 ft) above sea level. The groundwater appears to flow south, possibly along north-south trending faults. While these wells appear to have limited capacity, as most pump 15 to 30 gpm, the water quality is excellent, and it is worth looking at this water source in more detail.

Ethan Mamer collecting a water quality sample from a well near Dixon, New Mexico. *Photo by Robert Pine*

CHAPTER 4: ASSESSMENT OF GROUNDWATER RESOURCES FOR DIXON, NEW MEXICO

STUDY AREA

Dixon is located about 64 km (40 mi) north of Santa Fe and is adjacent to Embudo Creek, which feeds into the Rio Grande about 1.6 km (1 mi) west of the community (Fig. 4.1). Dixon had a population of 938 in 2020 (U.S. Census Bureau, 2024). Groundwater use in Dixon is primarily domestic and public supply. Surface water in the community is used for irrigation; as in other nearby communities, surface water is distributed by a network of acequias. Dixon MDWCA is the public water system for Dixon and serves 500 users, currently with one active well. Other nearby communities, such as Embudo, Canjilon, and Ojo Sarco, also have MDWCAs that use groundwater.

Local Geology

As in the other study areas, the youngest geologic unit is late Quaternary-age alluvium that underlies modern valleys and hosts the shallow aquifer. This unit consists of sand, silty-clayey sand, gravelly sand, and sandy gravel. The sediment is uncemented and weakly consolidated. Maximum thickness is up to around 30 m (100 ft), and the alluvium tends to thin toward the valley margins.

Dixon stratigraphy (Table 4.1) is somewhat similar to that of the northern Española Basin to the west. The primary sedimentary unit in the area is the Tertiary Tesuque Formation of the Santa Fe Group, which comprises basin-fill sediments associated with the opening of the Rio Grande rift. The Tesuque Formation is subdivided into four member-rank units described by Steinpress (1980, 1981), Koning and Aby (2003), and Aby and Koning (2004). The following description is synthesized from these previous works.

The four member-rank units of interest in the Tesuque Formation are (youngest to oldest) the Cejita, Ojo Caliente, Dixon, and Chama-El Rito Members; their distribution is shown in Figure 4.2. The Cejita Member is composed of at least 80 m (262 m) of sandy, pebble- to boulder-gravels with sparse lenses of coarse sand (Aby and Koning, 2004); this unit unconformably overlies either the Ojo Caliente Sandstone or the Dixon Member. The Ojo Caliente Sandstone is an eolian facies (sand dunes deposited by wind) made of weakly cemented fine to coarse sand. Similar to the Cejita Member, the Dixon Member shows channel and floodplain deposits, but the gravel size is smaller, and overall the unit is finer grained (15% mudstone per Steinpress [1980]).

Table 4.1. Descriptions of geologic units for the Dixon area. MYBP = millions of years before present.

	Geologic unit name	General description	Age (MYBP)	Geologic time period
	Quaternary alluvium	sand and silt deposits of modern floodplains and postglacial streams	2.5–0	Pleistocene–Holocene
Santa Fe Group—Tesuque Formation	Cejita Member	fluvial sandstones and conglomeratic channel deposits with some finer-grained floodplain deposits	12–5	Miocene
	Ojo Caliente Member (Tto)	eolian facies; pale brown, cross-stratified to thin planar-bedded sandstone; sand is fine to coarse grained	16–8	Miocene
	Dixon Member (Ttd)	channel and floodplain deposits	16–11	Miocene
	Chama-El Rito Member (Ttce)	channel deposits of volcaniclastic pebbly sandstone, pebble-conglomerate, and sandstone; minor overbank deposits of very fine- to fine-grained sandstone, siltstone, and mudstone in very thin to medium planar beds	16–11	Miocene
	Undivided crystalline rocks (Xu)	coarse-grained nonarkosic sandstones, conglomerates, gray shales, and some limestones	2,500–1,000	Proterozoic
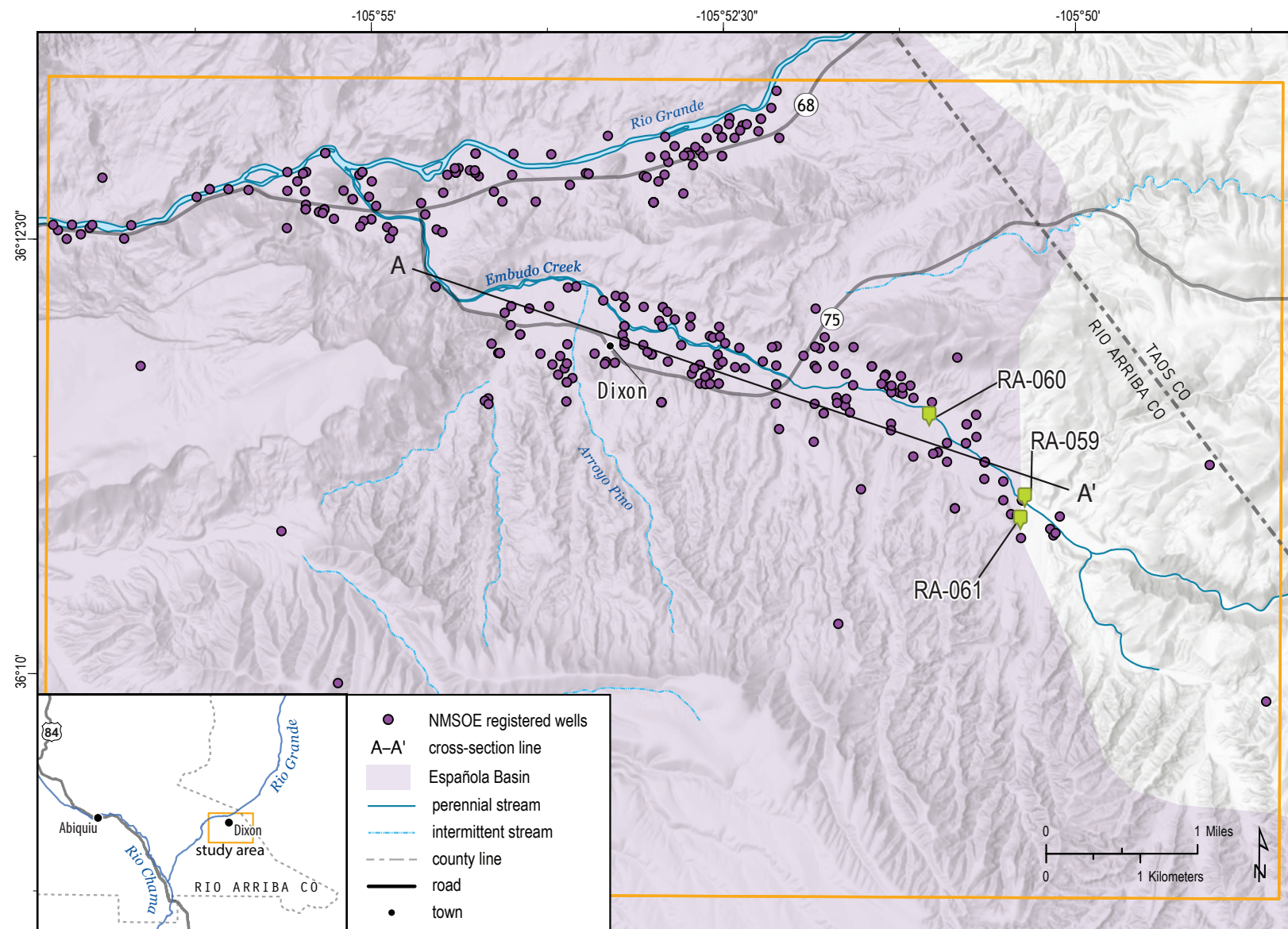
**Figure 4.1.** Study area boundary for the Dixon area, along with NMOSE-registered wells that have depth-to-water measurements and MDWCA wells (RA-060, RA-061, RA-059) that were sampled for this study.
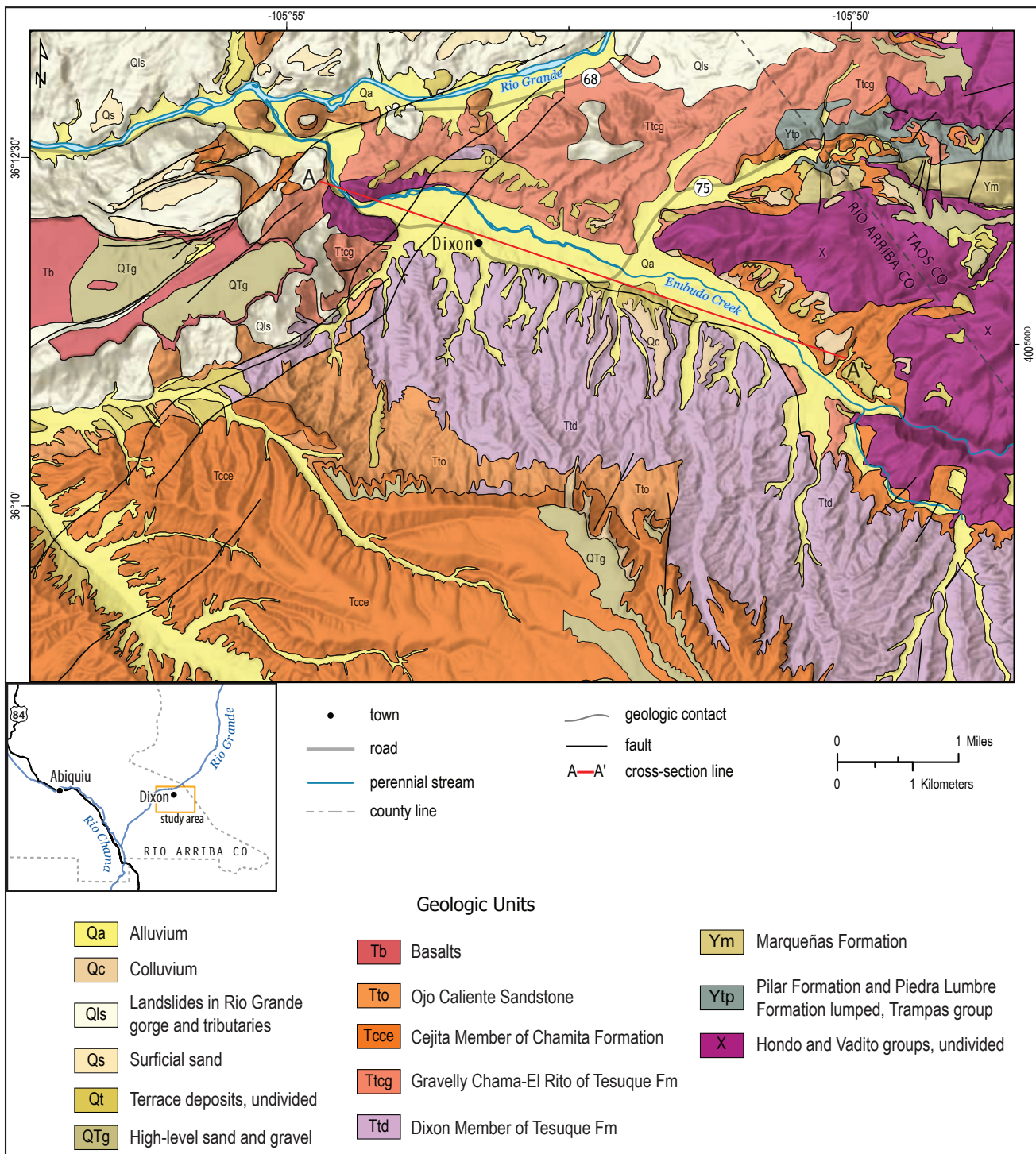
Figure 4.2. Geologic map of the Dixon study area with geologic cross-section line (A–A´). Modified from Koning et al. (2008) and Bauer et al. (2005). See those maps for detailed descriptions of map units.

The Dixon Member primarily underlies the Ojo Caliente Sandstone, but one tongue notably conformably overlies it. Both the Cejita and Dixon are interpreted to reflect fluvial deposition of Proterozoic and Paleozoic material eroded off the western flanks of the adjacent Sangre de Cristo Mountains. Beneath the Dixon Member is the Chama-El Rito Member of the Tesuque Formation, which is generally composed of channel deposits of volcaniclastic pebbly sandstone, pebble conglomerate, and sandstone. This member is relatively more gravelly and coarser than the Chama-El Rito Member exposed near the Medanales study area. The Cejita and Ojo Caliente Members are overall coarser grained and less consolidated than the Dixon and Chama-El Rito Members and are likely more permeable. However, these coarser members are located 110–150 m (360–490 ft) above Embudo Creek and do not supply water to current residents, although several springs are located near the contact of the Ojo Caliente Member and underlying Dixon Member.

Undivided Proterozoic basement rocks composed mostly of quartzite and schist crop out just west of Dixon (Fig. 4.2). The geologic cross section (Fig. 4.3) shows that this crystalline rock occurs at relatively shallow depths east of this outcrop and west of the Embudo fault zone, where it has an approximate maximum depth of 200 m (656 ft) below the surface. On the east end of the valley, gravelly strata at the base of the Chama-El Rito Member (Tesuque Formation) overlie Proterozoic granitic rocks.

A major geologic structure in the Dixon area, the Embudo fault, may have a significant impact on water quality. Faults are sparse east of the Embudo fault, in comparison to intensely faulted terrain near Medanales and Abiquiu. Several significant strike- and dip-slip splays of the Embudo fault zone generally strike northeast-southwest through the Dixon area. This pattern is interpreted as a result of a transfer zone between the Española Basin and the San Luis Basin to the northeast (Muehlberger, 1979; Aldrich, 1986; Koning and Aby, 2003; Koning et al., 2004b, 2013; Goteti et al., 2013). These two basins represent a right stepover of the Rio Grande rift. This stepover and the Embudo fault are aligned along the Jemez lineament, which is a northeast-southwest-trending crustal flaw that coincides with a series of volcanic centers extending from southeastern Arizona to northeastern New Mexico (Mayo, 1958; Aldrich, 1986). The Embudo fault zone deforms rocks of

the Tertiary Tesuque Formation and also exposes Proterozoic metamorphic rocks at the surface just west of Dixon (Koning and Aby, 2003). Here, Proterozoic basement rocks are in both depositional and fault contact with Cenozoic sedimentary deposits.

Groundwater that has a long residence time in crystalline rock can naturally exceed chemical standards for drinking water. A fault that displaces crystalline rock like the Proterozoic basement rocks near Dixon may act as a conduit that discharges poor-quality water at the surface.

Local Hydrogeology

Dixon is located along Embudo Creek about 3.2 km (2 mi) from the confluence of Embudo Creek and the Rio Grande. The nearest climate station is about 32 km (20 mi) to the southwest in Española. The average annual temperature is 11°C (51.6°F; Western Regional Climate Center, 2024). Winter temperatures average 0.2°C (32.3°F), with lows reaching less than -10°C (14°F). Summer temperatures average 21.6°C (70.9°F), with highs reaching around 30°C (86°F).

Average precipitation in Rio Arriba County displays general seasonal and spatial trends, where it is usually greater at higher elevations, during summer, and to the north. Seasonal variability occurs due to summer monsoon storms bringing moisture from the Gulf of Mexico and Gulf of California and winter frontal systems bringing moisture from the Pacific Ocean by prevailing winds. Española, which is about 150 m (500 ft) lower in elevation than Dixon, receives about 0.3 m (11.4 in.) of precipitation on average annually, with summer monsoon rains accounting for about 55% of annual precipitation. Because Dixon is slightly higher in elevation, precipitation amounts may be slightly larger.

Embudo Creek is a perennial stream that drains water from the Picuris Mountains to the northeast via Picuris Canyon and from the Sangre de Cristo Mountains to the southeast via the Rio Pueblo and the Rio Santa Barbara. Figure 4.4 shows a hydrograph for Embudo Creek at Dixon (USGS stream gage 08279000), illustrating natural flow fluctuations between 2010 and 2024. Flow rates in Embudo Creek usually increase to over 300 cfs during spring runoff (March through May) and monsoon season. However, in several instances, flow rates during these times have been 1 cfs or less, which correlates to years of low snowfall and monsoon precipitation.
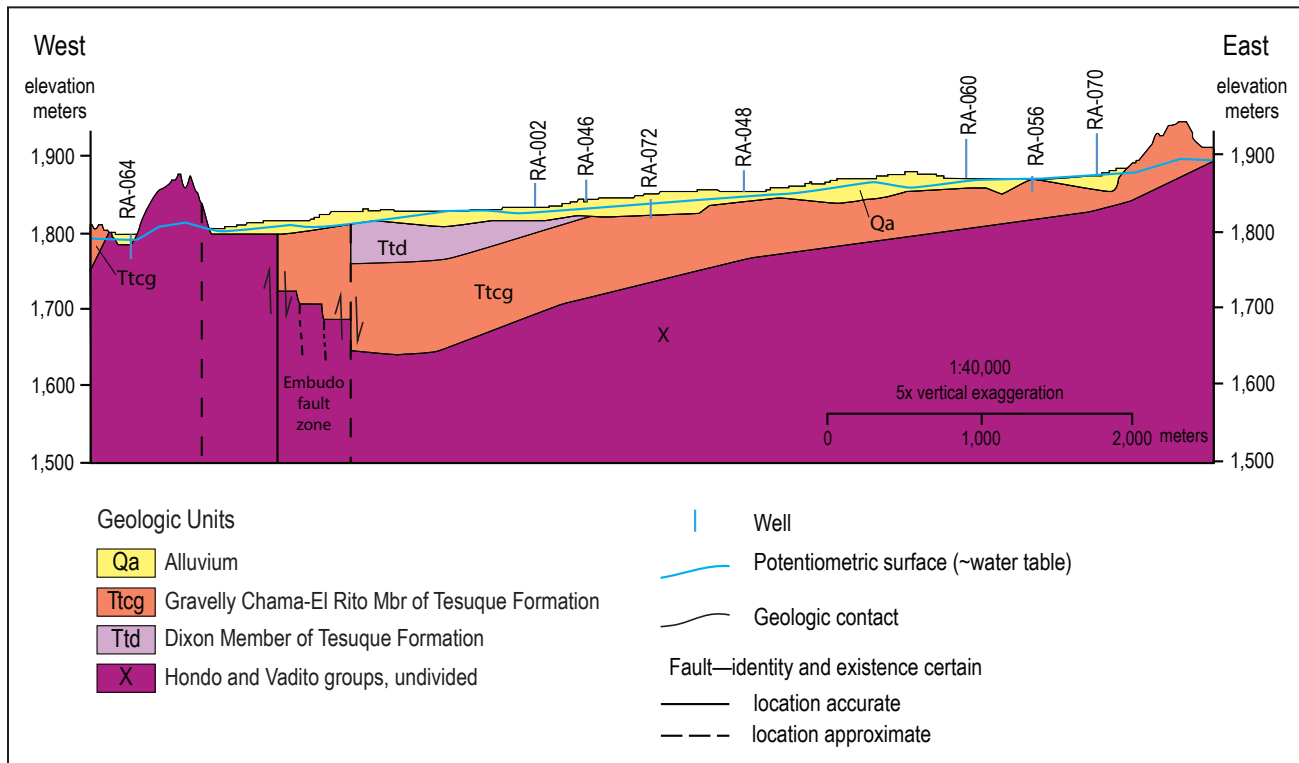
Figure 4.3. Geologic cross section parallel to Embudo Creek. Vertical exaggeration = 5×.
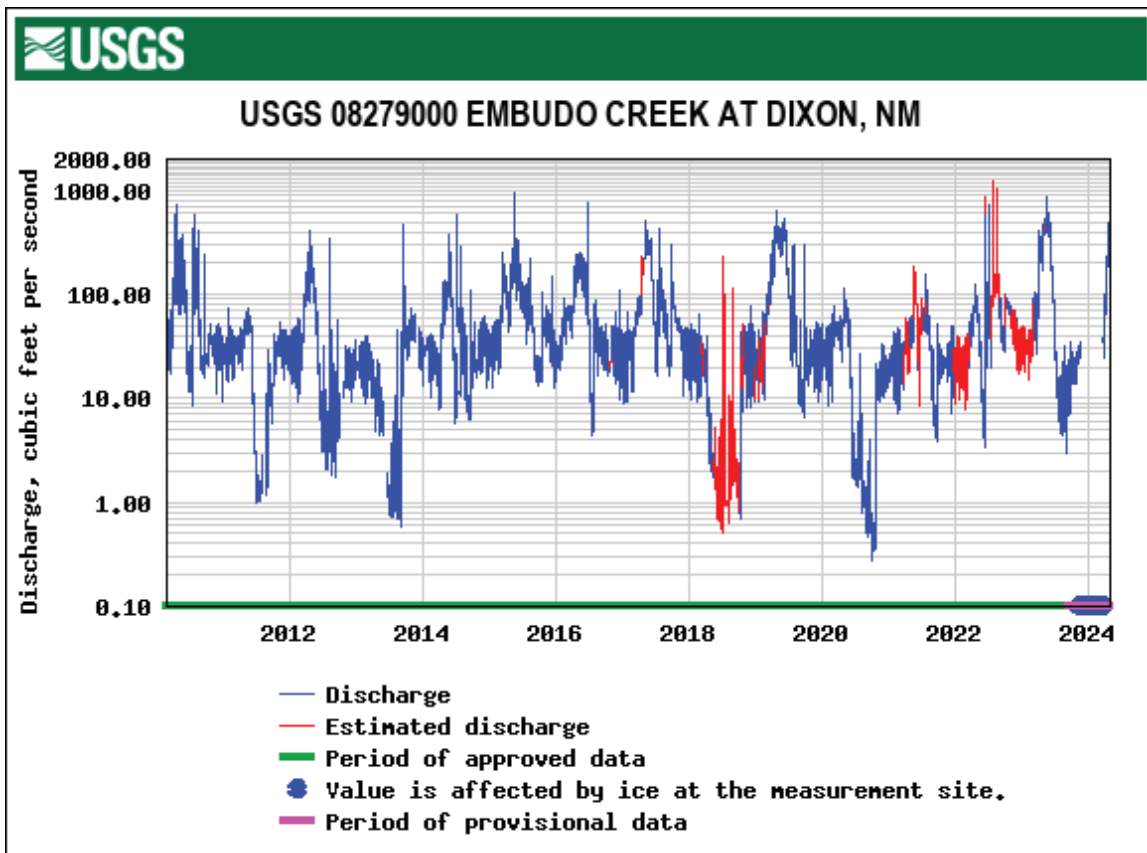

Figure 4.4. Hydrograph for Embudo Creek at Dixon. See Figure 1.1 for gage location.

Depth to water in most wells in the Dixon area is less than 15 m (50 ft), especially in the Embudo Creek valley, while many wells along the southern edge of the valley have depth-to-water measurements in the 15.2 to 45.7 m (50–150 ft) range. Most wells are completed 15.2 to 45.7 m (50–150 ft) deep in sand, gravel, and sometimes clay, with many completed 45.7 to 91.4 m (150–300 ft) and rarely over 100 m (328 ft). Examination of well logs suggests a maximum depth of the shallow alluvial aquifer of around 30 m (100 ft). All of the wells around Dixon are permitted for domestic use. Wells with total depths less than 10 m (33 ft) below the surface are completed in the shallow alluvial aquifer, but deeper wells are screened in the Chama-El Rito Member or a combination of the shallow aquifer and the Chama-El Rito Member.

DATA ASSESSMENT

Existing Data

Figure 4.1 shows registered wells that include depth-to-water measurements in the well records (NMOSE, 2024). Although existing water chemistry data for groundwater are scarce, some data for mutual domestic wells in the study area (Table 4.2), including the Apodaca MDWCA, were located, and we sampled those during this study (well RA-048). The data source was Drinking Water Watch (New Mexico Environment Department, 2024).

New Data

As part of this study, 31 wells in the Dixon area were inventoried. This entailed documenting the well location along with measuring the static depth to water. Twenty-one of these wells (Fig. 4.5) plus two springs (RA-1002 and RA-1003) were sampled for water quality. Criteria for sample site selection included maximized well coverage over the study area, accessibility, the ability of the well to be sampled, and the goal to sample wells that are completed in both shallow and deep aquifer systems. All samples were analyzed for general chemistry (major cations and anions), trace metals, the presence of bacteria, and the stable oxygen and hydrogen isotopes of water. In addition, we tested five of these samples for carbon-14 and tritium, which provides information about how long the water has been in the subsurface.

RESULTS

Water Levels

Figure 4.6 shows depth-to-water measurements for registered wells, which range from 0.3 to 223 m (1–732 ft). Total well depth measurements for these wells range from 2.4 to 400 m (8–1,312 ft) below the surface. Most wells are located within the valley bottom and have depth-to-water measurements of less than 10 m (33 ft) and well depths of less than 40 m (131 ft). These wells are likely completed in the shallow alluvial aquifer. Wells in the valley bottom that are deeper than this tap the deep aquifer system. Some wells located at slightly higher elevations to the south exhibit depth-to-water values between 10 and 20 m (33 and 66 ft) and well depths ranging from 20 to 80 m (66–262 ft), with a few wells with total depths greater than 80 m (262 ft) below the surface.

Table 4.2. General chemistry data for MDWCA wells in the Dixon study area, retrieved from Drinking Water Watch (New Mexico Environment Department, 2024).

| Water system number	MDWCA	Date	Calcium (Ca^{2+}) (mg/L)	Magnesium (Mg^{2+}) (mg/L)	Sodium (Na$^+$) (mg/L)	Potassium (K$^+$) (mg/L)	Bicarbonate (HCO$_3^-$) (mg/L)	Chloride (Cl$^-$) (mg/L)	Sulfate (SO$_4^{2-}$) (mg/L)	Total dissolved solids (mg/L)
3500721	Rio Embudo	08/06/1997	50.8	5.02	6.55	1.9	176	<10	14	190
3502621	Apodaca (RA-048)	11/05/1997	71.5	6.29	6.53	1.36	258	5	17.4	246
3556821	Ojo Sarco	03/29/1999	45.7	7.58	9.23	5	194	<10	<10	246
3556821	Ojo Sarco	10/08/1997	59.5	8.35	8.29	1.87	210	11	10.2	238
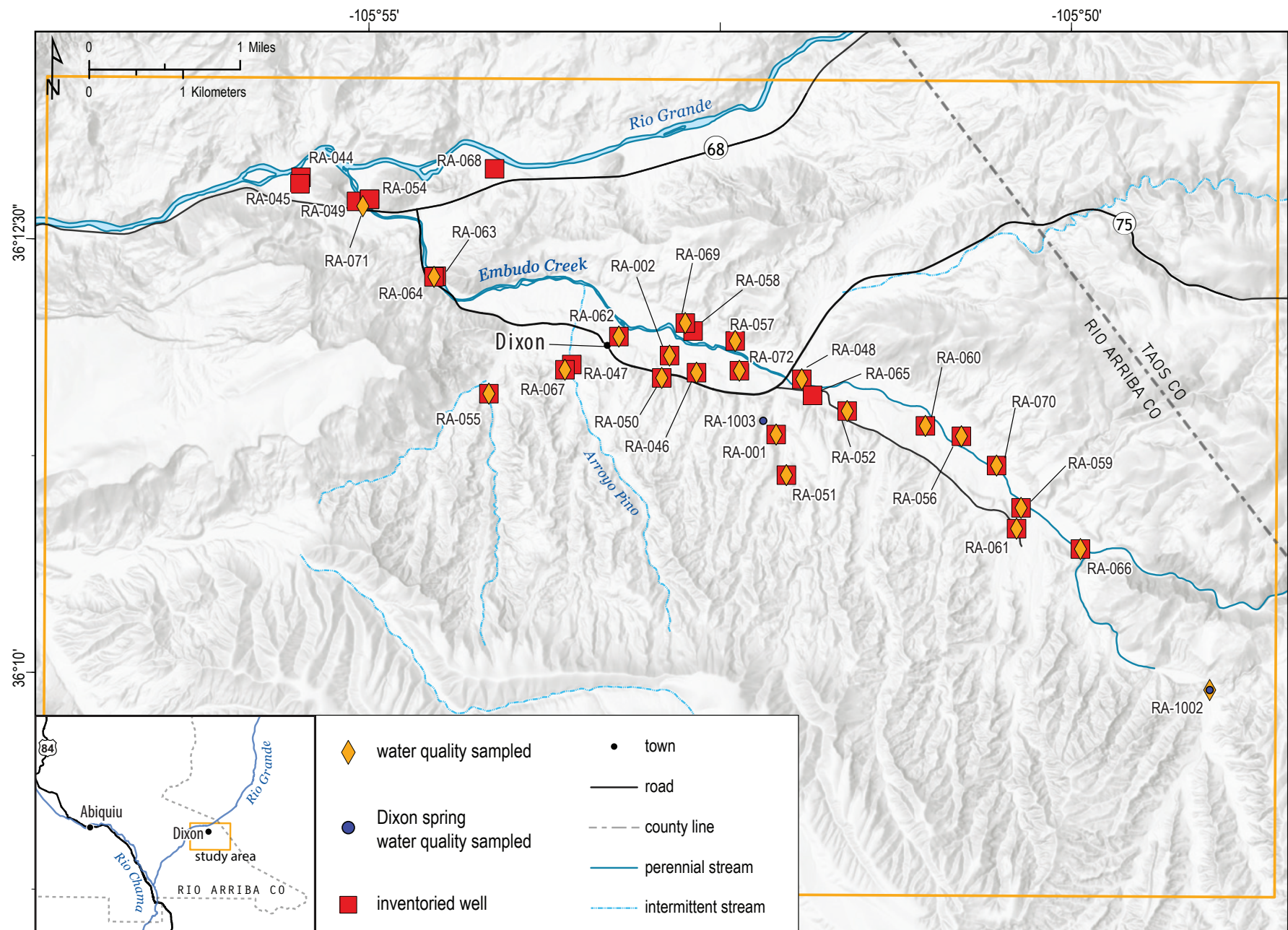
Figure 4.5. Locations of wells and springs that were inventoried and sampled for this study.
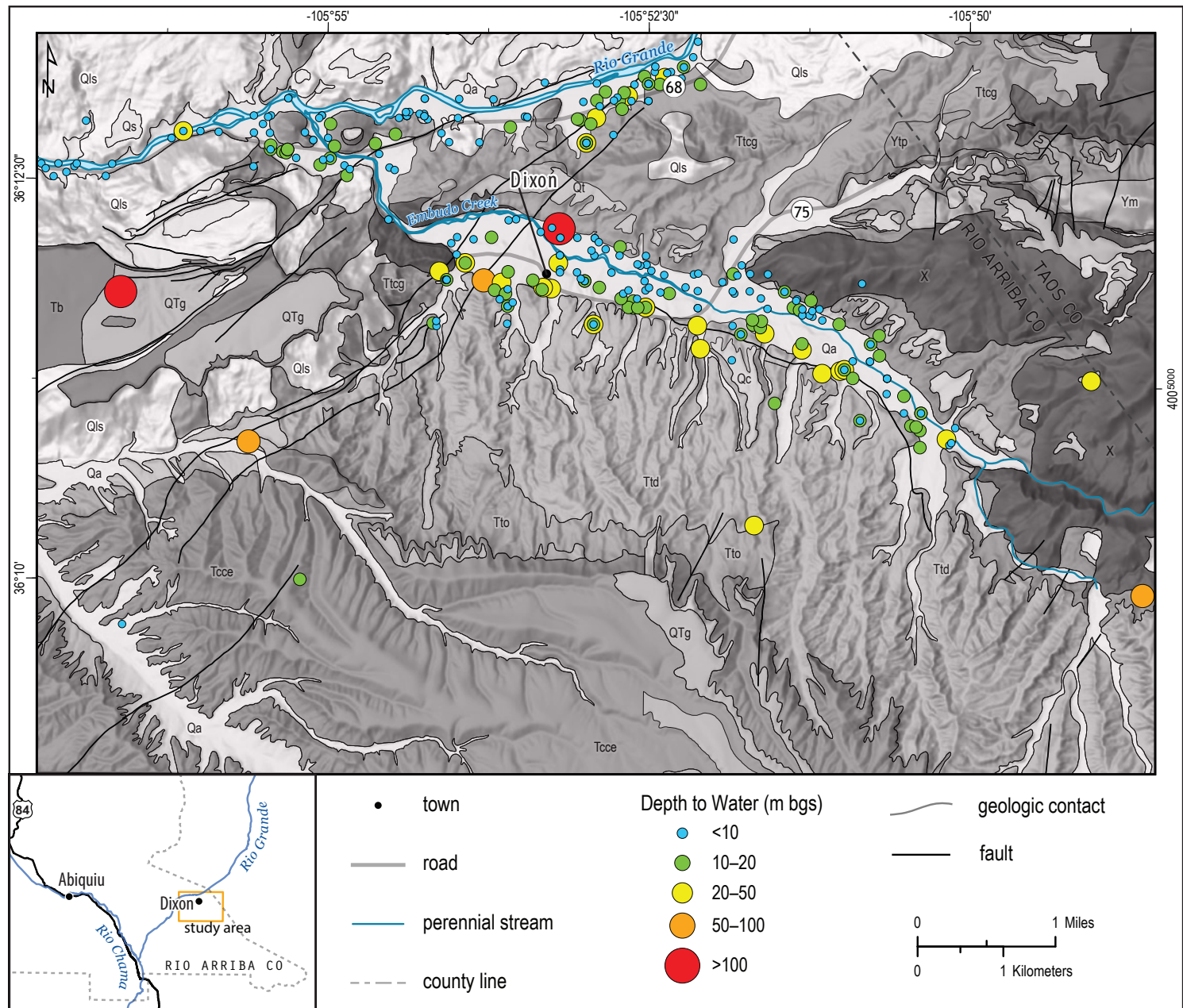
Figure 4.6. Registered wells shown with respect to local geology. The size of the points is proportional to depth to water. Refer to Figure 4.2 for a description of geologic units.

Figure 4.6 shows well locations with respect to local geology. Shallow wells in the floodplain are likely completed in Quaternary alluvium, while deeper wells go through the alluvium to older rocks below. Wells located south of the floodplain appear to penetrate through the Dixon Member (Ttbd) of the Tesuque Formation, which is exposed at the surface, but may be screened in the underlying Chama-El Rito Member.

Figure 4.7 shows a map of the water-table contours for the shallow alluvial aquifer in the study area. The contours represent the surface of the water table. In the Dixon area, our observations show the shallow alluvial aquifer is being recharged from the surrounding mountains and the Rio Embudo. This can be inferred from the gradient of the water table at the edges of the valley; the elevation of the water table near the valley boundaries is higher than in the valley center near the river. Near the center (axis) of the valley, water-table contours are either perpendicular to the river or form Vs that locally point downstream

or upstream. Downstream-pointed Vs suggest water infiltrates from the river and recharges the aquifer near the river. Upstream-pointed Vs suggest recharge to the river from the shallow aquifer. Thus, Embudo Creek appears to be a losing stream in some places and a gaining stream in others, depending on flow conditions. The water-table gradient in the area is around 1.5%. The saturated thickness in the valley is relatively thin in most places, ranging from 5 to 25 m (16.4–82 ft), and is thickest near the axis of the valley (Fig. 4.8).

Depth-to-water measurements for wells inventoried for this study are shown in Figure 4.9 and Table 4.3. Well logs that identified the total well depth, depth of the water-bearing unit, and unit description were not available for many wells. Wells were inferred to be completed in the shallow aquifer system or deep aquifer system based mainly on the depth-to-water measurements, where wells completed in the shallow alluvial aquifer exhibit depth to water of 20 m (66 ft) or less.

Table 4.3. Well details for wells inventoried in this study. Depth to water was measured for this study. Other information was extracted from well records, if available. bgs = below ground surface, gpm = gallons per minute.

| Well ID	Total depth (m)	Depth to water (m)	Top (m bgs)	Bottom (m bgs)	Aquifer system	Approximate yield (gpm)
			Water-bearing unit			
RA-001	17	10	8.2	16.7	deep	10+
RA-002	19	4.91	15	19	shallow	30
RA-046		16.97			shallow	
RA-048		4.52			shallow	
RA-050		17.01			deep	
RA-051		2.32			deep	
RA-052	17	15.04	30	54	deep	10–15
RA-055	102	38.76	79	102	deep	2–3
RA-056	15	7.65	5	14	deep	15
RA-057		2.41			shallow	
RA-059	15	9.06	10	15	shallow	30+
RA-060		4.13			shallow	
RA-061		17.41			shallow	
RA-062		4.06			shallow	
RA-064	30.48	1.83	12.192	30.48	deep	36
RA-066		1.55			shallow	
RA-067	39.624	12.92	15.24	30.48	shallow	10+
RA-069	16.764	3.71	45.72	54.864	deep	
RA-070		5.32			shallow	
RA-071		2.22			deep	2
RA-072	21.336	9.88	15.24	21.336	shallow	20
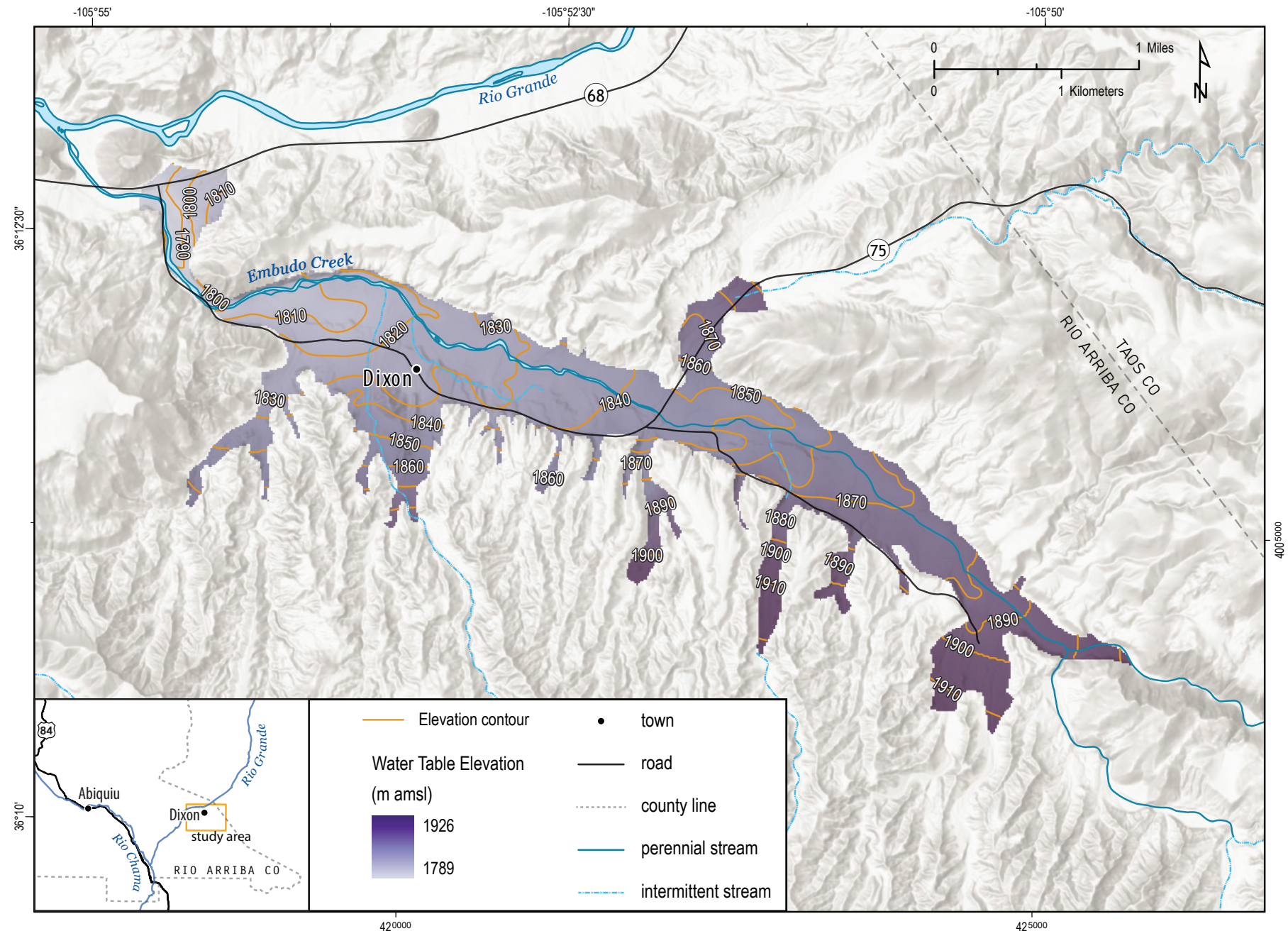
Figure 4.7. Water-table contours for the shallow alluvial aquifer in the Dixon area. Groundwater flows from high elevations to low elevations, generally perpendicular to contours.
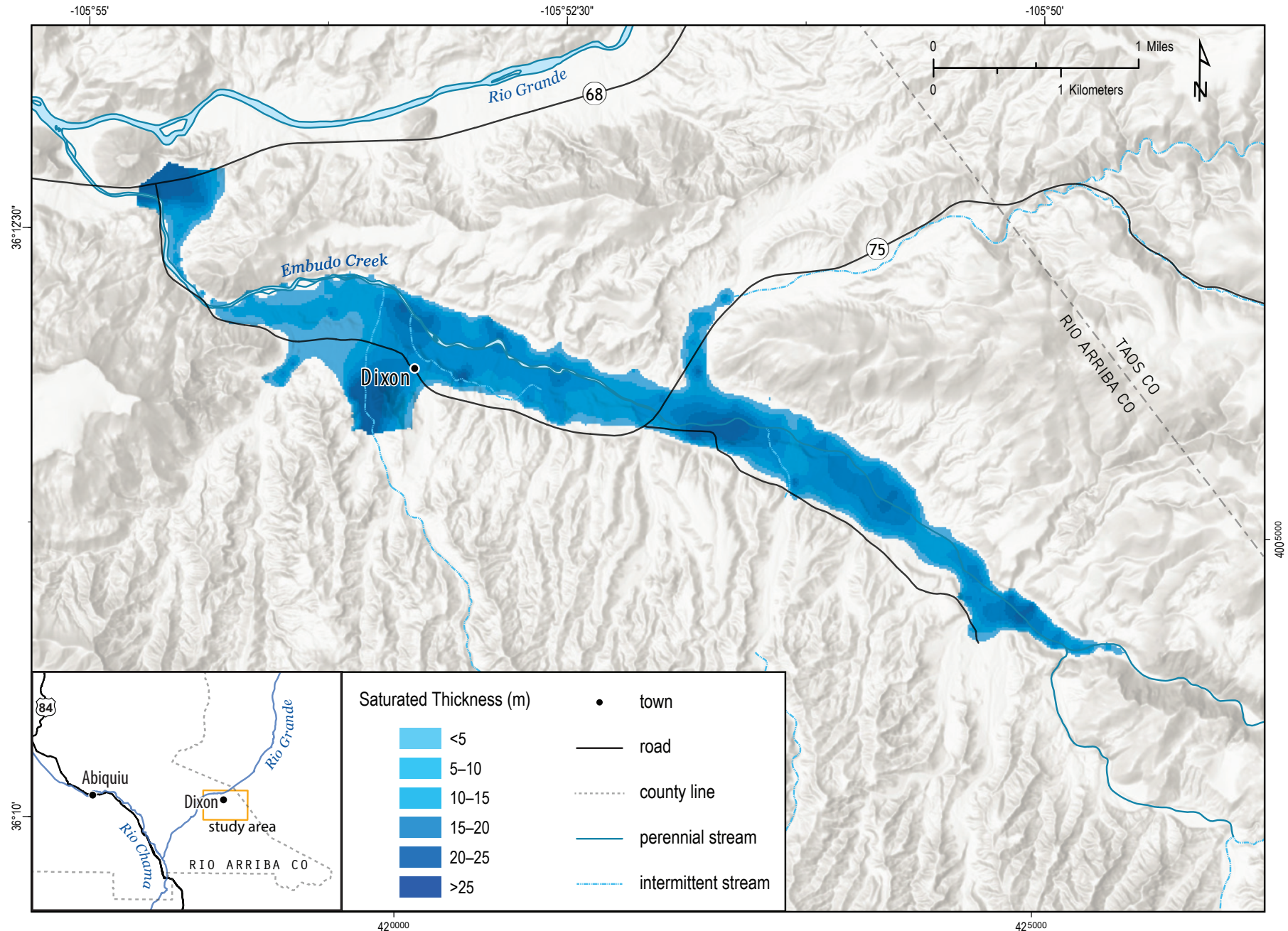
**Figure 4.8.** Saturated thickness of the shallow alluvial aquifer in meters.
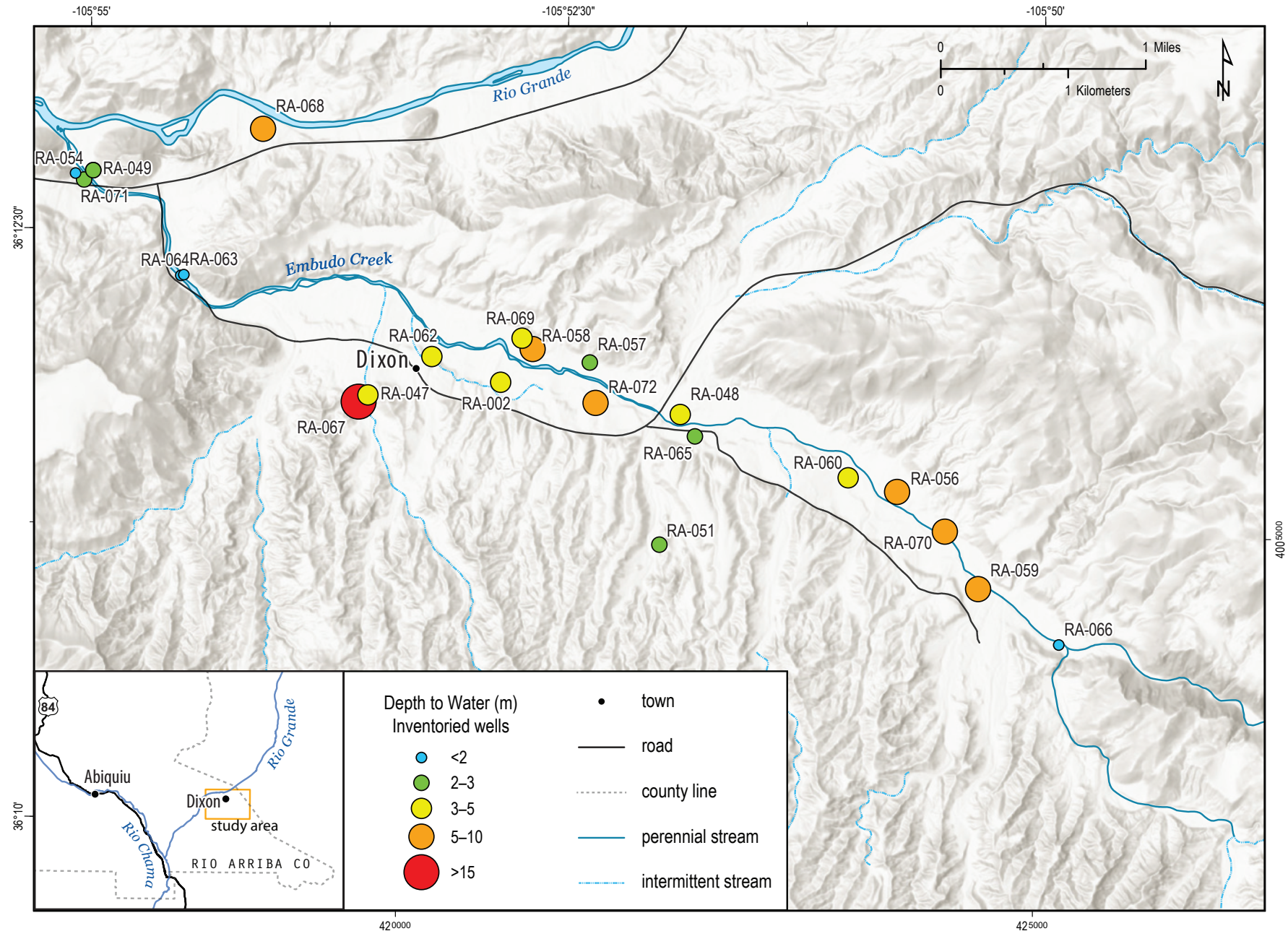
Figure 4.9. Depth-to-water measurements for wells inventoried in this study.

Water Chemistry Data

Water Quality

Table 4.4 shows major ion concentrations and other parameters for water samples. In general, water quality in the Dixon area is quite good, with TDS concentrations for all but two wells (RA-055 and RA-064) ranging from 258 to 434 mg/L (Fig. 4.10). For shallow aquifer system waters, TDS concentrations range from 117 to 211 mg/L—well below the secondary MCL of 500 mg/L. Wells RA-055 and RA-064 exhibit TDS concentrations of 756 mg/L and 9,220 mg/L, respectively. While water quality is generally good, some constituents were found to be above both the primary and secondary MCLs.

Groundwater sample results for coliform and several chemical constituents, including arsenic and fluoride, are depicted in Table 4.5. We tested all groundwater samples for the presence or absence of total coliform and *E. coli*. Only one shallow aquifer system well (RA-057) showed the presence of total coliform. Figure 4.11 shows arsenic concentrations for water samples; all but one deep well produce water that exceeds the primary MCL. Well RA-064 produces water with an arsenic concentration of 0.878 mg/L, which is over 80 times the MCL. The next-highest arsenic concentration was 0.0511 mg/L, observed for water produced by RA-069. No shallow aquifer system wells that were sampled produced water exceeding the arsenic primary MCL.

Table 4.4. Major ion and silica concentrations (mg/L), pH, and temperature (°C). S = shallow aquifer system, D = deep aquifer system, Sp = spring.

Point ID	Aquifer system	Calcium (Ca^{2+}) (mg/L)	Magnesium (Mg^{2+}) (mg/L)	Sodium (Na^+) (mg/L)	Potassium (K^+) (mg/L)	Bicarbonate (HCO_3^-) (mg/L)	Chloride (Cl^-) (mg/L)	Sulfate (SO_4^{2-}) (mg/L)	Total dissolved solids (mg/L)	Silica (SiO_2) (mg/L)	pH	Temperature (°C)
RA-002	S	87.9	7.95	11.4	1.31	288	6.89	29.5	309	17.6	7.3	12.5
RA-046	S	92.7	8.53	21.6	1.58	325	6.94	32.5	351	22.5	7.22	14.1
RA-048	S	80.6	7.6	8.49	1.23	256	5.27	27.4	275	15.1	7.35	12.3
RA-057	S	96.2	11	43.3	2.31	410	12	40.3	432	20.2	6.79	14.6
RA-059	S	36.7	2.84	55.7	1.12	185	19	35.9	263	15.8	7.75	13.6
RA-060	S	75.3	7.14	8.3	1.23	235	5.62	27.8	259	14.8	7.39	13.2
RA-061	S	85	7.12	19.7	1.33	288	6.59	30.4	318	20.4	7.34	15
RA-062	S	89.6	8.37	14.1	1.52	287	7.58	30.8	318	19.6	7.28	12.8
RA-066	S	83.9	12.8	54.3	2.41	383	25.9	30.5	431	24	7.59	15.3
RA-067	S	105	6.1	22.8	3.15	351	5.81	29.8	375	23.9	7.16	14.3
RA-070	S	94.7	8.97	9.66	1.57	291	7.03	37.2	323	16.8	7.02	15.7
RA-072	S	88.1	7.82	13.1	1.45	281	6.33	30.4	309	18.8	7.32	13.5
RA-001	D	23.9	2.92	93.3	5.64	273	9.91	42.5	372	50.6	7.87	15.9
RA-050	D	3.24	0.046	100	1.95	168	12.3	45.9	297	34.3	9.04	15.7
RA-055	D	8.38	0.295	236	3.83	244	91.1	232	756	59	8.6	17.1
RA-064	D	404	74.5	2,870	250	3,580	3,690	90.5	9,220	9.36	6.4	15.4
RA-052	D	50.9	3.48	79.7	1.88	312	11.6	35.5	363	19.8	7.77	14.6
RA-069	D	3.54	0.086	133	2.87	128	50.7	83.8	398	40.1	9.08	15.4
RA-051	D	4.15	0.091	100	1.34	196	12.2	36.6	287	24.9	8.91	15.3
RA-056	D	2.99	0.01	93.3	0.629	94	25.6	47.4	258	17.4	9.26	15.4
RA-071	D	57.6	6.58	65.2	3.77	288	35.1	20	355	19.8	7.31	13.4
RA-1002	Sp	86.1	17.5	47.6	1.7	414	24.8	6.09	434	38.2	7.57	12.1
RA-1003	Sp	4.25	0.138	93.5	1.29	200	8.1	34.3	271	22.5	8.54	12
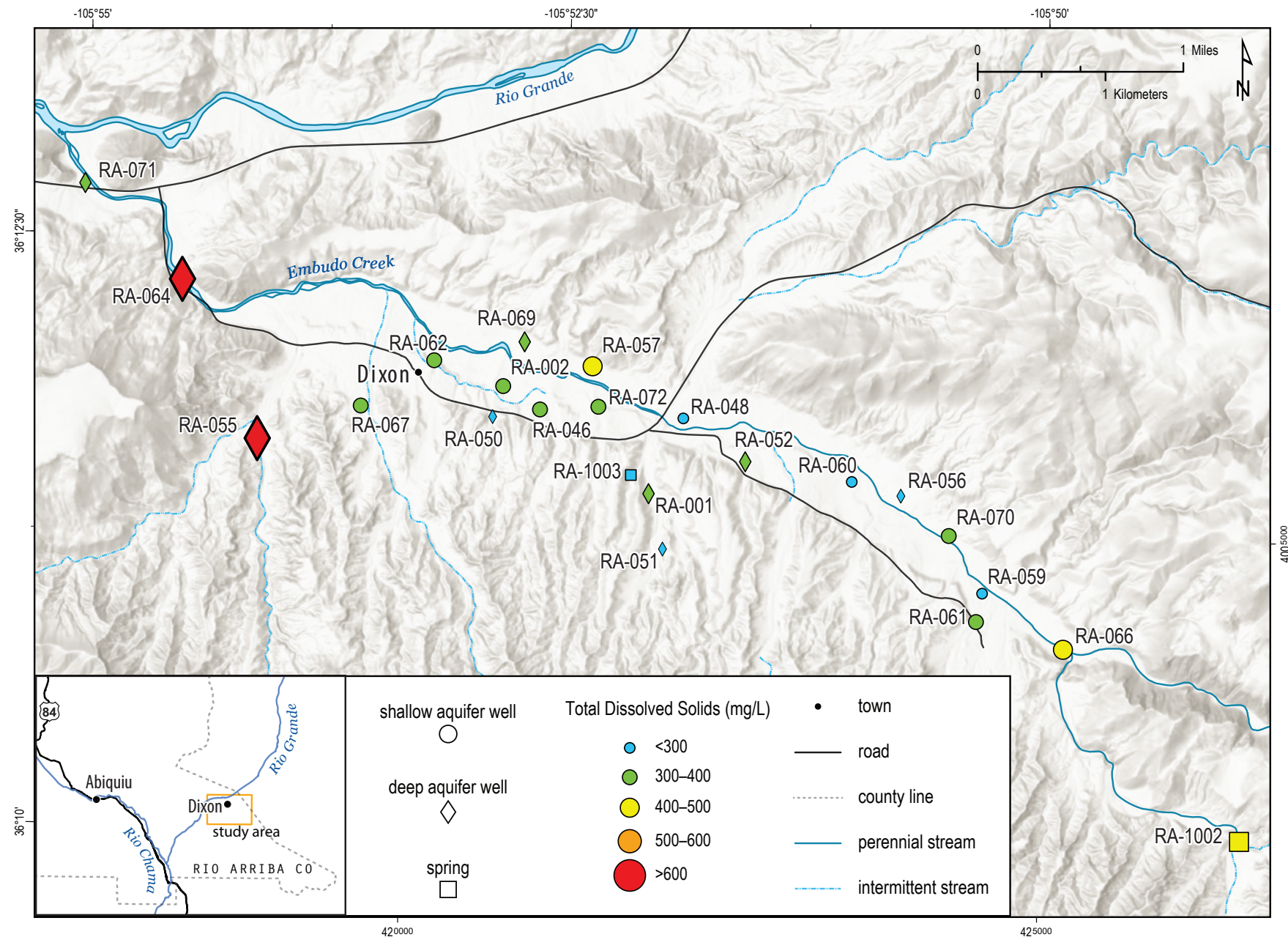
Figure 4.10. Sample locations, with point size proportional to TDS concentration.
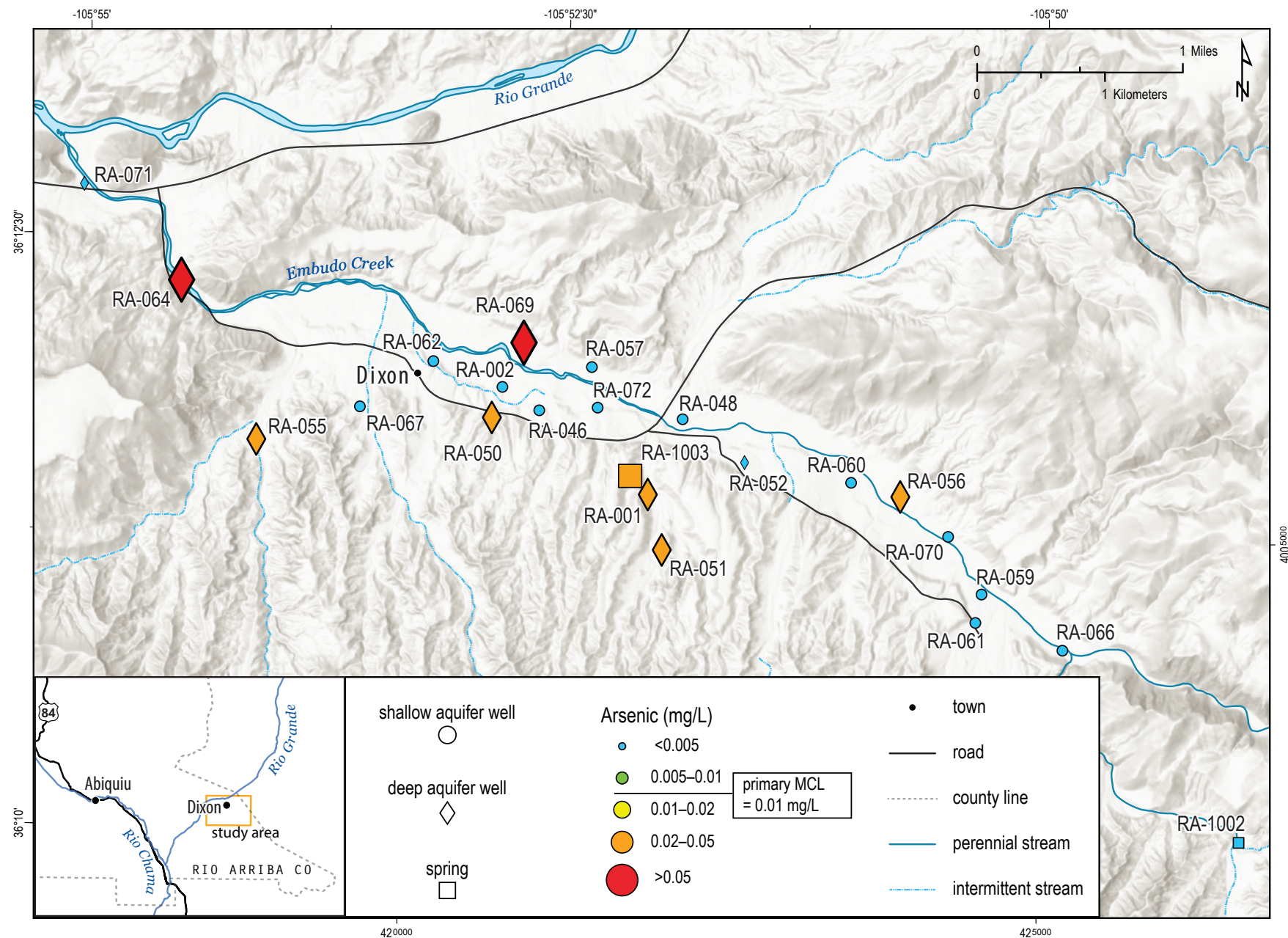
Figure 4.11. Arsenic (As) concentrations for water samples. Yellow, orange, and red points represent exceedance of the primary MCL.
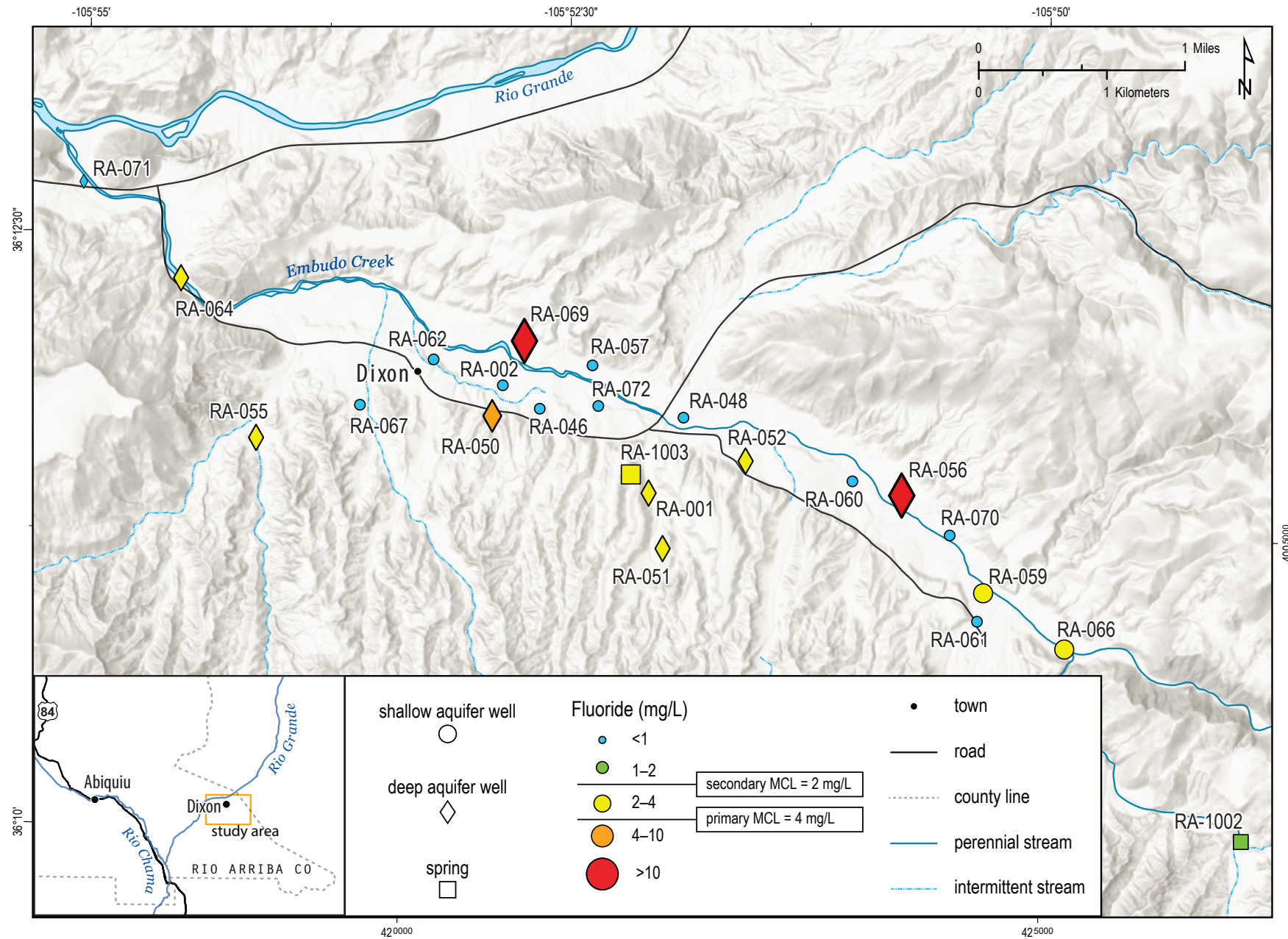
Figure 4.12. Fluoride (F⁻) concentrations for water samples. Yellow points represent wells producing water exceeding the secondary MCL, and wells shown in orange and red produce water that exceeds the primary MCL.

Figure 4.12 shows fluoride concentrations for water samples. Only three deep aquifer system wells produce water exceeding the primary MCL of 4 mg/L, and almost all other deep aquifer system wells produce water exceeding the secondary MCL of 2 mg/L. The two wells farthest upstream (RA-059 and RA-066) produce the only shallow aquifer system waters that exceed the secondary MCL of 2 mg/L. The spring RA-1003 discharges water that exceeds the primary MCLs for both arsenic and fluoride. A small number of wells (deep and shallow aquifer systems) produce water exceeding the secondary MCLs for iron and manganese. Well RA-064, located about 1 km (0.6 mi) downstream

from Dixon, produces very poor-quality water, with a TDS concentration of almost 10,000 mg/L and an extremely high arsenic concentration; it also exceeds MCLs for fluoride, uranium, chloride, iron, and manganese. Table 4.5 also shows that several deep wells produce water with pH values above 8.5, which is discussed in more detail below.

General Chemistry

Table 4.4 shows concentrations of major ions as well as TDS, silica (SiO_2), pH, and temperature. Figure 4.13 shows the groundwater chemistry for the water samples plotted on a Piper diagram. In all but one of the shallow aquifer system samples

Table 4.5. Concentrations of contaminants for which the EPA has established primary and secondary MCLs. Concentrations that exceed the primary MCL are highlighted red, and concentrations that exceed the secondary MCL are highlighted yellow. Bacterial tests show the presence (P) or absence (A) of total coliform and *E. coli*.

Point ID	Aquifer system	Total coliform	E. coli	Arsenic (As) (mg/L)	Fluoride (F⁻) (mg/L)	Uranium (U) (mg/L)	Chloride (Cl⁻) (mg/L)	Iron (Fe) (mg/L)	Manganese (Mn) (mg/L)	pH	Sulfate (SO₄) (mg/L)
EPA secondary drinking water MCL					2		250	0.3	0.05	<6.5 >8.5	250
EPA primary drinking water MCL				0.01	4	0.03					
RA-001	deep	A	A	0.0228	3.59	0.0116	9.91	<0.01	0.001	7.87	42.5
RA-002	shallow	A	A	0.001	0.41	0.0033	6.89	<0.01	<0.001	7.3	29.5
RA-046	shallow	A	A	0.0024	0.47	0.0049	6.94	<0.01	<0.001	7.22	32.5
RA-048	shallow	A	A	0.0007	0.28	0.0021	5.27	<0.01	<0.001	7.35	27.4
RA-050	deep	A	A	0.0356	7.49	0.0078	12.3	<0.01	0.002	9.04	45.9
RA-051	deep	A	A	0.0275	3.48	0.0124	12.2	0.011	0.005	8.91	36.6
RA-052	deep	A	A	0.0015	2.32	0.0092	11.6	1.14	0.074	7.77	35.5
RA-055	deep	A	A	0.0208	3.27	0.0261	91.1	<0.05	<0.005	8.6	232
RA-056	deep	A	A	0.0291	17.1	0.0056	25.6	0.026	0.002	9.26	47.4
RA-057	shallow	P	A	0.0041	0.59	0.0064	12	0.018	0.026	6.79	40.3
RA-059	shallow	A	A	0.0031	2.93	0.0225	19	0.112	0.006	7.75	35.9
RA-060	shallow	A	A	0.0007	0.38	0.0019	5.62	<0.01	0.001	7.39	27.8
RA-061	shallow	A	A	0.0046	0.96	0.0062	6.59	<0.01	<0.001	7.34	30.4
RA-062	shallow	A	A	0.0009	0.45	0.0039	7.58	<0.01	<0.001	7.28	30.8
RA-064	deep			0.878	2.6	0.118	3,690	14.1	1.92	6.4	90.5
RA-066	shallow	A	A	0.0012	2.19	0.0085	25.9	0.123	1.95	7.59	30.5
RA-067	shallow	A	A	<0.0005	0.17	0.0119	5.81	<0.01	<0.001	7.16	29.8
RA-069	deep	A	A	0.0511	13.9	0.0028	50.7	<0.01	0.002	9.08	83.8
RA-070	shallow	A	A	0.0005	0.33	0.0021	7.03	<0.01	<0.001	7.02	37.2
RA-071	deep	A	A	<0.0005	0.65	0.003	35.1	<0.01	0.013	7.31	20
RA-072	shallow	A	A	0.0016	0.42	0.0033	6.33	<0.01	0.001	7.32	30.4
RA-1002	spring			0.004	1.57	0.0033	24.8	1.26	0.616	7.57	6.09
RA-1003	spring			0.0243	4	0.012	8.1	<0.01	<0.001	8.54	34.3

(RA-059), Ca^{2+} is the dominant cation and HCO_3^- is the dominant anion, resulting from the dissolution of calcite. For all but one deep aquifer system water (RA-071), the dominant cation is Na^+; most deep aquifer system waters exhibit HCO_3^- as the dominant anion. Three deep aquifer system waters (RA-055, RA-069, and RA-056) show an increase in relative SO_4^{2-} concentrations. Water from the deep aquifer system well RA-064, which exhibits the highest TDS concentration, shows a very different anion composition, with Cl^- being the dominant anion.

Stoichiometric analysis, which accounts for the proportions in which elements or compounds react

with one another, confirms that almost all water samples showed some degree of cation exchange. Cation exchange is a water/mineral interaction where Na^+ ions that are adsorbed to clay minerals exchange with Ca^{2+} and Mg^{2+} ions that are dissolved in the groundwater. Because Ca^{2+} and Mg^{2+} have twice the charge of Na^+, for every one molecule of Ca^{2+} or Mg^{2+} that adsorbs to a mineral surface, two molecules of Na^+ are released into solution in the groundwater. This process can explain the overall trend observed for cations, which is a roughly linear arrangement from water that is Ca^{2+} dominant to Na^+ dominant. Mixing of different water sources is
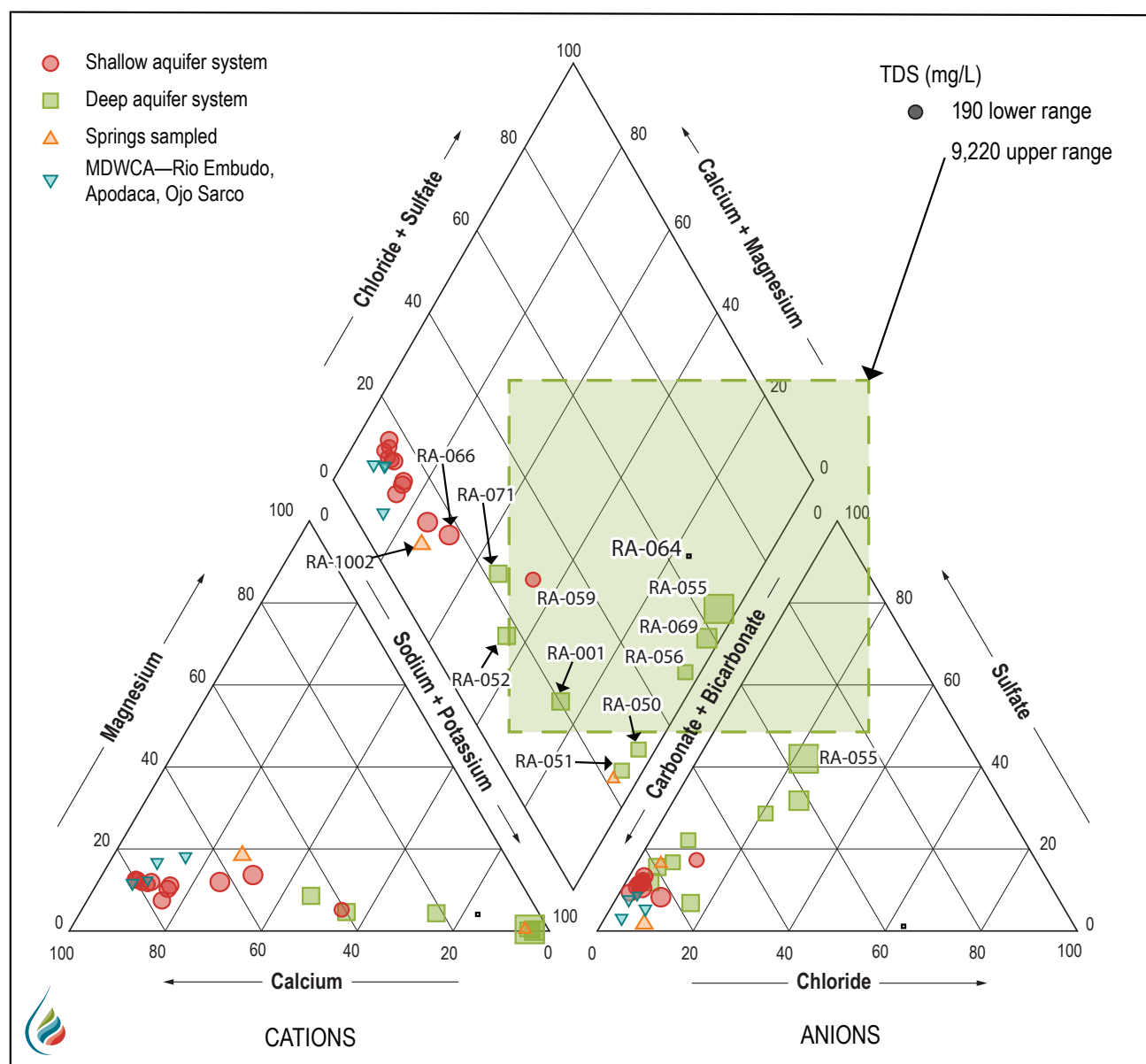

Figure 4.13. Major ion chemistry data for groundwater and spring samples and MDWCA wells plotted on a Piper diagram. The large green square is the data point for RA-064. Water produced by this well exhibited the highest TDS concentration (9,220 mg/L) of all wells sampled for this study.

the other main process that controls water chemistry in this aquifer system. The anion composition in Figure 4.13 shows possible mixing between shallow aquifer system waters and water chemically similar to that produced by well RA-055, which is located near the downstream end of the study area in the hills just south of Embudo Creek.

Stable Isotopes

As seen in Figure 1.7, all groundwater samples from all study areas appear to be primarily derived from winter precipitation and snowmelt. Figure 4.14 shows the same δD versus $\delta^{18}O$ graph as Figure 1.7 but focuses on the Dixon dataset. The global meteoric water line and the Rocky Mountains meteoric water line (Nordstrom et al., 2007) are included. All but one of the shallow aquifer system water samples plot in a group wherein a few points plot on the Rocky Mountains meteoric water line and the rest plot between the two meteoric water lines. The shallow

aquifer system well RA-066 plots close to the spring sample from Ojo Sarco (RA-1002) both in terms of stable isotopic composition (Fig. 4.14) and in terms of major ion composition (Fig. 4.13). Therefore, water from the spring RA-1002 and well RA-066 have likely undergone evaporation from an initial composition similar to other shallow aquifer system waters on the Rocky Mountains meteoric water line. Points that plot on the global meteoric water line include deep aquifer system samples RA-001 and RA-050 and the sampled spring RA-1003. The deep aquifer system well RA-064, which produces water with the highest TDS concentration, plots slightly to the right of the global meteoric water line. The two different meteoric water lines represent different recharge areas. Deep aquifer system waters that plot between the two meteoric water lines are mixtures of shallow aquifer system waters and deep aquifer system waters that plot on or near the global meteoric water line.
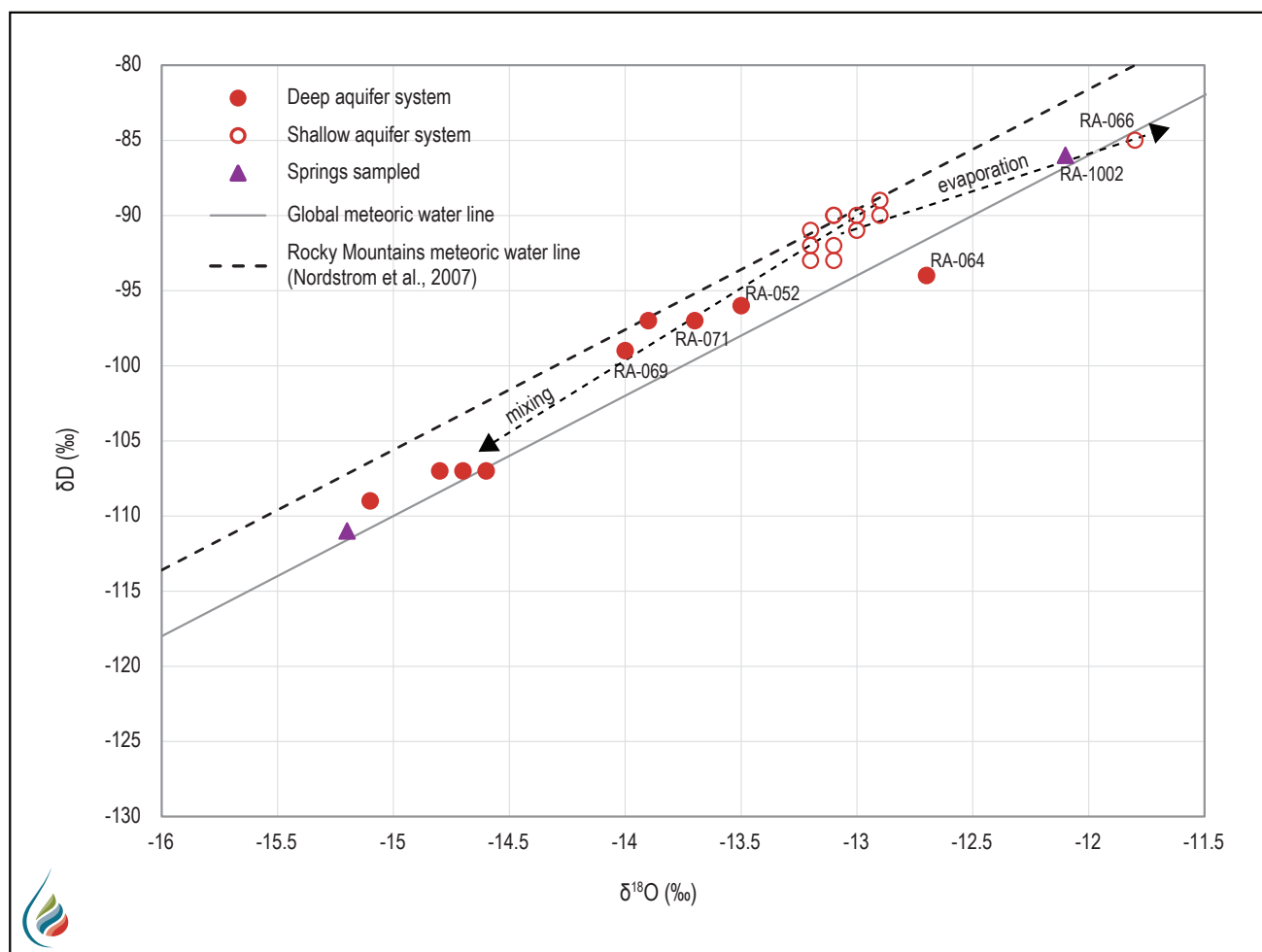

Figure 4.14. Stable isotopic composition of groundwater samples plotted on a δD versus $\delta^{18}O$ graph. Arrows indicate the different processes such as mixing and evaporation.

From these data, it is clear that waters in the shallow alluvial aquifer are primarily derived from winter precipitation and snowmelt in the Sangre de Cristo Mountains. The Rocky Mountains meteoric water line has a deuterium excess (y-intercept) of 14.4. Local meteoric water lines with deuterium excesses greater than that of the global meteoric water line are usually derived in mountainous areas where there is enough local moisture to evaporate and contribute to some of the local precipitation. Evaporation of such local moisture tends to be enriched in deuterium, hence the higher deuterium excess value of the Rocky Mountains meteoric water line. Deep waters sampled above the valley bottom to the south of Embudo Creek have a different origin, which probably reflects a high-altitude aquifer that was possibly recharged during a colder climate (hence the lighter isotopic values compared to the shallow aquifer data). Mixing between these older waters in the deep aquifer system and water in the shallow alluvial aquifer results in observed isotopic compositions for water samples from wells RA-069, RA-071, and RA-052.

Groundwater Ages

Table 4.6 shows results for ^{3}H, $\delta^{13}C_{DIC}$, and carbon-14 analyses in the Dixon region. Water produced by well RA-066 is very young according to both ^{3}H and carbon-14, which indicates it is about 20 years old. The other shallow aquifer system water (from RA-060) contains less ^{3}H (3.35 TU) and has an older corrected carbon-14 age of 426 YBP, indicating that this water has traveled along a longer flow path and/or has mixed with older, ^{3}H-free water along the way. The small negative ^{3}H (essentially zero) values for deep aquifer wells RA-069 and RA-051—both of which have high pH and are very rich in Na$^+$—are consistent with the old corrected carbon-14 ages of 27,409 and 35,535 YBP, respectively. Deep aquifer system water from RA-071, located at the far downstream end of the study area

just before the confluence with the Rio Grande, has a ^{3}H concentration of 2.76 TU and a corrected carbon-14 age of 160 YBP.

DISCUSSION AND CONCLUSIONS

For the following sections, refer to Figure 4.15, which is a hydrogeologic conceptual model based on the information and analyses discussed above.

Characterization of the Shallow Alluvial Aquifer

General Description

The shallow alluvial aquifer supplies groundwater for residents and communities along Embudo Creek, including Dixon. The aquifer is composed of Quaternary alluvium, including sand, silty-clayey sand, gravelly sand, and sandy gravel. Based on the reported pumping yields, which range from 20 to 60 gpm, hydraulic conductivities are quite high, meaning that water can easily flow through pores in the aquifer. The primary limitation of this aquifer is its physical size. Its spatial extent is limited to the valley bottom (Fig. 4.9), which is about 0.8 km (0.5 mi) wide in most areas. The saturated thickness is greatest—around 10 to 20 m (33–66 ft)—along the longitudinal axis of the streambed (Fig. 4.8). As seen in the geologic cross section (Fig. 4.3), many wells continue through the alluvium and are completed in Santa Fe Group rocks and sediments, which tend to produce water of lower quality, as discussed below.

Geochemical Description

Groundwater produced from shallow aquifer system wells is high quality, with TDS concentrations below 500 mg/L. Except for well RA-059, all shallow aquifer system wells are Ca^{2+}-HCO_3^- water type (Fig. 4.13), resulting from the dissolution of calcium carbonate ($CaCO_3$). Some variability observed for the cation composition is due to cation exchange and a small amount of mixing with other water sources.

Table 4.6. Tritium (^{3}H) concentrations, $\delta^{13}C_{DIC}$ data, and estimated carbon-14 (^{14}C) concentrations and ages for groundwater. TU = tritium unit, PMC = percent modern carbon, YBP = years before present.

| Site	System	^{3}H (TU)	$\delta^{13}C_{DIC}$ (‰)	^{14}C (PMC)	^{14}C age (YBP)	Corrected ^{14}C age (YBP)
RA-069	deep	-0.06	-7.6	2.3	30,290	27,409
RA-051	deep	-0.09	-8.3	0.94	37,470	35,535
RA-071	deep	2.76	-6.4	52.31	5,210	160
RA-060	shallow	3.35	-11.3	89.44	900	426
RA-066	shallow	5.8	-12	99.78	20	20
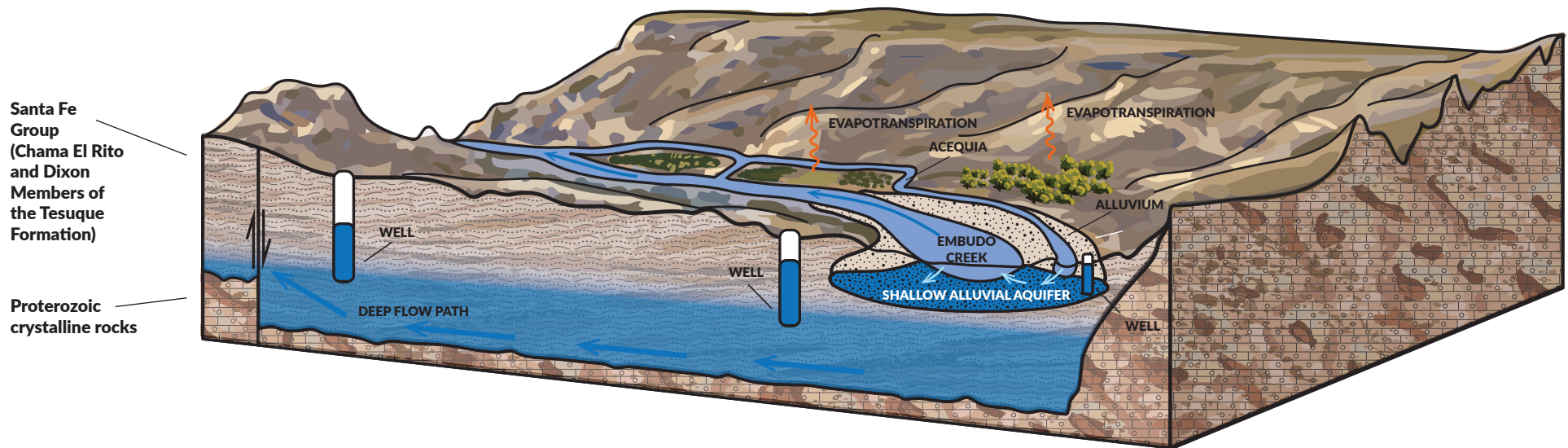
Figure 4.15. Hydrogeologic conceptual model for the Dixon area. The shallow alluvial aquifer is primarily recharged by rain and snow in the Sangre de Cristo Mountains, water from Embudo Creek, and acequias. Wells tapping the deep aquifer system are completed in Santa Fe Group rocks (Dixon and Chama-El Rito Members of the Tesuque Formation). The deep aquifer system likely sits on top of the Proterozoic crystalline rocks. Deep aquifer system water appears to increase in TDS concentrations with increasing depth. Deep groundwater flows to the west toward the Rio Grande. The Embudo fault zone forces these deep aquifer system waters to upwell into the shallow system on the other side of the fault zone. Groundwater in the deep aquifer system is generally low in TDS concentrations, high in relative sodium concentrations, and high in pH value (>8.5), which is likely due to dissolution of sodium-rich feldspars that make up much of the gravel and sand grains in the strata.

Groundwater Recharge and Discharge

Water from shallow aquifer system wells that was tested for tritium and carbon-14 contains tritium (Table 4.6), indicating that shallow aquifer system waters are a mixture of young groundwater that is less than 50 years old and older water that is more than 50 years old. Stable isotope data (Fig. 1.6) show that most shallow aquifer system waters are sourced from a high-elevation recharge area. These waters do not show any signs of evaporation, suggesting that Embudo Creek is likely a gaining stream much of the time. Therefore, much of the shallow groundwater is recent recharge, primarily from snowmelt and winter precipitation in the Sangre de Cristo Mountains to the southeast that is mixing with older shallow aquifer system waters that also originated in the Sangre de Cristo Mountains. However, some waters from the shallow aquifer system, such as well RA-066 and spring RA-1002, show evidence of evaporation (Fig. 4.14). The spring is located a short way up a small tributary to the south, and the well is located very close to the mouth of this tributary. These data suggest the tributary is a losing stream and recharges the shallow alluvial aquifer. Ultimately, water in the shallow alluvial aquifer discharges to Embudo Creek or the Rio Grande.

Characterization of the Deep Aquifer Systems

Groundwater produced by well RA-064 exhibits a TDS concentration of 9,220 mg/L, which is an order of magnitude higher than that exhibited by all other water samples (Fig. 4.13). This well is located west of the Embudo fault zone and is completed in Proterozoic rocks that crop out in that area. This well produces water that exceeds primary and secondary MCLs for almost all contaminants listed in Table 4.5, notably arsenic, which is exceeded by 80 times (Fig. 4.11). This water is likely very old (tens of thousands of years) and resides in fractures in Precambrian rocks. These rocks obviously do not constitute a suitable aquifer and should be avoided. Interestingly, the data shown here give no evidence this water is mixing into the shallow aquifer system.

Figure 4.16 shows the locations of five deep aquifer system wells and the spring RA-1003, all of which produce water with high pH values (>8.5) that exhibit relative Na$^+$ concentrations upward of 95% of total cations (Fig. 4.13). These waters appear to be discharging from the Chama-El Rito Member of the Tesuque Formation and exhibit TDS concentrations ranging from 258 to 756 mg/L. There is evidence that water chemically similar to water from RA-055, with a TDS concentration of 756 mg/L, is mixing with waters from the shallow alluvial aquifer system (Fig. 4.13). While these waters have relatively low TDS concentrations, they all exceed the primary MCL for arsenic (Fig. 4.11). Luckily, this mixing has not impacted the water quality of shallow aquifer system waters. Water with similar chemistry was observed for deep aquifer system wells in the Abiquiu Valley area, as described in Chapter 3. Similar water was also observed being produced from the Chama-El Rito Member of the Tesuque Formation in the San Luis Basin north of the Española Basin (Drakos et al., 2004). These high pH values are likely due to the dissolution of alkali feldspars (which are sodium-rich). When fresh meteoric water with very low TDS concentration comes in contact with these feldspars, Na$^+$ ions from the feldspar exchange with hydrogen ions (H$^+$), resulting in pH increasing to values between 8.5 and 10.

FUTURE WORK

Based on the recharge processes and small size of the aquifer in this study region, it is critical to consider the long-term sustainability of water supplies. The primary recharge to this region is snowmelt and winter precipitation. As climate changes in the future with increased temperatures and reduced recharge to aquifers (via less snowpack), it is critical to consider multiple water supply options. Further community discussions regarding consolidated water supplies are considered an important next step for this region. Having numerous private domestic wells in an area where the primary aquifer (a shallow alluvial aquifer) is thin and not extensive may cause wells to impact each other through pumping. By potentially consolidating groundwater supplies to a few productive wells with good water quality, community supply for the long term may be accomplished. Additional research on wells east of the Embudo fault zone in the formations at depth may provide additional options for water supply.
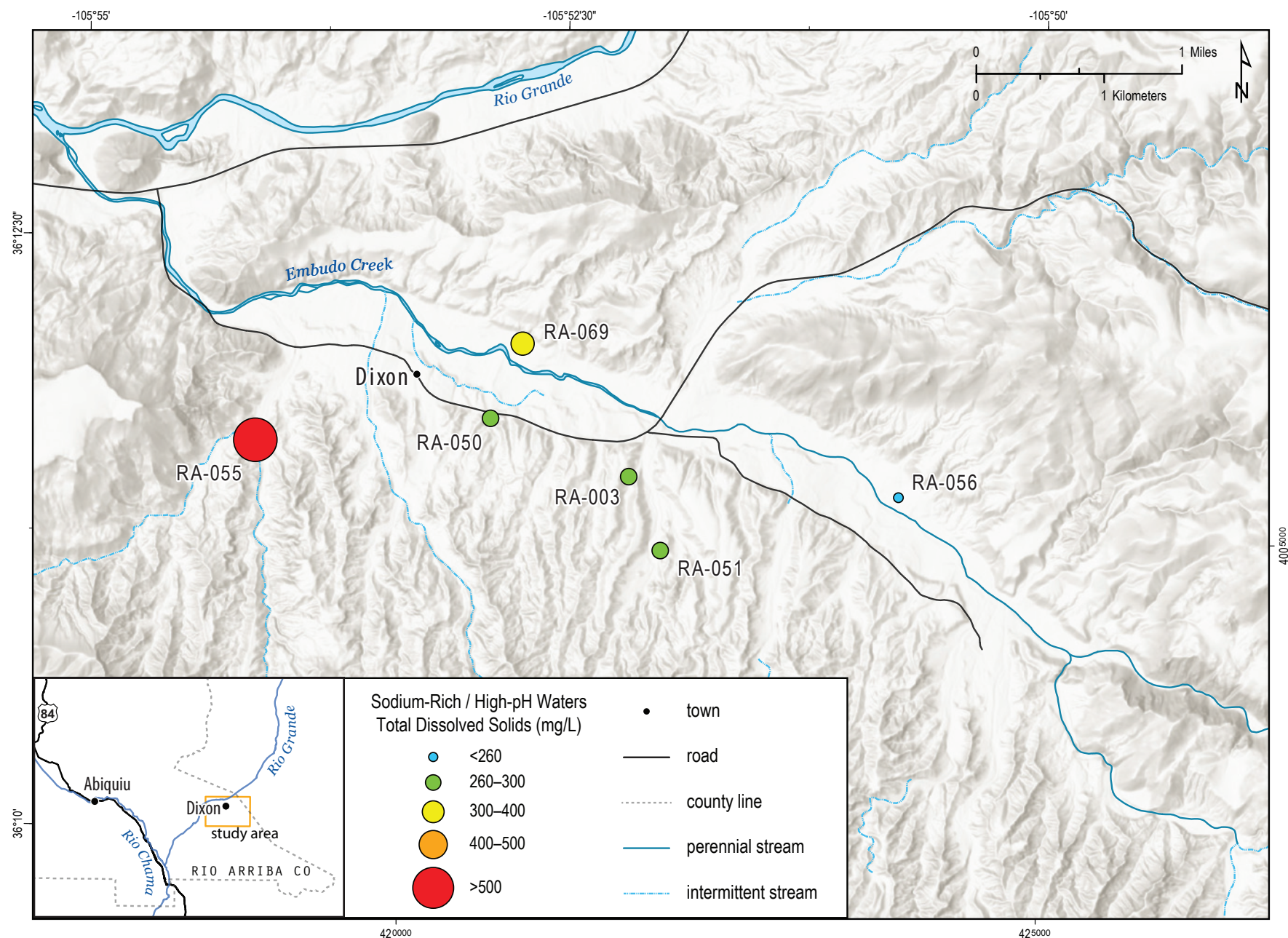
Figure 4.16. Locations of a spring and deep aquifer system wells that produce sodium-rich water exhibiting low TDS concentrations and pH values greater than 8.5.

REFERENCES

Aby, S.B., and Koning, D.J., 2004, Sedimentology of the Tesuque Formation and tectonics of the Embudo fault system near Dixon, New Mexico, *in* Brister, B.S., Bauer, P.W., Read, A.S., and Lueth, V.W., eds., Geology of the Taos Region: New Mexico Geological Society Fall Field Conference Guidebook 55, p. 351–358. https://doi.org/10.56577/FFC-55.351

Aldrich, M.J., 1986, Tectonics of the Jemez lineament in the Jemez Mountains and Rio Grande rift: Journal of Geophysical Research, v. 91, no. B2, p. 1753–1762. https://doi.org/10.1029/JB091iB02p01753

Baldridge, W.S., et al., 1994, The western margin of the Rio Grande rift in northern New Mexico—An aborted boundary?: Geological Society of America Bulletin, v. 106, no. 12, p. 1538–1551. https://doi.org/10.1130/0016-7606(1994)106<1538:TWMOTR>2.3.CO;2

Barker, F.B., 1958, Precambrian and Tertiary geology of the Las Tablas quadrangle, New Mexico: New Mexico Bureau of Mines and Mineral Resources Bulletin 45, 104 p. https://doi.org/10.58799/B-45

Bauer, P.W., Helper, M.A., and Aby, S., 2005, Geologic map of the Trampas 7.5-minute quadrangle, Rio Arriba and Taos Counties, New Mexico: New Mexico Bureau of Geology and Mineral Resources Open-File Geologic Map 104, scale 1:24,000. https://doi.org/10.58799/OF-GM-104

Brister, B.S., 1992, The Blanco Basin Formation (Eocene), San Juan Mountains region, Colorado and New Mexico, *in* Lucas, S.G., Kucs, B.S., Williamson, T.E., and Hunt, A.P., eds., San Juan Basin IV: New Mexico Geological Society Fall Field Conference Guidebook 43, p. 321–331. https://doi.org/10.56577/FFC-43.321

Clark, I., and Fritz, P., 1997, Environmental Isotopes in Hydrogeology: CRC Press, New York, 328 p.

Craig, H., 1961, Isotopic variations in meteoric waters: Science, v. 133, no. 3465, p. 3702–3703. https://doi.org/10.1126/science.133.3465.1702

Craigg, S.D., 2001, Geologic framework of the San Juan structural basin of New Mexico, Colorado, Arizona, and Utah, with emphasis on Triassic through Tertiary rocks: U.S. Geological Survey Professional Paper 1420, 70 p. https://doi.org/10.3133/pp1420

Dansgaard, W., 1964, Stable isotopes in precipitation: Tellus, v. 16, no. 4, p. 436–468. https://doi.org/10.3402/tellusa.v16i4.8993

Drakos, P., Sims, K., Riesterer, J., Blusztajn, J., and Lazarus, J., 2004, Chemical and isotopic constraints on source-waters and connectivity of basin-fill aquifers, *in* Brister, B., Bauer, P.W., Read, A.S., and Lueth, V.W., eds., Geology of the Taos Region: New Mexico Geological Society Fall Field Conference Guidebook 55, p. 405–414. https://doi.org/10.56577/FFC-55.405

Eastoe, C.J., Watts, C.J., Ploughe, M., and Wright, W.E., 2011, Future use of tritium in mapping pre-bomb groundwater volumes: Groundwater, v. 50, no. 1, p. 87–93. https://doi.org/10.1111/j.1745-6584.2011.00806.x

Ekas, L.M., Ingersoll, R.V., Baldridge, W.S., and Shafiqullah, M., 1984, The Chama-El Rito Member of the Tesuque Formation, Española Basin, New Mexico, *in* Baldridge, W.S., Dickerson, P.W., Riecker, R.E., and Zidek, J., eds., Rio Grande Rift—Northern New Mexico: New Mexico Geological Society Fall Field Conference Guidebook 35, p. 137–143. https://doi.org/10.56577/FFC-35.137

Fournier, R.O., and Potter II, R.W., 1982, A revised and expanded silica (quartz) geothermometer: Geothermal Resources Council Bulletin, v. 11, no. 329, p. 3–9.

Geohydrology Associates, Inc., 1979, Preliminary assessment of water resources near Las Placitas and El Rito, New Mexico: Prepared for Placitas Mutual Domestic Water Consumers Association, 67 p.

Goteti, R., Mitra, G., Beccene, A., Sussman, A., and Lewis, C., 2013, Three-dimensional finite-element modeling of fault interactions in rift-scale normal fault systems—Implications for the late Cenozoic Rio Grande rift of north-central New Mexico, *in* Hudson, M.R., and Grauch, V.J.S., eds., New Perspectives on Rio Grande Rift Basins—From Tectonics to Groundwater: Geological Society of America Special Paper 494, p. 157–184. https://doi.org/10.1130/2013.2494(07)

Ingersoll, R.V., Cavazza, W., Baldridge, W.S., and Shafiqullah, M., 1990, Cenozoic sedimentation and paleotectonics of north-central New Mexico—Implications for initiation and evolution of the Rio Grande rift: Geological Society of America Bulletin, v. 102, no. 9, p. 1288–1296. https://doi.org/10.1130/0016-7606(1990)102%3C1280:CSAPON%3E2.3.CO;2

International Atomic Energy Agency, 2017, Global network of isotopes in precipitation database: https://www.iaea.org/services/networks/gnip

Johnson, P.S., LeFevre, W.J., and Campbell, A., 2002, Hydrogeology and water resources of the Placitas area, Sandoval County, New Mexico: New Mexico Bureau of Geology and Mineral Resources Open-File Report 469, 191 p. https://doi.org/10.58799/OFR-469

Kelley, V.C., 1978, Geology of the Española Basin, New Mexico: New Mexico Bureau of Mines and Mineral Resources Geologic Map GM-48, scale 1:250,000, 1 sheet. https://doi.org/10.58799/GM-48

Kelley, S.A., Kempter, K.A., McIntosh, W.C., Maldonado, F., Smith, G.A., Connell, S.D., Koning, D.J., and Whiteis, J., 2013, Syndepositional deformation and provenance of Oligocene to lower Miocene sedimentary rocks along the western margin of the Rio Grande rift, Jemez Mountains, New Mexico, *in* Hudson, M.R., and Grauch, V.J.S., eds., New Perspectives on Rio Grande Rift Basins—From Tectonics to Groundwater: Geological Society of America Special Paper 494, p. 101–123. https://doi.org/10.1130/2013.2494(05)

Koning, D.J., and Aby, S., 2003, Geologic map of the Velarde 7.5-minute quadrangle, Rio Arriba and Taos Counties, New Mexico: New Mexico Bureau of Geology and Mineral Resources Open-File Geologic Map 79, scale 1:24,000. https://doi.org/10.58799/OF-GM-79

Koning, D.J., May, J., Aby, S., and Horning, R., 2004a, Geologic map of the Medanales 7.5-minute quadrangle, Rio Arriba County, New Mexico: New Mexico Bureau of Geology and Mineral Resources Open-File Geologic Map 89, scale 1:24,000. https://doi.org/10.58799/OF-GM-89

Koning, D.J., Ferguson, J.F., Paul, P.J., and Baldridge, W.S., 2004b, Geologic structure of the Velarde graben and southern Embudo fault system, north-central New Mexico, *in* Brister, B., Bauer, P.W., Read, A.S., and Lueth, V.W., eds., Geology of the Taos Region: New Mexico Geological Society Fall Field Conference Guidebook 55, p. 158–171. https://doi.org/10.56577/FFC-55.158

Koning, D.J., Aby, A., and Finch, S., 2007, Where is the water?—A preliminary assessment of hydrogeologic characteristics of lithostratigraphic units near Española, north-central New Mexico, *in* Kues, B.S., Kelley, S.A., and Lueth, V.W., eds., Geology of the Jemez Mountains Region II: New Mexico Geological Society Fall Field Conference Guidebook 58, p. 475–484. https://doi.org/10.56577/FFC-58.475

Koning, D.J., Smith, G.A., and Aby, S., 2008, Geologic map of the El Rito 7.5-minute quadrangle, Rio Arriba County, New Mexico: New Mexico Bureau of Geology and Mineral Resources Open-File Geologic Map 166, scale 1:24,000. https://doi.org/10.58799/OF-GM-166

Koning, D.J., Kempter, K.A., Peters, L., McIntosh, W.C., and May, J.S., 2011a, Miocene–Oligocene volcaniclastic deposits in the northern Abiquiu embayment and southern Tusas Mountains, New Mexico, *in* Koning, D.J., Karlstrom, K.E., Kelley, S.A., Lueth, V.W., and Aby, S.B., eds., Geology of the Tusas Mountains and Ojo Caliente: New Mexico Geological Society Fall Field Conference Guidebook 62, p. 251–274.

Koning, D.J., McIntosh, W., and Dunbar, N., 2011b, Geology of southern Black Mesa, Española Basin, New Mexico—New stratigraphic age control and interpretations of the southern Embudo fault system of the Rio Grande rift, *in* Koning, D.J., Karlstrom, K.E., Kelley, S.A., Lueth, V.W., and Aby, S.B., eds., Geology of the Tusas Mountains and Ojo Caliente: New Mexico Geological Society Fall Field Conference Guidebook 62, p. 191–214.

Koning, D.J., Grauch, V.J.S., Connell, S.D., Ferguson, J., McIntosh, W., Slate, J.L., Wan., E., and Baldridge, W.S., 2013, Structure and tectonic evolution of the eastern Española Basin, Rio Grande rift, north-central New Mexico, *in* Hudson, M.R., and Grauch, V.J.S., eds., New Perspectives on Rio Grande Rift Basins—From Tectonics to Groundwater: Geological Society of America Special Paper 494, p. 185–219. https://doi.org/10.1130/2013.2494(08)

La Calandria Associates, Inc., 2006, Rio Chama Regional Water Plan: Prepared for the Rio de Chama Acequias Association, Rio Arriba County, 191 p.

Langmuir, D., 1997, Aqueous Environmental Geochemistry (first edition): New Jersey, Prentice Hall, 600 p.

Maldonado, F., 2008, Geologic map of the Abiquiu quadrangle, Rio Arriba County, New Mexico: U.S. Geological Survey Scientific Investigations Map 2998, scale 1:24,000. https://doi.org/10.3133/sim2998

Maldonado, F., and Kelley, S.A., 2009, Revisions to the stratigraphic nomenclature of the Abiquiu Formation, Abiquiu and contiguous areas, north-central New Mexico: New Mexico Geology, v. 31, no. 1, p. 3–8. https://doi.org/10.58799/NMG-v31n1.3

Manley, K., 1981, Redefinition and description of the Los Pinos Formation of north-central New Mexico: Geological Society of America Bulletin, v. 92, no. 12, p. 984–989. https://doi.org/10.1130/0016-7606(1981)92<984:RADOTL>2.0.CO;2

Marçais, J., Gauvain, A., Labasque, T., Abbot, B.W., Pinay, G., Aquilina, L., Chabaux, F., Viville, D., and de Dreuzy, J.-R., 2018, Dating groundwater with dissolved silica and CFC concentrations in crystalline aquifers: Science of the Total Environment, v. 636, p. 260–272. https://doi.org/10.1016/j.scitotenv.2018.04.196

May, S.J., 1979, Neogene stratigraphy and structure of the Ojo Caliente-Rio Chama area, Española basin, New Mexico [PhD dissertation]: Albuquerque, University of New Mexico, 204 p.

May, S.J., 1984a, Miocene stratigraphic relations and problems between the Abiquiu, Los Pinos, and Tesuque Formations near Ojo Caliente, northern Española basin, *in* Baldridge, W.S., Dickerson, P.W., Riecker, R.E., and Zidek, J., eds., Rio Grande Rift—Northern New Mexico: New Mexico Geological Society Fall Field Conference Guidebook 35, p. 129–135. https://doi.org/10.56577/FFC-35.129

May, S.J., 1984b, Exhumed mid-Miocene volcanic field in the Tesuque Formation, southern Española basin, *in* Baldridge, W.S., Dickerson, P.W., Riecker, R.E., and Zidek, J., eds., Rio Grande Rift—Northern New Mexico: New Mexico Geological Society Fall Field Conference Guidebook 35, p. 171–178. https://doi.org/10.56577/FFC-35.171

Mayo, E.B., 1958, Lineament tectonics and some ore districts of the southwest: Transactions of the American Institute of Mining Engineers, v. 211, p. 1169–1175.

Molenaar, C.M., 1977, Stratigraphy and depositional history of Upper Cretaceous rocks of the San Juan Basin area, New Mexico and Colorado, with a note on economic resources, *in* Fassett, J.E., and James, H.L., eds., San Juan Basin III: New Mexico Geological Society Fall Field Conference Guidebook 28, p. 159–166. https://doi.org/10.56577/FFC-28.159

Moore, J.D., 2000, Tectonics and volcanism during deposition of the Oligocene–lower Miocene Abiquiu Formation in northern New Mexico [MS thesis]: Albuquerque, University of New Mexico, 144 p.

Muehlberger, W.R., 1967, Geology of the Chama quadrangle, New Mexico: New Mexico Bureau of Mines and Mineral Resources Bulletin 89, 114 p. https://doi.org/10.58799/B-89

Muehlberger, W.R., 1979, The Embudo fault between Pilar and Arroyo Hondo, New Mexico—An active transform fault, *in* Ingersoll, R.V., Woodward, L.A., and James, H.L., Santa Fe Country: New Mexico Geological Society Fall Field Conference Guidebook 30, p. 77–82. https://doi.org/10.56577/FFC-30.77

New Mexico Environment Department, 2024, Drinking Water Branch Drinking Water Watch: https://dww.water.net.env.nm.gov/NMDWW/ (accessed May 2024).

New Mexico Interstate Stream Commission, 2016, Rio Chama Regional Water Plan: New Mexico Office of the State Engineer, 188 p. https://www.ose.nm.gov/Planning/RWP/Regions/14_RioChama/2016/Reg%2014_Rio%20Chama%20Regional%20Water%20Plan%202016_July%202016_with%20appendices.pdf

New Mexico Office of the State Engineer, 2024, OSE POD Locations: https://gis.ose.state.nm.us/gisapps/ose_pod_locations/ (accessed June 19, 2024).

Newton, B.T., Rawling, G.C., Timmons, S.S., Land, L., Johnson, P.S., Kludt, T.J., and Timmons, J.M., 2012, Sacramento Mountains hydrogeologic study—Final technical report, prepared for Otero Soil and Water Conservation District: New Mexico Bureau of Geology and Mineral Resources Open-File Report 543, 84 p. https://doi.org/10.58799/OFR-512

Nordstrom, D.K., Wright, W.G., Mast, M.A., Bove, D.J., and Rye, R.O., 2007, Aqueous-sulfate stable isotopes—A study of mining-affected and undisturbed acidic drainage, *in* Church, S.E., von Guerard, P., and Finger, S.E., eds., Integrated Investigations of Environmental Effects of Historical Mining in the Animas River Watershed, San Juan County, Colorado: USGS Professional Paper 1651, p. 387–416. https://pubs.usgs.gov/pp/1651/downloads/Vol1_combinedChapters/vol1_chapE8.pdf

Phillips, F.M., and Thomson, B.M., 2022, Land-surface water budget, *in* Dunbar, N.W., Gutzler, D.S., Pearthree, K.S., Phillips, F.M., and Bauer, P.W., eds., Climate Change in New Mexico Over the Next 50 Years—Impacts on Water Resources: New Mexico Bureau of Geology and Mineral Resources Bulletin 164, p. 23–36. https://doi.org/10.58799/B-164

Ridgley, J.L., and Hatch, J.R., 2013, Geology and oil and gas assessment of the Todilto Total Petroleum System, San Juan Basin province, New Mexico and Colorado, *in* U.S. Geological Survey San Juan Basin Assessment Team, eds., Total Petroleum Systems and Geologic Assessment of Undiscovered Oil and Gas Resources in the San Juan Basin Province, Exclusive of Paleozoic Rocks, New Mexico and Colorado: U.S. Geological Survey Digital Data Series 69–F. https://pubs.usgs.gov/dds/dds-069/dds-069-f/REPORTS/Chapter3_508.pdf

Smith, H.T.U., 1935, The Tertiary and Quaternary geology of the Abiquiu quadrangle, New Mexico [PhD thesis]: Cambridge, Harvard University, 231 p.

Smith, H.T.U., 1938, Tertiary geology of the Abiquiu quadrangle, Rio Arriba County, New Mexico: The Journal of Geology, v. 46, no. 7, p. 933–965. https://doi.org/10.1086/624710

Smith, G.A., 1995, Paleogeographic, volcanologic, and tectonic significance of the upper Abiquiu Formation at Arroyo del Cobre, New Mexico, *in* Bauer, P.W., Kues, B.S., Dunbar, N.W., Karlstrom, K.E., and Harrison, B., eds., Geology of the Santa Fe Region: New Mexico Geological Society Fall Field Conference Guidebook 46, p. 261–270. https://doi.org/10.56577/FFC-46.261

Smith, G.A., 2004, Middle to late Cenozoic development of the Rio Grande rift and adjacent regions in northern New Mexico, *in* Mack, G.H., and Giles, K.A., eds., The Geology of New Mexico—A Geologic History: New Mexico Geological Society Special Publication 11, p. 331–358. https://doi.org/10.56577/SP-11

Steinpress, M.G., 1980, Neogene stratigraphy and structure of the Dixon area, Española basin, north-central New Mexico [MS thesis]: Albuquerque, University of New Mexico, 127 p.

Steinpress, M.G., 1981, Neogene stratigraphy and structure of the Dixon area, Española basin, north-central New Mexico—Summary: Geological Society of America Bulletin, v. 92, no. 12, p. 1023–1026. https://doi.org/10.1130/0016-7606(1981)92<1023:NSASOT>2.0.CO;2

Timmons, S.S., Land, L., Newton, B.T., and Frey, B., 2013, Aquifer Mapping Program technical document—Water sampling procedures, analysis and systematics: New Mexico Bureau of Geology and Mineral Resources Open-File Report 558, 14 p. https://doi.org/10.58799/OFR-558

Tolley, D.G., Frisbee, M.D., and Campbell, A.R., 2015, Determining the importance of seasonality on groundwater recharge and streamflow in the Sangre de Cristo Mountains using stable isotopes, *in* Lindline, J., Petronis, M., and Zebrowski, J., eds., Geology of the Las Vegas Region: New Mexico Geological Society Fall Field Conference Guidebook 66, p. 303–312. https://doi.org/10.56577/FFC-66.303

U.S. Census Bureau, 2024, Explore Census Data: https://data.census.gov (accessed May 2024).

U.S. Environmental Protection Agency, 2024, National Primary Drinking Water Regulations: https://www.epa.gov/ground-water-and-drinking-water/national-primary-drinking-water-regulations (accessed May 2024).

U.S. Geological Survey, 2019, Water-Use Terminology: https://www.usgs.gov/mission-areas/water-resources/science/water-use-terminology (accessed June 2024).

Vazzana, M.E., and Ingersoll, R.V., 1981, Stratigraphy, sedimentology, petrology, and basin evolution of the Abiquiu Formation (Oligo-Miocene), north-central New Mexico—Summary: Geological Society of America Bulletin, v. 92, no. 12, p. 2401–2483. https://doi.org/10.1130/GSAB-P2-92-2401

Western Regional Climate Center, 2024, Chama, New Mexico (291664): https://wrcc.dri.edu/cgi-bin/cliMAIN.pl?nm1664 (accessed May 2024).

Winter, T.C., Harvey, J.W., Franke, O.L., and Alley, W.M., 1998, Ground water and surface water—A single resource: U.S. Geological Survey Circular 1139, 79 p. https://doi.org/10.3133/cir1139

APPENDIX A: GROUNDWATER AGE DETAILS

Atmospheric carbon dioxide (CO_2) gas, which has an approximate carbon-14 (^{14}C) activity of 100 percent modern carbon (PMC; Clark and Fritz, 1997), is incorporated into the groundwater system (as bicarbonate, $H^{14}CO_3^-$) during infiltration of recharge through the vadose zone. As infiltration crosses the water table, dissolved inorganic carbon (DIC) is isolated from modern carbon-14 inputs from the atmosphere and soil zone reservoirs. The carbon-14 decays with time as the water travels along a flow path in the aquifer system. As a result, the amount of carbon-14 measured in the groundwater along a flow path gives an age, or the approximate time that has passed since the water recharged the aquifer system. In general, lower PMC indicates older groundwater. However, to properly quantify groundwater age, correcting the measured carbon-14 activity is usually necessary to account for hydrogeologic processes such as carbonate dissolution, isotopic exchange, and mixing of older and younger waters. In general, these processes result in apparent ages that are older than the actual age of the water.

The stable carbon isotopic composition for DIC in groundwater ($\delta^{13}C_{DIC}$) is not only useful for correcting the carbon-14 age for the dissolution of calcium carbonate ($CaCO_3$); it also provides important information about the type of vegetation in the recharge area. $\delta^{13}C_{DIC}$ is primarily a function of the carbon isotopic composition of the soil carbon dioxide in the recharge area and the carbon isotopic composition of the carbonate rock that has been dissolved (Clark and Fritz, 1997). The $\delta^{13}C$ of soil carbon dioxide is very similar to that of the local vegetation, which is a function of the metabolic pathway by which carbon dioxide is converted to carbohydrates during photosynthesis. The Calvin cycle (C_3–$\delta^{13}C$ ranges from -30‰ to -24‰) and the Hatch-Slack cycle (C_4–$\delta^{13}C$ ranges from -6‰ to -10‰) are the two principal photosynthetic cycles that account for about 90% of plants globally (Clark and Fritz, 1997). C_3 plants account for 85% of

plant species, including conifers, which are common in high elevations in New Mexico where most recharge occurs.

$\delta^{13}C_{DIC}$-BASED CARBON-14 AGE CORRECTION

The dissolution of carbon-dead (no detectable carbon-14) carbonate minerals, including calcite ($CaCO_3$), ultimately dilutes carbon-14 concentrations in groundwater, resulting in older apparent ages. Correction for this process requires an estimate of the dilution factor, q, in the following equation:

$$t = -8267 \cdot ln\left(\frac{a_t^{14}C}{q \cdot a_o^{14}C}\right)$$

where t = time in years and $a^{14}C$ = carbon-14 activity in PMC. We used the $\delta^{13}C$ mixing model as described by Clark and Fritz (1997) to correct carbon-14 ages for the dissolution of calcium carbonate:

$$q = \frac{\delta^{13}C_{DIC} - \delta^{13}C_{Carb}}{\delta^{13}C_{soil} - \delta^{13}C_{Carb}}$$

where $\delta^{13}C_{DIC}$ = measured $\delta^{13}C_{DIC}$ in groundwater, $\delta^{13}C_{soil}$ = $\delta^{13}C$ of the soil carbon dioxide, and $\delta^{13}C_{carb}$ = $\delta^{13}C$ of calcite being dissolved.

Corrections to apparent carbon-14 age dates were done only for samples collected from the Chama and Dixon study areas.

CHAMA

Refer to Table 2.5 in this report. Due to the very young age estimate (high PMC) and the low TDS concentration, we assumed the uncorrected carbon-14 age date for RA-029 was not in need of correction and that the $\delta^{13}C_{DIC}$ value was representative of the $\delta^{13}C_{DIC}$ value for recent recharge

in the recharge area, with no dissolution of calcium carbonate or calcite. Therefore, a similar $\delta^{13}C$ value was assumed to be $\delta^{13}C_{soil}$, and $\delta^{13}C_{carb}$ was assumed to be 0‰. While this correction seems reasonable for the shallow system waters, the corrected ages for the two deep system waters are more uncertain because the recharge area for the deep system waters may be different than that for the shallow system waters.

DIXON

Refer to Table 4.6 in this report. Due to the very young age estimate and the low TDS concentration, we assumed the uncorrected carbon-14 age date for RA-066 was not in need of correction and that the $\delta^{13}C_{DIC}$ value was representative of the $\delta^{13}C_{DIC}$ value for recent recharge in the recharge area, with no dissolution of calcium carbonate or calcite. Therefore, $\delta^{13}C_{soil}$ = -12‰ was assigned as the $\delta^{13}C_{soil}$ end member for the mixing model described above. $\delta^{13}C_{carb}$ was assumed to be 0‰. The correction for all apparent carbon-14 ages resulted in younger ages.

REFERENCE

Clark, I., and Fritz, P., 1997, Environmental Isotopes in Hydrogeology (first edition): New York, CRC Press, 328 p.

APPENDIX B: WELL INVENTORY

Well inventory data are available for download at
https://geoinfo.nmt.edu/publications/openfile/details.cfml?Volume=630

APPENDIX C: WATER LEVEL DATA

Water level data are available for download at
https://geoinfo.nmt.edu/publications/openfile/details.cfml?Volume=630

APPENDIX D: FIELD PARAMETERS AND WATER CHEMISTRY DATA

Field parameters and water chemistry data are available for download at
https://geoinfo.nmt.edu/publications/openfile/details.cfml?Volume=630

APPENDIX E: EXTERNAL DATA USED IN THE STUDY

Data from the USGS and New Mexico Drinking Water Watch are available for download at
https://geoinfo.nmt.edu/publications/openfile/details.cfml?Volume=630

NEW MEXICO
AQUIFER MAPPING

New Mexico Bureau of Geology and Mineral Resources
A research and service division of New Mexico Tech

geoinfo.nmt.edu

801 Leroy Place
Socorro, NM 87801-4796
(575) 835-5490